Functionalised macrocygles for tumour targeting

John Richard Morphy

FUNCTIONALISED MACROCYCLES FOR TUMOUR TARGETING

by

John Richard Morphy, B.Sc.(Hons.)

(Grey College)

University of Durham

A Thesis submitted for the degree of Doctor of Philosophy

September 1988

DECLARATION

The content of this thesis represents the work of the author unless indicated otherwise or acknowledged by reference. The thesis describes the results of research carried out in the Department of Chemistry of the University of Durham, the Department of Chemistry of Celltech Ltd., Slough and the Medical Research Council Radiobiology Unit, Harwell, between October 1985 and September 1988. It has not been submitted for a higher degree in any other academic institution.

ACKNOWLEDGEMENTS

I would like to express my sincere graditude to Dr. David Parker for his devoted supervision and enthusiastic guidance during the course of this research project.

I am also indebted to Dr. M. Crampton for innumerable and invaluable discussions and recommendations during the course of the kinetics experiments described here. Thanks also go to Dr. R. Kataky for her help in determining equilibrium constants.

I acknowledge the financial support provided by Celltech Ltd. (Slough), and Cyanamid Inc. (Wilmington) for the project and for my research assistantship. In particular, I should like to thank Drs. M. Eaton, A. Millican and R. Alexander (of Celltech) for their helpful guidance and co-operation, and for their hospitality during my frequent visits to Celltech.

A special thank you to Dr. A. Harrison of the MRC Radiobiology Unit (Harwell) for providing the majority of the radiochemical and biodistribution data contained within this thesis and for many fruitful discussions concerning its interpretation.

I am grateful to Dr. N.R.M. Smith for his expert typing of this thesis and to Mr. C. Greenhalgh for his help with the kinetics plots.

There are many more individuals, too numerous to mention by name, to whom I express my heartfelt thanks for their assistance, guidance and friendship; the technical and laboratory staff and my friends and colleagues in the Department of Chemistry and at Celltech.

Last but by no means least, I would like to thank my parents for their love, encouragement and support during the course of my three years of research.

ABBREVIATIONS

mac	Macrocycle
ab	Antibody
Mab	Monoclonal Antibody
$t_{\frac{1}{2}}$	Physical half-life
β (e^-)	Electron
β^+ (e^+)	Positron
EDTA	Ethylenediamine-tetraacetic Acid
DTPA	Diethylenetriamine-pentaacetic Acid
cyclam	1,4,8,11-tetraazacyclotetradecane
$13N_4$	1,4,7,10-tetraazacyclotridecane
TETA	1,4,8,11-tetraazacyclotetradecane-N,N^1,N^2,N^3-tetraacetic acid
TRITA	1,4,7,10-tetraazacyclotridecane-N,N^1,N^2,N^3-tetraacetic acid
DOTA	1,4,7,10-tetraazacyclododecane-N,N^1,N^2,N^3-tetraacetic acid
Ac	Acetate
Succ	Succinate
Ci	Citrate
HPLC	High Performance Liquid Chromatography
TLC	Thin Layer Chromatography
NMR	Nuclear Magnetic Resonance
IR	Infrared
UV	Ultraviolet
CI	Chemical Ionisation
DCI	Desorption Chemical Ionisation
FAB	Fast Atom Bombardment
Mpt	Melting Point
Acc.Mass	Accurate Mass
Anal	Analysis
TMS	Tetramethylsilane
THF	Tetrahydrofuran
DMF	Dimethylformamide
Pipes	1,4-Piperazinebis (ethane sulphonic acid)

FUNCTIONALISED MACROCYCLES FOR TUMOUR TARGETING

ABSTRACT

Monoclonal antibodies which recognise tumour-associated antigens provide a means of targeting radionuclides selectively to tumour cells. ^{99m}Tc and ^{64}Cu are potentially useful isotopes for radioimmunoimaging; ^{90}Y and ^{67}Cu may be suitable for radioimmunotherapy.

The synthesis of functionalised macrocycles for binding these four radioisotopes to antibodies is described. In each case, a macrocycle has been selected to provide a complex which is kinetically inert, thereby preventing dissociation of the radiolabel *in vivo*.

A novel strategy for conjugating a C-alkylated cyclam derivative (for binding Tc and Cu) to an antibody is described. This method facilitates the selective acylation of an exocyclic primary amino group in the presence of the secondary ring nitrogens.

Unfortunately, the labelling of antibody-bound cyclam with ^{99m}Tc required conditions (pH 11) which produced extensive binding of the radiolabel to the protein backbone. "Non-specific" ^{99m}Tc was subsequently found to dissociate *in vivo*. Pre-labelling the macrocycle with ^{99m}Tc solved the "non-specifics" problem but required a pH which meant that the conjugation step was too slow for sufficient specific activity to be bound. A phenol-pendent derivative of cyclam was found to incorporate ^{99m}Tc at a lower pH than cyclam itself.

The "non-specific" binding of copper to the protein was minimised using a low pH labelling strategy in conjunction with a chelate wash. Macrocyclic antibody conjugates labelled in this manner provided very promising biodistribution profiles in normal mice.

A labelling buffer was selected to enhance the rate of uptake of copper by the macrocycle at low pH. Macrocycle-antibody conjugates containing $13N_4$, which was found to provide faster association kinetics than cyclam, have been prepared and await radiolabelling studies.

A derivative of $13N_4$, containing 4 carboxylic acid donor sites, has been functionalised for conjugation to an antibody to act as a ^{90}Y binder.

J.R. MORPHY (1988)

CONTENTS PAGE

CHAPTER ONE

INTRODUCTION

1.1.1 What is Cancer?[1]

Cancer is a disorder of cells which normally appears as a *tumour* (a swelling), made up of a mass of cells. The visible tumour is the end result of a whole series of changes which may have taken many years to develop. Tumours contain cells which are capable of abnormal growth, since they no longer respond to normal growth-control mechanisms; thereby invading and damaging surrounding normal tissues. Strictly speaking a cancer is a *malignant* tumour (there are also *benign* types) capable of shedding cells which are carried to distant organs where they may produce secondary tumours (*metastases*).

Carcinogenesis is a multistage process - after an initiation step involving the carcinogen, another substance is required to promote growth of the tumour. The initiated cell may lie dormant for many years before its activation by the promoting agent. Carcinogens damage or destroy, as yet unknown, sequences of genes in the cellular DNA of the initiated cell. They may be *physical e.g* radiation and UV light, or *chemical e.g* nicotine, benzene, chlorinated hydrocarbons *etc*. Animal experiments suggest that *viruses* may be associated with the initiation of some forms of cancer (mainly leukaemias). There is considerable evidence that increased susceptibility to various forms of cancer may be inherited, although in the end environmental factors (*e.g* diet, tobacco, UV exposure *etc*.) usually determine whether or not the disease develops.

1.1.2 The Incidence of Cancer

Cancer is a common disease in the developed world, responsible for one death in every five. Most cancers develop late in life. Hence the elimination of the common diseases of childhood and of infectious diseases, since the middle of the 19th century, has dramatically increased the proportion of older people at risk.

Cancers can occur in any tissue of the body. The most common in the USA in 1984 were those of the lung, lower intestine (colon/rectum) and breast (Figure 1.1 top). In Japan, stomach cancer is a much more common cause of death (almost certainly diet-associated). These cancers are also amongst the most difficult to treat; the 5 year survival rates being relatively low (Figure 1.1 bottom). Improving the treatment available for these four types of cancer is the aim of this research project.

1.1.3 An Outline of the Project.

Although the exact nature of carcinogenesis remains largely unknown, it appears that potential cancer cells arise constantly within us ("initiation"). However the change in the character ("antigen complement") of these cells is usually sufficient to alert the immune system, whose white cells and natural antibodies seek out and destroy the mutinous cells. When the immune system fails to recognise these cells, cancer develops. This project aims to fight cancer by providing antibodies which the body itself has failed to produce. If these antibodies can be tagged with radioactive isotopes, it may be possible to detect and destroy tumour cells *in situ*, with minimal damage to normal tissue.

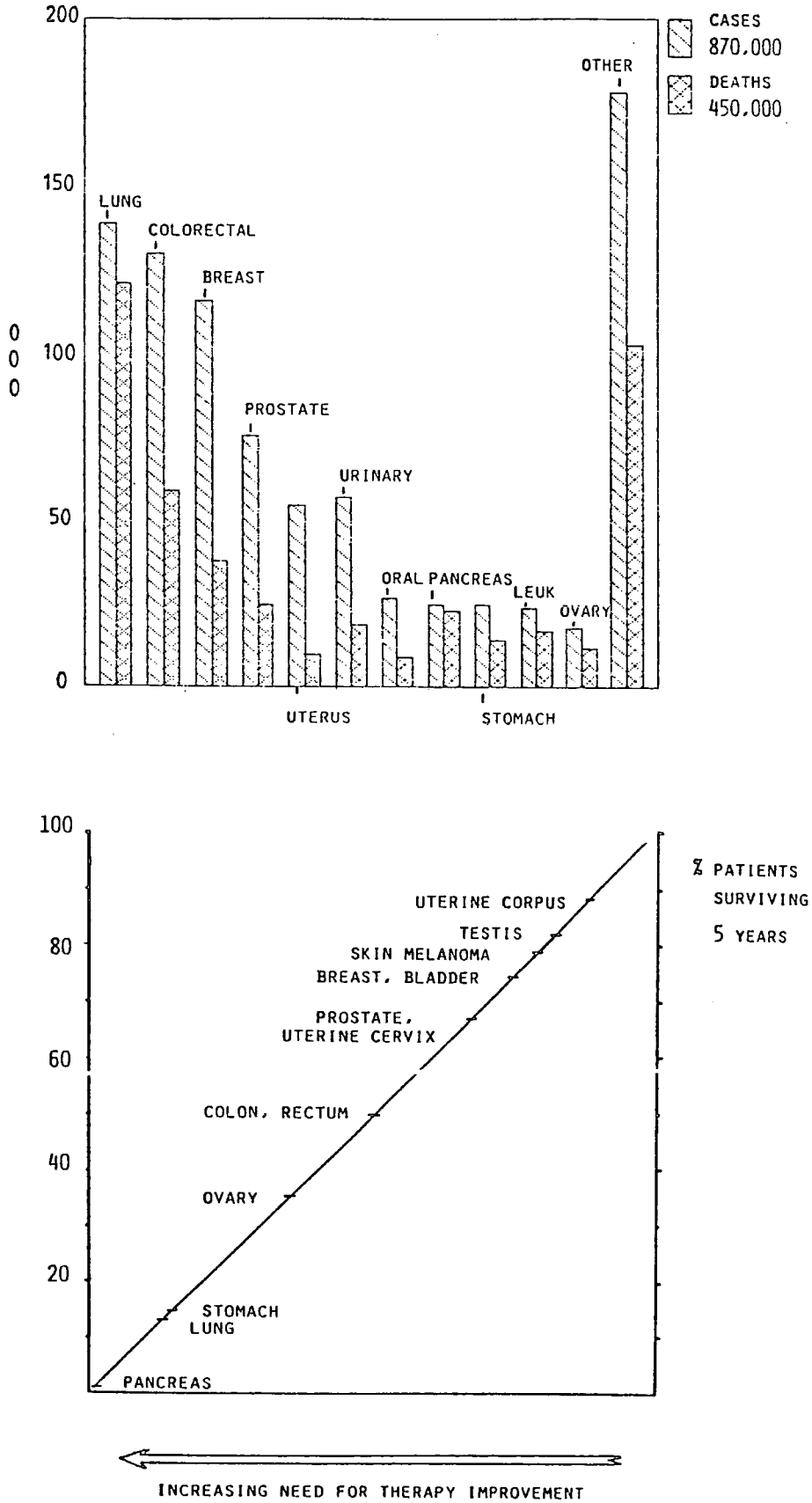

Figure 1.1 *Top: Estimated New Cases and Deaths (USA, 1984); Bottom: The Need for Therapy Improvement (5 year survival priority, USA).*

Since the project is multidisciplinary in nature, there are a number of research groups involved. Celltech Ltd. (of Slough) have expertise in the production and genetic engineering of monoclonal antibodies. The MRC Radiobiology Unit at Harwell provides wide experience of the use of radioisotopes in nuclear medicine. The Durham branch of the project aims to develop appropriate methods for attaching radioisotopes to monoclonal antibodies.

1.2 ANTIBODIES[1-5]

1.2.1 What are antibodies ?

Antibodies are proteins, called Immunoglobulins, produced by vertebrates in response to infection by pathogens and other foreign substances. They invoke a response by the immune system which ultimately leads to the elimination of that substance from the body. Antibodies are produced by the white blood corpuscles called B-lymphocytes. B-cells are manufactured in the bone marrow but migrate soon afterwards to the lymphatic system, especially the lymph nodes and spleen. There they remain dormant until alerted to the presence of foreign substances by another group of white cells called T-lymphocytes. Once alerted they proliferate rapidly and produce huge quantities of antibodies which recognise the invading substance as foreign, stimulating its destruction by a third group of white cells, the macrophages.

Antibodies recognise a foreign material, the *antigen* by binding with partial structures (determinants) on its surface in a highly specific manner. Each B-lymphocyte produces a single type of antibody with specificity for one determinant on one antigen - a *monoclonal*

antibody. The specificity of monoclonal antibodies is generally so precise that higher animals can produce antibodies to a wide range of foreign molecules which differ only slightly from the animal's own molecules. The key to this specificity lies in the highly complex three-dimensional structure of the protein.

1.2.2 The Structure and Specificity of Antibodies

Antibodies are symmetrical molecules and consist, in the case of Immunoglobulin G (IgG - the most common type in the bloodstream) of two identical "heavy" chains (50000 daltons) and two identical "light" chains (25000 daltons). The four polypeptide chains are linked by disulphide bonds, the light chains to the heavy chains and the heavy chains to one another in the "hinge region". Although the overall effect is a complex three-dimensional structure, it can be approximated to a two-dimensional "Y" form (Figure 1.2).

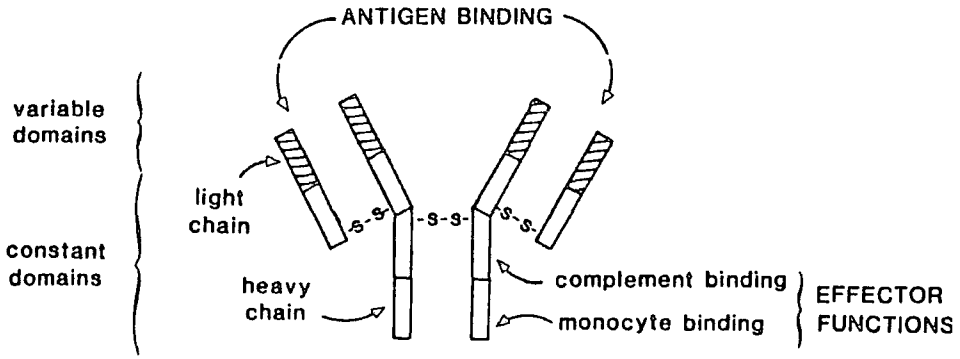

Figure 1.2 *The structure of IgG*

Each heavy chain consists of a variable domain and three constant domains; the light chain contains a variable domain and a single constant domain. The variable and constant domains of one light chain

fold over the variable and first constant domain of a heavy chain to give a "Fab" arm (Fab = fragment antigen binding) which contains a single antigen binding site. Each antibody molecule is therefore bivalent, having two identical binding sites. The other constant domains of the heavy chain form the stem of the molecule, the "Fc" portion (Fc = fragment crystallisable), which interacts with the immune system through its effector functions.

It is principally the spatial arrangement of amino acid residues in the variable domains which determines the individual antigen-binding specificity of an antibody molecule. These antigen-binding sites constitute unique 3D structures called "idiotypes" and are complementary in shape to that of the determinant.

1.2.3 Antibodies for Cancer Treatment

The development of monoclonal antibodies in recent years has revitalised the search for a so-called "magic bullet" treatment for cancer. The theoretical basis of this concept is a simple one. Tumour cells have upon their surfaces specific molecules, termed "tumour-associated antigens", which are not found, or at least are less numerous, on the surfaces of normal cells. Pressman was the first to realise that an antibody with the relevant specificity for these antigens could be used to carry radioactivity to the site of a tumour, where it would accumulate preferentially. The main obstacle to the development of this approach was the difficulty of raising antibodies with sufficiently high specificity for the target antigen.

1.2.4 Polyclonal Antibodies

Antibodies are raised by injecting the tumour-associated antigen into mice and collecting the antibody-producing B-cells from the spleen. However the normal antibody response of an animal to a foreign antigen is to produce an enormous diversity of antibody structures directed against different antigens, different determinants of a single antigen and even different antibody structures against the same determinant - these are *polyclonal antibodies*. Since individual antibody molecules are extremely similar chemically, once mixed in a polyclonal serum, they cannot be separated from one another. Were these polyclonal antibodies to be tagged with radioactivity and injected into a patient, they would bind non-specifically to tissue not associated with the tumour, damaging normal as well as malignant cells.

1.2.5 Monoclonal Antibodies

It was not until the development of "hybridoma" technology by Köhler and Milstein[6] in 1975 that antibodies with sufficiently high specificity for tumour targeting (monoclonal antibodies) were available. B-lymphocytes from the spleen of mice, immunised against a sheep antigen, were immortalised by fusion with mouse myeloma cells (X63-Ag8), in the presence of a fusion-promoting agent (Sendai virus; polyethylene glycol 4000; dimethylsulphoxide), to produce hybrid cells called hybridomas (Figure 1.3).

A myeloma is a malignant B-lymphocyte tumour whose cells normally secrete immunoglobulins but X63-Ag8 was specifically selected for its inability to produce Ig.

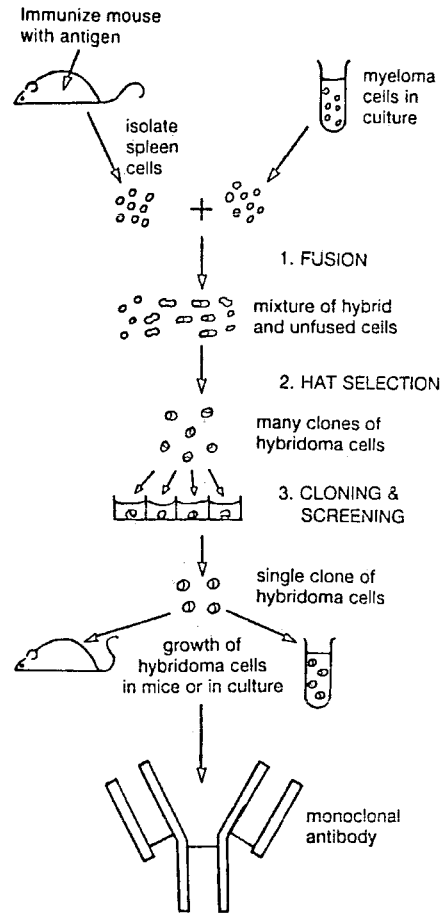

Figure 1.3 *Production of a monoclonal antibody*

The hybridoma inherits both the capacity of the myeloma cell-line for continuous proliferation and the capacity of the B-lymphocyte to synthesise and secrete a single specific antibody.

In the second stage of the protocol, the so-called "HAT" selection, hybridoma cells are separated from unfused myeloma cells by growing the cell mixture in a culture containing nutrients which are useful in the synthesis of hybridomal DNA but not myelomal DNA. Finally the mixture of purified hybridoma cells is screened to identify and isolate those hybridoma clones which secrete the antibody of interest. This is usually done by diluting the suspensions of hybridoma cell mixtures into individual wells of plastic microtitre plates such that each well contains, on average, less than one cell. The clones are allowed to grow and the content of each well is assayed for the presence of the

desired antibody. The dilution procedure is repeated until the cell-line producing this antibody is truly monoclonal. Virtually unlimited quantities of highly specific antibody can be produced in this way.

1.2.6 Human Monoclonal Antibodies

One factor which limits the usefulness of mouse monoclonal antibodies (murine Mab's) for cancer treatment in humans is that they are inherently immunogenic. Human Mab's would be less immunogenic since they possess the same constant domains as normal human Ig. Unfortunately the production of human Mab's by the hybridoma method is much more difficult than that of murine Mab's. Human B-lymphocytes are necessarily more difficult to obtain since tumour-associated antigens can hardly be injected into humans. In some cases, they may be recovered from the blood of individuals already exposed to the antigen, such as cancer patients who have the ability to make antibodies against tumour antigens. Furthermore human B-cells are more difficult to fuse with suitable human myeloma cell-lines, of which there are few.

Other ways of immortalising human antibody-forming cells are being sought; in the meantime, two other methods for reducing immunogenicity in humans are being explored - antibody fragments and chimaeric antibodies.

1.2.7 Antibody Fragments

Since the antigen-binding site lies within the variable region of the antibody, the remaining portion, the Fc region, is not necessary for targeting radioisotopes. Moreover, the appreciation that the Fc region of murine Mab's could be immunogenic in humans, and reduce the

specificity of the antibody for the tumour, led to the use of antibody fragments rather than the whole molecule.

Where the first and second constant domains of the heavy chain meet, there is a short mobile polypeptide piece ("switch region") containing the functionally important hinge region where the two heavy chains are joined by disulphide bonds. This region is particularly susceptible to attack by protease enzymes. The enzymes plasmin and papain cleave the IgG molecule into Fc and two monovalent Fab fragments (Figure 1.4 left). Pepsin cleaves IgG into Fc' and one $F(ab')_2$ fragment (Figure 1.4 right).

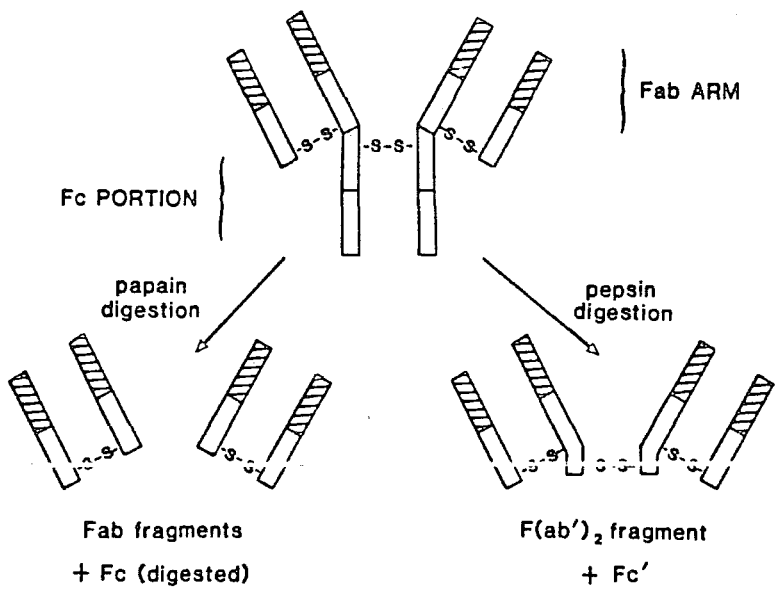

Figure 1.4 *Proteolytic fragments of IgG*

The use of Fab and $F(ab')_2$ fragments may have other advantages besides reducing immunogenicity. Their smaller size should improve access to more hindered sites within the tumour. Since they are cleared more rapidly from the circulation than intact Ig, the radiation background and whole body dose may be minimised.

1.2.8 Chimaeric Antibodies[7]

Using recombinant DNA technology, it is now possible to combine portions from one antibody gene with segments from another to produce completely novel types of antibody. Chimaeric antibodies contain the variable region of a murine Mab joined to the constant regions of a human Mab. Chimaerics may be less likely to trigger an immune response in humans than all-mouse Mab's provided that the immune attack is primarily directed against the constant region.

1.2.9 Tumour-Associated Antigens

When a normal cell becomes malignant it can express antigens which are not produced by the parent cell such as altered carbohydrates and proteins and oncofoetal antigens which reflect the tendency of tumour cells to become more primitive (Figure 1.5). These antigens may be tumour specific or, more commonly, highly selective for certain types of tumour cells.

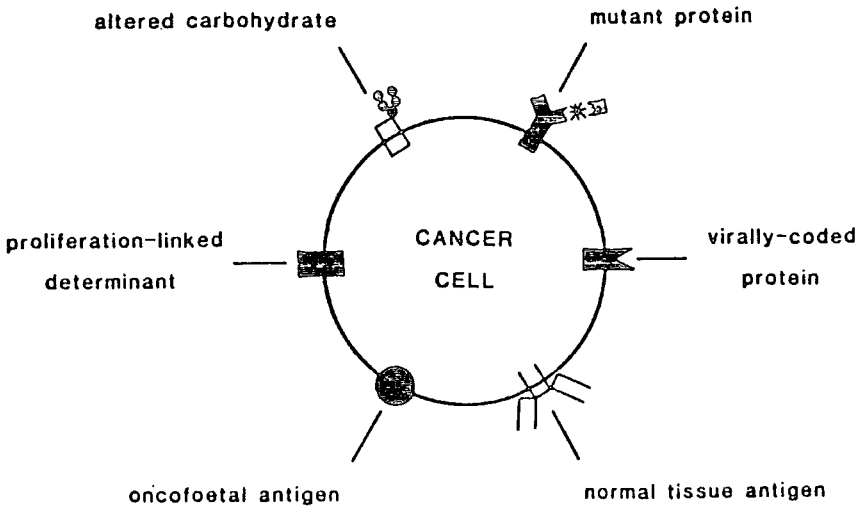

Figure 1.5 *Target Antigens*

It is actually quite rare for an individual Mab to bind exclusively to the target cell since normal tissue may express either the same antigen or a structurally indistinguishable molecule. Since a tumour cell membrane expresses a large number of antigens, the key to successful targeting is to identify those which are most characteristic of that individual cell-type.

Consideration must also be given to the tendency of certain antigens to be shed from the tumour into the bloodstream. In addition many tumours have regions which are devoid of a particular antigen. The importance of these "cold regions" will be discussed in section (6.1). Judicious choice of the target antigen, and its complementary Mab, is therefore crucial for the overall success of this approach.

1.3 RADIOISOTOPES FOR TUMOUR TARGETING

1.3.1 General Criteria for the Selection of Radioisotopes[8-11]

The primary consideration governing the choice of a suitable radioisotope is the purpose for which the antibody is to be radiolabelled. The desired physiological effect of the radiation is markedly different depending upon whether the primary aim is diagnostic (radioimmunoimaging) or therapeutic (radioimmunotherapy).

For imaging purposes, minimal interaction of radiation is desired with the tissues of the patient and maximum interaction with a detector located outside the body. Gamma emitters may be suitable in this respect if they deliver photons of appropriate energy to escape from the body and with sufficient density to achieve the necessary resolution for tumour imaging.

In radioimmunotherapy, the intention is to deliver as much energy as possible at the target site, thereby delivering a sterilising dose of typically 500-2000 rads. Suitable sources emit largely particulate radiation, α particles or, more commonly, β particles, with little or no gamma component. The contrasting radiation requirements for imaging and therapy are summarised below:

Therapy	Diagnosis
Beta rays are useful since they deliver ionizing radiation to the limited area that is to be treated.	Beta rays can not be visualized externally and only increase tissue radiation exposure.
Gamma rays are of little therapeutic value (except those of very low energy) since they distribute the radiation exposure over a wide area.	Gamma rays are of primary importance in imaging (except those of low energy, which do not penetrate the tissue).
There may be a role for longer lived radionuclides if the radiation has to be delivered over a period of time.	Short-lived radionuclides are preferred since they do not have to be present after the initial images are obtained.

Another important factor which differs for imaging and therapy is the physical half-life of the radioisotope, usually being longer for therapy than for imaging. The physical $t_{\frac{1}{2}}$ of an imaging radioisotope is the minimum time necessary for localisation of the radiolabelled Mab in the tumour, followed by the diagnostic procedure itself, in order to limit the radiation dose to the patient. For therapy, the desire is to maximise the radiation dose to the tumour. Providing the Mab is sufficiently specific towards the target tissue and has a suitably long biological half-life, it is useful to deliver sterilising radiation over a period of several days from a longer-lived radioisotope.

In addition to the aforementioned criteria, there are also a number of additional factors governing the choice of radionuclide which are common to both imaging and therapy.

The decay of the radioisotope should ideally produce a stable

daughter product in order to reduce the hazard to the patient. The recoil produced by particulate emissions, especially of α particles, may rupture the bond between the radionuclide and the antibody allowing it to diffuse randomly throughout the body. In addition, radioactive decay usually produces a different element with different chemical properties for which the mode of attachment to the antibody may be less suitable, allowing it to become detached from the protein. If active daughter products are produced, they should be rapidly eliminated from the body.

The method of production of the radionuclide should be straightforward and relatively economical, such that the radioisotope is readily available for medical use. Its chemical properties must be sufficiently different from those of the nuclide from which it is prepared (the "carrier" material) to permit its purification by chemical means. The use of "carrier-free" material is particularly important for therapy, since a sterilising dose can only be delivered if a substantial amount of active material is attached to each antibody molecule.

Finally the chemical properties of the radionuclide must allow its attachment to the antibody by a stable radionuclide-protein bond, and in sufficient quantity to provide the specific activity necessary to produce the desired effect, whilst retaining the the immunoreactivity of the antibody. Metals are usually better than non-metals in this respect since they allow more flexibility for the chemist and usually form stronger radionuclide-antibody bonds.

Suitable radionuclides for therapeutic applications are discussed further in section (6.2). For now, the emphasis will be placed on the selection of radioisotopes for imaging and their attachment to Mab's.

1.3.2 *In vivo* Imaging[12]

Often the life-threatening nature of cancer arises not from the primary tumour but from the spread of the disease to other critical organs. The development of *in vivo* imaging as a means of detecting a broad spectrum of cancerous growths within a patient, including smaller secondary growths called metastases, is crucial to the success of antibody-based cancer therapy. Large accessible tumours are probably best removed by surgery, smaller less accessible metastases by radioimmunotherapy[1] (Figure 1.6). As well as providing useful information about the size, morphology and location of tumour deposits, *in vivo* imaging is vital for prognosis and for monitoring the effect of therapeutic radiation upon the tumour during the course of the treatment.

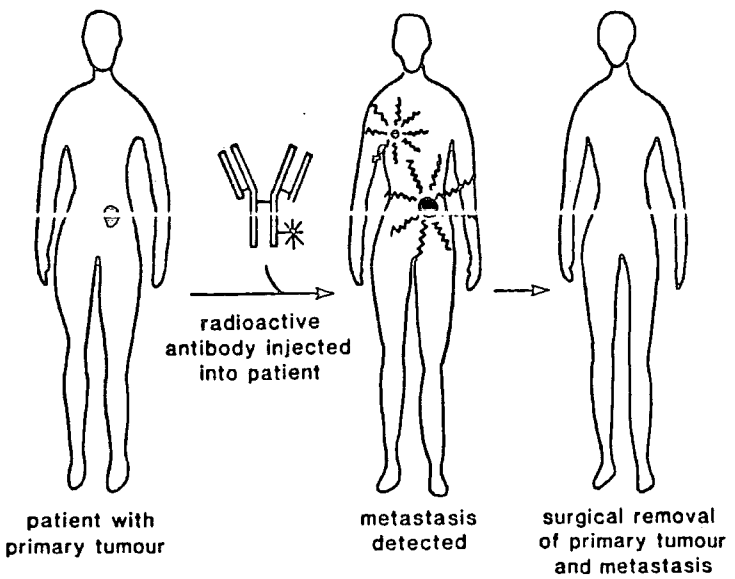

Figure 1.6 *The Principle of radioimmunoimaging*

Electromagnetic radiation of suitable energy for *in vivo* imaging, to which the human body is "transparent", has a frequency of either less

than 10^{10} Hz or greater than 10^{18} Hz. Nuclear medicine exploits the high energy gamma ray "window". At the low energy side of the spectrum, imaging techniques based upon nuclear magnetic resonance are being developed.

NMR imaging[13,16] exploits the differences in the relaxation times of water protons depending upon their location within the body. If a superparamagnetic nucleus can be targeted to a tumour site, the relaxation times of tumour-associated protons will be sufficiently shorter than those of protons in the surrounding tissue to allow the tumour to be imaged by NMR. Unlike gamma radiation, radiofrequency waves are thought to be completely harmless to the patient. However the field of NMR imaging is still in its infancy and it may be several years before it can compete with gamma ray imaging in terms of cost, sensitivity and resolution.

Gamma rays suitable for radioimaging can be produced in two different ways. Either they result directly from the nuclear decay of the isotope - single photon emitters - or the isotope emits a positron (β^+) and creates two opposing 511 keV gamma rays by electron-positron annihilation. The two techniques are completely different in terms of the method of detection of the gamma ray and the type of image thereby obtained.

1.3.3 Single Photon Emission

A static Anger camera is required to provide an image of the tumour (Figure 1.7). In view of the random direction of emission from single photon-emitting isotopes, a collimator is required to localise the radiation upon the detector. The detector is a NaI (Tl) crystal which produces a flash of light when struck by a gamma particle. These light

flashes are amplified with photomultipliers and counted as electrical pulses. The resolution of an Anger camera is typically 1-2 cm, which is much coarser than that obtainable using X-ray techniques.

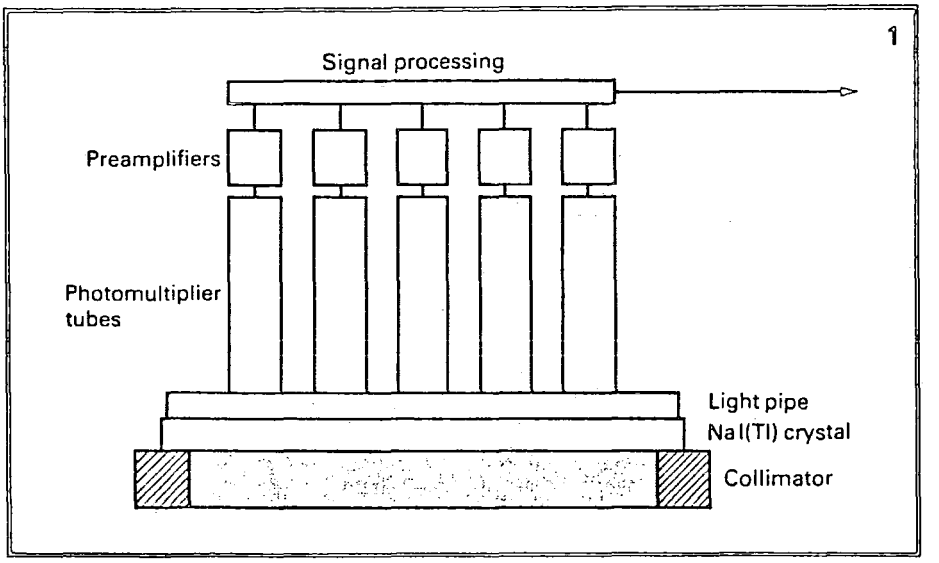

Figure 1.7 *The Anger camera layout*

1.3.4 Tomography[1,12]

A two-dimensional image of a tumour on a plate often contains artefacts and false positive regions. It is preferable to assemble a three-dimensional picture of the tumour by recording the activity from a series of slices taken across the body of the patient - this process is called *tomography*. Tomography can be carried out by mounting the Anger camera on a rotating gantry, recording multiple images at different angles of the patient and reconstructing the activity distribution through a back-projection process. The need for physical collimation, which reduces the count-rate at the crystal surface 1000 fold, makes single photon emitter computerised tomography (SPECT) a much less

sensitive and accurate technique than positron emission tomography (PET).

1.3.5 Positron Emission Tomography[14]

The data provided by positron emitters can be processed to give tomographic information without the need for physical collimation, by virtue of the directional nature of the emission ("electronic collimation"). The annihilation of a positron "at rest" by a standstill electron implies the emission of two perfectly anti-parallel quanta. Due to the relative motion of positron and electron, the distribution is actually gaussian about 180^0 ($\pm$ 0.5^0).

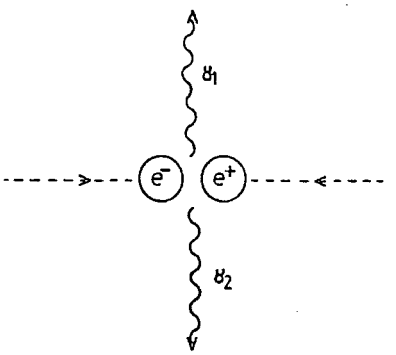

In PET, the two gamma rays are detected at each side of the source. This confines the annihilation event to a single line joining the two detectors (Figure 1.8).

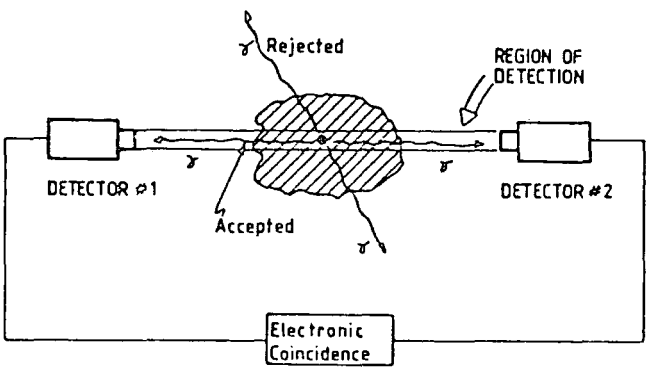

Figure 1.8 *Schematic drawing of the first PET scanner*

In conventional PET, a distribution plot of the radioisotope throughout the tumour is constructed from the pattern of coincidences as the two scanners are rotated around the patient. More modern detector configurations are shown in Figure 1.9; a planar annular ring of scintillators, a large area planar detector and the most recent development, multiring configurations.

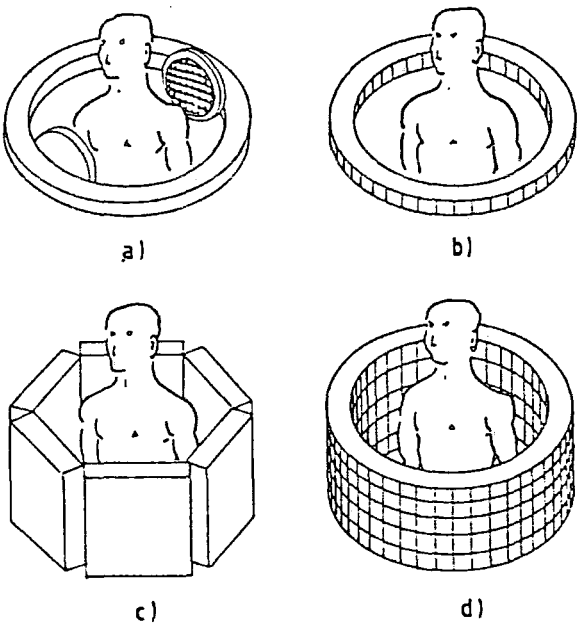

Figure 1.9 *Examples of PET camera configurations: a) two opposite Anger cameras; b) single ring; c) hexagon planar camera; d) multiring*

In "Time-of-Flight" PET, the position of the isotope can be found very precisely by calculating the difference in the time of arrival of the 2 photons (t_1-t_2) onto opposite detectors 1 and 2, using the relation:

$$(d_1-d_2)/c = t_1-t_2$$

where d is the distance from the detector and c is the speed of light.

Generally PET techniques produce very high resolution images, theoretically down to 3-4 mm, which are vastly superior to those given

by SPECT. The main disadvantage of PET is that the special camera presently required is very expensive, typically ten times the cost of an Anger camera. This will remain the main obstacle to the widespread application of PET as a routine tool for *in vivo* imaging until cheaper equipment becomes available.

1.3.6 Choice of Single Photon Emitters[8,9,10]

In addition to fulfilling the general criteria outlined in section (1.3.1), single photon emitters suitable for radioimaging are characterised by

(1) a half-life of between 6 hours and 8 days

(2) a gamma energy of between 80 and 240 keV

(3) high energy single gamma abundance per decay

(4) zero or small abundances of low-energy particulate radiations

(5) chemical properties which facilitate their attachment to antibodies

Examples of radionuclides which fulfill some or all of these criteria are given in Table 1.1

Nuclide	$t_{\frac{1}{2}}$	E_{max} β (MeV)	E_{photon} (keV %)	Source
^{99m}Tc	6.02h	---	141(89)	generator
^{123}I	13h	---	159(83)	cyclotron
^{125}I	60.00d	---	27(138)	cyclotron
^{131}I	8.05d	0.188	364(82)	reactor
^{111}In	2.83d	---	171(88)	reactor

Table 1.1 *Radionuclides used or useful for radioimmunoimaging*

Technetium[15-18]

^{99m}Tc† has been the most widely used radioisotope in nuclear medicine for many years for two principal reasons.

Firstly it delivers gamma rays of an almost ideal energy (140 keV) for detection by the NaI (Tl) crystal of an Anger camera. ^{99m}Tc is relatively safe - there are no particulate emissions and the abundance of single energy gamma rays allows a low specific activity to be used.

Secondly, since ^{99m}Tc is obtained from a ^{99}Mo generator, it is readily available in a "carrier-free" form. It can be transported easily from the production to the application site and is cheap and convenient to use. Radioactive generators are column-chromatographic devices which can separate the components of a radioactive decay chain. In this case, the daughter isotope ^{99m}Tc ($t_{\frac{1}{2}}$ = 6h) can be separated from its parent isotope ^{99}Mo ($t_{\frac{1}{2}}$ = 66h) by eluting an alumina/silica column, onto which the parent is absorbed, with an isotonic (0.9%) saline solution (Figure 1.10). The eluate, a saline solution containing ^{99m}Tc, is collected with a lead-shield evacuated vial. Since ^{99}Mo continuously decays to ^{99m}Tc, after a suitable time delay further batches of ^{99m}Tc may be eluted from the column. One major benefit of the generator system is that it provides supplies of the daughter isotope for much longer than its own half-life allows. For example a single ^{99}Mo generator provides a supply of ^{99m}Tc for a period of up to 7 days.

Iodine isotopes[2,15]

Three isotopes of iodine, ^{123}I, ^{125}I and ^{131}I, have been investigated for diagnostic use. ^{123}I shares with ^{99m}Tc the benefit of abundant, single energy gamma emissions particularly suitable for detection using

---

†"m" stands for "metastable" and signifies an excited nuclear state with an unusually long life-time.

an Anger camera. However unlike ^{99m}Tc, ^{123}I is a cyclotron‡ product and is consequently much more difficult and expensive to produce in a "carrier-free" form. ^{125}I is much less suitable for diagnosis by virtue of its long half-life (60 days) and the low energy of its gamma emissions.

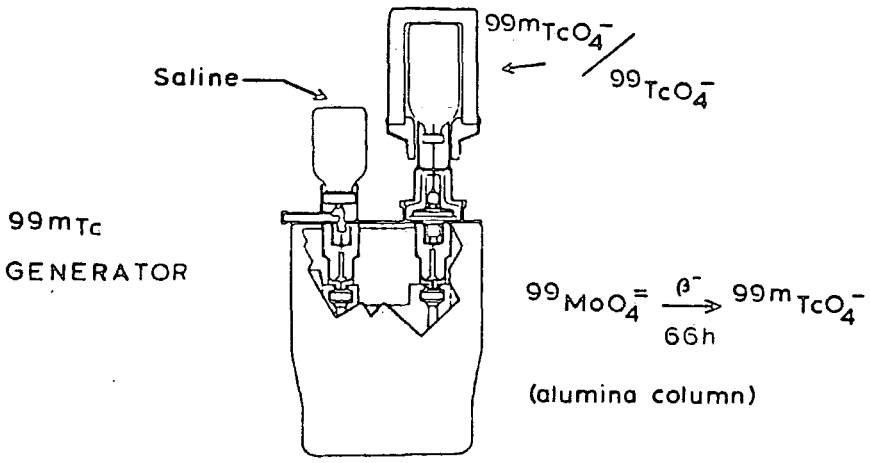

Figure 1.10 *Technetium-99m generator*

^{131}I was the first isotope to be used for radiolabelling antibodies with the intention of imaging tumours, but has now fallen into disfavour. Its gamma energy (364 keV) is rather too high to be detected efficiently using a Anger camera and its particulate (β) emissions increase the absorbed radiation dose to the patient unnecessarily.

Iodine isotopes also suffer from the disadvantage of rapid de-iodination from the Mab *in vivo*, releasing the radioisotope to circulate randomly through non-target tissue and to accumulate in the thyroid gland.

---

‡A cyclotron is a type of particle accelerator in which a target material is bombarded with projectiles *e.g* protons accelerated under the influence of magnetic and electrical fields.

Indium

An isotope of indium, ^{111}In, is the only serious competitor to ^{99m}Tc as a gamma source for scintigraphy. Although its gamma emissions are less well matched to an Anger camera than those of ^{99m}Tc, ^{111}In has the advantage of a longer half-life (2.83 days) which allows more time for the radiolabelled antibody to accumulate in the tumour and clear from the bloodstream. Often useful tumour : background relationships are only available after 2 days[2], less than one half-life for ^{111}In. For ^{99m}Tc, less than 0.5% of the original activity will remain after 2 days, probably insufficient for imaging purposes unless a high initial specific activity is used. If the accumulation/clearance time can be reduced by use of antibody fragments[2], Fab and $F(ab')_2$ (section 1.2.7), ^{99m}Tc will be less disfavoured. On the grounds of cost and availability, ^{99m}Tc is the easy winner - it can be obtained from a generator, ^{111}In cannot.

Clearly neither ^{99m}Tc nor ^{111}In has ideal nuclear properties in every respect. Their relative merits and drawbacks are summarised in Table 1.2. Also included in the table are a number of other considerations, largely influenced by the chemical rather than the nuclear properties of the isotopes. Some of these factors only came to light during the course of our work and will be discussed in more detail in subsequent chapters. For the time being, suffice it to say that either one of these isotopes is worthy of serious consideration for *in vivo* imaging.

1.3.7 Choice of Positron Emitters

The positron emitters ^{82}Rb and ^{68}Ga are widely used in PET studies since they are readily available from ^{82}Sr and ^{68}Ge generators respectively[14].

However their physical half-lives, 1.4 and 1.1 minutes, are too short for our purposes; there being insufficient time for localisation of the radiolabelled antibody in the tumour.

TECHNETIUM	INDIUM
Merits	Merits
1. Abundant single E gamma emissions	1. No "non-specific" labelling of antibodies
2. Ideal E (141 keV) for detection	2. Longer half-life (2.83 days) than ^{99m}Tc
3. Cheap and readily available from a generator	
Drawbacks	Drawbacks
1.Very short $t_{1/2}$ (6.0 h)	1.Lower abundance of suitable energy gamma rays than ^{99m}Tc
2.Difficult and largely unknown tracer level chelation chemistry	2.Existing chelating agents for binding ^{111}In to antibodies are unsatisfactory esp.EDTA
3."Non-specific" binding to antibodies	3.Hydrolyses easily to form colloids which increase the non-target dose.
	4.Not available from a generator - 10x more expensive than ^{99m}Tc

Table 1.2 *Advantages and disadvantages of ^{99m}Tc and ^{111}In for radioimmunoimaging*

^{64}Cu is more suitable for antibody-based PET imaging by virtue of its longer half-life (12.8 hours). It has two modes of decay, the dominant one being positron emission (see diagram overleaf). ^{64}Cu also has a very small gamma component (0.6%; 1.34 MeV). It is made from ^{64}Zn by a (n,p) reaction (section 4.1.1). The major disadvantage of ^{64}Cu is its cost, 100 times that of ^{99m}Tc and 10 times that of ^{111}In.

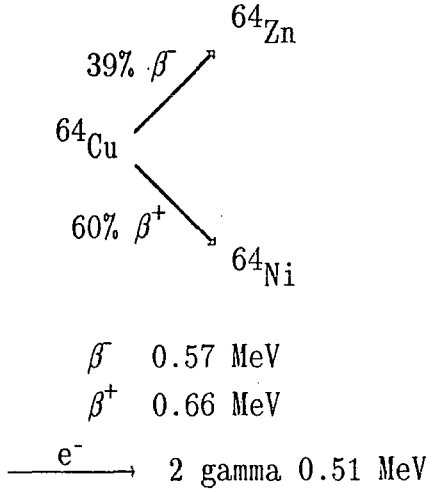

1.4 THE BINDING OF METALLIC RADIONUCLIDES

Metallic radionuclides *e.g* ^{99m}Tc, ^{64}Cu, ^{111}In must be attached to monoclonal antibodies using a strong binding ligand. The donor atoms of the chelate may form part of the antibody itself or, more usually, belong to a separate chelating agent, selected for its high affinity for the radiometal, which is suitably attached to the Mab.

1.4.1 Direct Labelling of Antibodies[15,19]

Direct labelling exploits the functional groups of the amino acids, which constitute the protein, to complex the metal. The great advantage of this method is its experimental simplicity, an important factor in the preparation of any radiopharmaceutical. Unfortunately, direct protein-radiolabel bonds are usually labile if the stereochemistry of the donor groups does not match the preferred coordination geometry of the metal. ^{99m}Tc has been used to directly label Mab's but the *in vivo* stability of the majority of the protein-metal bonds thus formed is low.

There are however a limited number of sites within the antibody, thought to be associated with thiol groups, which bind ^{99m}Tc more avidly[20] (section 3.1.5).

1.4.2 Use of Bifunctional Chelating Agents

By far the most successful strategy for attaching radiometals to Mab's employs bifunctional chelating agents. The advantage of chelators is that they form bonds to metals which are generally much more stable than those formed by direct labelling. It is possible to tailor the choice of chelating group to match the distinctive coordination requirements of the radiometal which must be bound, optimising the "hardness" and number of donor atoms and the coordination geometry such that the complex is sufficiently stable for use *in vivo*.

Suitable chelating agents are bifunctional in the sense that they possess one site, containing a number of donor atoms, which binds the metal and another site through which the chelator can be linked to the antibody. The preferred form of the latter functionality will be discussed in section (1.7). The metal-binding functionality forms the basis of the current discussion.

1.4.3 Thermodynamic and Kinetic Stability of Chelate Complexes for *In Vivo* Applications

It is well known that complexes formed between metals and chelating ligands are generally more thermodynamically stable than those involving monodentate donor groups - this is the so-called "chelate effect". The strong driving force for complexation is often cited to be the large increase in translational entropy which accompanies the displacement of

a given number of solvent molecules by a smaller number of ligand molecules, *e.g.*

$$M(H_2O)_6 + 3L \longrightarrow ML_3 + 6H_2O$$

$$M(H_2O)_6 + 2L \longrightarrow ML_2 + 6H_2O$$

The greater the denticity of the ligand, the larger the positive entropy contribution and the more thermodynamically stable the complex (assuming that enthalpy effects are minor!).

Although thermodynamic stability provides a useful bench-mark by which we can judge the suitability of a particular chelate for *in vivo* use, it is not the major consideration. No matter how high the stability constant of the complex may be, the establishment of equilibrium inside the body will encourage dissociation of the metal. This is a consequence of the extremely low concentration of radioactive chelates *in vivo* compared to the relatively high concentrations of competing chelatable metals (*e.g* Zn^{2+}, Ca^{2+}) and competing chelating ligands, notably the metal-binding proteins, albumin and transferrin[21].

Dissociation of metals from chelating agents occurs by either an acid-catalysed or an acid-independent mechanism. Since the former process is much more rapid, the majority of the flux of the dissociation reaction occurs *via* this route. As a general rule, a metal-chelate complex becomes progressively less thermodynamically stable as it is more highly protonated (ML > MLH > MLH_2 > MLH_3 etc):

$$ML \underset{k_{-1}}{\overset{K_1}{\rightleftharpoons}} MLH \underset{k_{-2}}{\overset{K_2}{\rightleftharpoons}} MLH_2 \underset{k_{-3}}{\overset{K_3}{\rightleftharpoons}} MLH_3 \quad etc.$$

A more important factor governing *in vivo* stability than the stability constant of ML is therefore the *kinetic inertness* of the complex towards protonation (k_1, k_2, k_3 etc should be slow). Additionally, the

protonation constants (K_1, K_2, K_3 etc) should be low, such that the pH at which ML becomes extensively protonated and seriously destabilised is lowered.

1.4.4 EDTA and DTPA Chelating Agents

The first chelate-protein conjugates which were considered sufficiently stable for *in vivo* use were based upon the polyaminocarboxylate ligands, ethylenediaminetetraacetic acid (EDTA) and diethylene tri-aminopentaacetic acid (DTPA):

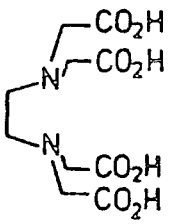

EDTA

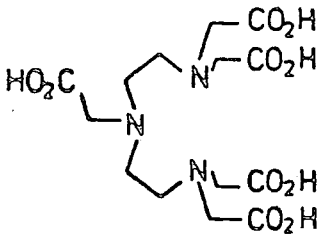

DTPA

These ligands form complexes with a huge number of different metal ions; EDTA being a chelator for at least 70 different elements[21]. However, many of these complexes are insufficiently stable for use *in vivo*. The very fact that EDTA forms complexes with so many elements, with a great range of chemical properties, implies that it is not tailored to satisfy the often distinctive coordination requirements of individual elements - it is "jack-of-all-trades and master-of-none"!

For some metals the particular combination of N and O donor atoms found in EDTA and DTPA is ideal, for others a combination containing "harder" or "softer" donors may be preferred. In some cases, there are insufficient donor sites for the metal to be coordinatively saturated, for other metals there are too many and carboxylate arms hang free.

The carboxylic acid arms of EDTA and DTPA are deprotonated when bound to metals, often resulting in anionic complexes. Inside the body, anionic complexes attract protons and other metal cations *e.g* Ca^{2+} and Zn^{2+}. Since the main pathway for cleavage of metal-nitrogen bonds involves acid (or metal) catalysis, metal complexes of EDTA and DTPA normally have low kinetic stability *in vivo*. This problem is particularly serious in those regions of the body where the pH is low. In the stomach and liver, the pH may be as low as 2. Under such acidic conditions, the metal-chelate complex is protonated and the overall species has a much reduced thermodynamic stability and a strong tendency to dissociate.

1.4.5 Macrocycles for Metal Binding[22,23]

In order to bind labile metal ions in such a manner that they are stable *in vivo*, nature often uses macrocyclic ligands; for example, the iron- and magnesium-porphyrins of haemoglobin and chlorophyll and the cobalt-corrin complex of vitamin B_{12}. The basic skeleton of the porphyrin ring contains 16 atoms.

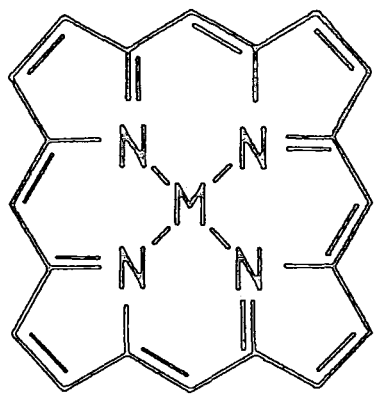

Figure 1.11 *Basic skeleton of naturally occurring porphyrins*

The metal sits in the plane of the four nitrogen donors which are arranged to give a sequence of 6-membered chelate rings (Figure 1.11). The corrin ring has a total of 15 atoms and a sequence of three 6- and one 5-membered chelate rings. In view of their unique chelation properties, many synthetic analogues of naturally-occurring tetraamine macrocycles have been synthesised during the last 3 decades and have been found to form complexes with a wide variety of metal ions. To fully encircle a first-row transition metal ion, a macrocyclic ring size of between 13 and 16 members is appropriate, providing that the nitrogen donors are arranged to give five-, six- or seven-membered chelate rings (Figure 1.12). Smaller rings *e.g* $12N_4$ can only be accommodated if the macrocyclic folds and does not completely encircle the metal ion on coordination.

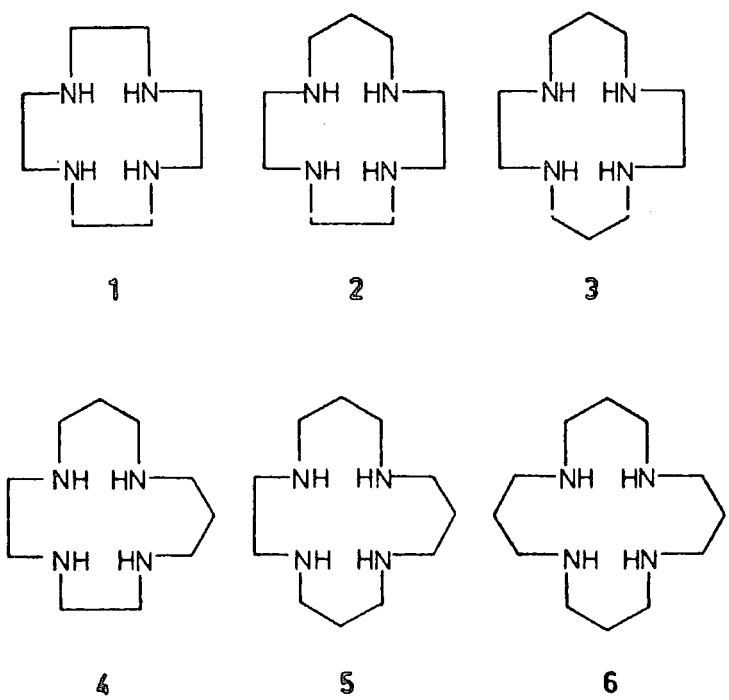

Figure 1.12 *Tetraamine Macrocycles 1)$12N_4$; 2)$13N_4$; 3) cyclam; 4) isocyclam; 5) $15N_4$; 6) $16N_4$*

Larger rings must be sufficiently conformationally mobile to achieve a favourable coordination geometry about the central transition metal ion. Ligands with more than 4 donors may be able to accommodate more than one metal ion.

1.4.6 The Macrocyclic Effect

Macrocyclic complexes are, almost without exception, more stable thermodynamically and kinetically than their corresponding open-chain analogues. Termed the "macrocyclic effect" by its discoverers, Margerum and Cabbiness[24], it is a more profound feature of macrocyclic complexes than simply an increased "chelate effect" arising from the presence of an additional chelate ring.

The high thermodynamic stability of macrocyclic complexes may be attributed to either a favourable enthalpy or entropy contribution or to a combination of both. For example, Margerum *et al.*[25] found that the enthalpy term is dominant when the formation of the Ni(II) complex of the [14]-membered tetraamine macrocycle ("cyclam") and its non-cyclic analogue are compared. However, for other complexes, the entropy term is primarily responsible for the increased thermodynamic stability (section 1.5.6).

The enhanced thermodynamic stability associated with the "macrocyclic effect" was attributed to the kinetic inertness of the macrocycle versus acyclic complexes. Open-chain ligands can undergo successive S_N1 displacement steps. and in acidic media, the dissociated groups are rapidly protonated. However, dissociation of a macrocyclic complex requires distortion of the ligand to minimise electrostatic repulsion between the first dissociated and protonated site and the central metal, and to allow the approach of the incoming ligand. The

requirement for rearrangement of the ligand upon protonation raises an energy barrier to decomplexation, imparting higher kinetic stability upon the complex (section 1.5.3).

The reasons for the slow *association* kinetics of tetraamine macrocycles are discussed in section (5.1.2).

It is popular to ascribe the enhanced stability of macrocyclic complexes to the "fit" between the metal ion diameter and the size of a relatively rigid cavity in the centre of the macrocycle. Although this may be a valid concept for explaining the selectivity of crown-ether ligands for alkali metal ions[26], the correlation between stability and "fit" is less certain for tetraamine macrocycles and is metal-dependent.

Hancock *et al.*[27] found that the larger cations, Pb^{2+} and Cd^{2+}, formed their most stable complexes with a [12]-membered tetraamine ligand. For the smaller Cu^{2+} cation, larger [13]- and [14]-membered ligands were preferred. The first observation may be explained in terms of the metal lying outside the "cavity" with the ligand in a folded ("cis") conformation. This type of ligand conformation is usually more strained so, as for acyclic complexes, the overriding stability factor is the sequence of chelate ring sizes. However the overall stability of the complex may still be higher than the open-chain analogue due to a more favourable entropy factor. In cases where the metal ion precisely "fits" the macrocyclic cavity, the metal-nitrogen bond distances are optimised, the ligand conformation is unstrained and the overriding stability factor is usually the enthalpy. The factors determining enthalpy and entropy contributions to thermodynamic stability are assessed in section (1.5), for complexes of Cu^{2+} with a series of tetraamine macrocycles.

1.5 COPPER RADIOISOTOPE BINDING

1.5.1 Basic Copper Chemistry[28]

The dipositive state is the most important one for copper. The d^9 electronic configuration makes Cu(II) complexes subject to Jahn-Teller distortion‡† if placed in cubic (octahedral or tetrahedral) environments and this profoundly affects the stereochemistry and stability of its complexes. When six-coordinate, the "octahedron" is severely distorted along one 4-fold axis, such that there is a planar array of four short equatorial Cu-L bonds and two long axial Cu-L bonds. In fact copper(II) forms many complexes in which the elongation is so pronounced that the coordination environment is essentially square planar. Usually the cases of tetragonally distorted "octahedral" coordination and square coordination are not easily differentiated.

There are few tetrahedral complexes containing copper(II), examples being the chloro complex $CuCl_4^{2-}$ and the bis(salicylaldiminato) complex $(Me_3C\text{-}N{=}CH\text{-}(C_6H_4)\text{-}O\text{-})_2Cu$. Most copper(II) complexes have distorted "octahedral" or square planar symmetries.

In aqueous solution, Cu(II) salts give the aqua ion $[Cu(H_2O)_6]^{2+}$ in which two of the water molecules are further from the metal than the other four. Addition of nitrogen-containing ligands to aqueous solutions leads to successive displacement of water ligands since transition metal ions such as Cu^{2+} prefer "softer" nitrogen donors to "harder" oxygen donors. However the addition of the fifth and sixth nitrogen donors is difficult due to the Jahn-Teller effect. For

‡†The Jahn-Teller theorem predicts that the unsymmetrical occupancy of a degenerate energy level will be unstable and the system will undergo distortion so as to remove the degeneracy. The driving force for the distortion is a reduction in the overall energy of the occupied "d" orbitals.

example, $[Cu(NH_3)_6]^{2+}$ can only be formed in liquid ammonia and $[Cu(en)_3]^{2+}$ is formed only at extremely high concentrations of ethylene diamine. Amine complexes of Cu(II) are much more intensely blue than the aqua ion because amines produce a stronger ligand field which causes a high frequency shift in the position of the "d-d" absorption band.

1.5.2 Copper Binding using EDTA, DTPA and TETA

Meares *et al.*[29,30] reported that ^{67}Cu complexes of EDTA or DTPA, whether in the free-form or antibody-bound, were extensively decomposed by human serum within 24 hours. In contrast copper chelates made from the macrocyclic ligand "TETA" and its antibody conjugates were found to be much more stable in serum, 94-98% remaining intact after 5 days (Table 1.3).

CHELATE	DAY		
	0	3	5
^{67}Cu-DTPA-N-butylamide	100	35	33
^{67}Cu-DTPA-antibody	100	6	5
^{67}Cu-NO_2 Benzyl EDTA	95	18	18
^{67}Cu-Benzyl-EDTA-antibody	94	4	5
^{67}Cu-NO_2-Benzyl-TETA	100	98	98
^{67}Cu-Benzyl-TETA-antibody	100	96	94

Table 1.3 *Decomposition of Copper Chelates in Serum. Intact Chelate Remaining (%) at Various Times*

These results are surprising on the basis of the relative thermodynamic stabilities of the chelates - Cu-TETA is actually less stable than Cu-EDTA or Cu-DTPA at pH 7 (Table 1.4). Moreover the EDTA complex of cobalt(II) has a higher serum stability than Cu-EDTA even though it is less thermodynamically stable[31]. This was explained in terms of the high

rate of ligand exchange characteristic of Cu(II) relative to Co(II) complexes and the high concentration of competing ligands (*e.g* albumin) in serum. The enhanced *in vivo* stability of Cu-TETA must be explained in terms of the "macrocyclic effect" and the kinetic inertness which it conveys upon copper(II) complexes of [14]-membered macrocyclic tetraamines.

LIGAND	STRUCTURE	log K_{CuL}
EDTA	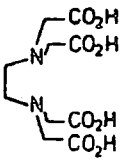	18.7
DTPA	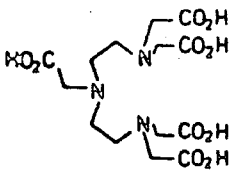	21.4
TETA	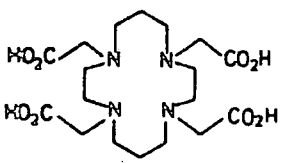	18.6

Table 1.4 *Stability constants of Aminocarboxylate Ligands; 20°C; I=0.1*

1.5.3 The Macrocyclic Effect for Copper(II) Cyclam Complexes

The rôle of the "macrocyclic effect" in accounting for the observed thermodynamic and kinetic stabilities of copper-tetraamine complexes is well-illustrated by considering the parent $14N_4$ cycle "cyclam" and its acyclic analogue, 1,4,8,11-tetraazaundecane (2,3,2-tet), as examples (structures overleaf). Kimura and Kodama[32] found the copper complex of cyclam to be 2000 times more stable than that of the linear tetraamine (Table 1.5).

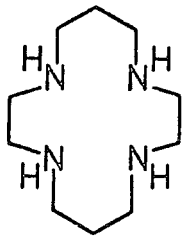

cyclam

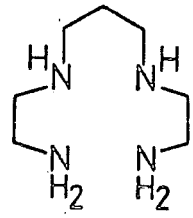

2,3,2-tet

LIGAND	log K_{CuL}	-ΔH (kcal mol^{-1})	ΔS (cal $K^{-1}mol^{-1}$)
CYCLAM	27.2‡‡	30.4	22.4
2,3,2-TET	23.9	27.7	16.5

Table 1.5 *(25^0C; $I=0.2$ mol dm^{-3})*

They proposed that the observed "macrocyclic effect" was due to a combination of favourable enthalpy (ca 60%) and entropy (ca 40%) contributions. Earlier the Ni(II)-cyclam complex had been found to exhibit a solely enthalpy-governed "macrocyclic effect".

Hinz and Margerum[25] explained the enthalpy contribution for Cu(II) cyclam in terms of decreased free ligand solvation; less energy being required for desolvation prior to complexation. Fabrizzi and Paoletti[33,34] prefer to explain the effect in terms of the conformation of the free ligand being perfectly pre-orientated for copper complexation. In the acyclic system, energy must be expended for the required conformational change. Indeed this represents the popular notion of a relatively rigid macrocycle cavity (cyclam) accommodating a metal ion of "best fit" with strong planar Cu-N bonds and a large heat of formation (-ΔH).

‡‡Cu(II) cyclam is thought to be a mixture of two isomers, a blue isomer and a more thermodynamically stable red isomer. The reported formation constant would then be a composite of the values for the individual isomers.

Another manifestation of the "macrocyclic effect" for Cu(II) cyclam is its kinetic inertness, especially towards acid-catalysed dissociation. In fact it is so inert that decomplexation only occurs to an appreciable extent in very strong (5-6M) acid[35]. The dissociation of copper from tetraamines occurs in two steps for cyclam but one step for the linear tetraamine, 1,5,8,12-tetraazadodecane (3,2,3-tet):

$$Cu(cyclam)^{2+} \underset{k_{-1}}{\overset{k_1}{\rightleftharpoons}} Cu(Hcyclam)^{3+} \xrightarrow{k_2} Cu^{2+} + (H_4cyclam)^{4+}$$

$$Cu(3,2,3\text{-tet})^{2+} \xrightarrow{k_1'} Cu^{2+} + (H_4tet)^{4+}$$

The cleavage of the first Cu-N bond in $Cu(cyclam)^{2+}$ requires distortion of two stable chelate rings (Figure 1.13 left) and is *via* a protonation pathway. Similar cleavage in $Cu(3,2,3\text{-tet})^{2+}$ requires distortion of a single chelate ring only (Figure 1.13 right) and is *via* a solvation pathway.

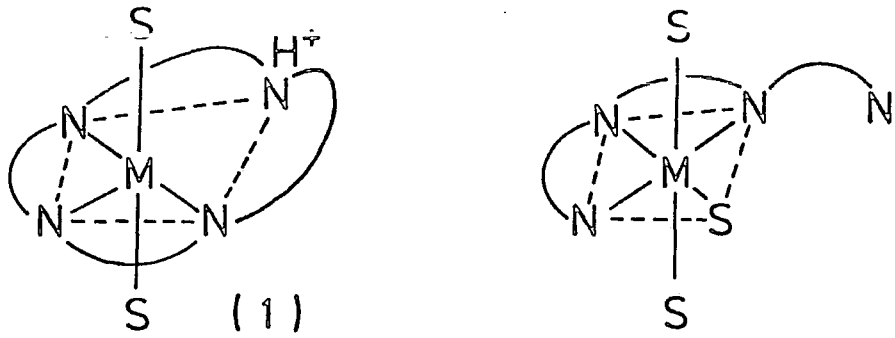

Figure 1.13 *Species resulting from first Cu-N bond cleavage*

Thus the cleavage of the first Cu-N bond of $Cu(3,2,3\text{-tet})^{2+}$ is much more rapid (10^4 - 10^5 times) than that for $Cu(cyclam)^{2+}$. Since solvation of (1) is hindered by the steric constraints of the macrocyclic ligand, k_{-1}

is larger than k_2 and the cleavage of the second Cu-N bond is rate-determining for $Cu(cyclam)^{2+}$.

1.5.4 Crystal Structures of Copper(II) Cyclam Complexes

The X-ray structure[36] of the perchlorate salt of Cu(II) cyclam is shown in Figure 1.14. The 4 N donors lie in the same plane as the metal with all four Cu-N bonds of equal length (2.02 Å). The tetragonally distorted "octahedron" is completed by the oxygen atoms of perchlorate in the two axial positions (Cu-O = 2.57 Å). The ligand adopts a least-strained "trans-III" conformation in which the six-membered chelate rings are in a stable chair form on opposite sides of the N_4 plane. The five-membered chelate rings adopt a stable gauche form.

In the crystal structure[37] of Cu-NbzTETA (Figure 1.15), the expected tetragonal distortion is also observed. However in this case the equatorial positions are occupied by 2 N and 2 O donors, with Cu-donor bond lengths of 2.0 Å. The remaining two Cu-N bonds are elongated and occupy axial positions (2.428 and 2.367 Å). The strong interaction of the carboxylate oxygens is surprising in view of the usual preference of Cu^{2+} for N donors.

It is interesting that the crystal structure[38] of the copper(II) complex of the 1,8-diacetic acid derivative of cyclam is similar to that of $[Cu(cyclam)]^{2+}(ClO_4^-)_2$, in that the four strongest bonds are to nitrogen with relatively weak Cu-O axial bonds (Figure 1.16). Thus it would appear that the N_2O_2 coordination of Cu-TETA is unique amongst the known copper complexes of cyclam derivatives, resembling more closely the copper complexes of EDTA and DTPA.

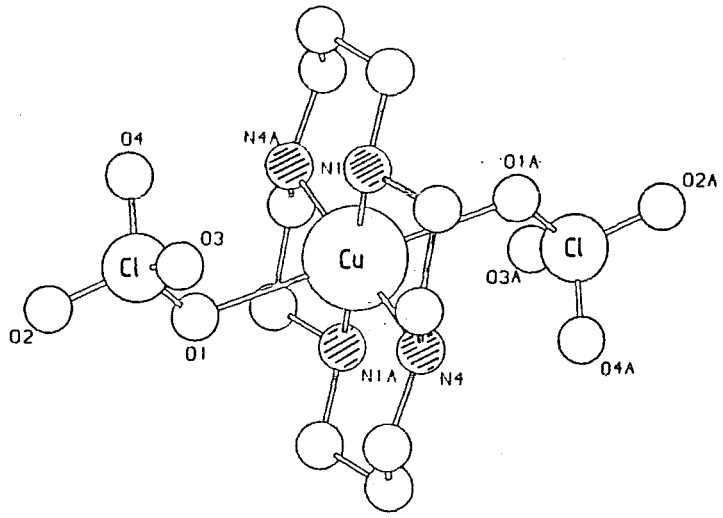

Figure 1.14 *Crystal Structure of [Cu(cyclam)].ClO_4*

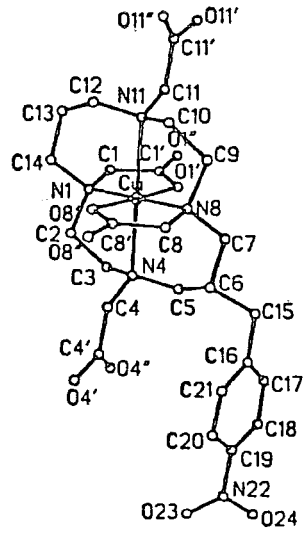

Figure 1.15 *Crystal Structure of Cu [6-(p-$NO_2C_6H_4CH_2$TETA]*

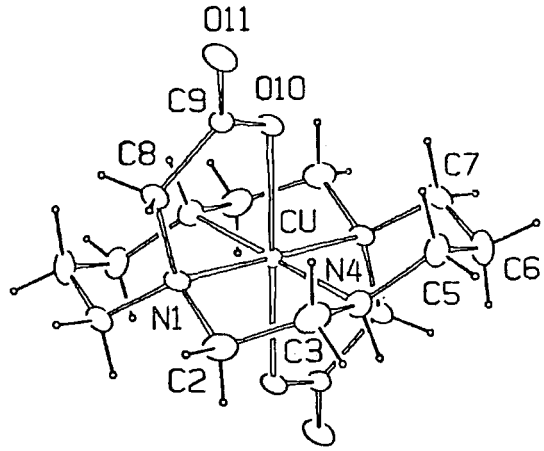

Figure 1.16 *Crystal Structure of Cu [1,8-N,N'-bis(carboxy-methyl)-cyclam*

1.5.5 Comparison of TETA and cyclam for copper binding

Since the structure of a copper-tetraamine complex in solution is expected to resemble that in the solid-state, Meares *et al.*[37] proposed that the unusual N_2O_2 donor set conveyed upon Cu-TETA a special kinetic inertness over and above that expected for a cyclam complex from the "macrocyclic effect". The complex was said to have a structural rigidity which shields the copper ion from attacking ligands. The assertion that N_2O_2-coordinated Cu-TETA is more kinetically stable than than N_4-coordinated Cu-cyclam is highly controversial. Peralkylated cyclams are generally accepted to have faster metal-dissociation kinetics than the parent cycle (section 2.2.4). In addition, the anionic nature of Cu-TETA will attract protons and other metal ions into the vicinity of the complex. As noted earlier for EDTA and DTPA, these species catalyse dissociation of metal ions. Although Cu-TETA was shown by Meares *et al.* to be inert in serum at pH 7 (section 1.5.2), its weak axial Cu-N bonds will be particularly susceptible to acid-catalysed cleavage in the more acidic parts of the body.

Cationic complexes *e.g* $Cu(cyclam)^{2+}$ forming strong Cu-N bonds should be more kinetically stable *in vivo*. Unfortunately the rate of dissociation of copper from cationic macrocyclic tetraamine complexes is so slow that it has proved difficult to measure rate constants through which we can compare the suitabilities of a series of macrocycles for *in vivo* copper binding (only a value for Cu-cyclam has so far been measured)[35]. It is therefore necessary at present to consider the thermodynamic stability and rate of association of a Cu(II) complex as a rough guide to its suitability.

1.5.6 Thermodynamic Stabilities of Copper(II) Polyamine Complexes

The stability constants of the copper(II) complexes of a series of macrocyclic ligands (Figure 1.12) are given in Table 1.16[32].

LIGAND	log K
Cu-12N_4	24.8
Cu-13N_4	29.1
Cu-15N_4	24.4
Cu-cyclam	27.2
Cu-isocyclam	22.4

Table 1.16 *Stability constants for a series of tetraamine macrocycles at 25°C and I=0.2 mol dm^{-3}*

With increasing ring size, the stability of copper-tetraamine complexes reaches a maximum value (29.1) for 1,4,7,10-tetraazacyclotridecane ("13N_4"), then decreases again. It is noteworthy that the copper complex of iso-cyclam is significantly less stable than Cu(II) cyclam. The unsymmetrical arrangement of 5- and 6-membered rings introduces steric strain into the conformation of the bound ligand[34].

Interestingly, the origin of the "macrocyclic effect" varies for different ring sizes. Kimura *et al.*[39] found that the increased stability of Cu-12N_4 was primarily due to a more favourable entropy contribution. This arises from the free ligand being more "rigid" and more highly solvated than the acyclic ligand, giving rise to favourable configurational and translational entropy changes on complexation. For the Cu-13N_4 system[40], the entropy contribution is lower but it is more than offset by a more favourable enthalpy factor giving a larger stability constant overall. The enhanced enthalpy contribution arises from stronger Cu-N bonds, a less strained ligand conformation for a larger cycle and possibly lower solvation in the free ligand. As discussed previously (section 1.4.3), the "macrocyclic effect" for Cu-

cyclam is predominantly enthalpy-driven.

In view of their high thermodynamic stabilities, the tetraamine macrocycles, cyclam and $13N_4$ were shortlisted for further investigation as potential bifunctional chelating agents for ^{64}Cu and ^{67}Cu.

1.5.7 Phenolic Macrocycles as Copper Binders

In a series of papers[41-45], Kimura *et al.* reported the metal-binding potential of tetraamine macrocycles bearing phenolic side chains. The [14]-membered phenolic cycle (2) forms complexes with Ni(II) and Fe(II) in which the phenol is bound to the metal as an axial phenolate donor (Figure 1.17).

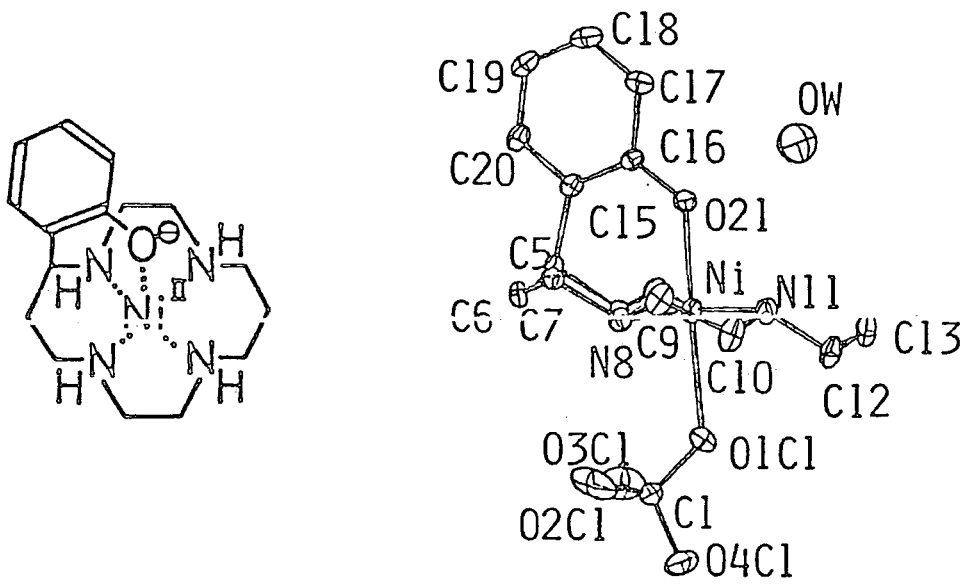

Figure 1.17 *Molecular Structure of a Nickel(II) Complex with Phenol-pendent cyclam (2)*

The pK_a values for the phenols in the NI(II) and Fe(II) complexes of (2), a measure of the strength of the axial interaction, are 6.30 and 6.8 respectively, compared to 8.86 for the free ligand. Incidentally,

the phenol in the free ligand is more acidic than phenol itself (pK_a 10) due to stabilisation of the phenolate by intramolecular electrostatic attraction with the dipositively charged ring (pK_1 11.75; $pK_2$10.84). When bound, the phenolate imparts special properties upon the chelate, stabilising complexes which are not normally formed by the parent cycle *e.g* Fe^{III}-(2) and Ni^{III}-(2).

The phenol pK_a for the Cu(II) complex (9.2) is high indicating that axial interaction is weak (Jahn-Teller distortion). The stabilising influence of an axially bound phenolate donor is therefore likely to be irrelevant for the Cu(II) complex except at higher than physiological pH (Table 1.7).

	log K (25^oC; I=0.2 mol dm^{-3})
Cu-cyclam	27.2
CuL	29.2
pKa 9.2	
$CuH_{-1}L$	32

Table 1.7 *Stability constants of Cu(II) complexes of cyclam and phenol pendent cyclam; L-2*

Nonetheless, the suitability of phenol-pendent derivatives of cyclam and $13N_4$ for binding copper (and technetium) will be discussed in more detail in Chapters 2,3,4 and 5.

1.6 TECHNETIUM RADIOISOTOPE BINDING

1.6.1 Basic Technetium Chemistry[18,46]

Despite the widespread use of ^{99m}Tc in nuclear medicine, the chemistry

of technetium is still poorly developed. However the ready availability in recent years of macroscopic amounts of a longer-lived radionuclide ^{99}Tc, a β-emitter ($t_{\frac{1}{2}}$ = 2.13 x 10^5 yr), has encouraged much effort to elucidate basic technetium chemistry. It appears that technetium has an extensive coordination chemistry, with a variety of inorganic and organic ligands, exhibiting oxidation states from -1 (d^{10}) to +7 (d^0) displaying coordination numbers from 4 to 9.

Those Tc complexes most relevant to nuclear medicine contain the metal in the oxidation state +1, +3, +4 or +5. Since ^{99m}Tc is obtained as the pertechnetate (TcO_4^-) ion from a ^{99}Mo generator, it must be reduced from the +7 oxidation state to a lower oxidation state. For example a tin(II) salt is normally used for the two-electron reduction of Tc(VII) to Tc(V):

$$Tc^{VII}O_4^- \xrightarrow[(-H_2O)]{2H^+,2e^-} "Tc^{V}O_3^-"$$

$$"Tc^{V}O_3^-" \xrightarrow{2H^+\ (-H_2O)} "Tc^{V}O_2^+"$$

$$"Tc^{V}O_2^+" \xrightarrow[(-H_2O)]{2H^+} "Tc^{V}O^{3+}"$$

Only one oxo group is removed in the reduction step; others being removed by protonation and loss of water.

In general Tc(IV) and Tc(V) complexes have technetium-oxo cores in order to satisfy their high-charge requirements. In particular, Tc(V) can be satisfied by one oxo group and four good π-bonding ligands (*e.g* TcO^{3+} core in $TcOCl_4^-$) or by two oxo groups and one σ-donating ligand (*e.g trans*-TcO_2^+ core in $[Tc(py)_4O_2]^+$). Technetium-oxygen bonds have been found by X-ray analysis to be sufficiently short to be formulated as (σ + π) double bonds (Tc=O). The Tc=O bond length in complexes with a TcO^{3+} core is usually shorter (by about 0.1 Å) than that in complexes

containing *trans*-TcO_2^+ groups. The former can be 5-, 6-, or 7-coordinate, the latter are always 6-coordinate. The TcO group demonstrates a powerful trans effect and influence. In complexes containing "hard" or π-acidic ligands in the cis-position, solvent molecules (water or alcohol) occupying the sixth position will subsequently be deprotonated to give a *trans*-TcO_2^+ core (Figure 1.18).

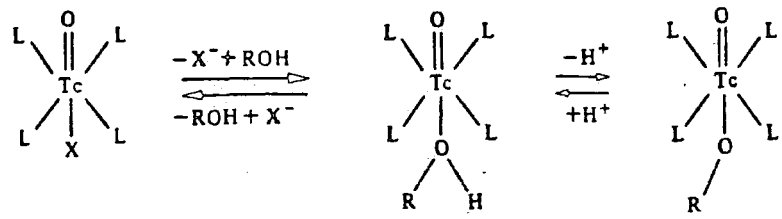

where L = *cis* ligands, R = Me .

For R = H the reaction can proceed further :

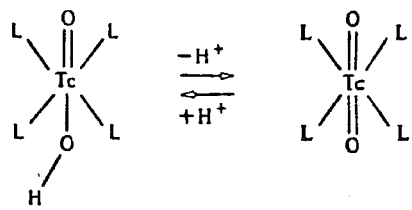

Figure 1.18 *Formation of trans-TcO_2^+ species in aqueous solution*

In Tc(I) and Tc(III) complexes, there are no oxo groups *ie.* TcL_n, Tc_2L_n *etc.* Low valent complexes of technetium most often contain π-acceptor ligands which can accept electron density from the metal *e.g* phosphines, arsines, carbon monoxide *etc.* Technetium at the "carrier-added" level (*ie.* ^{99}Tc) also forms a variety of polynuclear species, containing for example $Tc_2O_2^{6+}$ cores. In contrast "carrier-free" ^{99m}Tc rarely forms polynuclear species since its molar concentration is so low. It is important to recognise that the chemistry of technetium may differ between "carrier-free" and "carrier-added" levels.

1.6.2 ^{99m}Tc radiopharmaceuticals

A wide variety of tissues can be imaged using ^{99m}Tc radiopharmaceuticals which localise passively within these regions by virtue of their size, lipophilicity, charge etc., rather than by antibody targeting[16,18]. An enormous number of chelators for ^{99m}Tc have been synthesised in an attempt to achieve the required selectivity for the target tissue, a few of which are described below.

Brain[47,48]

In order to penetrate the highly lipophilic blood-brain barrier, technetium complexes must be neutral with small hydrophobic ligands. Three ^{99m}Tc complexes designed for SPECT brain imaging (^{99m}Tc-BAT, ^{99m}Tc-GTS and ^{99m}Tc-PnAO) are given in Figure 1.19.

Heart

The first heart imaging agents[49] containing Tc(I) had the structure $Tc[D_2X_2]^+$ where D = ditertiary arsine or phosphine and X = Cl^-, Br^-, or I^-. However they showed disappointing uptake in human myocardium and have been superceded by second generation isonitrile-Tc(I) complexes $[^{99m}Tc(CNR)_6]^+$, developed by Davison *et al.* (Figure 1.20).

Kidney

^{99m}Tc-DTPA has been widely used for glomerular filtration imaging. Davison *et al.*[50] complexed ^{99m}Tc with N,N-bis-(mercaptoacetamido)-ethylene diamine (DADS) to produce an imaging agent for renal tubular secretion. However another complex ^{99m}Tc-MAG_3 (MAG_3 = mercaptoacetyl-glycylglycylglycine) was found[51] to be more effective than ^{99m}Tc-DADS (Figure 1.21).

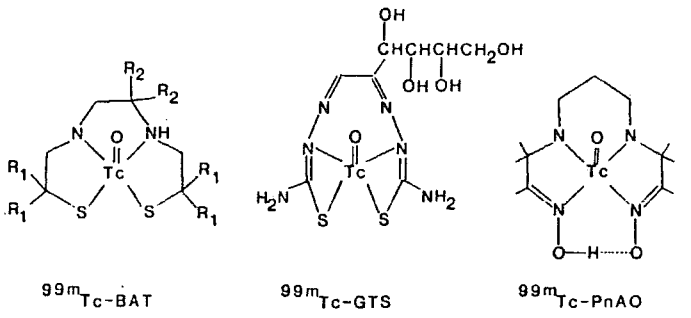

Figure 1.19 *^{99m}Tc complexes designed for SPECT brain imaging; BAT=bis-aminoethane thiol; GTS=glucobis-thiosemicarbazone; PnAO=propyleneamine oxime.*

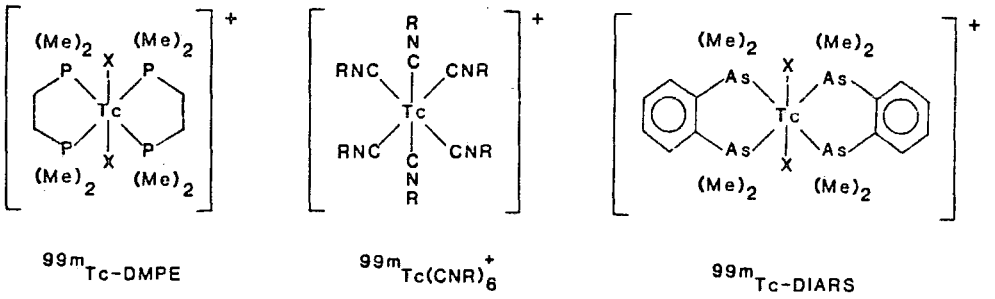

Figure 1.20 *Structures of ^{99m}Tc heart-imaging agents.*

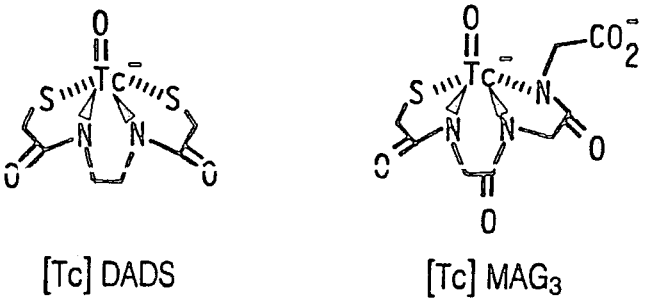

Figure 1.21 *Structures of ^{99m}Tc kidney-imaging agents.*

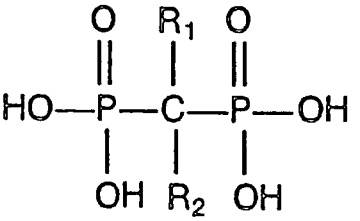

Figure 1.22 *Structure of diphosphonate ligands for ^{99m}Tc bone imaging; MDP: R_1=R_2=H; HEDP: R_1=OH, R_2=CH_3*

Bone

Bone-scanning using ^{99m}Tc-phosphate complexes is the most common application of ^{99m}Tc in diagnostic medicine. The use of diphosphonate ligands provides particularly high resolution images; methylene diphosphonate (MDP) and hydroxyethylidene diphosphonate (HEDP) being especially popular (Figure 1.22).

1.6.3 Antibody-bound Technetium Chelators

Some workers have attempted to adapt some of the acyclic ligands developed for conventional ^{99m}Tc-radiopharmaceuticals for use as antibody-bound chelators, particularly DTPA[52]. Although ^{99m}Tc-DTPA gives better results than "direct-labelling" of the antibody (section 1.4.1), there are still the problems of excessive re-oxidation to TcO_4^- and transchelation to serum components.

Other workers[53] have employed acyclic ligands containing nitrogen and sulphur donors to produce more stable ^{99m}Tc chelates than ^{99m}Tc-DTPA. Another approach is to replace DTPA with a tetraamine macrocycle, the advantages of which have been discussed *vide ante* in connection with copper binding.

1.6.4 ^{99m}Tc Complexes of Macrocyclic Ligands

In 1980, Volkert *et al.*[54] reported that the macrocyclic tetraamine, cyclam, formed a kinetically inert chelate with ^{99m}Tc. Complexes could be formed from pertechnetate in higher than 95% yield at pH 11 in 10^{-3} M cyclam using 5 x 10^{-6} M stannous chloride as the reducing agent. The yield of complex was decreased at more acidic pH, and with decreasing concentrations of ligand and reducing agent. The ^{99m}Tc-cyclam complex

was resistant to oxidation (air, O_2, H_2O_2) and exposure to 0.05 M NaOH, although there was slight decomposition in 0.05 M HCl. In a later paper[55], the overall charge of ^{99m}Tc-cyclam was reported to be +1, with technetium in oxidation state +5, consistent with the structural formula $[TcO_2(cyclam)]^+$. Since the longer-lived isotope ^{99}Tc formed identical complexes with cyclam in comparable yield to ^{99m}Tc, sufficient complex was isolated to grow an X-ray quality crystal[56].

The ^{99m}Tc-cyclam complex was isolated as the perchlorate salt, *trans*-$[Tc(cyclam)O_2].ClO_4.H_2O$. There are no bonding interactions between cation and anion or water molecules. The cation consists of a *trans*-$OTcO^+$ core with the ligand in the favoured *trans*-III conformation. The structure has a centre of symmetry at the metal, which sits in the N_4 plane with the axial oxo donors completing a near-perfect octahedron (Figure 1.23). The Tc-O distance (1.751 Å) is greater than that found in a mono-oxo complex and the Tc-N distance (average 2.125 Å) is the longest observed for any cyclam complex (cf. Cu(II) 2.02 Å). It is suggested that the donor distance might impose a small amount of steric strain upon the conformation of the ligand.

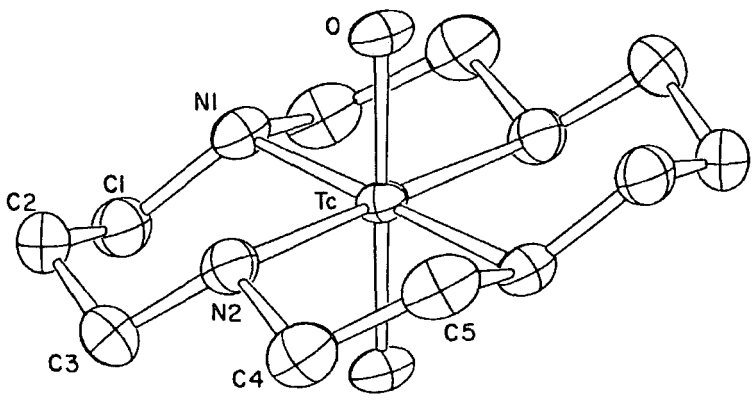

Figure 1.23 *ORTEP drawing of the cation trans-$[Tc(cyclam)O_2]^+$. Probability ellipsoids are shown at the 50% level. Hydrogen atoms are not included.*

In conclusion, cyclam binds ^{99m}Tc rapidly at pH 11, forming a kinetically inert complex suitable for *in vivo* applications. One problem which will be addressed in Chapters 2 and 3 is the slow rate of complexation of ^{99m}Tc by cyclam at neutral pH (preferred by antibodies). At low pH, electrostatic repulsion between the protonated ligand and cationic Tc(V) species is an important factor determining rate. One possible solution is to employ an axial anionic donor in an attempt to reduce electrostatic repulsion and enhance the rate of uptake. In particular, the phenol-pendent cyclam (2) will be investigated as a potential Tc-binder at lower pH.

1.7 CONJUGATION OF CHELATING AGENTS TO ANTIBODIES

1.7.1 Use of Acylating Agents

Practically all reported methods of conjugation employ a reaction between an electrophilic group on the chelating agent and a nucleophilic group on the antibody. The most useful nucleophilic residues on the antibody are amines: the terminal amino groups, the isoindoles of histidine but more particularly the ϵ-amino group of lysine. The most commonly-used chelating ligand, DTPA, is easily converted to more reactive acylating agents *e.g* anhydrides, carbodiimides or activated esters.

Anhydrides

There are two anhydride methods for conjugating DTPA to antibodies. Originally, Krejcarek and Tucker[57] used a mixed anhydride (MA-DTPA) prepared from DTPA and isobutylchloroformate. However this anhydride

was found to be so unstable that a second route based on a cyclic dianhydride (CA-DTPA), prepared from DTPA and acetic anhydride , was devised[58,59]. It was presumed that the site of attachment of DTPA was the lysine ϵ-amino group (Figure 1.24). Although the CA-DTPA is more stable than MA-DTPA and less easily hydrolysed in the aqueous reaction medium, there is a greater probability of loss of antibody immuno-reactivity by internal or external cross-linking since CA-DTPA has two reactive groups.

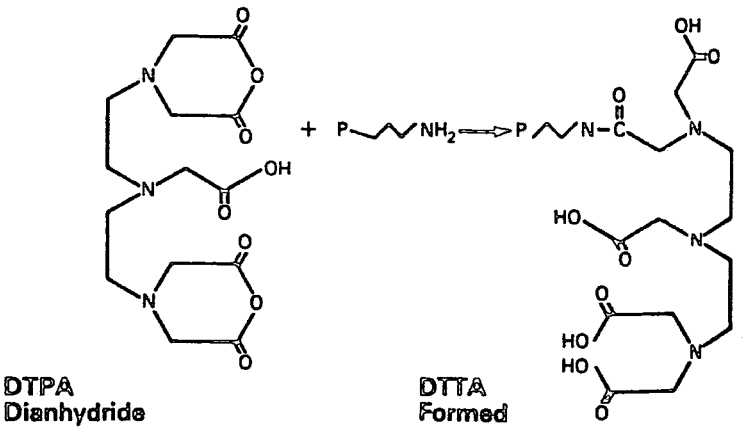

Figure 1.24 *Conjugation of DTPA Dianhydride (CA-DTPA) to lysine ϵ-NH_2 groups of an antibody.*

Carbodiimide method

A water soluble carbodiimide, 1-ethyl-3(3-dimethyl-aminopropyl) carbo-diimide (EDC) has been used to conjugate the carboxy groups of DTPA to amino groups on Mab's[60]. The reaction mechanism involves an intermediate O-acylisourea species. This method apparently produces an even higher level of Mab deactivation than CA-DTPA.

N-hydroxysuccinimide ester method

Najafi *et al.*[61] synthesised an N-hydroxysuccinimide pentaester of DTPA from CA-DTPA and N-hydroxysuccinimide which was more stable than CA-DTPA

and therefore gave a higher DTPA conjugation yield. However the presence of 5 active ester groups causes considerable cross-linking and deactivation of Mab's.

The main advantage of using acylating agents for conjugating chelates is the simplicity of the protocol since the chelate itself is the starting material. However in the case of DTPA, the main disadvantage is the loss of a potential binding site. The loss of denticity makes DTTA, a less efficient binder of ^{111}In and other radionuclides than DTPA itself, such that the radiolabel is lost more rapidly *in vivo*[62].

1.7.2 Use of Aromatic Amine-Derived Reagents

Historically, the first chelate-protein conjugates to be stable enough for *in vivo* use were derived by reaction of azophenyl-EDTA with Mab amines[63]. However the complexity of the synthesis of chelate side-chains, such as azophenyl, hindered the further development of this approach until Meares *et al.*[64] developed a shorter procedure using amino acids and aromatic amine intermediates (Figure 1.25).

Unfortunately azophenyl-EDTA, derived by diazotisation of aminophenyl-EDTA, proved to be non-specific for lysine residues, reacting instead with tyrosine (OH) and histidine (NH)[15].

The use of thiocyanate groups (R-N=C=S) for coupling fluorescent probes, spin labels etc. to proteins is well known. They are mild reagents obtained by reacting aromatic amines with thiophosgene and are specific for amino groups. Both Meares *et al.*[65] and Gansow *et al.*[62] have used thiocyanate groups ("CITC") extensively and effectively for conjugating EDTA and DTPA to antibodies (Figure 1.26).

Another class of coupling agents derived from aromatic amines, by

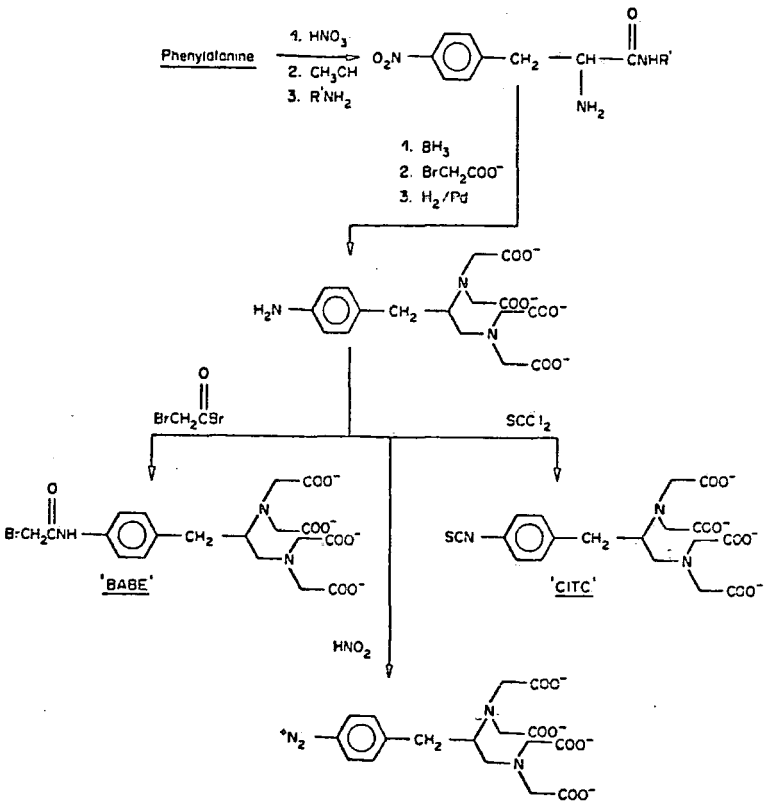

Figure 1.25 *Synthesis of functionalised EDTA derivatives (azophenyl-, "BABE" and "CITC" from amino acids.*

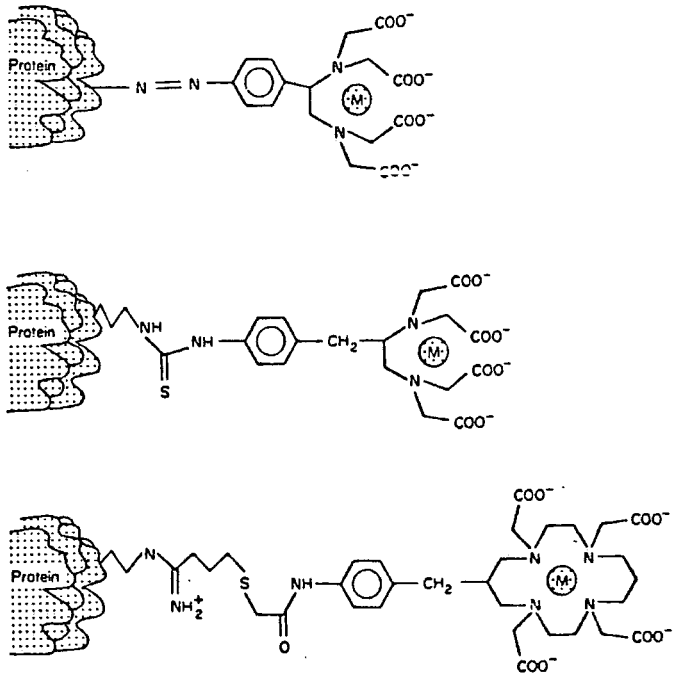

Figure 1.26 *Protein conjugates of azo-phenyl EDTA (top), "CITC" (middle) and α-bromoacetamido-TETA (bottom), through a C_4S spacer group to lys.ε-NH_2.*

reaction with α-bromoacetyl bromide, are the α-bromoacetamides ("BABE"). These reagents were used by Meares *et al.* to couple EDTA[65] and TETA[29] to Mab amines for use as ^{111}In and ^{67}Cu binders respectively. Although this method apparently worked well for the ^{111}In binder, the ^{67}Cu binder was found to be effective only if the lysine side-chain was first extended with "Traut's reagent" to include a free thiol group (section 2.4.2). The α-bromoacetamide was then conjugated *via* a thioether bridge (Figure 1.26). The effectiveness of this coupling method, as determined by our own experiments, will be explored further in Chapter 2.

The difficulty of the synthesis of functionalised chelates containing aromatic amine-derived coupling agents makes this strategy more complex than the anhydride method. However since the metal-binding site is unaffected by conjugation, the stability of the resulting radionuclide bond *in vivo* is greatly enhanced. An additional advantage is the greater selectivity of coupling reactions employing thiocyanates and α-bromoacetamides; there being less deactivation of the antibody.

1.7.3 Use of Maleimide-Based Reagents

The use of maleimides as coupling reagents for proteins was first described by Kitagawa *et al.*[66] in 1976. The water soluble maleimide ester used in this initial work, N-maleimidobenzoyl-N-hydroxysuccinimide ester (MBS) is now commercially available as a cross-linking agent. MBS was used to link the thiol groups of the enzyme β-D-galactosidase to the lysine residues of insulin, by reaction with the maleimide and N-HS ester respectively. Several other maleimide cross-linkers have since been synthesised with the intention of improving the stability of the maleimide ring at higher pH (section 2.4.3). One of these, succinimidyl-

4-(N-maleimidomethyl)-cyclohexane-1-carboxylate (3) is reported[67] to be more stable than MBS.

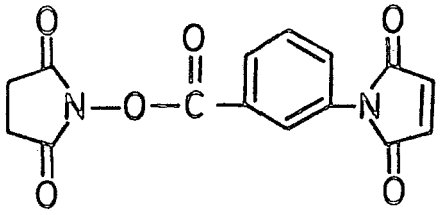

(MBS)

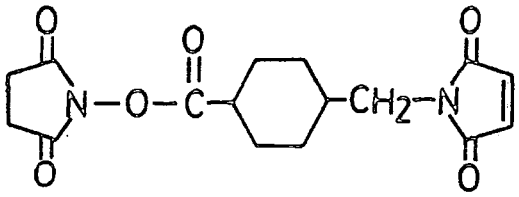

(3)

In addition to our own work involving maleimides (section 4.2), Volkert *et al.*[68] reported a coupling method using MBS to conjugate a di-N-alkylated cyclam, with a thiol-containing side chain, to Mab lysine residues. A potential problem arises from the incorporation of highly reactive maleimide residues into the antibody itself, rendering the modified protein highly sensitive to changes in pH. It seems to us preferable to use maleimides on the chelate side chain and thiol groups on the Mab when using cross-linkers such as MBS and (3).

1.7.4 Antigen-Site Binding

A potentially very exciting method of conjugating chelates to Mab's is to raise an antibody which recognises the chelate as an antigen, binding it reversibly in the variable region. Meares *et al.*[69] developed an antibody which recognises ^{111}In-benzyl-EDTA. Since, in this case, the antigen binding site is occupied and cannot recognise tumour associated antigens, the antibody must accumulate passively inside the tumour. A

solution to this problem is to develop a bifunctional antibody in which one Fab arm recognises the chelate, or preferably a cluster of chelates, and the other recognises the tumour associated antigen. This approach is far more complex than those described *vide ante*, and may take many years to develop to fruition, but in the long term, it could well prove to be a relatively simple method for conjugating large concentrations of chelates to Mab's without impairing immunoreactivity.

1.8 THE SCOPE OF THIS WORK

The majority of this thesis is concerned with the development of novel functionalised macrocyclic ligands for binding isotopes of technetium and copper to antibodies, in a manner suitable for radioimmunoimaging and radioimmunotherapy. The most appropriate ligands for this purpose are derivatives of cyclam and $13N_4$.

Chapter 2 contains a discussion of the factors influencing the choice of a suitable side-chain functionality for the macrocycles, cyclam and $13N_4$, their preferred methods of synthesis and the development of a novel conjugation procedure for attaching functionalised macrocycles to Mab's.

Chapters 3 and 4 contain the results of ^{99m}Tc and ^{64}Cu radiolabelling experiments using the antibody-macrocycle conjugates described in Chapter 2. In Chapter 5, the kinetics of association of copper(II) with cyclam, $13N_4$ and derivatives thereof, are discussed.

Chapter 6 includes a review of current progress in the field of radioimmunotherapy. Also discussed: the development of functionalised macrocycles for binding ^{90}Y and radiolabelling experiments involving ^{67}Cu; both isotopes being favoured for therapeutic applications.

Chapter 7 contains experimental procedures for the synthesis of tetraamine macrocycles, macrocycle-linker conjugates and macrocycle-antibody conjugates. Non-synthetic experimental is reported at the end of the chapter in which it is discussed.

1.9 REFERENCES

1. E.J. Wawrzynczak and P.E. Thorpe, "*Introduction to the Cellular and Molecular Biology of Cancer*", Chapter 18, 379 (1986)
2. F.R. Seiler, P. Gronski, R. Kurrle, G. Lüben, H.-P. Harthus, W. Ax, K. Bosslet and H.-G. Schwick, *Angew.Chem.Int.Ed.Engl.*, 24, 139 (1985)
3. G. Köhler, *Angew.Chem.Int.Ed.Engl.*, 24, 827 (1985)
4. C. Milstein, *Angew.Chem.Int.Ed.Engl.*, 24, 816 (1985)
5. N.K. Jerne, *Angew.Chem.Int.Ed.Engl.*, 24, 810 (1985)
6. G. Köhler and C. Milstein, *Nature*, 256, 495 (1975)
7. J.L. Marx, *Science*, 229, 455 (1985)
8. W. Wolf and J. Shani, *Nucl.Med.Biol.Int.J.Radiat.Appl.Instrum. Part B*, 13(4), 319 (1986)
9. R.W. Wessels and R.D. Rogus, *Med Phys*, 11(5), 638 (1984)
10. R.P. Spencer, "*Therapy in Nuclear Medicine*", 3 (1978)
11. J.L. Humm, *J.Nucl.Med.*, 27(9), 1490 (1986)
12. R.D. Neirinckx, *Chem.Br.*, 335, April Edit., (1986)
13. M. Golman, *Physica.Scripta*, T19, 476 (1987)
14. A. Del Guerra, *Physica.Scripta*, T19, 481 (1987)
15. W.C. Enkelman and C.H. Paik, *Nucl.Med.Biol.Int.J.Radiat.Appl. Instrum. Part B*, 13(4), 335 (1986)
16. R.L. Rawls, *C&EN*, 26 (Sept 1986)
17. D.J. Hnatowich, *Nucl.Med.Biol.Int.J.Radiat.Appl.Instrum. Part B*, 13(4), 353 (1986)
18. T.C. Pinkerton, C.P. Desilets, D.J. Hoch, M.V. Mikelsons and G.M. Wilson, *J.Chem.Ed.*, 62(11), 965 (1985)

19. B.A. Khaw, W. Strauss, A. Carvalho, E. Locke, H.K. Gold and E. Haber, *J.Nucl.Med.*, 23(11), 1011 (1982)

20. C.H. Paik, W.C. Eckelman and R.C. Reba, *Nucl.Med.Biol.Int.J.Radiat. Appl.Instrum. Part B*, 13(4), 359 (1986)

21. C.F. Meares, *Nucl.Med.Biol.Int.J.Radiat.Appl.Instrum. Part B*, 13(4), 311 (1986)

22. J.C.A. Boeyens and S.M. Dobson, "*Stereochemical and Stereophysical Behaviour of Macrocycles*", (Elsevier), 1 (1987)

23. L.F. Lindsay, *Chem.Soc.Rev.*, 4, 421 (1975)

24. D.K. Cabbiness and D.G. Margerum, *J.Am.Chem.Soc.*, 91, 6540 (1969)

25. F.P. Hinz and D.G. Margerum, *J.Am.Chem.Soc.*, 96, 4993 (1974); *Inorg.Chem.*, 13, 2941 (1974)

26. R.M. Izatt, J.S. Bradshaw, S.A. Nielson, J.D. Lamb and J.J. Christensen, *Chem.Rev.*, 85, 271 (1985)

27. R.D. Hancock and M.P. Ngwenya, *J.Chem.Soc.Dalton Trans.*, 2911 (1987)

28. F.A. Cotton and G. Wilkinson, "*Advanced Inorganic Chemistry*", (4th Edition), 811 (1980)

29. M.K. Moi, C.F. Meares, M.J. McCall, W.C. Cole and S.J. DeNardo, *Anal.Biochem.*, 148, 249 (1985)

30. S.V. Deshpanda, S.J. DeNardo, C.F. Meares, M.J. McCall, G.P. Adams, M.K. Moi and G.L. DeNardo, *J.Nucl.Med.*, 29, 217 (1988)

31. W.C. Cole, S.J. DeNardo, C.F. Meares, M.J. McCall, G.L. DeNardo, A.L. Epstein, H.A. O'Brien and M.K. Moi. *Nucl.Med.Biol. Int.J.Radiat.Appl.Instrum. Part B*, 13(4), 363 (1986)

32. M. Kodama and E. Kimura, *J.Chem.Soc.Dalton Trans.*, 1473 (1977)

33. L. Fabrizzi, P. Paoletti and R.M. Clay, *Inorg.Chem.*, 17, 1042 (1978)

34. L. Fabrizzi, M. Micheloni and P. Paoletti, *J.Chem.Soc.Dalton Trans.*, 1581 (1979)

35. L.-H. Chen and C.-S. Chung, *Inorg.Chem.*, 27, 1880 (1988)

36. P.A. Tasker and L. Siklar, *J.Cryst.Mol.Struct.*, 5, 329 (1975)

37. M.K. Moi, M. Yanuck, S.V. Deshpanda, H. Hope, S.J. DeNardo and C.F. Meares, *Inorg.Chem.*, 26, 3458 (1987)

38. D. Parker, I. Helps, J. Chapman and G. Ferguson, accepted for publication in *J.Chem.Soc., Chem.Commun.* (1988)

39. M. Kodama and E. Kimura, *J.Chem.Soc.Dalton Trans.*, 116 (1976)

40. M. Kodama and E. Kimura, *J.Chem.Soc.Dalton Trans.*, 1720 (1976)

41. E. Kimura, T. Koike and M. Takahashi, *J.Chem.Soc., Chem.Commun.* 385 (1985)

42. Y. Iitaka, T. Koike and E. Kimura, *Inorg.Chem.*, 25, 404 (1986)

43. E. Kimura, K. Uenishi, T. Koike and Y. Iitaka, *Chem.Letts.*, 1137 (1986)

44. E. Kimura, M. Yamaoka, M. Morioka and T. Koike, *Inorg.Chem.*, 25, 3883 (1986)

45. E. Kimura, T. Koike, K. Uenishi, M. Hediger, M. Kuramoto, S. Joko, Y. Arai, M. Kodama and Y. Iitaka, *Inorg.Chem.*, 26, 2975 (1987)

46. A.G. Jones and A. Davison, *Int.J.Appl.Radiat.Isot.*, 33, 867 (1982); 33, 875 (1982)

47. D.P. Nowotnik *et al.*, W.A. Volkert *et al.*, *Nucl.Med.Comm.*, 6, 499 (1985)

48. S. Jurisson, E.O Schlemper, D.E. Troutner, L.R. Canning, D.P. Nowotnik and R.D. Neirinckx, *Inorg.Chem.*, 25, 543 (1986)

49. J.-L. Vanderhayden, M.J. Heeg and E. Deutsch, *Inorg.Chem.*, 24, 1666 (1985)

50. D. Brenner, A. Davison, J. Lister-James and A.G. Jones, *Inorg.Chem.*, 23, 3793 (1984)

51. A.R. Fritzberg, S. Kasina, D. Eshima and D.L. Johnson, *J.Nucl. Med.*, 27, 111 (1986)

52. R.L. Childs and D.J. Hnatowich, *J.Nucl.Med.*, 26, 293 (1985)

53. Y. Arano, A. Yokoyama, Y. Mageta, K. Horiuchi, H. Saji and K. Torizuka, *Appl.Radiat.Isot. Int.J.Radiat.Appl.Instrum. Part A*, 37(7), 587 (1986)

54. D.E. Troutner, J. Simon, A.R. Ketring, W. Volkert and R.A. Holmes, *J.Nucl.Med.*, 21, 443 (1980)

55. J. Simon, D.E. Troutner, W.A. Volkert and R.A. Holmes, *Radiochem. Radioanal. Letts.*, 47(1), 111 (1981)

56. S.A. Zuckman, G.M. Freeman, D.E. Troutner, W.A. Volkert, R.A. Holmes, D.G. Van Derveer and E.K. Barefield, *Inorg.Chem.*, 20, 2386 (1981)

57. G.E. Krejcarek and K.I. Tucker, *Biochem.Biophys.Res.Commun.*, 77, 581 (1977)

58. D.J. Hnatowich, W.W. Layne and R.L. Childs, *Int.J.Appl.Radiat. Isot.*, 33, 327 (1982)

59. C.H. Paik *et al.*, *J.Nucl.Med.*, 24, 1158 (1983)

60. C.H. Paik *et al.*, *Hybridoma*, 2, 248 (1983)

61. A. Najafi, R.L. Childs and D.J. Hantowich, *Int.J.Appl.Radiat. Isot.*, 35, 554 (1984)

62. M.W. Brechbiel, O.A. Gansow, R.W. Atcher, J. Schlom, J. Esteban, D.E. Simpson and D. Colcher, *Inorg.Chem.*, 25, 2772 (1986)

63. M.W. Sundberg, C.F. Meares, D.A. Goodwin and C.I. Diamanti, *J.Med. Chem.*, 17, 1304 (1974)

64. S.M. Yeh, D.G. Sherman and C.F. Meares, *Anal.Biochem.*, 100, 152 (1979)

65. C.F. Meares, M.J. McCall, D.T. Rearden, D.A. Goodwin, C.I. Diananti and M. McTigue, *Anal.Biochem.*, 142, 68 (1984)

66. T. Kitagawa and T. Aikawa, *J.Biochem.*, 79, 233 (1976)

67. B. Yoshitake, Y. Yamada, E. Ishikawa and R. Masseyeff, *Int.J. Biochem.*, 101, 395 (1979)

68. J.Franz, G.M. Freeman, E.K. Barefield, W.A. Volkert, G.J. Ehrhardt and R.A. Holmes, *Int.J.Radiat.Appl.Instrum. Part B*, 14(5), 479 (1987)

69. D.A. Goodwin, C.F. Meares *et al.*, *Int.J.Radiat.Appl.Instrum. Part B*, 13(4), 383 (1986)

CHAPTER TWO

THE SYNTHESIS OF MACROCYCLE-ANTIBODY CONJUGATES

PART A: SYNTHESIS OF FUNCTIONALISED MACROCYCLES

2.1 INTRODUCTION

2.1.1 The Need for Functionality

The preferred type of macrocycle for binding isotopes of technetium and copper, a [13] or [14]-membered tetraamine, must be functionalised with a side chain through which attachment to the antibody will take place. There are many factors which must be considered when deciding upon a particular type of side chain and many criteria must be fulfilled.

Firstly, the side chain should render the ligand both soluble and stable in aqueous media over a wide pH range and it should be unreactive towards the secondary amines of the ring. Secondly the steric constraints imposed upon the ring should be minimised such that the binding characteristics of the functionalised and parent cycles are of the same order. Thirdly the synthesis of the functionalised cycle should be as straightforward as possible. Given the complexity of many macrocyclisation reaction mixtures, an ultraviolet active side chain, typically an aromatic group, would help in the monitoring and purification of the reaction products. Finally the functionality of the pendent group must allow the cycle to be linked selectively to the antibody without damaging the integrity of the tetraamine system of the ring.

2.1.2 The Use of Aromatic Amine Side Chains

As discussed in section (1.7.2), Meares *et al.* reported in 1984[1] a

method of conjugating chelates, such as EDTA, to antibodies using an α-bromoacetamide side chain. In view of the apparent success of this method, it was decided to pursue in the first instance, the synthesis of macrocyclic tetraamines functionalised with aromatic amine side chains which could later be converted to α-bromoacetamides using α-bromoacetyl bromide.

2.2 PHENOL-PENDENT TETRAAMINE MACROCYCLES

2.2.1 The Use of Phenolic Side Chains

As suggested in section (1.6.4), phenol-pendent macrocycles are potentially useful for binding technetium-99m. In particular, the effect of the phenol group on the kinetics of association and dissociation of the radiolabel is of interest.

The decreasing rate of uptake of technetium(V) by cyclam at lower pH is almost certainly due to electrostatic repulsion between the cationic oxo-technetium species, TcO^{3+} or TcO_2^+, and the increasingly protonated ligand. Antibody-bound macrocycles should ideally be labelled at physiological pH (7.0-7.8) to avoid damage to the protein but the rate of complexation at this pH and at the "no carrier added"† level is slow. Negatively charged pendent groups could serve to reduce the charge density on the macrocycle thereby enhancing the kinetics of complexation.

The pK_a value for the phenol in Kimura's macrocycle (2) is

†"No carrier added" material contains a single radioactive isotope only; since no "cold" isotopes are present, the molar concentration of metal in radiolabelling experiments is necessarily low.

significantly lower (8.8) than for the phenol itself (10)[2]. At pH 9 the phenol will be substantially deprotonated reducing the net positive charge on the macrocycle by one unit (Figure 2.1).

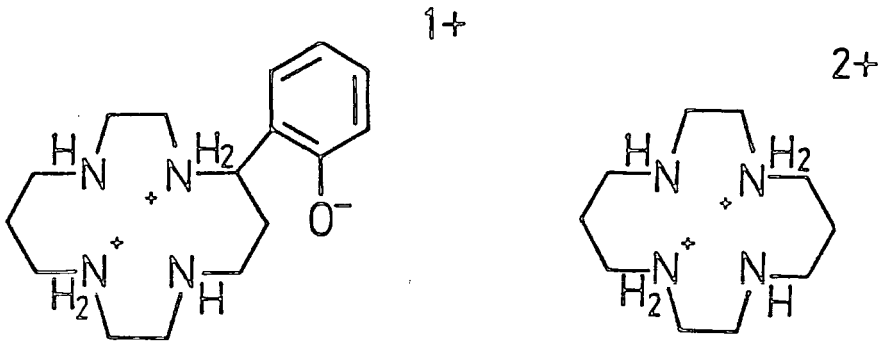

Figure 2.1 *Dominant species at pH9 for cyclam and (2)*

Alternatively, or in addition to electrostatic effects, the phenol might serve to orientate the incoming technetium cation for rapid incorporation into the ring. There is even the possibility that the phenolic group might act as an axial donor for technetium, as was observed in the Ni^{2+} and Fe^{2+} complexes of (2)[2,3], replacing one of the oxo donors and conferring extra thermodynamic or kinetic stability on the complex. These factors will be considered further in Chapter 3.

2.2.2 Synthesis of p-Aminophenol-pendent Cyclams

The attachment of a pendent group to cyclam containing both phenolic moieties is possible by way of Kimura's macrocyclisation of the linear tetraamine, 1,4,8,11-tetraazaundecane with 6-nitrocoumarin[2]. The

proposed scheme is given in full in Figure 2.2. The macrocyclic amide (4) may be reduced with diborane to give the tetraamine (5). To facilitate selective acylation by α-bromoacetylbromide at the exocyclic aromatic amine, it would be necessary to protect, with methyl groups, the more nucleophilic secondary amines of the ring. In turn this would require prior protection of the phenol as a suitable ether. Finally the nitro group would be hydrogenated to give the aminophenol-pendent cyclam (6) and converted to the α-bromoacetamide (7).

It was found that the presence of an electron-withdrawing nitro group increased the reactivity of the coumarin ring, reducing the reaction time from 2 weeks to 5 days. The desired macrocyclic amide (4) was then separated by painstaking column chromatography on gravity silica. Providing the elution rate is not too fast (overall elution time 18 hours), the amide may be obtained in reasonable yield (21%) and of sufficient purity not to require recrystallisation. The yields of macrocyclic amides of this type were improved by using only anhydrous solvents for the cyclisation step.

It became apparent that a solution of diborane-dimethyl sulphide complex in THF reduced both amide and nitro groups of (4), if the reaction time was 6 days. This was primarily established from the ^{13}C NMR spectrum; the signal due to the aromatic carbon bearing a nitro group (*ca.* 140 ppm) was replaced by a signal attributable to an aromatic amine (118-127 ppm region). Aromatic nitro groups are not usually attacked by diborane[4] but the presence of an electron-donating phenol in the para position apparently activates this system towards reduction. Selective reduction of the amide group to give cycle (5) was subsequently achieved with a solution of diborane in THF by limiting the reaction time to 24 hours.

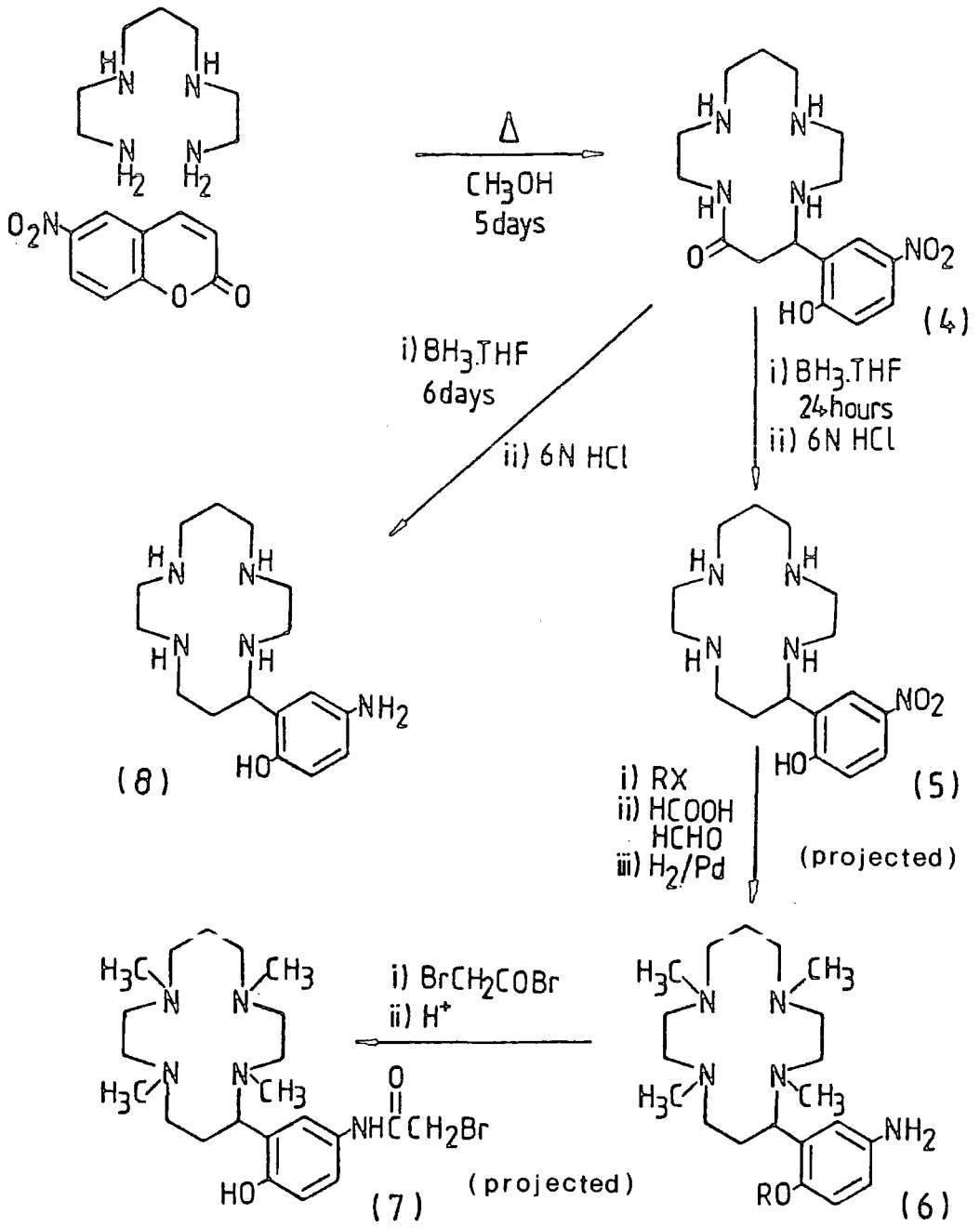

Figure 2.2 The Synthesis of para-Aminophenol-pendent Cyclams

R = Tr
X = Cl

2.2.3 Redox reactions of p-Aminophenols

It was apparent from the behaviour of the fully reduced cycle (8) in aqueous solution that the p-aminophenol moiety was unstable, especially at alkaline pH. A solution of the free amine in water was found to darken on standing and in time an intractable dark brown solid precipitated. This instability was attributed to the propensity of p-aminophenols to oxidise in basic solution to p-iminoquinones[5]:

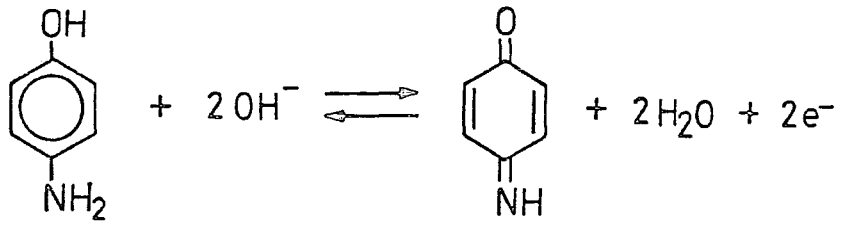

The darkening of the solution may be explained by the formation of a charge-transfer complex involving the p-aminophenol as an electron donor and the p-iminoquinone as an electron acceptor. The redox reactions of p-aminophenols clearly make them less than ideal for conjugating macrocycles to antibodies and alternative side chains were required.

Two further problems came to light regarding the use of aromatic amines as pendent groups for tetraamine macrocycles. The necessity for peralkylation of the secondary amines and the lack of selectivity in the reaction of bromoacetyl bromide with aromatic amines. These subjects will be considered in sections (2.2.4) and (2.2.5) respectively.

2.2.4 Binding Characteristics of Per-N-Alkylated Cyclams

The methyl groups of N-tetramethylcyclam (9) impose steric constraints upon the structure of its metal complexes. The metal is displaced from

the plane of the four nitrogen donors. Barefield *et al.*[6] used space-filling models to show that a metal in the coordination plane forces the methyl groups into positions close to possible axial donors. This finding is supported by our own molecular modelling studies on a dioxo-technetium (V) complex of (10) which shows steric crowding about the axial oxo groups due to the proximity of the methyl groups. Relief of steric strain would require the metal to sit outside the coordination plane, almost certainly weakening the Tc-N bonds and reducing the stability of the complex. In his thesis[7], J. Simon reported that tetra-methylcyclam was a much less efficient technetium binder than cyclam itself which he attributed to steric hindrance by the methyl groups bonded to the nitrogens.

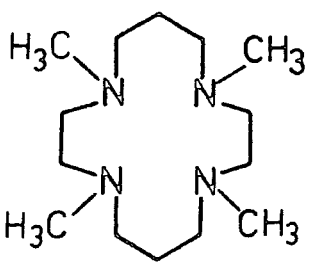

(9)

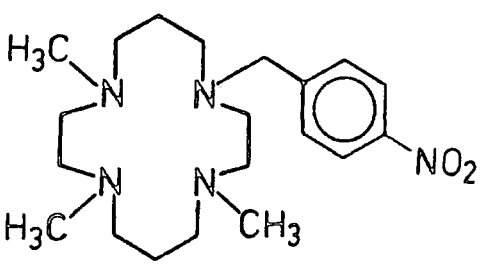

(10)

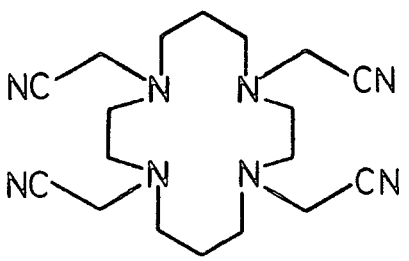

(11)

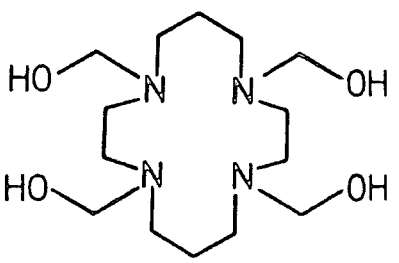

(12)

The ruthenium (VI) dioxo complex of N-tetramethylcyclam $[Ru^{VI}O_2(tmc)]^+$, which is isoelectronic with the technetium (V) complex $[Tc^{V}O_2(tmc)]^+$, is rather unstable both in solution and in the solid state[8]. This instability has been associated with steric interactions between the N-Me groups and the oxygen lone pairs.

The presence of alkyl groups on all four nitrogens of cyclam is equally undesirable for copper binding. Barefield and Wagner[9] showed that the copper complexes of N-tetramethylcyclam (9) are formed more rapidly than those of cyclam, but dissociation of the metal is also more facile. Subsequent studies by Hay *et al.*[10,11] using the ligands N-tetrakis-(2-cyanoethyl)-cyclam (11) and N-tetrakis-(2-hydroxyethyl)-cyclam (12) indicate that their copper complexes also dissociate readily in acid solution.

2.2.5 Competitive Alkylation and Acylation of Aromatic Amines

Some model reactions using cyclam and aromatic amines showed it was not possible to selectively acylate the amine with α-bromoacetyl bromide. A mixture of N-alkylated and N-acylated products was suggested by the appearance of two methylenic resonances in the 3.5-4.5 ppm region of the ^1H NMR spectrum (Figure 2.3). This observation was subsequently supported by the work of Gansow *et al.*[12] who reported that N-alkylation of the aromatic amine of aminobenzyl-EDTA, by α-bromoacetyl bromide, occurs to a greater extent than N-acylation (70% alkylation/30% acylation). The lack of selectivity of the amine towards acylation would cause intermolecular reaction of a pair of macrocycles to produce aggregates such as (13) destroying their potential to be linked to antibodies.

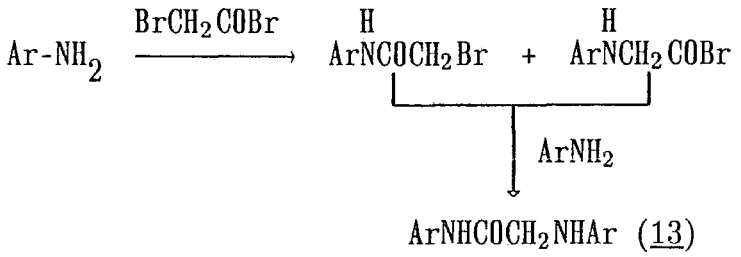

Figure 2.3 *Competitive Alkylation and Acylation of aromatic amines by α-bromoacetyl bromide*

2.2.6 Synthesis of p-Aminomethylphenol-pendent Macrocycles

By using a primary aliphatic amine group in place of the aromatic amine, it was hoped to overcome the problems outlined above. In addition to resisting oxidation in aqueous base, the p-aminomethyl phenol derivatives should prove easier to acylate selectively at the exocyclic amine by virtue of its enhanced nucleophilicity relative to the aromatic amine of cycle (8). This is illustrated by the difference in basicity between the two types: $pK_a \approx 10$ for primary aliphatic amines; $pK_a \approx 5$ for primary aromatic amines[13]. This type of cycle can be synthesised using an analogous two step route from 6-cyanocoumarin and a linear tetraamine. However unlike 6-nitrocoumarin, 6-cyanocoumarin is not commercially available and must be made by reducing the former to 6-aminocoumarin followed by diazotisation in the presence of copper (I) cyanide (Figure 2.4). In the first step, the yield of 6-aminocoumarin was optimised by modifying the procedure of Micklethwaite *et al.*[14] such that the product is extracted into chloroform rather than crystallised directly from hot sodium bicarbonate solution. Unreacted 6-nitrocoumarin was removed by dissolving the mixture in aqueous acid and extracting exhaustively into chloroform.

The standard diazotisation procedure outlined in Vogel's handbook[15] was followed for the conversion of 6-aminocoumarin to 6-cyanocoumarin.

However to ensure complete dissolution of 6-aminocoumarin hydrochloride, 3N, rather than 6N, hydrochloric acid was used. The 6-cyanocoumarin recovered from the chloroform layer was found to be sufficiently pure to be used in the next step. A small amount was recrystallised from hot water for analytical purposes.

The duration of the cyclisations of the linear tetraamines (14) and (15) with 6-cyanocoumarin were of the same order as those observed for 6-nitrocoumarin, in accord with the electron withdrawing effect of the nitrile group. The yield of the [13]-membered macrocyclic amide (16) was consistently lower than that of the [14]-membered analogue (17), possibly due to increased conformational strain arising from the replacement of a propylenic unit by an ethylenic unit.

The macrocyclic amides (16) and (17) were isolated in a similar manner to (4) through column chromatography and reduced to pentaamines (18) and (19) using diborane-THF. Excess borane was consumed with methanol to give easily removed trimethylborate. The resulting pentaaminoborane was hydrolysed to the pentahydrochloride salt with 6N HCl. It was possible to isolate cycles (18) and (19) as clear oils simply by dissolving the crude hydrochloride salt in aqueous base and extracting into chloroform. The poorer yield of the [13]-membered cycle (18) may result from either a less clean borane reduction or a less favourable partition of the cycle between chloroform and aqueous base. Attempts to recrystallise cycles (18) and (19) proved unsuccessful due to their high solubility but it was found, by cation exchange HPLC, that the material in each case was sufficiently pure ($\geq$ 95%) to proceed with conjugation to the antibody.

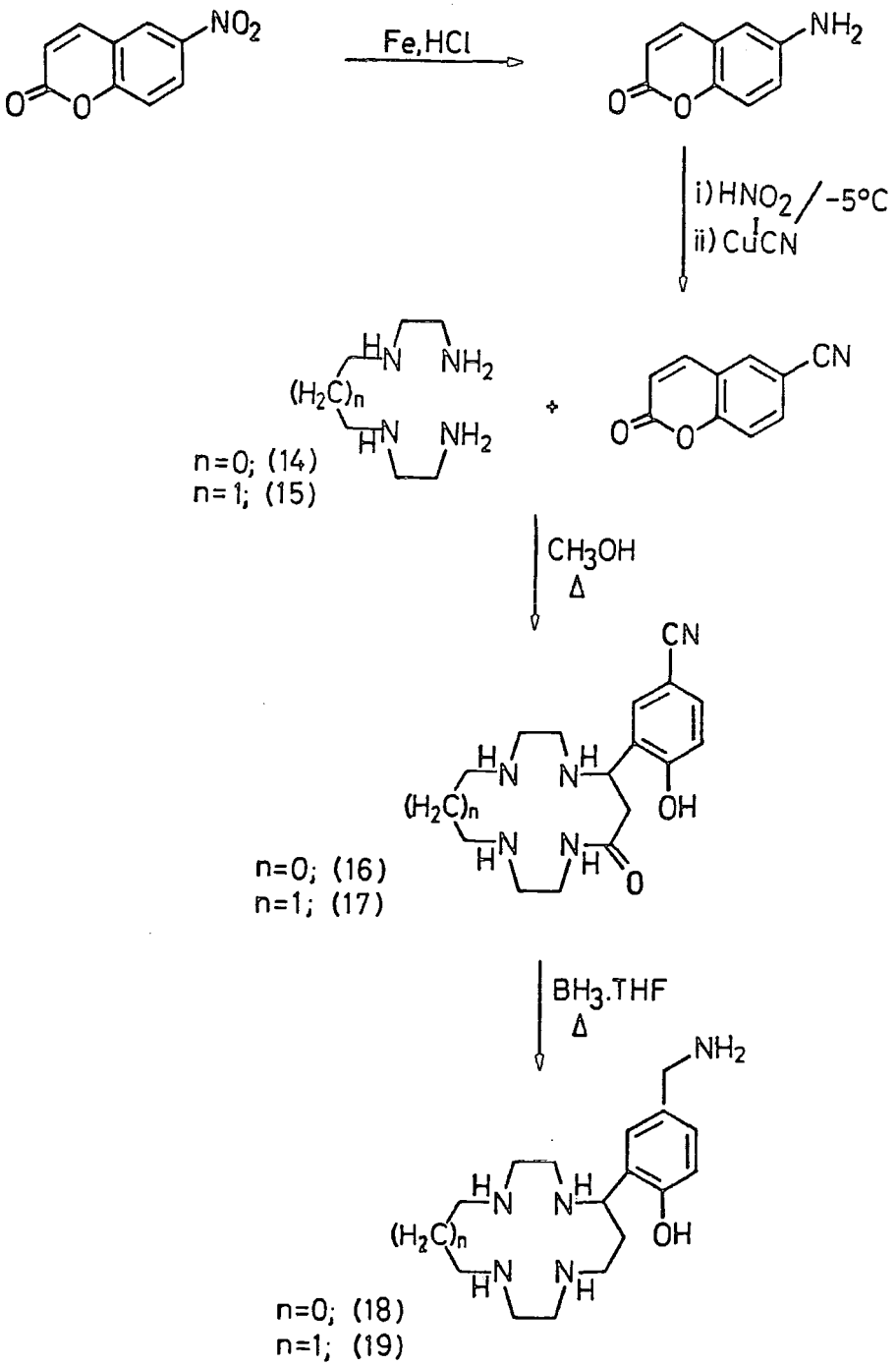

Figure 2.4 *Synthesis of [13]- and [14]-membered para-Aminomethylphenol-pendent Macrocycles.*

2.3 NON PHENOL-PENDENT TETRAAMINE MACROCYCLES

2.3.1 The Use of Non-Phenolic Side Chains

The synthesis of non-phenolic functionalised cyclam and $13N_4$ is equally important for two main reasons. Firstly it permits an investigation of the possible role of a phenol-pendent group in technetium binding; we require a non-phenolic analogue as a control. Secondly, Kimura *et al.*[16] reported that the phenol is interacting very weakly (pK_a 9.2) in the copper complex of (2) and stabilises the system only at high pH (section 5.1.3). Non-phenolic cyclam and $13N_4$ should therefore suffice as ^{64}Cu and ^{67}Cu binders.

It is possible to conjugate the macrocycles either through a carbon or through a nitrogen atom of the ring. Each method has merits and drawbacks which will be considered in sections 2.3.2 and 2.3.3.

2.3.2 Synthesis of N-functionalised Cyclams

The main advantage of N-functionalised cyclam derivatives is their easy synthesis from cyclam itself, which is commercially available. Reaction of excess cyclam with a suitably substituted benzyl bromide, according to the method of Volkert *et al.*[17], proceeds cleanly to give the mono-N-alkylated derivative in high yield. Pendent groups attached through carbon must be introduced into the backbone before macrocyclisation. The synthesis of C-functionalised macrocycles is consequently more complex and much more expensive, in view of the costly starting materials, low yielding reactions and time-consuming chromatography for their purification.

In the first instance, when our efforts were directed towards aromatic amine-based side chains, cyclam was alkylated using p-nitrobenzyl bromide in chloroform at room temperature. With cyclam in large excess, exclusively monoalkylated product (20) is obtained (Figure 2.5). Unreacted cyclam can be filtered off after extracting the product into diethyl ether and is easily recovered by sublimation.

Selective reaction of α-bromoacetyl bromide at the exocyclic aromatic amine requires methylation of the three remaining secondary amines using the Eschweiler-Clarke method[18]. The final step, hydrogenation of the nitro group of (21) to give cycle (22) was never completed due to a shift in emphasis away from aromatic amines towards a new strategy based on aliphatic primary amines. It was noted previously (section 2.2.6) that the use of an aliphatic amine-based side chain should permit conjugation of a phenol-pendent macrocycle without the risk of acylation of the ring. Likewise cycle (24) should possess similar advantages over (22) and can be made simply, by monoalkylating cyclam with α-bromotolunitrile followed by reduction of the nitrile group using diborane-THF (Figure 2.6). Both reactions proceed in high yield to give the free amine form of (24), isolated as a clear oil by extracting a basic solution of the crude hydrochloride salt with chloroform. In accord with the behaviour of pentaamines (18) and (19), cycle (24) could not be recrystallised using a wide range of solvent systems but was deemed sufficiently pure for conjugation purposes, as determined by ^{1}H NMR and DCI mass spectroscopy.

2.3.3 Binding Characteristics of Mono-N-Alkylated Cyclams

Although per-N-alkylated cyclams are unquestionably poorer technetium and copper binders than cyclam itself, there is uncertainty about the

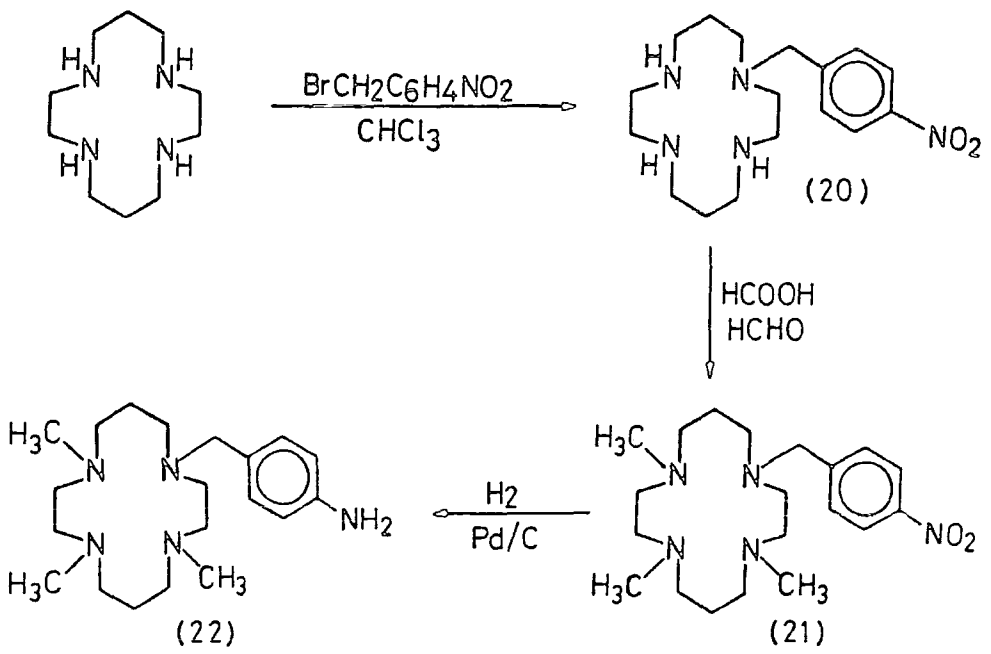

Figure 2.5 *Synthesis of N-(aminobenzyl)-pendent Cyclams.*

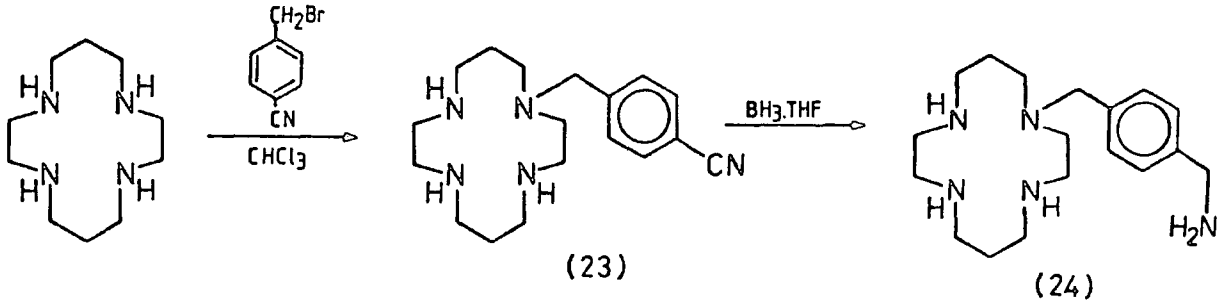

Figure 2.6 *Synthesis of N-(aminomethylbenzyl)-pendent Cyclams.*

binding efficacy of mono-N-alkylated cyclams.

J. Simon[7] recommended that, wherever possible, derivatisation of cyclams for technetium binding should be made through carbon rather than nitrogen. Technetium complexes of a series of mono-N-alkylated cyclams were prepared by Ketring *et al.*[17] in greater than 90-95% yield at pH 11.5 but a temperature of 80-90^{o}C was quoted. The same workers reported in an earlier paper[19] that cyclam itself incorporates technetium in similar yield at room temperature (pH 11). If a temperature of 80-90 ^{o}C is required for complexation by mono-N-alkylated cycles, their use for binding technetium to antibodies, which denature above 40 ^{o}C, would be precluded. Few copper complexes of mono-N-alkylated cyclams have been reported. Kaden *et al.*[20] prepared a series of copper (II) complexes of N-carboxyalkylcyclams, which do not appear to differ appreciably in their binding characteristics from cyclam itself.

It is conceivable that we would need to use protecting groups *e.g* benzyl,Z for conjugating certain types of macrocycle to the antibody. Hydrogenolysis of these protecting groups would probably cleave the side chain from the macrocycle in the same step.

2.3.4 Synthesis of C-functionalised Macrocycles

C-functionalisation appears to be preferable to N-functionalisation in view of the greater resistance of the carbon-carbon bond to cleavage and the superior binding characteristics of macrocycles with four secondary amines in the ring.

The preferred route to C-functionalised [13] and [14]-membered tetraamines employs a double condensation reaction between a linear tetraamine and a functionalised malonate ester to form a macrocyclic diamide which can then be reduced to the tetraamine using diborane

(Figure 2.7). This route was first reported by Tabushi *et al.* in 1977[21] and has since been used by Meares *et al.*[22] to functionalise TETA with an aromatic amine side chain.

Diethyl p-cyanobenzylmalonate (25) can be made by alkylating the sodium salt of diethylmalonate with α-bromotolunitrile. A two fold excess of diethylmalonate prevents significant dialkylation occurring.

Condensation between the functionalised malonate ester and the linear tetraamine requires several days under reflux in anhydrous ethanol. The [13]-membered diamide (26) conveniently precipitates from solution as it is formed and can be recrystallised from hot ethanol. The [14]-membered diamide (27) must be purified by lengthy chromatography on silica. The yield of (26) is again lower than for (27), the yields of the diamides are broadly similar to those obtained for the corresponding phenolic amides (16) and (17), but the diamides are easier to purify in both cases.

Reduction of the amide and nitrile groups proceeds smoothly with diborane, both pentaamines can be isolated in good yield by extracting from basic solution into chloroform.

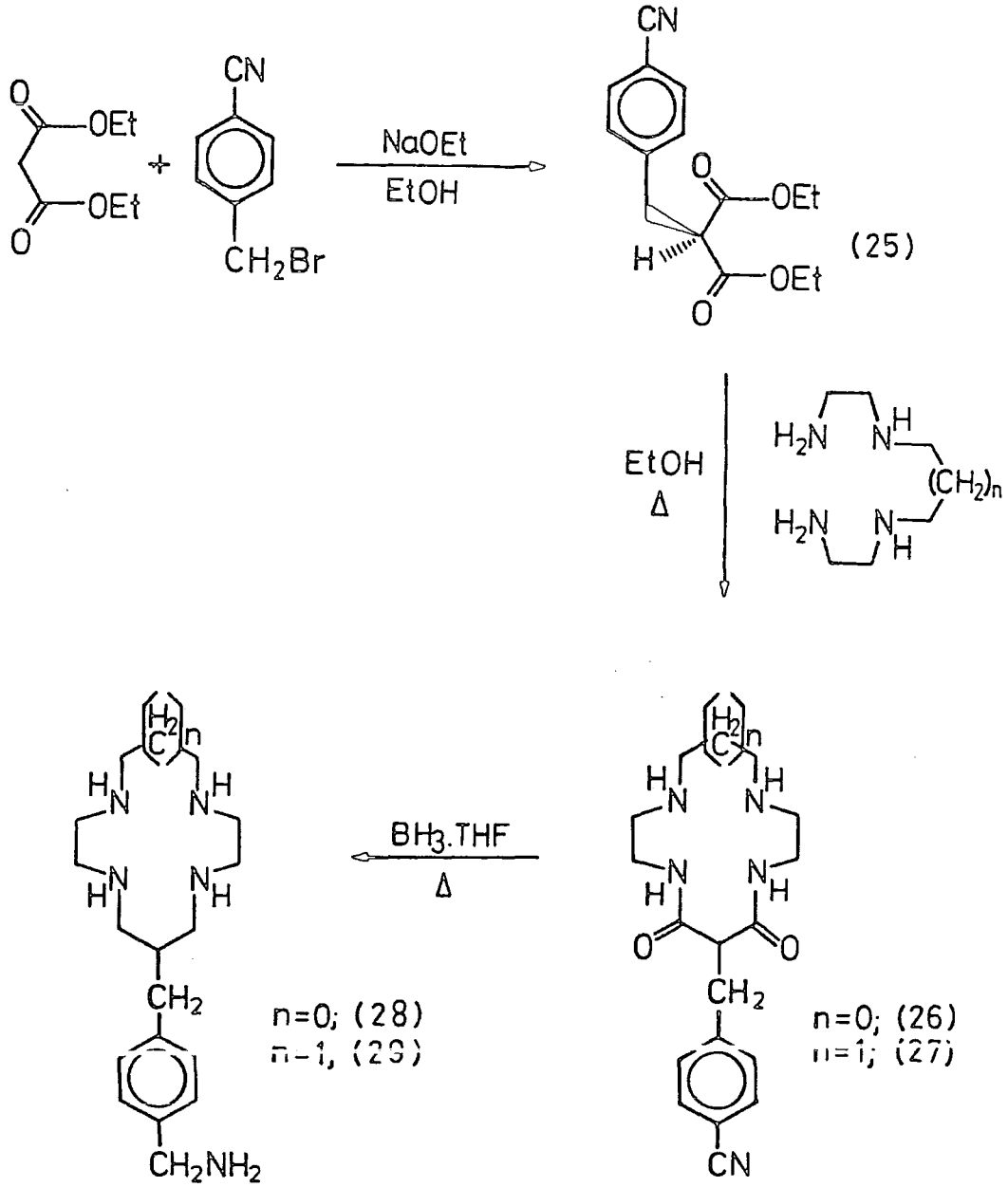

Figure 2.7 *Synthesis of C-functionalised [13]- and [14]-membered macrocycles.*

PART B: SYNTHESIS OF CROSS-LINKING AGENTS AND ANTIBODY CONJUGATION

2.4 INTRODUCTION

2.4.1 Heterobifunctional Linker Molecules

The preferred form of the functionalised macrocycle, containing a nucleophilic aliphatic amine in the side chain, must be attached to nucleophilic residues on the monoclonal antibody. This requires the use of a heterobifunctional cross-linker with two distinct groups, one specifically reactive towards the macrocycle side chain, the other towards suitable groups on the antibody.

2.4.2 Modification of the antibody with Traut's reagent

It has been reported by Meares *et al.*[22] that labelling of the macrocyclic ligand TETA with ^{67}Cu is only effective if a "spacer" group is employed between the macrocycle and the antibody. The conjugate obtained by reacting α-bromoacetamidobenzyl-TETA directly with amine residues on the antibody "Lym-1" could not be labelled successfully unless the copper was added to the macrocycle prior to conjugation to the protein. This observation implies that in the absence of a spacer group, the macrocycle is inaccessible to the radioisotope, possibly "buried" within the complex macrostructure of the protein.

Similarly, Arano *et al.*[23] reported that the efficacy of the labelling of bifunctional chelators with technetium-99m was related to the length and lipophilicity of the chain separating chelator and antibody. If the chain was too short or too lipophilic, the chelate was

"buried" within the protein and was unavailable for radiolabelling.

The spacer group employed by Meares *et al.* was introduced by reaction of lysine ϵ-amino groups with 2-iminothiolane ("Traut's Reagent"). For their purposes, the resulting thiol group was then reacted with the bromoacetamide of the functionalised TETA derivative (30) to form a thioether bridge (Figure 2.8).

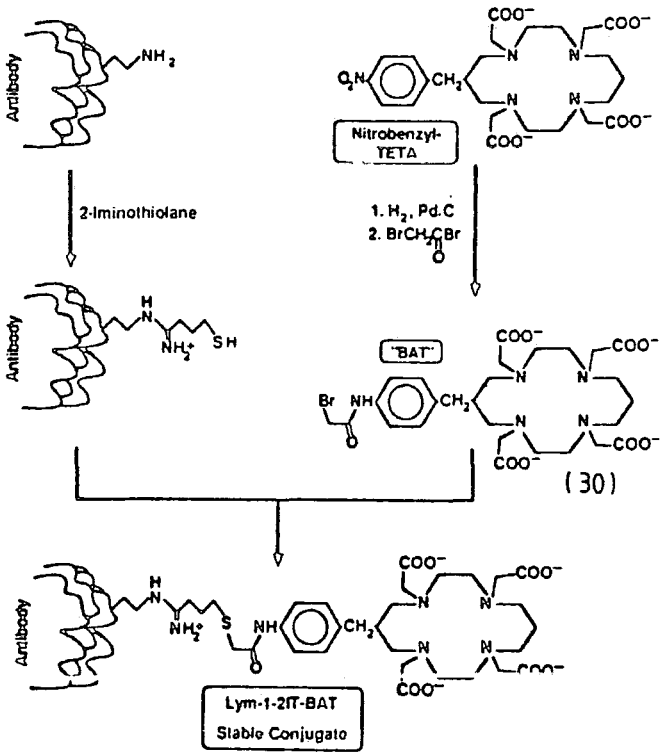

Figure 2.8 *"Trauting" of lysine residues produces thiol-containing "spacer" groups for attachment of functionalised macrocycles.*

"Trauting" of the antibody also allows us to control more precisely the number, but not the location, of macrocycles bound to each antibody. An excessive number of chelators bound to the antigen binding region, which also contains lysine, would reduce the immunoreactivity of the antibody and must be avoided. The conversion of a limited number of lysines,

typically five, to thiols would enable us to control the conjugation of macrocycles bearing thiol-specific functional groups. Normally, Immunoglobulin G does not contain free thiol groups but its Fab fragments‡ do, in which case the use of thiol-specific macrocycle conjugates would be equally applicable.

2.4.3 Cross-Linking Agents of the Prior Art

A suitable bifunctional linker molecule must provide a terminus which reacts with the exocyclic primary amino group of the functionalised macrocycle and another which reacts specifically with the antibody thiols. The use of activated esters *e.g* of p-nitrophenol, N-hydroxysuccinimide, in place of acyl halides should allow greater selectivity and control in the acylation of the exocyclic amine. In addition however, protection of the ring nitrogens with metal ions or by pH control will still be necessary.

The use of α-bromoacetamides as thiol specific reagents, although favoured by Meares *et al.*[1,22], is unsuitable for our purposes since reaction also occurs at the secondary nitrogens of unsubstituted macrocyclic tetraamines giving complex oligomeric mixtures. At higher pH α-haloacids are readily hydrolysed to α-hydroxyacids, of which the aldehyde tautomer is essentially non-specific for thiol groups, reacting with amine residues as well (Figure 2.9).

Heterobifunctional cross-linkers which employ maleimides as the thiol-specific group are commercially available[24,25]. Generally these are highly reactive and tend to hydrolyse readily at high pH ($\geq$ 7.5) to maleamic acid (Figure 2.9). It would appear that the less favoured

---

‡See section (1.2) for a definition of the terms Immunoglobulin G and Fab fragments.

orbital symmetry of the ring-opened form renders it unreactive towards thiol residues. In addition maleimides generally show relatively poor selectivity for thiols over amines *e.g* lysine, histidine, especially at high dilutions and at higher pH *i.e* above 7.5.

The use of cross-linkers which have low specificity for thiols, such as α-bromoacetamides and maleimides, would result in the formation of complex polymeric mixtures through reaction at amino groups on both the antibody and the unsubstituted macrocycle.

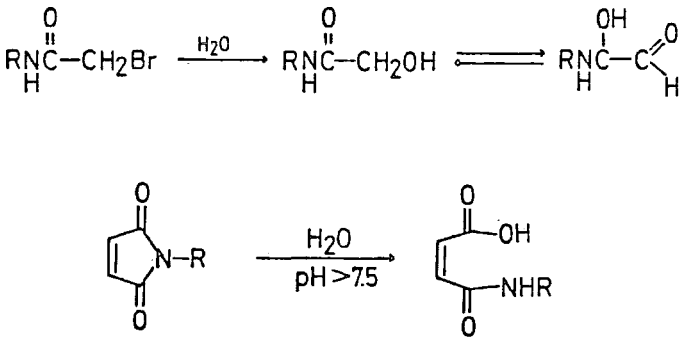

Figure 2.9 *Hydrolysis reactions of α-bromoacetamides and maleimides.*

2.5 VINYL PYRIDINE LINKER MOLECULES

2.5.1 Vinyl Pyridines as Thiol-Specific Reagents

In 1970, Cavins and Friedman[26] announced a new internal standard for amino acid analyses based on S-β-(4-pyridylethyl)-L-cysteine. The thiol group of cysteine was found to be 300 times more reactive towards 4-vinylpyridine than the amino group and reacted selectively to give (31). In view of the superior thiol specificity of vinyl pyridines, compared to the reagents of the prior art, a new generation of bifunctional

linker molecules was developed in collaborative work with Celltech. Both 2- and 4-vinylpyridine derivatives were found to react selectively with thiols in the pH range 5 to 9.

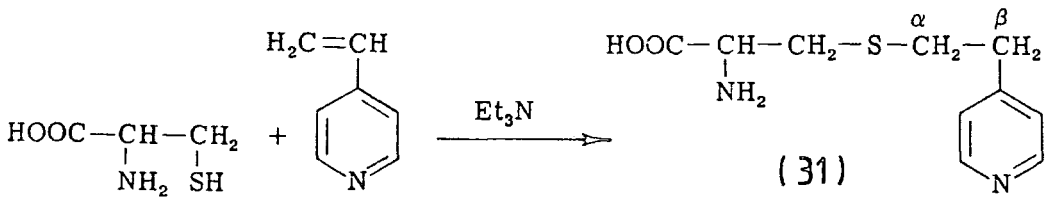

In separate experiments, both isomers were found to be unreactive towards the amino group of the dipeptide, Ala-Pro-NH_2 at pH 9. (Ala = Alanine; Pro = Proline). The relative rates of reaction of 2- and 4-vinyl pyridines with N-acetyl-cysteine and Ala-Pro-NH_2 are presented in Figure 2.10.

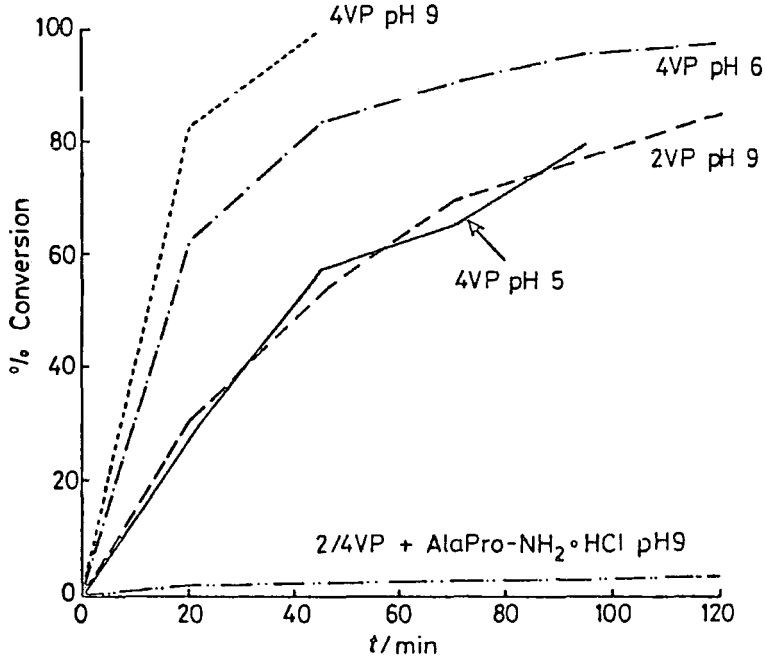

Figure 2.10 *Reaction of 2- and 4-vinylpyridine with N-acetyl cysteine and Ala-Pro-NH_2*

Thiols react with a number of α,β-unsaturated compounds at rates determined by the electron deficiency of the terminal position[27]. The π orbitals of 2- and 4-vinyl groups have appropriate symmetry for conjugation with the π orbitals of the pyridine ring. The characteristic electron-deficiency of the pyridine ring is thus delocalised to the terminal position of the vinyl group (Figure 2.11). The more highly conjugated 4-vinylpyridine derivative is more electron deficient at the terminal position and therefore more reactive towards thiols than 2-vinylpyridine. However since heterobifunctional cross-linkers containing 2-vinylpyridine are considerably easier to synthesise from commercially available materials than their 4-vinyl analogues, they were preferred in the first instance.

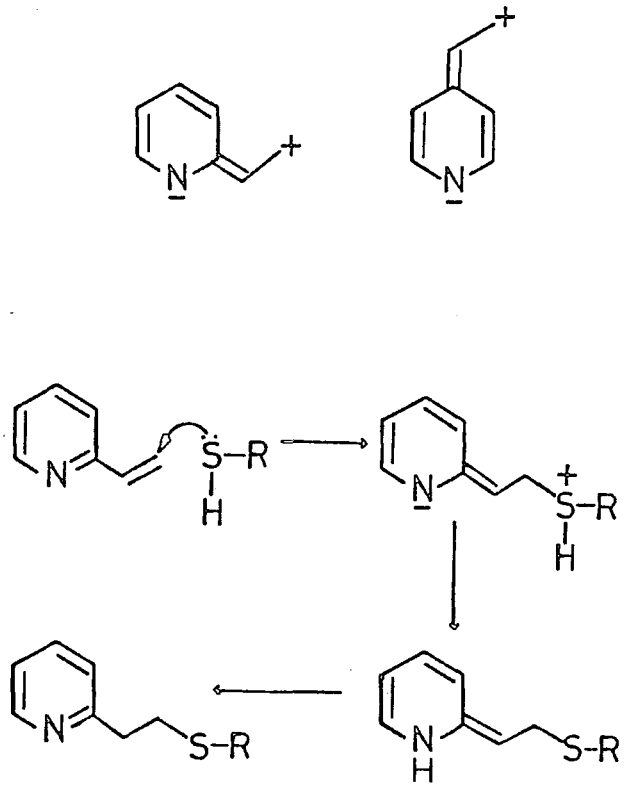

Figure 2.11 *Valence bond structures of 2- and 4-vinylpyridine; mechanism of the reaction of 2-VP with thiol groups.*

2.5.2 Synthesis of a Vinyl Pyridine Cross-linker

The linker molecule, 2-vinyl-6-methoxyacetic acid pyridine-p-nitrophenol ester, can be synthesised in six steps from commercially available 2,6-bis(hydroxymethyl) pyridine (Figure 2.12). The synthetic route, devised primarily at Celltech, aims to convert one hydroxymethyl group to a vinyl group and the other to a p-nitrophenyl ester. Initially one of the hydroxy groups is protected as an acid-labile dimethoxytrityl ether whilst the other is alkylated to give a relatively stable methyl ester. Having removed the DMT group with either p-toluenesulphonic acid or zinc(II) bromide, the liberated alcohol (33) can be oxidised to an aldehyde (34) using an activated form of manganese dioxide[28] (obtained from Fluka). The conversion of the aldehyde to a vinyl group was higher yielding when the Peterson reagent[29], trimethylsilylmethylmagnesium chloride, was used rather than a conventional Wittig reagent. The use of thionyl chloride to promote 1,2-elimination from the intermediate silyl alcohol gave satisfactory yields of product (35). The final step, exchange of methyl and p-nitrophenyl esters, requires that the lithium salt of the acid be converted to its pyridinium salt before condensing with p-nitrophenol. It is thought that the pyridinium cation is acting catalytically as a proton donor since neither lithium nor triethyl-ammonium salts of the acid are reactive. The p-nitrophenyl ester (36) is highly reactive and must be stored at -18 ^{o}C under nitrogen to prevent rapid retro-hydrolysis to the acid.

The synthesis of the more reactive 4-vinylpyridine linker molecules is more complex since 2,4-bis(hydroxymethyl)-pyridine is both commercially unavailable and more difficult to mono-protect selectively at the 2-position.

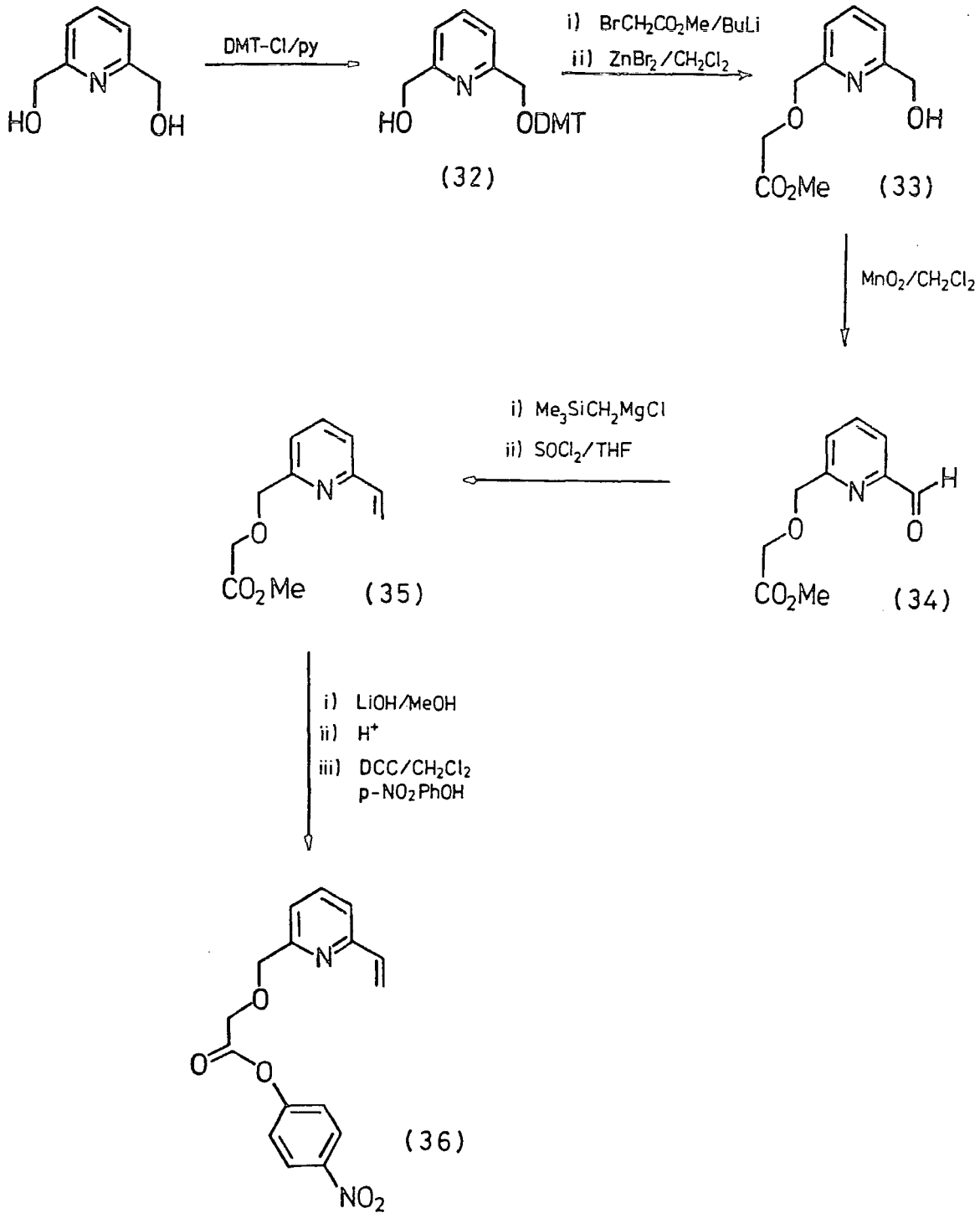

Figure 2.12 *Synthesis of a 2-Vinylpyridine-active ester Linker Molecule.*

2.6 SELECTIVE ACYLATION OF EXOCYCLIC AMINO GROUPS

2.6.1 Strategies for Selective Acylation

Since exocyclic primary amines are much more nucleophilic than aromatic amines, milder acylating reagents such as active esters can be used in place of acyl halides. However since secondary amines are also susceptible to acylation by activated esters, the ring must be protected. The most obvious answer would be to protect the ring with a metal ion which could be removed once acylation was complete.

2.6.2 Metal Ion Protection

Lithium and sodium are known to form weak complexes with cyclam. We have investigated the possibility of using alkali metal ions as protection for the tetraamine system of cycle (29) during acylation of its exocyclic primary amino group with α-bromoacetyl bromide. However the precipitation of oligomeric material from solution suggests that lithium and sodium ions cannot prevent acylation of the ring.

Zinc forms complexes with cyclam[30] which we hoped would be sufficiently stable (log K = 15.5) to protect the ring in aqueous solution, yet which allow removal of the metal under relatively mild conditions. However when a p-nitrophenyl ester was added to an aqueous solution containing (29) and zinc(II) bromide no reaction occurred. This suggests that the acidity of zinc(II) ions in water is promoting excessive protonation of the primary amine. The use of aprotic solvents, such as acetonitrile, would avoid protonation but the zinc complex of (29) was found to be insufficiently soluble in such media.

Copper and nickel form sufficiently strong complexes with cyclam to

protect the ring but subsequent removal of the metal ion requires such forcing conditions that their use is impracticable. Removal of nickel(II) ions requires the complex to be boiled in sodium cyanide solution[31]. Copper(II) ions cannot be removed even as the insoluble sulphide following treatment with H_2S. They will eventually dissociate in boiling 6N HCl but cannot be separated from the free ligand under these conditions. If the pH is raised or the temperature dropped, copper is bound by the ligand again.

2.6.3 Controlling pH

In view of our failure to identify a suitable metal for protecting the ring, it was decided to investigate the role of pH in the relative rates of acylation at the primary and secondary centres. It was discovered that by buffering the reaction mixture to pH 7, acylation could be confined to the exocyclic amine of the functionalised macrocycle. The four successive protonation constants of cyclam itself are 11.5, 10.2, 1.7 and 1.0[32]. At neutral pH, the ligand will bind two protons shared equally between the four equivalent nitrogens. As a result of the extensive hydrogen bonding and extremely rapid exchange of protons, each nitrogen will effectively "see" half a proton. It would appear that 2 protons are sufficient to lock up all four nitrogen lone pairs and prevent acylation occurring in the ring (Figure 2.13).

At pH 7 the benzylamine side chain of (29) will also be extensively protonated ($pK_a \approx 9.5$), less than 1% existing as the free form. However this is much greater than the concentrations of monoprotonated and unprotonated cyclam, 0.04% and 0.002% respectively, and it is clearly sufficient to allow exocyclic acylation to occur.

Another important factor could be the low intrinsic reactivity of

the diprotonated form of the ring. Although protons are exchanged rapidly within the ring, the loss of a proton will require a change in the conformation of the ring, imposing a kinetic barrier to deprotonation. If this is the case, the kinetic barrier for deprotonation of the exocyclic amine would almost certainly be lower, allowing more rapid deprotonation to occur.

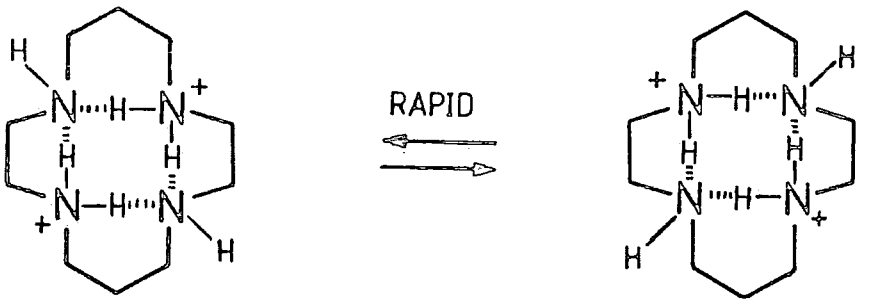

Figure 2.13 *Hydrogen Bonding and Proton Exchange in Diprotonated Cyclam*

2.6.4 Synthesis of Macrocycle-linker Conjugates

A solution of "Pipes" buffer (0.5M) provides a pH in the range 6.8 to 7.0 for the condensation of the macrocyclic primary amine with the p-nitrophenyl ester (36) (Figure 2.14). The macrocycle is dissolved in aqueous buffer and a 2 fold excess of ester is added in an equal volume of p-dioxane. Should the pH of the solution deviate significantly from 6.8 to 7.0, it can be adjusted with either 1N NaOH or 1N HCl.

The reaction is equally applicable to non-phenolic and phenolic macrocycles and is generally complete within 4 hours at 40 ^{o}C. The

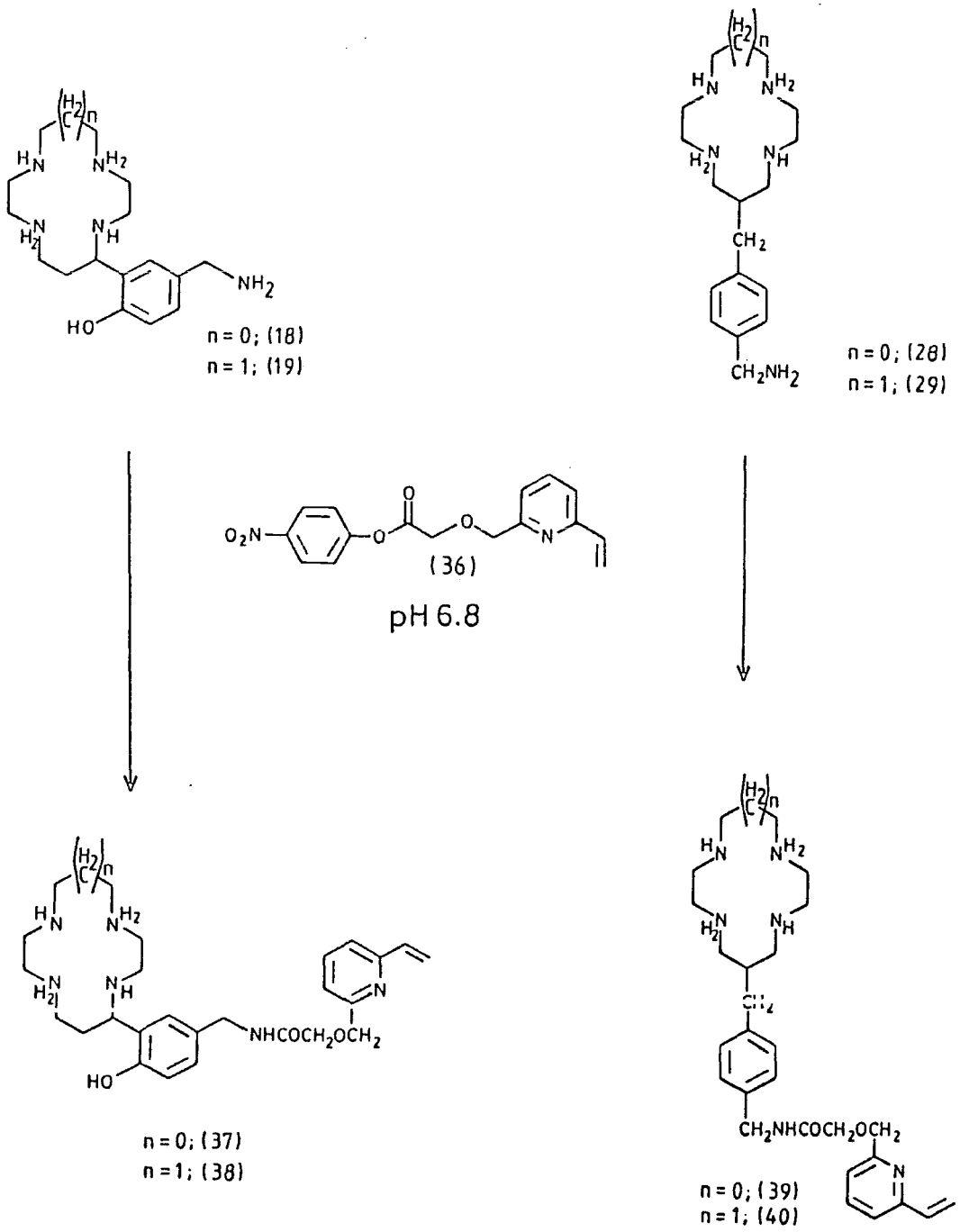

Figure 2.14 *Selective Acylation of the Exocyclic Amino Groups of Functionalised [13]- and [14]-membered Macrocyclic tetraamines.*

dicationic macrocycle-linker conjugate can be separated from unreacted macrocycle (charge +3) using cation exchange HPLC, by virtue of the charge difference. The HPLC profile for the reaction of the [13]-membered phenol (18) is shown in Figure 2.15.

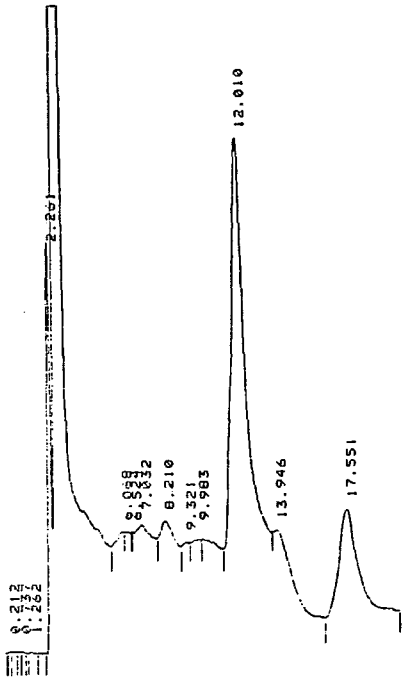

Figure 2.15 *Cation Exchange HPLC profile for reaction between (18) and (36), showing (37) at 12 minutes and (18) at 17.5 minutes*

Retention times vary between 11 and 14 minutes, being slightly earlier for the phenolic macrocycle conjugates. Isolated as diacetate salts, the non-phenols are colourless oils, the phenols slightly yellow solids. Yields varied from 80% for (40) to 50% for (37). The long term stability of the conjugates is good, both in the solid state and in aqueous solution. The conjugates were characterised by ^{1}H NMR spectroscopy and FAB mass spectroscopy, the 3 methylenic resonances in the 4.7-4.1 ppm region being particularly diagnostic. Typical NMR and FAB spectra are presented in Figure 2.16.

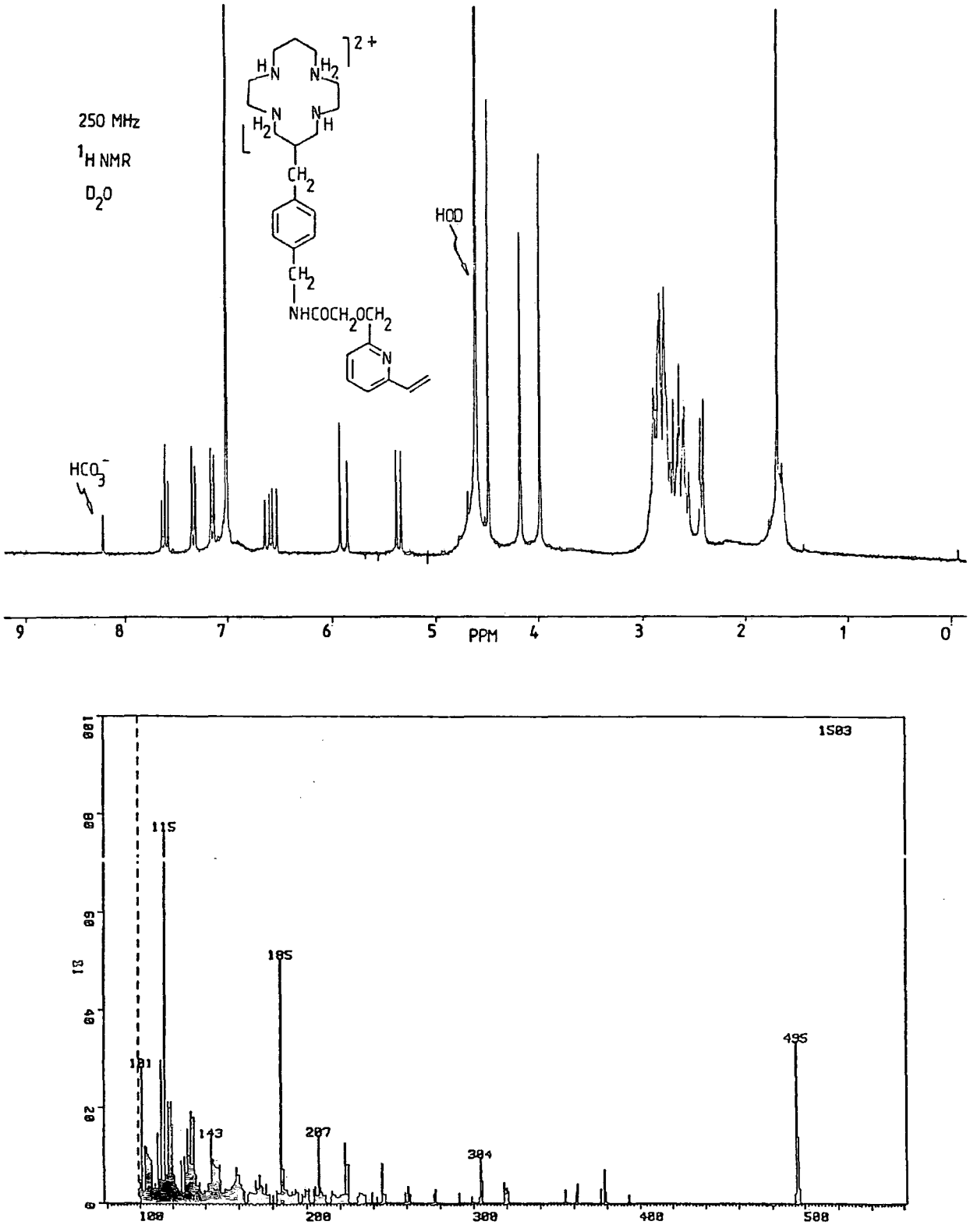

Figure 2.16 *NMR and FAB Spectra*

2.7 ANTIBODY CONJUGATION

2.7.1 Choosing the Antibody

Having made the macrocycle-vinyl pyridine conjugates (37) to (40), the next step is to attach them to a suitable monoclonal antibody. The antibody of first choice, "B72.3", binds to tumour-associated glycoprotein (TAG-72) found in human colon and breast cancer[33,34]. Monoclonal B72.3 is an attractive choice for research work since it is readily available, has a low affinity for normal tissue types and has a complement antigen (TAG-72) with a high incidence (> 80%) in colon carcinoma tissue.

2.7.2 Introduction of Free Thiol Groups on the Antibody

The need for derivatisation of the antibody with Traut's reagent[35] has been discussed previously (section 2.4.2).

A solution of antibody (2 mg) in 0.2M phosphate buffer (pH 7.4) was treated with 75 μl of 20 mM 2-iminothiolane in 50 mM triethanol-HCl (pH 8) in the presence of 2-mercaptoethanol at 4 ^{o}C. After 60 minutes at 4 ^{o}C, the conjugated antibody was separated from small molecules by filtration through Sephadex G-50 (0.1 M sodium phosphate buffer pH 8).

Using Traut's method, the number of free thiols introduced per antibody was found to vary from 2 to 5, as determined by titration against Ellman's reagent, 6,6'-dinitro-3,3'-dithiobenzoic acid (DTNB)[36]. Antibody thiols cleave the disulphide bonds of DTNB to form a mixed disulphide (41) and, in the process, liberate a molecule of 6-nitro-3-thiobenzoic acid (Figure 2.17). Since the titration is performed at high pH, the liberated thiol is deprotonated and the resulting thiolate

anion (42) has an intense yellow colouration. Knowing the λ_{max} (412 nm) and extinction coefficient (13600) of its absorption band, the concentration of thiolate and, by extrapolation, the concentration of antibody thiols can then be calculated.

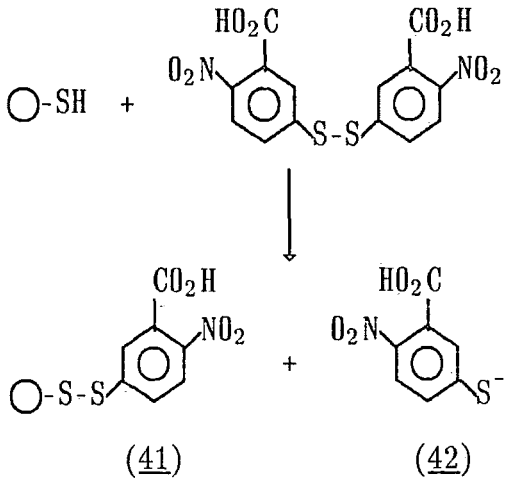

Figure 2.17 *Ellman's Assay for Free Thiol Groups*
○ = *antibody*

2.7.3 Conjugation of the Antibody

A solution of "trauted" antibody in 0.1M phosphate buffer (pH 8.0), containing 2 mM EDTA to sequester trace metals, was divided into two equal fractions. Both fractions were then incubated for 18 hours at 4 ^{o}C under argon, one fraction containing excess macrocycle-vinyl pyridine conjugate, the other fraction acting as a control. The first fraction was centrifuged through Sephadex G-50 to separate the antibody-chelator conjugate from unreacted vinylpyridine. Both fractions were then assayed for free thiols using Ellman's reagent. It was apparent that some thiols had been "lost" from the control antibody due to oxidation. However a greater number had been "lost" by the antibody exposed to the macrocycle-vinylpyridine conjugate. The difference in the number of

free thiols between the two fractions gave an indication of the number of thiols capped by macrocycles.

Before radiolabelling studies were performed using these antibody-chelator conjugates, those thiol groups which had oxidised were re-reduced and all free thiols were then capped with α-iodoacetamide (or 4-vinylpyridine) to prevent their participation in metal-binding (see section 3.1.5).

2.8 MONITORING ANTIBODY CONJUGATION

2.8.1 The Importance of Monitoring Conjugation

It is important to quantify the number of macrocycles bound per antibody as accurately as possible. The number of bound chelators must be optimised to provide as large a chelator concentration as possible for rapid metal binding without compromising the immunoreactivity of the antibody[37]. Additionally, quality control in the manufacture of a radiopharmaceutical dictates that we monitor the number of macrocycles per antibody to determine accurately the radiation dose to the patient.

The Ellman's assay, described in section (2.7.3), gave an indication of the macrocycle:antibody ratio by relating the number of free thiols in the derivatised and control antibodies. However for greater accuracy we require a method which counts the number of bound chelators directly, rather than by inference from the number of "lost" thiol groups. A variety of techniques have been employed by other workers for this purpose, incorporating either radioactive or fluorescent markers.

2.8.2 Radioactive Assay

In order to monitor the number of molecules of functionalised EDTA bound to B72.3, Gansow *et al.*[12] used ^{14}C labelled bromoacetic acid in its synthesis. Knowing the concentration of protein, they could calculate the chelator:antibody ratio from the amount of specific activity bound to the antibody.

The TLC assay developed by Meares *et al.*[1] uses a solution of radioactive cobalt (^{57}Co) in citrate buffer to quantify the protein-bound chelator. The antibody bound ^{57}Co-chelate remains at the origin whilst ^{57}Co-citrate moves with $R_f > 0.2$, in ammonium acetate/methanol.

Although radio-assays allow the quantification of very low concentrations of antibody-bound chelator, they possess a number of disadvantages. The ^{14}C labelling method is only useful at the research stage. If employed for quality control in the final product, its β-emissions would increase the dose to the patient unnecessarily.

The utility of Meares' method based on radioactive cobalt is limited by the presence in solution of trace metals which occupy a sizeable proportion of the ligands at low chelator concentrations. In addition, there is the prospect of cobalt binding non-specifically to the protein backbone. An EDTA wash needs to be performed to avoid over-estimation of the true chelator concentration.

2.8.3 Fluorescent Assay

Alternative assays based on fluorescent markers have been used extensively in protein chemistry. Our initial line of approach was to incorporate a fluorescent 1-dimethylaminonaphthalene-5-sulphonyl or "dansyl" group[38] into a prospective linker molecule based on a Z-

protected lysine. It was planned to react the p-nitrophenyl ester of the functionalised lysine (43) with the exocyclic primary amino group of cycle (29), remove the Z group then attach the macrocycle-linker conjugate (44) to the antibody thiols using α-bromoacetyl bromide (Figure 2.18). However the poor solubility of the lysine derivative (43) in aqueous media, due to the lipophilicity of the dansyl residue, inhibited further development of this approach. Furthermore it is conceivable that the incorporation of a bulky fluorescent group, such as dansyl, into the chain linking macrocycle and antibody might trigger a greater immunogenic response to the modified antibody. It is intrinsically preferable to employ a fluorophore which need not be part of the linker molecule itself.

2.8.4 Ortho-phthalaldehyde (OPA) Assay

The reaction between o-phthalaldehyde and primary amines in the presence of 2-mercaptoethanol, produces highly fluorescent products[39]. The isoindole product (45) exhibits greater sensitivity than either ninhydrin or fluorescamine (detection limit is ca. 10^{-11} M). The o-phthalaldehyde adducts are completely soluble and stable in aqueous buffers and since they are considerably less expensive than alternatives based on fluorescamine, they may be used routinely for quality control.

Exhaustive hydrolysis of the antibody conjugate with 6N HCl (16 hours at 110 ^{o}C) gives a mixture of amino acids and protonated functionalised macrocycle. Reaction of the liberated primary amino groups with o-phthalaldehyde and 2-mercaptoethanol gives a series of isoindole adducts which may be detected spectrofluorimetrically (λ_{exc} 334 nm; λ_{fluor} 453 nm). Separation of the macrocycle-isoindole compound (45) from derivatised amino acids was achieved using cation-exchange

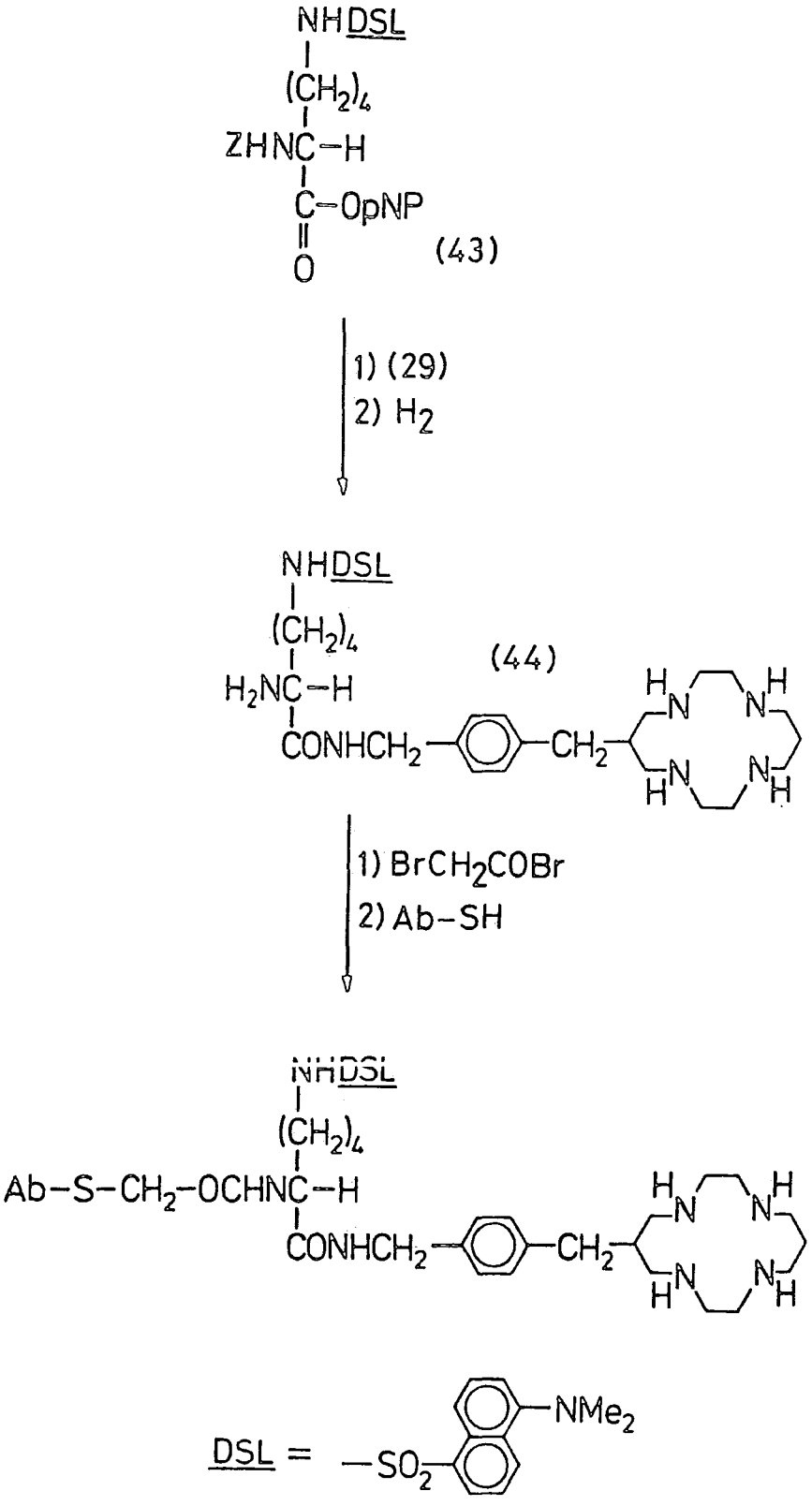

Figure 2.18 *Synthesis of a Linker Molecule containing a Fluorescent "Dansyl" Group.*

HPLC, by virtue of its dipositive charge at pH 6.5 (Figure 2.19). Typically, the derivatised antibodies were found to contain, by the OPA method, between 2 and 3 macrocycles per antibody. This level of conjugation was consistent with that given by the previously described Ellman's assay.

2.9 IMMUNOREACTIVITY - THE EFFECTS OF CONJUGATION

The immunoreactivity of the derivatised B72.3 antibody was assayed by affinity chromatography. This technique measures the percentage of the total antibody which retains an affinity for the TAG-72 antigen, suitably attached to a chromatographic plate. The immunoreactivity was tested for levels of conjugation between 1 and 9 macrocycles per antibody. It was found that up to 3 macrocycles could be conjugated without unduly diminishing the immunoreactivity. However when the average number of chelators bound was increased from 3 to 9, the affinity of the antibody for TAG-72 was progressively reduced.

Other workers also found an inverse relationship between the number of chelating groups per antibody and immunoreactivity. Meares *et al.*[1] found 77-84% retention of immunoreactivity by the anti-lymphoma Mab, "Lym-1", when conjugated with 0.4 to 2.3 molecules of EDTA per antibody. In their experience, 3 or 4 chelators per antibody did not seriously degrade the immunoreactivity but this may depend upon the type of chelator, the method of conjugation and the type of antibody used.

Using the macrocyclic ligand TETA as a copper-67 binder, Meares *et al.*[22] found a retention of 70-75% with 2.7 chelators bound per antibody. Paik *et al.*[37] noted retentions of 67% and 47% for 0.8 and 3.4 molecules

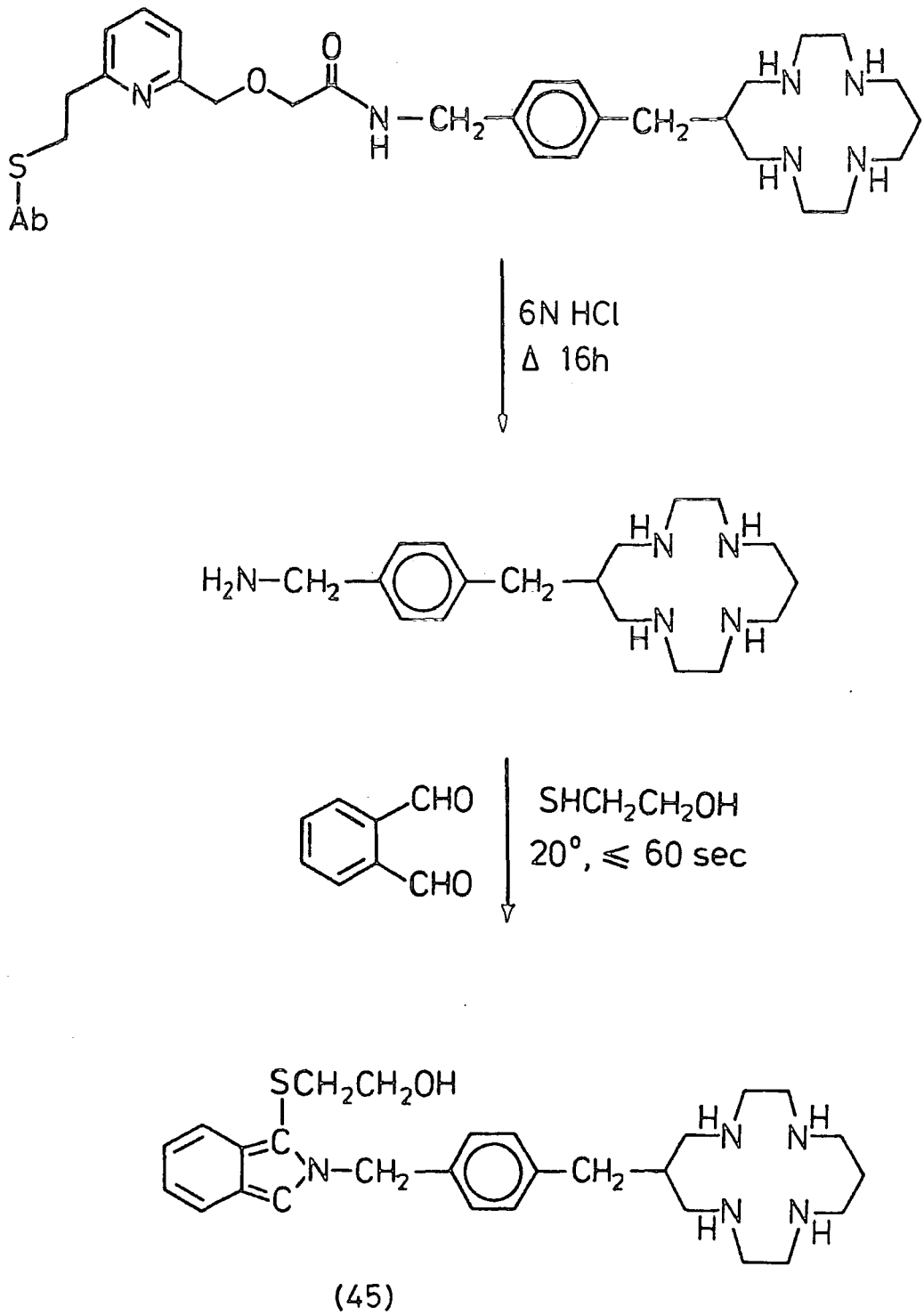

(45)

Figure 2.19 *Ortho-phthalaldehyde Assay for the Number of Macrocycles bound per antibody.*

of DTPA per antibody, bound using the carbodiimide method, and 100% retention for 2 molecules of DTPA per antibody, bound by the cyclic anhydride method (see section 1.7.1). Hnatowich[40] reported that conjugation of 4.3 DTPA molecules per protein using the cyclic anhydride method gave a retention of immunoreactivity of 51%.

Volkert *et al.*[41] attached up to 4.2 functionalised cyclam macrocycles to the Mab, anti-HSA IgG (HSA = human serum albumen), with 90% retention of immunoreactivity. Using the same Mab as ourselves, B72.3, Gansow *et al.*[12] attached up to 1 molecule of EDTA or DTPA using the anhydride or isothiocyanate methods (section 1.7.2) without loss of antigen affinity. However when more than 3 ligands were attached, a serious deterioration was noted. The nature of the chelator was important; EDTA being worse than DTPA with respect to loss of affinity: EDTA: 36% retention (2.8 per Mab); DTPA: 75% retention (2.7 per Mab).

The inverse relationship between the level of conjugation and the immunoreactivity of an antibody is valid for a given chelator conjugated by a given technique. However Paik *et al.*[37] reported that antibodies bearing equal numbers of chelating groups can, under certain circumstances, be either active or inactive. There would appear to be a more subtle relationship between immunoreactivity and derivatisation, involving the positioning of the chelating groups with regard to the variable region.

The method of conjugation outlined in section 2.7 introduces (at lys ϵ-NH_2) thiol groups and concomitant macrocycles with a completely random distribution along the protein backbone. It is intrinsically preferable to locate chelating groups specifically outside the immunologically important variable region. In future, genetically engineered antibodies, developed by Celltech, will permit "site-specific"

attachment of the chelator outside the binding region. The chelator concentration on the antibody could then be increased, thereby enhancing its metal binding characteristics, without impairing its immunological integrity.

2.10 REFERENCES

1. C.F. Meares, M.J. McCall, D.T. Rearden, D.A. Goodwin, C.I. Diamenti and M. McTigue, *Anal. Biochem.*, 142, 68-78 (1984)
2. E. Kimura, T. Koike and M. Takahashi, *J.Chem.Soc. Chem.Commun.*, 385 (1985)
3. Y. Iitaka, T. Koike and E. Kimura, *Inorg.Chem.*, 25, 402 (1986)
4. W. Carruthers, "*Some modern methods of organic synthesis*" (2nd Edition), 270 (1978)
5. J.D. Roberts and M.C. Caserio, "*Basic Principles of Organic Chemistry*" (2nd Edition), 1311 (1977)
6. K.D. Hodges, R.G. Wollman, S.L. Kesser, D.N. Hendrickson, D.G. Van Deveer and E.K. Barefield, *J.Am.Chem.Soc.*, 101, 906 (1979)
7. J. Simon, Diss.Abstr.Int.B (1980)
8. C.M. Ché, K.Y. Wong and C.K. Poon, *Inorg.Chem.*, 24, 1797 (1985)
9. E.K. Barefield and F. Wagner, *Inorg.Chem.*, 12, 2435 (1973)
10. R.W. Hay and R. Bembi, *Inorg.Chim.Acta.*, 65, L227 (1982)
11. R.W. Hay, M.P. Pujari, W.T. Moodie, S. Craig, D.T. Richens, A. Perotti and L. Ungaretti, *J.Chem.Soc. Dalton Trans.*, 2605 (1987)
12. M.W. Brechbiel, O.A. Gansow, R.W. Atcher, J. Schlom, J. Esteban, D.E. Simpson and D. Colcher, *Inorg.Chem.*, 25, 2772 (1986)
13. J.D. Roberts and M.C. Caserio, "*Basic Principles of Organic Chemistry*" (2nd Edition), 1101 (1977)
14. G.T. Morgan and F.M.G. Micklethwaite, *J.Chem.Soc.*, 85, 1230 (1904)
15. A.I. Vogel, "*Practical Organic Chemistry*" (3rd Edition), 607 (1956)
16. E. Kimura, M. Yamaoka, M. Morioka and T. Koike, *Inorg.Chem.*, 25, 3883 (1984)
17. A.R. Ketring, D.E. Troutner, T.J. Hoffman, D.K. Stanton, W.A.

Volkert and R.A. Holmes, *Int.J.Nucl.Med.Biol.*, 11(2), 113 (1984)

18. Leuckart, *Org.Reactions*, 5, 307 (1949)

19. D.E. Troutner, J. Simon, A.R. Ketring, W. Volkert and R.A. Holmes, *J.Nucl.Med.*, 21, 443 (1980)

20. T.A. Kaden, *Helv.Chim.Acta*, 69, 2081 (1986)

21. I. Tabushi, Y. Taniguchi and H. Kato, *Tetrahedron Lett.*, 12, 1049 (1977)

22. M.K. Moi, C.F. Meares, M.J. McCall, W.C. Cole and S.J. Denardo, *Anal.Biochem.*, 148, 249 (1985)

23. Y. Arano, A. Yokoyama, Y. Magata, K. Horiuchi, H. Saji and K. Torizuka, *Appl.Radiat.Isot.; Int.J.Radiat.Appl.Instrum. Part A*, 37(7), 587 (1986)

24. T. Kitagawa and T. Aikawa, *J.Biochem.*, 79, 233 (1976)

25. B. Yoshitake, Y. Yamada, E. Ishikawa and R. Masseyeff, *Int.J. Biochem.*, 101, 395 (1979)

26. J.F. Cavins and M. Friedman, *Anal.Biochem.*, 35, 489-493 (1970)

27. J.S. Wall and M. Friedman, *J.Org.Chem.*, 31, 2888 (1986)

28. *J.Chem.Soc.*, 1094 (1952)

29. Peterson, *J.Org.Chem.*, 33, 780 (1968)

30. M. Kato and T. Ito, *Inorg.Chem.*, 24, 509 (1985)

31. E.K. Barefield, *Inorg.Syntheses*, 16, 224 (1976)

32. M. Kodama and E. Kimura, *J.Chem.Soc., Dalton Trans.*, 1720 (1976)

33. A.J. Paterson and J. Schlom, *Int.J.Cancer*, 37, 659 (1986)

34. D. Colcher, P. Horan-Hand, M. Nati and J. Schlom, *Proc.Nat.Acad. Sci.USA*, 78, 3199 (1981)

35. R. Traut *et al.*, *Biochem.*, 12, 3266 (1973)

36. G.L. Ellman, *Arch.Biochem.Biophys.*, 82, 70 (1959)

37. W.C. Eckelman and C.H. Piak, *Nucl.Med.Biol., Int.J.Radiat.Appl. Instrum. Part B*, 13(4), 335 (1986)

38. G. Weber, *J.Biochem.*, 51, 155 (1952)

39. J.R. Benson and P.E. Hare, *Proc.Nat.Acad.Sci.USA*, 72(2), 619 (1975)

40. R.L. Childs and D.J. Hnatowich, *J.Nucl.Med.*, 26, 293 (1985)

41. J. Franz, W.A. Volkert, E.K. Barefield and R.A. Holmes, *Nucl. Med.Biol., Int.J.Radiat.Appl.Instrum. Part B.* 14(6), 569 (1987)

CHAPTER THREE

RADIOLABELLING STUDIES USING TECHNETIUM-99m

3.1 THE LABELLING OF MACROCYCLE-ANTIBODY CONJUGATES

3.1.1 ^{99m}Tc for Radioimmunoimaging

The suitability of ^{99m}Tc for imaging tumours has been discussed in the introduction (section 1.3.3). Its ideal gamma energy (140 eV) and availability from a ^{99}Mo generator have made ^{99m}Tc by far the most widely used radioisotope in diagnostic nuclear medicine (90% of all current applications involve ^{99m}Tc!). In addition, its ability to form "strong" complexes with macrocyclic ligands such as cyclam (section 1.6.7) make ^{99m}Tc an attractive choice for radiolabelling tumour-specific Mab's.

3.1.2 The Labelling of Cyclam-Antibody Conjugates with ^{99m}Tc

In 1980, Volkert *et al.*[1] described the formation of thermodynamically and kinetically stable ^{99m}Tc-cyclam complexes (Figure 3.1) by reducing pertechnetate (TcO_4^-) with stannous chloride in the presence of the macrocycle at pH 11. The yield of complex was reduced at lower pH due to electrostatic repulsion between an increasingly protonated ligand and the oxo-technetium cationic species.

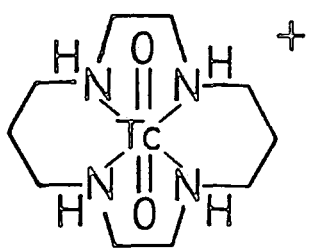

Figure 3.1 *Structure of the ^{99m}Tc complex of cyclam*

The same workers later reported[2] that the rate of incorporation of

technetium by cyclam at pH 7 could be improved dramatically if a weak anionic ^{99m}Tc-citrate complex was used as a carrier species. This method appeared to be ideal for the labelling of cyclam-antibody conjugates since the use of a pH close to physiological pH (7-7.8) would reduce the risk of damaging the antibody. However our fellow workers at Celltech found that the citrate transfer method was ineffective for labelling cyclam-antibody conjugates at pH 7. It would appear that ^{99m}Tc-citrate is more stable at pH 7 than was reported by Volkert *et al.* and it is thought that these workers may have measured the pH of the buffer before addition of the highly basic macrocycle (this makes the buffer much more alkaline).

The incorporation of ^{99m}Tc into antibody-bound cyclam was sufficiently rapid only at pH > 10. It was hoped that the Mab would not be unduly affected by this alien pH. Pertechnetate was pre-reduced in phosphate buffer at pH 6.0 using stannous chloride since there was evidence that reduction at more alkaline pH produces a higher yield of ^{99m}Tc-colloids which cannot then be incorporated by the macrocycle. The reduced technetium was then added to a solution of cyclam-antibody conjugate in bicarbonate buffer at pH 10.8:

$$TcO_4^- \xrightarrow[\text{pH 6/SnCl}_2]{\text{phosphate}} \text{"}TcO_2^+\text{"} \xrightarrow[\text{bicarbonate pH 10.8}]{\text{cyclam-ab}} TcO_2\text{-cyclam-ab}$$

ab = antibody "B72.3"

3.1.3 The Need for Biodistribution Studies

Serum stability studies give a rough indication of the suitability of a ^{99m}Tc-labelled macrocycle-antibody conjugate for *in vivo* diagnosis. If transchelation to serum components is observed, the conjugate is

unequivocably unsuitable. If the conjugate is stable in serum it may be suitable; conclusive evidence of suitability can only be obtained by conducting a biodistribution study in normal (non-tumour bearing) mice. The conjugate is injected intravenously into the tail vein of the mouse and is evenly distributed throughout the cardiovascular system within a matter of seconds. The level of cardiovascular activity falls quite steeply initially as the radiolabelled Mab diffuses from the blood into the extracellular fluid (ECF) until an equilibrium is reached between the blood and the ECF (typically 50% in 24 hours, Figure 3.2). The activity in the blood-pool will then fall more slowly at a rate determined by the rate of antibody catabolism.

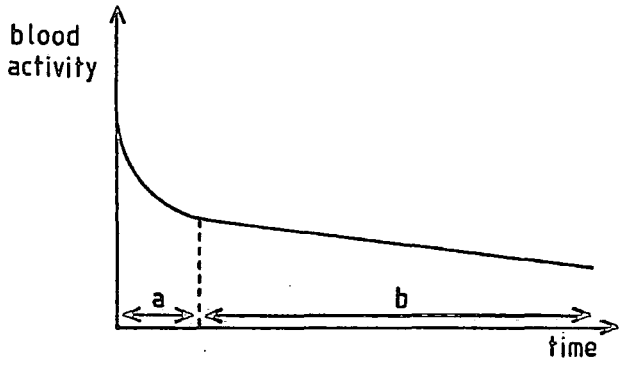

Figure 3.2 *Decreasing cardiovascular activity with time after injection; a= equilibration (~ 24 hours); b= catabolism (several days).*

If the cardiovascular activity falls in a given time by more than the theoretical amount, the radiolabel may have dissociated from the antibody or the antibody may have been damaged and removed from the blood by the liver.

Some accumulation of activity in the liver is inevitable as a result of its blood content (~ 30% by mass) and the leakage of activity from blood capillaries into the extracellular spaces. Higher than

expected levels of activity in the liver may signify that the antibody has suffered damage during the radiolabelling procedure. The free thiol groups of "trauted" antibodies may form disulphide bonds which cross-link individual IgG to form aggregates which would accumulate in the liver. Alternatively high liver activity may be due to dissociation of metal ions from the antibody to form complexes with other metal-binding proteins, *e.g* transferrin, albumin which are subsequently degraded in the liver. Although the exact nature of metal extraction by the liver is unknown, it appears that there are receptors which can bind a variety of metals. In particular there are thiol receptors which seem to extract technetium avidly unless it is strongly chelated to a protein.

It is also important to limit the accumulation of activity in other organs to that arising from their blood content and from the initial equilibration. The interpretation of the activity in the kidney is complicated by virtue of it being the organ of excretion. Small molecules (including proteins of mass < 60000 daltons) can be excreted rapidly into the urine. Several biodistribution time points are required to determine whether there is excessive accumulation in the kidney relative to the blood.

3.1.4 Biodistribution of ^{99m}Tc-cyclam-antibody conjugates

The cyclam-antibody conjugate was labelled at pH 11 (section 3.1.2), then purified from small molecules *e.g* excess $SnCl_2$, using a PD10 column (Sephadex G-25). The biodistribution data at 4 and 24 hours is given in Table 3.1. Two indicators of tissue activity are given: %dose g^{-1} and %dose. The former gives a direct indication of the relative activity in equal masses of different tissues and therefore measures any accumulation of activity in a particular organ over and above that

expected from its blood content and equilibration. However the total dose in that organ depends upon its total mass, which can vary between smaller and larger animals. It is therefore usual to quote the percentage of the total dose contained within an organ in addition to the %dose g^{-1}. The quoted figures are mean values (typically 2 mice per time-point), corrected for decay to time zero (the standard deviations are also given).

Tissue	4 Hours		24 Hours	
	%D g^{-1}	%Dose	%D g^{-1}	%Dose
BLOOD	16.0 ± 0.1	---	7.8 ± 0.4	---
KIDNEYS	13.1 ± 1.3	7.1 ± 0.9	6.9 ± 3.0	3.7 ± 1.8
LIVER	8.8 ± 0.1	13.2 ± 1.0	5.7 ± 1.1	8.7 ± 1.4

Table 3.1 *Biodistribution data for pH 11 conventional labelling; 2 mice per time point.*

At both time-points, the level of activity in the blood is considerably lower than would be expected from equilibration alone. Together with the relatively high kidney levels, this suggests that most of the activity has been excreted within 24 hours. ^{99m}Tc may have been dissociated from the protein as TcO_4^- which is rapidly excreted. Alternatively, the thioether bond linking macrocycle and antibody may be unstable *in vivo* (thiol-vinylpyridine additions are potentially reversible). The liberated ^{99m}Tc-cyclam complex would be eliminated rapidly from the body.

Technetium bound by the macrocycle is unlikely to dissociate *in vivo* due to its kinetic inertness. If the low levels of cardiovascular activity are due to dissociation of ^{99m}Tc form the Mab, technetium must also be bound "non-specifically" by other chelating groups on the protein.

3.1.5 Non-Specific Metal Binding

In addition to a small number of macrocyclic ligands (typically 2 or less), the derivatised antibody contains a multitude of other sites which are capable of binding transition metals, albeit less strongly. Thus cyclam-antibody conjugates contain two types of binding sites - "specific" sites (the macrocycles) and "non-specific" sites (the protein itself). Non-specific binding sites can successfully compete with much "stronger" ligands such as macrocycles by virtue of their higher concentration on the antibody.

It is known that non-specific binding sites which chelate ^{99m}Tc are of two different types: high capacity, low affinity sites and low capacity, high affinity sites. The addition of a 10 fold excess of DTPA can prevent the binding of technetium to low affinity sites but no amount of DTPA can prevent binding to high affinity sites. Paik *et al.*[3,4] reported that high affinity sites were related to free thiol groups produced by the reduction of the disulphide bridges linking the two heavy chains (section 1.2.2). They proposed the use of high affinity sites to bind ^{99m}Tc strongly to Mab's without the need for conjugating chelating agents such as DTPA. Although equal to conjugated DTPA in terms of effectiveness, with a much simpler protocol, this method of binding ^{99m}Tc cannot compete, in terms of *in vivo* kinetic inertness, with the use of a macrocyclic ligand *e.g* cyclam.

3.1.6 Prevention of Non-Specific Binding

Since the majority of non-specific technetium is bound by low affinity sites it can be removed using a *chelate wash*. In addition to EDTA and DTPA, other suitable chelates may include amino acids *e.g* histidine

responsible for non-specific binding or thiol-containing ligands *e.g* 2-mercaptoethanol. Whatever the choice of chelate, there remains a limit to the amount of non-specifically bound ^{99m}Tc which can be removed - 15% remains bound according to Paik *et al.*[4], but the quantity probably varies for different Mab's.

The only effective way to reduce non-specific metal-binding to zero is to label the macrocycle before it is coupled to the antibody - this strategy is called *pre-labelling*.

3.2 PRE-LABELLING

3.2.1 Conventional versus Pre-Labelling

The direct or "conventional" labelling of cyclam-antibody conjugates with ^{99m}Tc produces a large excess of non-specifically bound radiolabel (Figure 3.3) which dissociates *in vivo* lowering the tumour:background activity ratio. Pre-labelling of the macrocycle with ^{99m}Tc in the absence of the Mab would seem to provide the ideal solution to this problem. Once radiolabelled, the macrocycle is conjugated to thiols on the antibody in the usual manner (Figure 3.4).

The pH and temperature of the radiolabelling buffer is no longer restricted to close to physiological pH by the presence of the antibody. The macrocycle can therefore be labelled at a pH at which incorporation is known to be rapid. Another advantage of pre-labelling is that the Mab does not come into contact with the stannous chloride reducing agent, so the risk of damage to disulphide bridges is absent.

Unfortunately pre-labelling is not a perfect solution to the problem of non-specific binding since it adds greater complexity to the

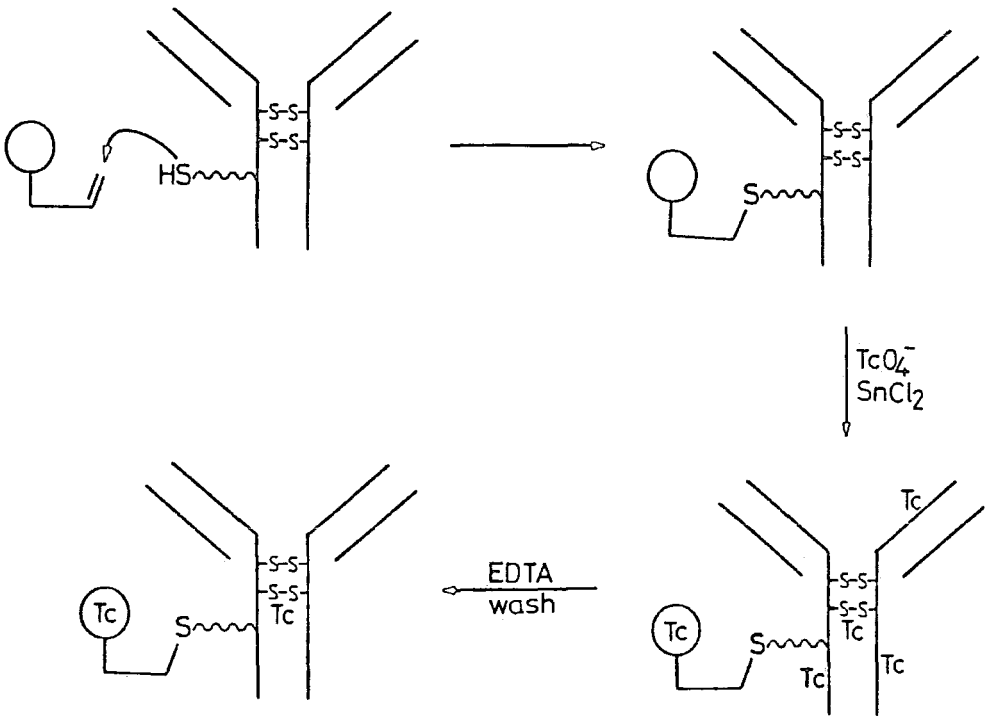

Figure 3.3 *The Conventional Labelling Strategy*

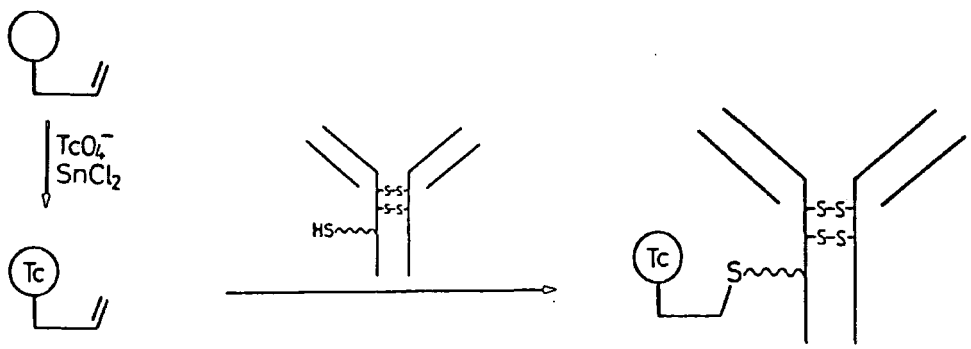

Figure 3.4 *The Pre-labelling Strategy*

preparation of the radiopharmaceutical. There are two reactions and purifications which must be performed by a hospital clinician, both involving potentially hazardous radioactive materials. Pre-labelling is also more time-consuming, especially if the conjugation step is slow; an important consideration in view of the short half-life of ^{99m}Tc (6.02h)! The advantages and disadvantages of conventional and pre-labelling protocols are summarised in Table 3.2.

CONVENTIONAL LABELLING	PRE-LABELLING
Advantages	Advantages
* Simple one-pot protocol	* No Non-Specific Binding
Disadvantages	* pH and temperature of labelling not restricted by antibody.
* Reduced Tc binds non-specifically.	* Tc insertion into macrocycle rapid and easily quantifiable.
* Some non-specifics cannot be removed by a chelate wash.	* Antibody does not "see" reducing agent.
* High liver uptake of non-specific Tc *in vivo*.	Disadvantages
	* More steps
	* Duration of conjugation step critical due to short half-life.

Table 3.2 *Conventional Labelling and Pre-Labelling Compared*

3.2.2 A Pre-Labelling Strategy for ^{99m}Tc

A radiolabelled macrocycle-linker conjugate was prepared by reacting reduced ^{99m}Tc ($SnCl_2$; pH 6) with the cyclam-2-vinylpyridine conjugate (40) at pH 11 (80°C):

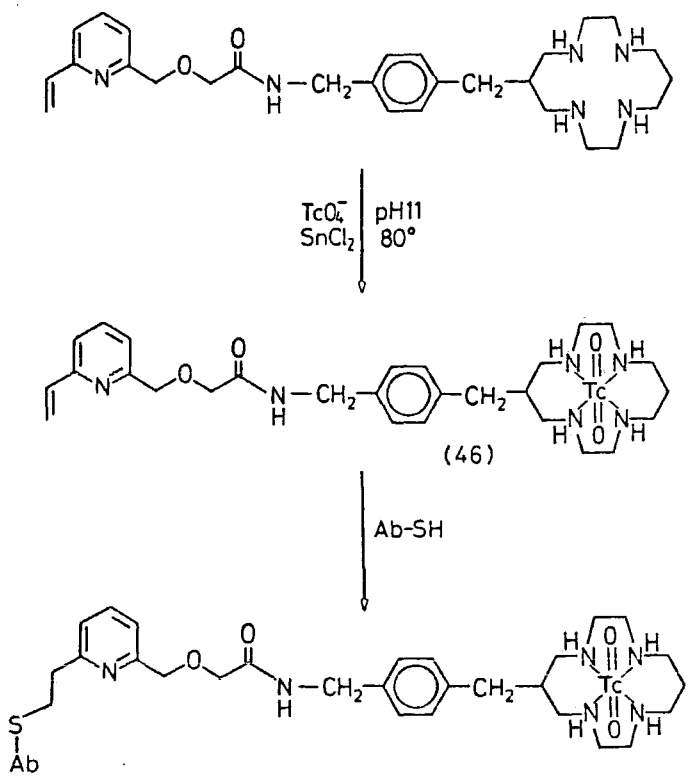

The incorporation was greater than 95% under these conditions and the 2-vinylpyridine group was apparently unaffected by the high pH and temperature. The ^{99m}Tc complex was separated from excess free macrocycle and TcO_4^- using cation exchange HPLC. The recovery of activity from the column was poor (< 50%). The purified radiolabelled conjugate (46) was then reacted with the trauted antibody (B72.3) for 2 hours at 37°C. The yield of ^{99m}Tc-mac-ab was poor (< 0.5% of the activity was associated with the protein) due to the low reactivity of 2-vinylpyridines towards thiols.

The ^{99m}Tc-mac-ab conjugate was purified using a PD10 column and injected into mice. The biodistribution data at 19.5 hours is given in Table 3.3. The blood level is higher than that given by the conventional labelling strategy - 13.4% dose g^{-1} at 19.5 hours for pre-labelling, compared to 7.8% dose g^{-1} at 24 hours for conventional labelling. However the level of activity in the liver is extremely high, indicating accumulation of the radiolabel. On this occasion, the build up of

activity in the liver cannot be due to non-specifically bound ^{99m}Tc, of which there is none, nor to cleavage of the macrocycle-antibody bond since ^{99m}Tc-cyclam is rapidly excreted by the kidneys. It is therefore likely that the high liver activity is due to aggregated protein, arising from intermolecular cross-linking of free thiol groups, but this cannot be a definitive statement on the basis of a single experiment.

Tissue	%D g^{-1}	%Dose
BLOOD	13.4 ± 1.8	32.4 ± 5.4
KIDNEYS	4.3 ± 0.0	2.5 ± 0.2
LIVER	14.1 ± 3.7	22.6 ± 2.2

Table 3.3 *Biodistribution of a pre-labelled ^{99m}Tc-cyclam antibody conjugate at 19.5 hours; 2 mice per time point.*

3.2.3 Xenograft Studies using Pre-labelled Antibody Conjugates

A sample of the pre-labelled ^{99m}Tc-mac-ab conjugate was injected intravenously into mice containing *xenografts* (human tumours implanted into immunosuppressed mice) displaying the antigen (TAG-72) recognised by B72.3. Another ^{99m}Tc-mac-ab conjugate was prepared as a control, containing the non-specific Mab MOPC21. The biodistribution data at 16 hours and the tumour:blood and tumour:liver ratios are given in Tables 3.4 and 3.5 respectively.

%D g^{-1}	MOPC21	B72.3
TUMOUR	4.2	7.3
BLOOD	13.6	10.9
LIVER	7.0	6.5
KIDNEY	4.9	4.5
COLON	1.7	1.3
SPLEEN	4.2	3.8

Table 3.4 *Biodistribution data for tumour-bearing animal at 16 hours.*

	TIME	TUMOUR/BLOOD	TUMOUR/LIVER
^{99m}Tc-MOPC21	(16h)	0.31	0.6
^{99m}Tc-B72.3	(16h)	0.67	1.1
^{125}I-MOPC21	(24h)	0.44	1.7
^{125}I-B72.3	(24h)	0.90	3.9

Table 3.5 *Comparison of B72.3 Animal Data for ^{99m}Tc and ^{125}I*

The tumour: blood and tumour:liver ratios for ^{99m}Tc-B72.3 are roughly twice those of the control Mab (MOPC21), indicating selective accumulation of activity in the tumour. However this level of selectivity is lower than that obtained using ^{125}I-B72.3 - in particular the tumour:liver ratio is inferior for ^{99m}Tc. This suggests that the method of attaching the ^{99m}Tc-binding macrocycle may be more damaging than the method used for iodination of the antibody. Aggregated Mab's produce higher liver levels, deactivated Mab's lower tumour levels. Aggregated Mab's are not removed using a PD10 column; size exclusion HPLC being required for their separation. However HPLC is not a practicable procedure for a hospital clinician to follow. Site-specific labelling would help reduce aggregation of Mab's and loss of immunoreactivity if the macrocycle was suitably located outside the antigen-binding region.

The specific activity of ^{99m}Tc which could be attached to B72.3 using the 2-vinylpyridine method was much too low for the tumour to be imaged externally. If the length of the conjugation procedure was extended, the yield of Tc-mab-ab could be improved but would be more than offset by the decay of ^{99m}Tc to ^{99}Tc ($t_{\frac{1}{2}}$ 6.02h).

3.3 MORE REACTIVE THIOL-SPECIFIC CROSS-LINKERS

3.3.1 Enhancing the Reactivity of Vinyl Pyridines

The usefulness of a pre-labelling strategy for short-lived ^{99m}Tc depends upon the kinetics of attachment of the labelled macrocycle being sufficiently rapid. Conjugation of a 2-vinylpyridine conjugate is simply too slow for sufficient specific activity to be attached to the Mab. For this reason a number of other vinyl-substituted nitrogen heterocycles are currently being tested by our collaborators at Celltech for enhanced reactivity towards antibody thiols *e.g* 4-vinylpyridine (47), vinyl-2,2-dipyridine (48) and 4-vinylpyrimidine (49):

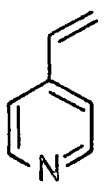

(47)

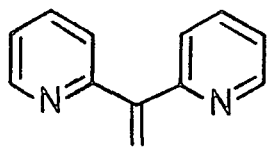

(48)

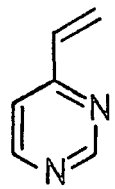

(49)

Unfortunately many macrocycle-linker conjugates containing faster-reacting nitrogen heterocycles have proved much more difficult to synthesise than the 2-vinylpyridine derivative. Others have exhibited only modest improvements in reactivity.

3.3.2 Maleimide Cross-Linking Agents

Maleimides are much more reactive towards thiols than even the fastest-reacting vinylpyridine[5-7]. Problematically, they are also more reactive towards other groups on the antibody (less thiol-specific). Maleimides are also more sensitive to pH; losing their reactivity through ring

opening at high pH (section 2.4.3).

If these problems can be overcome, or at least minimised, maleimides are potentially useful as part of a pre-labelling strategy. Moreover since several maleimide cross-linkers are commercially available, no long synthetic procedures would be required for the preparation of macrocycle-linker conjugates.

3.3.3 The pH Sensitivity of Maleimides

One of the main shortcomings of maleimides for pre-labelling is their tendency to ring-open and/or react with amine groups at high pH. Since cyclam can only be labelled successfully above pH 10 and most maleimides ring-open below pH 7, the pre-labelling of a cyclam-maleimide conjugate is not a realistic option. However some maleimide cross-linkers are somewhat less pH sensitive than others[8,9]. One such derivative is commercially available: sulfosuccinimidyl-4-(N-maleimidomethyl) cyclohexane-1-carboxylate (50):

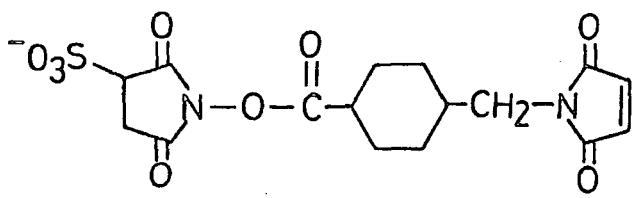

(50)

It was found that the maleimide group of (50) was stable for at least 9 hours in aqueous buffer at pH 6.5 in the presence of equimolar amounts of cyclam, as determined by ^{1}H NMR. The integral of the maleimide singlet (δ 6.83) remained unchanged throughout the experiment. The only hydrolysis reaction which occurred was that of the N-hydroxysuccinimide

ester group.

This stability study suggests that the maleimide group of a macrocycle-(50) conjugate could be sufficiently stable towards ring opening and unreactive towards secondary ring nitrogens to allow ^{99m}Tc labelling at neutral pH.

3.4 LOWERING THE pH OF ^{99m}Tc LABELLING

3.4.1 Phenols versus Non-Phenols as Tc binders

As discussed in section (2.2.1), it was hoped to enhance the kinetics of uptake of ^{99m}Tc by cyclam by providing an additional anionic donor site in the form of a phenol-pendent group.

The influence of the phenol upon the kinetics of uptake was monitored radiochemically using acetylated forms of the functionalised phenolic and non-phenolic macrocycles (19) and (29).

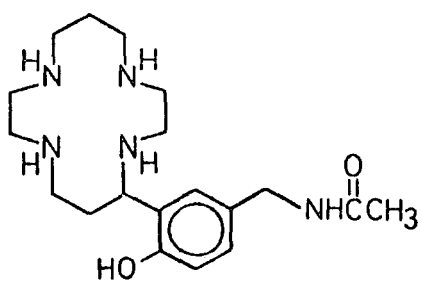

(51)

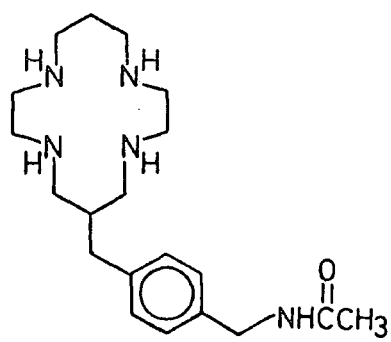

(52)

The synthesis of the aminomethyl forms of these macrocycles has been described elsewhere (section 2.2.6 and 7.3.1). The exocyclic amino group can be acetylated selectively, with p-nitrophenyl acetate, using the strategy of pH control described in section 2.6.3. Acetylation

prevents any possible influence of the primary amino group upon the kinetics of association, thereby simulating the circumstances of the conjugated macrocycle. Cycles (51) and (52) were transferred to our collaborators at Celltech for radiolabelling experiments.

The rates of uptake of ^{99m}Tc by (51) and (52) were compared using cation exchange HPLC radiometry. At pH 10.8, the phenolic cycle was found to incorporate ^{99m}Tc at an essentially similar rate to the non-phenol. However at lower pH (8.95), the difference between the two cycles was much more marked (Figure 3.5). After 30 minutes, the non-phenol had bound a mere 13% of the available activity, whereas the phenol had bound 72%. After 60 minutes the contrast between the 2 cycles was slightly less pronounced. The incorporation by the non-phenol had increased substantially (to 23%), the phenol only slightly (to 75%). The total amount of activity recovered from the HPLC column was less than 100% of the TcO_4^- activity for the non-phenol, indicating that uncomplexed Tc had been retained on the column. The activity ascribed to a single ^{99m}Tc-(51) complex actually comprised 2 peaks eluting very close together, suggesting two complexes with similar charge.

The phenolic group of (51) must be implicated to explain its rapid association kinetics compared to (52). At pH 8.95 the phenol group of (2) is substantially ionised (pK_a 8.86); interacting strongly with the diprotonated ring and reducing the overall charge of the ligand from +2 to +1 (Figure 3.6)[10].

The rate enhancement could be explained purely on the grounds of lower electrostatic repulsion towards the incoming technetium cation, without invoking bond formation between technetium and the phenol. Alternatively the phenol could serve to pre-orientate the "TcO_2^+" species for rapid incorporation into the ring (Figure 3.7).

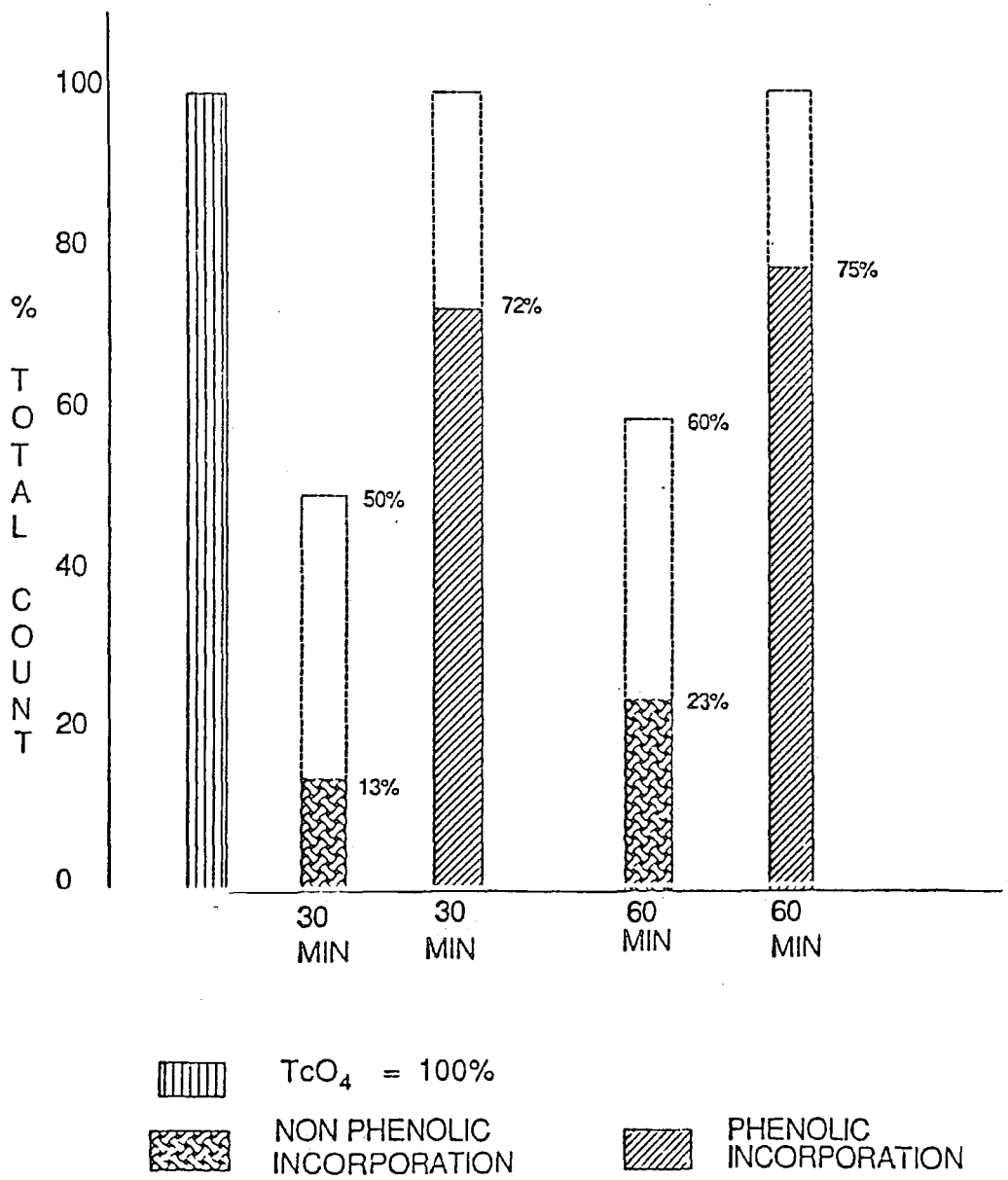

Figure 3.5 *The Incorporation of Reduced ^{99m}Tc by Phenolic and Non-Phenolic Cyclam Derivatives at pH 8.95 (1.0M $NaHCO_3$); Reduction in 0.5M phosphate (pH 6.0); 20°C.*

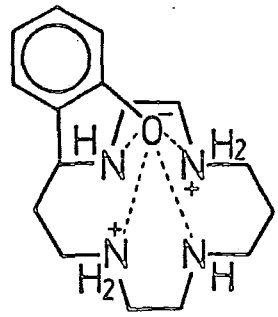

Figure 3.6 *Stabilisation of the phenolate anion of (2)*

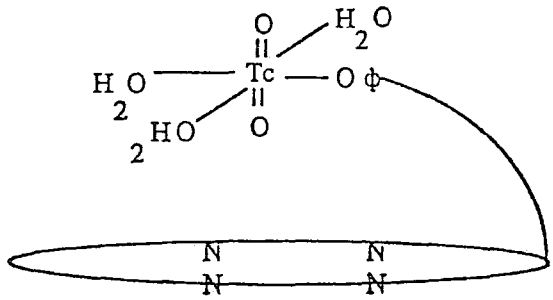

Figure 3.7 *Potential Intermediate Species in the Complexation of ^{99m}Tc by Phenolic Cyclam.*

The explanation for the apparent existence of two ^{99m}Tc-(51) species may lie with the ability of the phenol to act as an extra axial donor (section 1.5.7). One species may involve axial phenolate coordination whilst the other may contain unbound phenol (Figure 3.8).

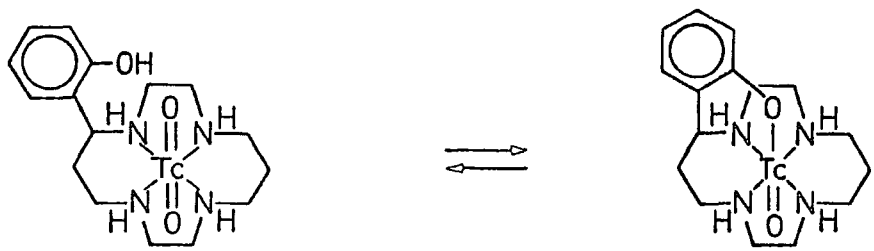

Figure 3.8 *A Possible Role for Axial Phenolate Binding*

To the author's knowledge there is no precedent for Tc(V)-amine complexes containing mono-oxo rather than dioxo cores. However, if the oxidation state of Tc were to be reduced from +5 to +4 by phenolate binding, the overall charge (+1) of the complex would not change, consistent with the observed HPLC profile.

Whatever the exact rôle of the phenol group in the kinetics of association, the implication for radiolabelling is readily apparent. Antibody-bound phenolic cyclam may be labelled satisfactorily at a lower pH than is possible for cyclam itself. However the pH must be reduced still further if maleimides are to provide a viable pre-labelling strategy.

3.4.2 Nitrophenol-pendent Cyclams for Tc Binding

If the increased rate of Tc binding observed for (51) at pH 8.95 is related to deprotonation of the phenol at that pH, it may be possible to achieve further rate-enhancing effects at even lower pH by reducing the pK_a of the phenol still further.

Generally electron-withdrawing substituents increase the acidity of phenols. The reduction of the pK_a is dependent upon the number of substituents, their electron-withdrawing power and their position in the ring. Ortho and para-substituted nitro groups are particularly effective:

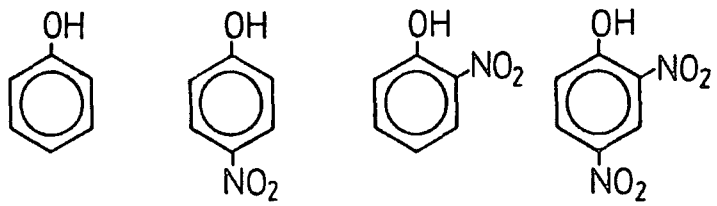

pK_a	10.0	7.15	7.17	4.10

Kimura *et al.*[11] found that the pK_a's of 4-nitrophenol and 2,4-dinitrophenol are even lower when attached to tetraamine macrocycles due to the stabilisation of the phenolate anion by the dipositive charge of the ring (Figure 3.6).

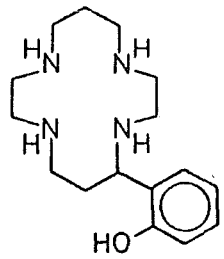

(2)

pK_a 8.86

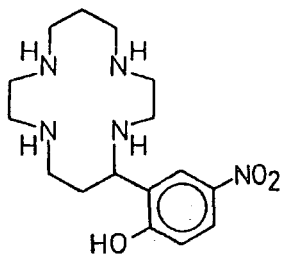

(5)

6.37

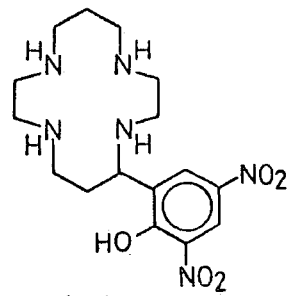

(53)

2.90

The mononitrophenol of cycle (5) is substantially deprotonated at pH 7. The dinitrophenol of (53) is completely ionised. Both cycles may therefore be compatible with the use of maleimide linker molecules. The synthesis of a functionalised nitrophenol-pendent cyclam is described below.

3.4.3 Synthesis of a Functionalised Nitrophenol-pendent cyclam

A procedure reported by Kimura *et al.*[11] was adapted for the synthesis of a functionalised ortho-nitrophenol-pendent cycle (54) (see overleaf). The pentaamine (19) was protected with trifluoroacetic anhydride in an attempt to prevent N-nitration, *ipso* nitration and/or oxidative cleavage of the aryl group from the macrocycle. After nitration with HNO_3/H_2SO_4 (3:2), the protecting groups were removed with aqueous base in methanol. On acidification (acetic acid), a yellow solid precipitated which was identified by ^1H NMR and Negative FAB mass spectroscopy to be a pure

sample of the dinitrophenolic cycle (53). The absence of benzylic methylene protons ($\delta \sim 4$ ppm) in the ^{1}H NMR spectrum was diagnostic.

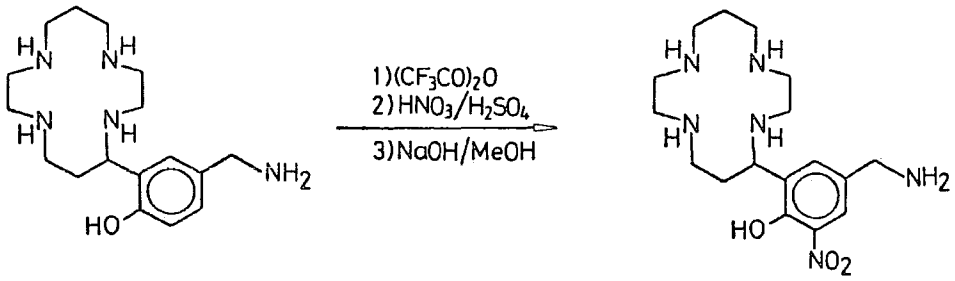

(19) (54)

It was apparent that *ipso*-nitration had occurred at the para position bearing the protected aminomethyl substituent (followed by loss of the amido substituent). It is possible that primary trifluoroacetamides are less robust than secondary trifluoroacetamides in the nitrating mixture of concentrated acids, HNO_3 and H_2SO_4. Certainly the alkyl substituted ortho position will be more hindered (by the macrocycle) than the para position towards attack by nitronium ions. Perhaps this explains why predominantly dinitro compound is obtained. A small amount of the desired product (54) was isolated as a yellow solid by cation exchange HPLC from the crude material which remained in solution in aqueous acetic acid. Since the overall yield of (54) was a meagre 2.3%, this would not appear to be a viable route.

3.4.4 Sulphonic Acid-Phenol-pendent Cyclams for Tc Binding

There are few electron-withdrawing groups which can be introduced in a one-pot reaction of the functionalised pentaamine (19). One such group, a sulphonic acid, is easily introduced by dissolving the macrocycle in 98% H_2SO_4. Low temperature sulphonation generally produces a mixture of ortho and para isomers. At higher temperatures, the more

thermodynamically stable meta isomer is formed[12]. In terms of reducing the pK_a of the phenol, sulphonic acid substituents are much less effective than nitro groups. However sulphonic acid groups themselves are ionised at neutral pH and it would be instructive to investigate the effect of another charged species other than phenol upon the rate of uptake of ^{99m}Tc at this pH.

One ortho and two meta positions in the phenol group of cycle (19) are available for sulphonation. The cycle was dissolved in 98% H_2SO_4 and heated to 100°C for 1 hour. Somewhat surprisingly in view of the elevated temperature used, the major isomer in the product mixture was the ortho derivative (55); the meta coupling (2.2 Hz) of the two protons of the aromatic ring being diagnostic. A small sample of (55) was isolated by cation-exchange HPLC as the triacetate salt, for analytical purposes and ^{99m}Tc labelling studies (section 3.5.1).

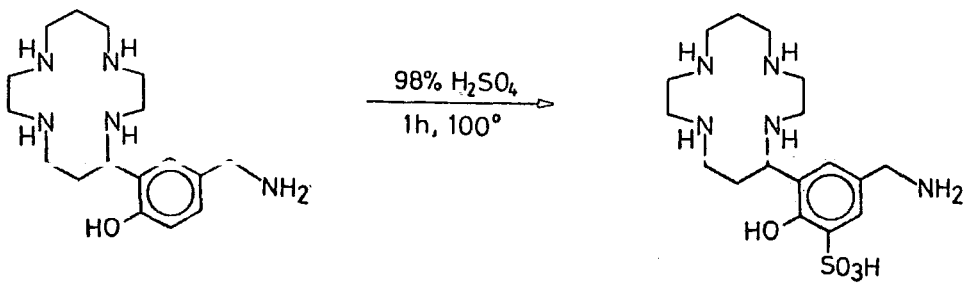

(19) (55)

3.5 TECHNETIUM LABELLING STUDIES AT NEUTRAL pH

3.5.1 The Potential of a Series of Tetraamine Ligands for pH7 Labelling

In experiments conducted at the MRC Radiobiology Unit, Harwell for safety reasons, the author tested the binding efficacy of a series of

tetraamine ligands towards ^{99m}Tc at neutral pH (section 3.7). The aim was to identify cycles which might be used in conjunction with maleimides in a pre-labelling protocol.

Eight ligands were investigated: 6 macrocyclic and 2 open-chain tetraamines (Figure 3.9).

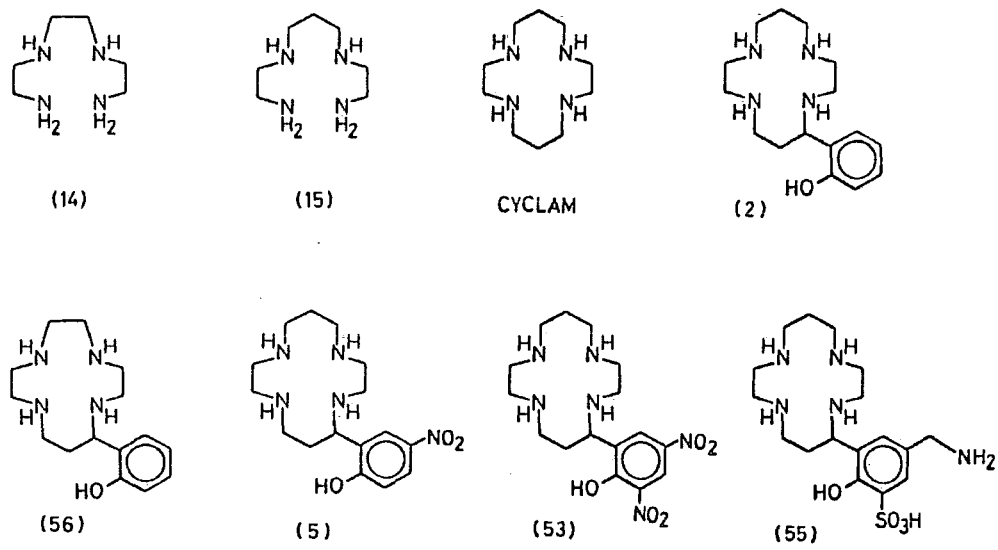

Figure 3.9 *Candidate tetraamine ligands for neutral pH* ^{99m}*Tc labelling.*

By analogy with the association kinetics of copper(II) and tetraamine ligands (section 5.1.2), the rate of incorporation of ^{99m}Tc by open-chain ligands is expected to be substantially faster than for macrocycles, under a pH régime (*e.g* pH 7) where both ligands are protonated. The application of open-chain ligands for binding transition metals *e.g* Tc is usually limited by the instability of their chelate complexes *in vivo* (section 1.4). However the work of Volkert *et al.*[2] could not distinguish between the stability of ^{99m}Tc-cyclam and the ^{99m}Tc complex of the open-chain tetraamine, 1,5,8,12-tetraazadodecane with respect to acid-induced decomplexation.

The basic cyclam system is included as a reference, even though its rate of uptake is likely to be very slow at this pH. The phenolic ligands (2), (5), (53) and (55) have been discussed *vide ante*. The inclusion of the $13N_4$ cycle (56) should provide an indication of the rôle of the phenol in a smaller macrocycle. Volkert *et al.*[13] hinted that the Tc-N bonds in ^{99m}Tc-cyclam might be slightly longer than their optimum value (section 1.6.4). The slightly smaller cavity of $13N_4$ might enhance *in vivo* stability still further.

3.5.2 Results of the Labelling Studies

The labelling yields for all 8 ligands, as determined by HPLC radiometry, were relatively low at pH 7 (Table 3.6). However these figures are misleading because the recovery of activity from the cation exchange column was very poor. An injection of TcO_4^- gave a recovery of activity of only 34% (TcO_4^- should pass straight through the column). This suggests that the generator eluent was impure (a previous generator had produced 2 separate peaks for an injection of supposedly pure TcO_4^-!). It was therefore decided to relate the labelling yields to the amount of recovered rather than injected TcO_4^- (Table 3.6).

3.5.3 Discussion of Labelling Yields

As expected, cyclam did not incorporate measurable amounts of ^{99m}Tc at pH 7 due to electrostatic repulsion between the diprotonated ring and incoming TcO^{3+} and TcO_2^+ species.

The phenolic groups of (2) and (56), with pK_a's 8.86 and 8.71 respectively, will also be substantially protonated at pH 7. However since both ligands show significant uptake of ^{99m}Tc, it is conceivable

that sufficient is ionised to reduce the charge on the ring and its electrostatic repulsion towards the oxo-technetium cation.

LIGAND	Reaction Time(mins)	% Labelling Yield vs TcO_4^- standard	% Labelling Yield vs TcO_4^- injection
(14)	48	7.8	23
(15)	46	20.8	60
CYCLAM	25	0.0	0
(2)	33	(i) 5.6 (ii) 12.7	(i) 16 (ii) 38
(56)	34	12.2	36
(5)	38	15.5	46
(53)	32	2.5	7
(55)	32	4.0	11

Table 3.6 *Labelling Yields for a series of Tetraamine Ligands with* ^{99m}Tc.

There does not seem to be a direct correlation between the pK_a of the phenol and the rate of uptake. The dinitrophenolic cycle (53) shows very low incorporation at pH 7 even though its phenol is completely ionised (pK_a 2.90). The mononitrophenol (5) shows much better incorporation even though its phenol is not completely deprotonated at pH 7 (pK_a 6.37). However the sulphonic acid-phenol cycle (55) shows much lower incorporation than (2) which is consistent with the lower acidity of the phenol ($pK_a \sim 12$). There would not appear to be a rate-enhancing effect arising from the negative charge on the sulphonic acid group at this pH.

A most curious feature of ^{99m}Tc binding by (2) is the appearance of two peaks (Figure 3.10). These peaks are more widely separated on HPLC than those observed previously for the acetamidomethyl derivative (51). The second peak (at 9 minutes) may be due to a dicationic species in

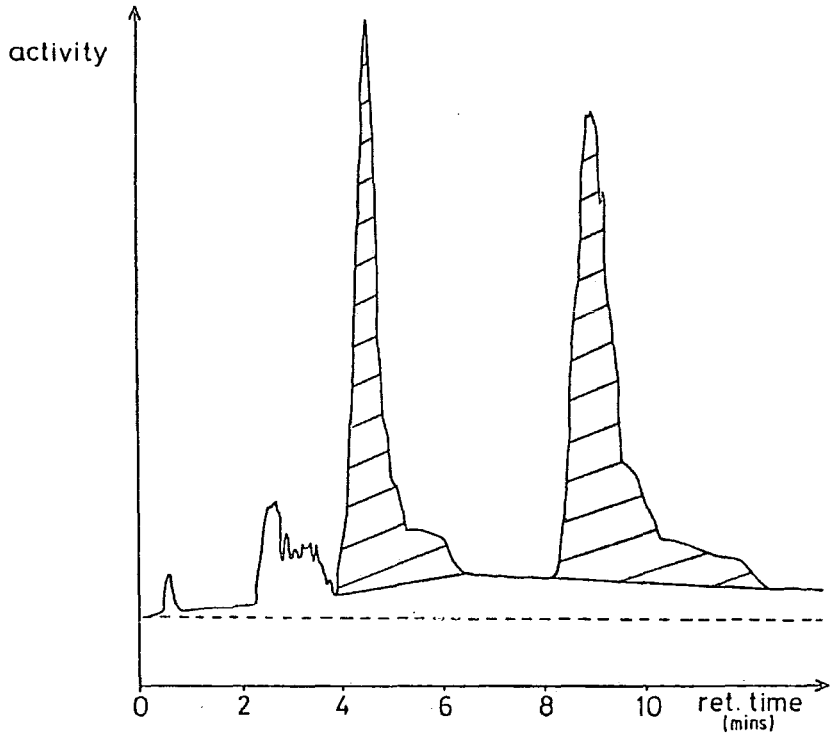

Figure 3.10 *HPLC Radiometry Profile for the Reaction between Reduced ^{99m}Tc and (2) at pH7 (33 min; 20°C).*

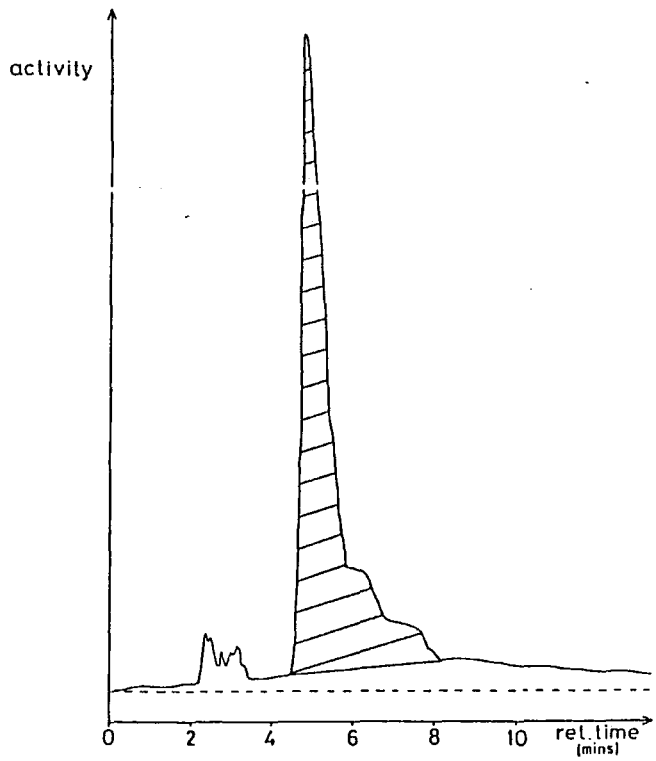

Figure 3.11 *HPLC Radiometry Profile for the Reaction between Reduced ^{99m}Tc and (15) at pH7 (46 min; 20°C).*

which an axial phenolate group (one e^- donor) has replaced one of the oxo groups (two e^- donor) (Figure 3.8). If both species were mono-cationic, technetium would be present in the +4 rather than +5 oxidation state in the complex where the phenolate was bound. It is a mystery why no secondary peaks are observed for (56), (5), (53) and (55). If the two peaks are taken together, the uptake of ^{99m}Tc by (2) is better than for any of the other macrocycles (54%).

The best incorporation of all (60%) was provided by the acyclic tetraamine, 1,4,8,11-tetraazaundecane (15), essentially a single peak eluting at 5.1 minutes (Figure 3.11). In contrast, 1,4,7,10-tetraaza-undecane (14) gave a disappointing incorporation (23%) and the reaction mixture contained large quantities of TcO_4^-. In fact several of the samples contained TcO_4^-, whether from re-oxidation or incomplete reduction is not clear on the basis of one result. Many of the peaks were broad - this may be improved using a gradient eluent system.

The reason for the generally low recovery of injected ^{99m}Tc from the column, even in the case of TcO_4^-, is unclear. The recovery of activity was particularly poor for those ligands which gave little or no peaks with retention times 4-5 minutes. This suggests that reduced uncomplexed ^{99m}Tc sticks to the column.

Since these results are based on a single experiment, it would be unwise to draw too many conclusions from the data. In view of the necessity to conduct all radiolabelling experiments at Harwell, it was not possible to substantiate these observations in repeat experiments. However it is likely that this work will be continued by other workers.

3.6 CONCLUSIONS

It has been established by a number of workers, including our collaborators at Celltech, that ^{99m}Tc binds non-specifically to the protein when Mab's are labelled directly with reduced technetium. Non-specifically bound Tc dissociates *in vivo* and is removed from the blood-pool. Pre-labelling solves the problem of non-specific binding but introduces other constraints. The only cross-linker which could withstand the pH required for ^{99m}Tc labelling of cyclam (pH 11), a 2-vinylpyridine derivative, reacted too slowly for sufficient specific activity to be attached to the Mab B72.3 for imaging a xenograft bearing the antigen TAG-72. The tumour uptake was also relatively low presumably due to damage to the antigen-binding site caused by the "trauting" and conjugation procedure - site-specific labelling would be better.

Commercially available cross-linkers containing maleimide groups should be more effective in a pre-labelling strategy by virtue of their greater reactivity towards thiols. However, since maleimides are unstable at the high pH required for ^{99m}Tc labelling of cyclam, alternative macrocycles which could be labelled at neutral pH were required. A phenol-pendent cyclam derivative was found to incorporate reduced Tc more rapidly at pH 9 than cyclam itself. With this result in mind, the rate of uptake of ^{99m}Tc by a series of derivatised phenolic macrocycles and acyclic ligands was investigated by the author. At this pH, cyclam did not incorporate ^{99m}Tc at all. The phenolic derivatives were much better although yields were lower than at pH 9. An acyclic ligand, 1,4,8,11-tetraazaundecane gave the best uptake of all at neutral pH. It may prove to be useful for pre-labelling if the *in vivo* stability of its ^{99m}Tc complex is sufficiently high.

The phenolic cyclam (2) was the only ligand to produce two distinct ^{99m}Tc complexes. It is possible to speculate that the phenol is bound (as phenolate) to technetium in one of these complexes (Figure 3.8) but this postulation cannot be substantiated from experiments at the tracer level. A crystal structure of the ^{99}Tc complex of (2) would be required to ascertain whether or not the phenol coordinates to Tc. Similarly association kinetics experiments at the macroscopic level (using ^{99}Tc) would be required to rationalise the rôle of the phenol in enhancing the rate of uptake at low pH.

There did not appear to be a direct relationship between the rate of uptake at lower pH and the pK_a of the phenol, although these results are based upon a single experiment and should not be over-interpreted at this stage.

In conclusion it appears that pre-labelling is the only effective strategy for avoiding non-specific Tc binding. Several phenol-pendent macrocycles and acyclic ligands show promising rates of uptake of reduced Tc at neutral pH. Their use in conjunction with maleimide cross-linkers as part of a pre-labelling strategy is worthy of further investigation.

3.7 EXPERIMENTAL

3.7.1 Reagents

The ligands, 1,4,8,11-tetraazacyclotetradecane (cyclam), 1,4,7,10-tetraazadecane (2,2,2-tet) and 1,4,8,11-tetraazaundecane (2,3,2-tet) were purchased from Aldrich, Fluka and Strem respectively and were used without further purification.

The phenolic macrocycles, 11-(2-hydroxyphenyl)-1,4,7,10-tetraaza-cyclotridecane (56), 5-(2-hydroxyphenyl)-1,4,8,11-tetraazacyclotetra-decane (2) and 5-(2-hydroxy-5-nitrophenyl)-1,4,8,11-tetraazacyclotetra-decane (5) were synthesised according to the method of Kimura *et al.*[10,11] (see sections 7.3.1 and 7.3.5 for synthetic procedures).

The dinitrophenolic cycle, 5-(2-hydroxy-3,5-dinitrophenyl)-1,4,8,11-tetraazacyclotetradecane (53) was synthesised accidentally during the nitration of (19) (see sections 3.4.4 and 7.3.6). The synthesis of 5-(2-hydroxy-3-sulphonic acid-5-aminomethylphenyl)-1,4,8,11-tetraazacyclotetradecane (55) is described in section 3.4.5 and outlined in section 7.3.6.

Stannous(II) chloride was purchased from Aldrich and all buffer materials were obtained from BDH. The $^{99m}TcO_4^-$ was eluted from a sterile ^{99}Mo-^{99m}Tc shielded "Amertec 11" generator (Amersham) with 0.9% saline. Doubly distilled deionised water was used throughout.

3.7.2 Stock Solutions

Ligands

Most of the stock solutions were 20mM in ligand. However the nitro-phenol-pendent cycles (5) and (53) could only provide a 14.3 mM stock solution due to their poor solubility in water.

Stannous chloride

Stock solutions of $SnCl_2$ (2.18 mM) were prepared daily by dissolving *e.g* 17.5 mg $SnCl_2$ in 4.23g of 10mM HCl (21.8 mM), followed by a ten-fold dilution in distilled water.

Buffers

0.5M phosphate (pH 7.0) and 0.2M citrate (pH 6.0) buffers were prepared.

Technetium

The eluent volume was adjusted each day (to allow for decay of the generator) to provide a stock solution which contained an activity of 5.6 μCi/μL at 10:00h on the morning of the labelling experiment.

3.7.3 Labelling

Pertechnetate (11.2 μCi; 21.3 x 10^{-15} mol) was reduced using stannous chloride (54.7 μM) in the presence of the tetraamine ligand (1 mM) at pH 7.0 (0.5M phosphate) at room temperature.

The reaction mixture (total volume 100 μL) was prepared from the following ingredients:

1) $^{99m}TcO_4^-$ (11.2 μCi† in 2 μL saline)
2) $SnCl_2$ (2.5 μL of 2.188 mM solution in 1 mM HCl)
3) Phosphate buffer (90.5 μL of 0.5M solution)
4) Ligand (5μL of 20 mM solution)

The reaction mixtures containing the less soluble nitrophenolic ligands were prepared using 7 μL of 14.3 mM ligand stock solution with correspondingly less phosphate buffer (88.5 μL).

3.7.4 Monitoring the Rate of Incorporation

The rate of uptake of ^{99m}Tc was monitored by HPLC radiometry. After a reaction period of between 25 and 48 minutes, 20 μL of the reaction

---

†at 10:00h on the morning of the experiment

mixture was mixed with 10 μL of 0.2M citrate buffer (pH 6.0). 20 μL of the resulting solution was injected onto the HPLC column (cation exchange resin CM300 "Synchropak") and eluted isocratically with pH 6.5 buffer (6% 1.0M NH_4OAc; 30% CH_3CN; 64% H_2O) at a flow-rate of 1.4 cm^3 min^{-1}.

3.7.5 Recovery of Activity

The total eluent from each injection (flow time ~ 15 mins) was collected and counted separately to establish the activity recovered relative to that retained on the column. The recovered activity was compared to the amount of injected activity. A TcO_4^- standard was used for this purpose: 20 μL of a solution containing 2 μL of TcO_4^- stock solution in 98 μL phosphate buffer was diluted with 10 μL citrate buffer and 20 μL was counted. The time at which the TcO_4^- standard was counted was recorded such that all further counts could be time-corrected for decay using the equation:

$$A_t = A_o \, e^{-\lambda t}$$

where A_t = activity at time, t,

A_o = activity at time, t_o and

λ = transformation constant = $0.693/t_{\frac{1}{2}} = 0.63/6 = 0.105\ h^{-1}$ for ^{99m}Tc

For example, a sample giving 2100 cpm at 12:00h will give at 14:30h on the same day:

$$2100 \times e^{-(2.5 \times 0.693)/6} = 1573 \text{ cpm.}$$

It became clear at an early stage that a large amount of activity was sticking to the column despite the use of citrate buffer in an attempt to chelate unreacted reduced technetium. In fact an injection of TcO_4^- as a control gave a recovery of activity of only 34%. All the reaction

mixtures produced lower recoveries, although several were above 30%. The percentage recovery values relative to the TcO_4^- standard, time corrected for decay, are given in Table 3.7.

3.7.6 Calculation of Incorporation of ^{99m}Tc into macrocycles

All samples, except that containing cyclam, produced HPLC peaks between 4.27 and 5.20 minutes which were consistent with a monocationic complex containing a *trans*-TcO_2^+ core (*e.g* 2,3,2-tet, Figure 3.11). Variable amounts of activity were also eluted between 1 and 3.2 minutes which might be attributed to neutral *e.g* TcO_2 or anionic species *e.g* TcO_4^-.

The phenolic cyclam (2) was the only ligand which gave a peak with a much longer retention time (8.94 mins), in addition to one at 4.27 minutes. When repeated with freshly prepared ligand stock solution the same result was obtained: peaks at 4.39 and 8.68 minutes (Figure 3.10). All ligands were later found to be stable in aqueous stock solution (20 mM) for a period of more than 10 days, as determined by ^1H NMR spectroscopy.

The percentage of recovered activity contained within the major peak (some ligands produced multiple peaks) with a retention time between 4.27 and 5.20 minutes was determined by cutting out and weighing the shaded areas (Figures 3.10 and 3.11) and comparing this with the weight of the total area above the dotted baseline. The baseline represents the background level of activity at the start of each run. For the phenolic cyclam (2), each of the two peaks was weighed separately.

Approximate percentage values (C), for the degree of incorporation of ^{99m}Tc by the series of ligands, have been calculated by multiplying the percentage activity recovered from the column relative to injected

TcO_4^- (A) by the percentage activity contained within the shaded areas (B). The values of A, B and C for each of the 9 systems are given in Table 3.7.

LIGAND	COUNTS RECOVERED	% COUNTS RECOVERED vs STAND TcO_4^-	% COUNTS RECOVERED vs INJECT TcO_4^- (A)	% SHADED PEAK (B)	% INCORPORATION (C)
(14)	25761	23	68	34	23
(15)	35327	32	93	65	60
CYCLAM	17985	16	47	0	0
(2)	34920	31	92	(i) 18 (ii) 41	(i) 16 (ii) 38
(56)	36734	33	97	37	36
(5)	36739	33	97	47	46
(53)	27740	25	73	10	7
(55)	19947	18	52	22	11
STAND TcO_4^-	38001	34	--		
INJECT TcO_4^-	111147				

Table 3.7 *Recovery of Activity and Calculated Incorporation of ^{99m}Tc for a series of Tetraamine Ligands.*

3.8 REFERENCES

1. D.E. Trautner, J. Simon, A.R. Ketring, W. Volkert and R.A. Holmes, *J.Nucl.Med.*, 21, 443 (1980)

2. W.A. Volkert, D.E. Trautner and R.A. Holmes, *Int.J.Appl.Radiat. Isot.*, 33, 891 (1982)

3. C.H. Paik, J.J. Hong, M.S. Sahumi, S.C. Heald, R.C. Reba, J. Steigman and W.C. Eckelman, *Int.J.Nucl.Med.Biol.*, 12, 3 (1985)

4. C.H. Paik, W.C. Eckelman and R.C. Reba, *Nucl.Med.Biol.Int.J.Radiat. Appl.Instrum. Part B*, 13(4), 359 (1986)

5. M.J. O'Sullivan *et al.*, *Anal.Biochem.*, 100, 100 (1979)

6. J.W. Freytag *et al.*, *Clin.Chem.*, 30, 417 (1984)

7. R.J. Youle *et al.*, *Proc.Nat.Acad.Sci.USA*, 77, 5483 (1984)

8. T. Kitagawa and T. Aikawa, *J.Biochem.*, 79, 233 (1976)

9. B. Yoshitaka, Y. Yamada, E. Ishikawa and R. Masseyeff, *Int.J. Biochem.*, 101, 395 (1979)

10. E. Kimura, T. Koike and M. Takahashi, *J.Chem.Soc. Chem. Commun.*, 385 (1985)

11. E. Kimura, T. Koike, K. Uenishi, M. Hediger, M. Kuramoto, S. Joko, Y. Arai, M. Kodama and Y. Iitaka, *Inorg.Chem.*, 26, 2975 (1987)

12. S. Coffey (Editor) "*Rodd's Chemistry of Carbon Compounds*", (2nd Edition; Elsevier), 374 (1971)

13. S.A. Zuckerman, G.M. Freeman, D.E. Trautner, W.A. Volkert, R.A. Holmes, D.G. Van Derveer and E.K. Barefield, *Inorg.Chem.*, 20, 2386 (1981)

CHAPTER FOUR

RADIOLABELLING STUDIES USING COPPER-64

4.1.1 ^{64}Cu for Positron Emission Tomography

The advantages of positron emission tomography (PET) for imaging tumours and the choice of ^{64}Cu as a suitable positron emitter have been discussed in the introduction (sections 1.3.5 and 1.3.7). Copper isotopes form kinetically inert complexes with a number of macrocyclic tetraamine ligands, in particular the [14]-membered system cyclam and its phenol-pendent derivative (2) (section 1.5).

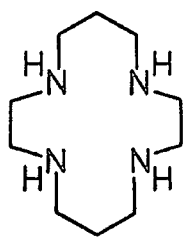

cyclam

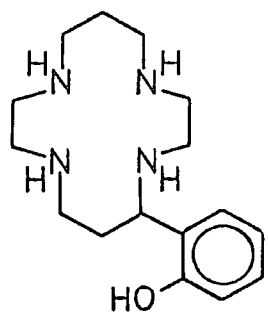

(2)

Copper(II) cyclam complexes are much easier to prepare than those containing Tc(V) since there is no need to use a reducing agent *e.g* $SnCl_2$ or a high pH régime. Any copper(II) salt may be used in aqueous solution at pH 7.

Unfortunately ^{64}Cu is much more expensive and less readily available than ^{99m}Tc. It is made from ^{64}Zn by a (n,p) reaction:

$$^{64}Zn + n \longrightarrow {}^{64}Cu + p$$

6 mCi of ^{64}Cu was made at Harwell by bombarding spectral grade ZnO_2 with neutrons, the first time ^{64}Cu had been produced in a "carrier-free" form in the U.K. The "carrier-free" material was extracted electrochemically;

the electrode being washed with 0.04N HCl to give a solution of $^{64}CuCl_2$.

4.1.2 Conventional Labelling of Macrocycle-Antibody Conjugates with ^{64}Cu

The opportunity to label antibody-bound cyclam with ^{64}Cu at neutral pH removes the risk of damaging the sensitive macrostructure of the protein during labelling (for ^{99m}Tc, pH 11 is required).

The macrocycles, cyclam and its phenolic derivative (2), as their 2-vinylpyridine conjugates, were conjugated to "trauted" Mab (B72.3) in the manner described in section 2.7.3, then labelled with $^{64}CuCl_2$ at pH 7. The *in vivo* stability of the radiolabelled mac-ab conjugate was compared with that of a radiolabelled native antibody in biodistribution studies. The radiolabelled Mab was separated from unbound ^{64}Cu using a PD10 column, then injected into mice. The animal data is presented in Table 4.1 (the interpretation of biodistribution data is discussed in section 3.1.3).

	— ^{64}Cu-mac$_1$-ab —		— ^{64}Cu-mac$_2$-ab —		— ^{64}Cu-ab —	
TISSUE	%Dg^{-1}	%Dose	%Dg^{-1}	%Dose	%Dg^{-1}	%Dose
BLOOD	8.1 ±0.8	21.7 ±1.2	9.6 ±1.5	26.4 ±4.1	2.1	5.6
KIDNEYS	6.1 ±0.4	3.3 ±0.3	5.4 ±0.8	3.1 ±0.6	9.1	4.1
LIVER	19.5 ±2.1	33.5 ±2.0	15.4 ±2.9	27.7 ±6.5	12.4	21.7

Table 4.1 *Biodistribution data for pH 7 conventional labelling; 24 hours, mac$_1$=cyclam; mac$_2$=(2); ab=B72.3; no.of mice per dataset=2.*

The level of cardiovascular activity after 24 hours is higher for the macrocycle-containing antibody conjugates than for the native Mab indicating a greater *in vivo* stability for the radiolabel. However the accumulation of activity in the liver is much higher than would be expected from its blood content. The liver is roughly 30% blood by

weight so the expected % dose g^{-1} for the liver should not be significantly greater than one third of the % dose g^{-1} for the blood-pool. The fact that the liver % dose g^{-1} is roughly twice that of the blood may be attributed to either the removal, by the liver, of "aggregates" of labelled antibody or the dissociation of copper from the Mab (non-specifics)†. Free copper is rapidly removed from the blood by the liver and kidneys where it accumulates readily. It is not possible on the basis of the present data to differentiate the contributions of these two effects to the loss of cardiovascular activity, but it seems likely that both are implicated.

4.2 A PRE-LABELLING STRATEGY FOR ^{64}CU

If the high liver activity is due to non-specifically bound copper dissociating from the antibody, a pre-labelled ^{64}Cu-mac-ab conjugate should reduce the activity in the liver and give a correspondingly higher cardiovascular activity. (The pre-labelling protocol is reviewed in section 3.2). Any excess liver accumulation could then be attributed to the removal, by the liver, of aggregates of IgG from the blood.

4.2.1 Pre-labelled ^{64}Cu-Cyclam Conjugates

Since cyclam macrocycles can be labelled with copper(II) at neutral pH, there is no restriction upon the use of maleimide cross-linkers for pre-labelling (unlike ^{99m}Tc: see section 3.3).

A macrocycle-maleimide conjugate (57) was prepared by reacting the

†See sections 3.1.4 and 3.1.5 for definitions of the terms "aggregates" and "non-specifics".

functionalised non-phenolic cyclam macrocycle (29) with the commercially available cross-linker (50), sulfosuccinimidyl-4-(N-maleimidomethyl)-cyclohexane-1-carboxylate, in "Pipes" buffer at pH 6.8 (Figure 4.1). The conjugate (57) was then labelled with $^{64}CuCl_2$ at pH 6.5 and conjugated to the "trauted" Mab (B72.3) in the usual manner.

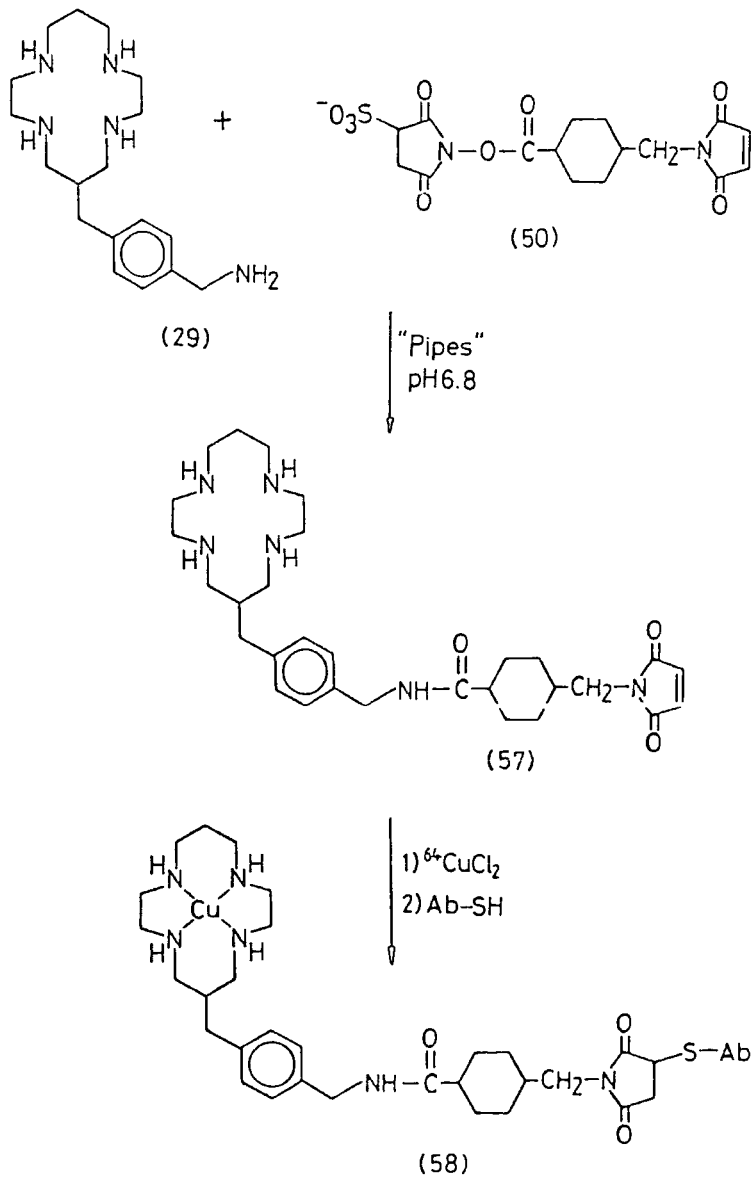

Figure 4.1 *Synthesis of ^{64}Cu-mac-ab conjugates using maleimide-based pre-labelling.*

After 2 hours reaction more than 60% of the total activity was associated with the protein. This compares with a paltry 0.5% for ^{99m}Tc-cyclam, conjugated to "trauted" B72.3 using a 2-vinylpyridine linker molecule (section 3.2.2), and well-illustrates the merit of a more reactive maleimide cross-linker for pre-labelling.

4.2.2 Biodistribution of the Pre-labelled Conjugate

The radiolabelled conjugate (58) was purified from small molecules *e.g* (57) and ^{64}Cu-(57) using a PD10 column (Sephadex G-25) and was injected into mice. The biodistribution data at 18 hours is given in Table 4.2

TISSUE	PD10 (Seph.G-25) %Dg^{-1}	PD10 (Seph.G-25) %Dose	HPLC (GF-250) %Dg^{-1}	HPLC (GF-250) %Dose
BLOOD	17.5 ±0.7	47.8 ±1.2	18.4 ±1.2	55.8 ±0.7
KIDNEYS	5.7 ±0.8	2.9 ±0.2	6.3 ±1.2	3.3 ±0.4
LIVER	8.9 ±0.4	16.0 ±0.9	6.0 ±0.5	12.3 ±1.1
LUNGS	7.8 ±1.0	1.4 ±0.1	8.1 ±0.6	1.5 ±0.2
SPLEEN	5.2 ±0.3	0.4 ±0.0	5.1 ±0.5	0.4 ±0.1

Table 4.2 *Biodistribution data for pre-labelling; 18 hours; non-phenolic cyclam; no.of mice per dataset=3.*

The level of cardiovascular activity is much higher than was observed previously (Table 4.1) for the ^{64}Cu-mac-ab conjugate prepared by conventional labelling. In addition, the liver activity is substantially reduced. This suggests that non-specifically bound copper (which is absent from pre-labelled conjugates) may have been responsible for the low cardiovascular and high liver activities produced by conventionally-labelled conjugates *in vivo*.

If the PD10-purified conjugate is further purified using size-exclusion HPLC (Dupont GF-250), the blood:liver activity ratio can be improved still further (Table 4.2). The blood level (55.8 %Dose) is

close to the theoretical maximum value after 18 hours, predicted by the equilibration of IgG with the extracellular tissues (section 3.1.3). The liver activity is little more than one third of the cardiovascular level, consistent with its blood content and with equilibration. The fact that HPLC purification improves the blood:liver ratio suggests that aggregated protein still presents a problem. HPLC can remove aggregates and fragments (PD10 does not) but unfortunately cannot be used routinely in hospitals for this purpose - steps must be taken to prevent protein damage *e.g* site-specific labelling.

4.2.3 Conclusions

The observation that a pre-labelled ^{64}Cu-cyclam-antibody conjugate remains in the blood, unless the protein itself is damaged, confirms the view that the ^{64}Cu-cyclam complex is kinetically stable *in vivo*.

Additionally the bonds linking macrocycle and antibody (amide, thioether, amidine) would also appear to possess high *in vivo* stability. Thus by preventing non-specific metal binding, pre-labelling allows stable ^{64}Cu-mac-ab conjugates to be prepared. However it is not considered to be an ideal procedure for preparing radiopharmaceuticals routinely (section 3.2.1). Conventional labelling involves a much simpler one-pot protocol and would be preferred if the problem of non-specific binding could be overcome.

There is little doubt that much of the non-specifically bound copper could be removed using a chelate wash *e.g* EDTA, DTPA, cyclam but as for ^{99m}Tc, it seems unlikely that all would be readily removed in a single and rapid treatment. A more effective approach is to prevent non-specific binding from occurring in the first place by using a low pH labelling régime. To understand this approach, it is necessary to

consider the origin of non-specific binding of copper by proteins.

4.3 LABELLING MACROCYCLE-ANTIBODY CONJUGATES WITH ^{64}CU AT LOW pH

4.3.1 The pH Dependence of Non-Specific Copper Binding

According to Pettit *et al.*[1,2], copper(II) binds to most peptides (HL) below pH 5 through the terminal-NH_2 group and the carbonyl oxygen of the neighbouring peptide linkage. This Cu-O bond is weak such that the complex formed $[CuL]^+$ has only a small range of existence. Above pH 5, Cu(II) promotes deprotonation of the adjacent peptide nitrogen to form a more stable Cu-N bond with a 5-membered chelate ring. As the pH is raised, further chelate rings are formed by bonding to successive peptide nitrogens. Hence the final complex with tetraglycine will involve displacement of 3 peptide hydrogens to give the NNNN-bonded complex $[CuH_{-3}L]^{2-}$. With a tripeptide (*e.g* triglycine) the final species will be a NNN-bonded complex, the fourth centre to coordinate being the carboxylate group. Stepwise coordination of copper(II) by triglycine is shown in Figure 4.2. The species distribution plot for the copper(II) complex of tetraglycine is given in Figure 4.3.

At high pH, copper(II) coordinates readily to any sequence of amino acids except those containing large amounts of proline (proline does not possess an ionisable hydrogen and cannot form a typical Cu-N peptide bond). Hence coordination of copper(II) by deprotonation of the peptide nitrogens of the backbone of proteins is the primary origin of the non-specific binding of this metal at neutral pH. From the species distribution curves of Figure 4.3, it is clear that Cu^{2+} is not bound by tetraglycine at pH 4. By analogy, ^{64}Cu should not bind non-specifically

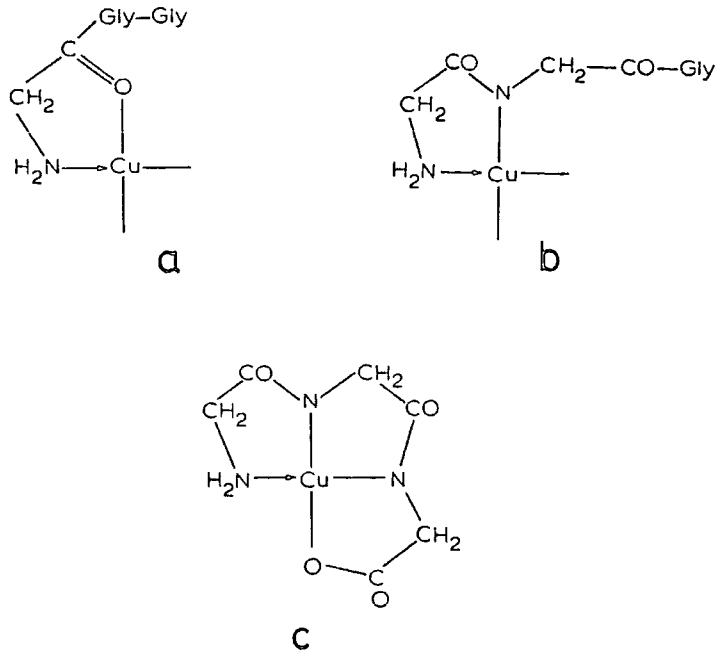

Figure 4.2 *Copper(II) Complexes of Triglycine (HL); a:[CuL] b:[CuH$_{-1}$L]; c:[CuH$_{-2}$L] species.*

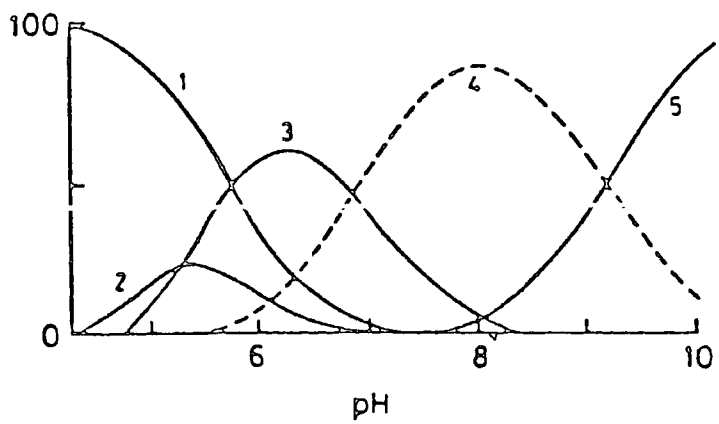

Figure 4.3 *Species distribution curves (%) for the Cu^{2+} complex of tetraglycine in a 1:1 solution of 0.001 mol dm^{-3}. 1:Cu^{2+}; 2:[CuL]; 3:[CuH$_{-1}$L]; 4:[CuH$_{-2}$L]; 5:[CuH$_{-3}$L].*

to macrocycle-antibody conjugates if the pH of the labelling buffer is reduced from 7 to 4.

4.3.2 Enhancing the Kinetics of Uptake at Low pH

The success of the low pH strategy for avoiding non-specific binding depends upon the rate of uptake of ^{64}Cu by the macrocycle being sufficiently rapid. At pH 4, the macrocycles, cyclam and phenolic cyclam (2), are almost exclusively diprotonated. The rate of reaction between Cu^{2+} and diprotonated macrocycles is generally slow due to electrostatic repulsion in the outer-sphere complex (section 5.1.2). Kimura *et al.*[3] found that the rate of reaction between Cu^{2+} and diprotonated cyclam was faster in acetate buffer by virtue of reduced electrostatic effects. In kinetics experiments at Durham, it was found that a succinate buffer enhanced the rate of incorporation still further (section 5.2.1).

4.3.3 Radiolabelling Studies with ^{64}Cu at pH 4

The effects of low pH (*i.e* 4) and of stripping agents (chelate wash) upon the incorporation of ^{64}Cu by a control antibody and a macrocycle-antibody conjugate were investigated by our collaborators at Celltech and Harwell.

A mac-ab conjugate (mac = phenolic cyclam (2); ab = B72.3), containing 0.24 macrocycles per antibody, was incubated for 30 minutes with $^{64}CuCl_2$ in 0.3M phosphate buffer (pH 7). The radiolabelled conjugate was purified using a PD10 column: 38.6% of the added ^{64}Cu activity was associated with the protein fraction. The labelling was repeated for the control antibody (B72.3); 4.7% of the activity being

bound by the protein.

The effect of lowering the pH was then investigated using a 0.2M succinate buffer at pH 4.0. The effect of a stripping agent was also investigated by incubating the labelled conjugate with a 150 fold excess (over Mab) of cyclam for 30 minutes. The activities associated with conjugated and control Mab's (after PD10 purification) and the conjugated:control activity ratios are summarised in Table 4.3.

BUFFER	pH	STRIPPING AGENT	mac-ab (X)	control-ab (Y)	RATIO (X/Y)
0.3M PHOSPHATE	7	---	38.6	4.7	8.2
0.2M SUCCINATE	4	---	33.2	0.64	52.0
0.2M SUCCINATE	4	CYCLAM	35.3	0.20	176.0

Table 4.3 *Percentages of ^{64}Cu activity bound; mac=(2); ab=B72.3; 30 minutes; 20^{0}C.*

The use of a pH 4 succinate buffer seems to be a very effective method for reducing the non-specific binding of copper(II) to the control antibody. The reduction in the activity associated with the mac-ab conjugate is of a similar magnitude, presumably due to a decrease in non-specific binding rather than a reduction in specific binding by the macrocycle. If true, the use of a succinate buffer to provide rapid association kinetics at pH 4 is vindicated. The mac-ab:control-ab ratio is much superior at pH 4 than at neutral pH.

The incubation of the control antibody (radiolabelled at pH 4) with excess cyclam reduced the activity associated with the protein still further. This suggests that a small amount of non-specific ^{64}Cu may be bound even at pH 4. Washing the ^{64}Cu-mac-ab conjugate with cyclam does not make a significant difference to the amount of associated activity.

4.3.4 Biodistribution Studies Using Conjugates Labelled at Low pH

A sample of ^{64}Cu-mac-ab conjugate (mac = (2); ab = B72.3), prepared in succinate buffer at pH 4.0 and purified using PD10, was injected intravenously into mice. The biodistribution data at 21 hours is given in Table 4.4. Another sample of ^{64}Cu-mac-ab, prepared similarly, was further purified using size-exclusion HPLC to separate the IgG peak from other radiolabelled components. The biodistribution data for this second sample at 21 hours is also given in Table 4.4.

TISSUE	PD10 (Seph.G-25)		HPLC (GF-250)	
	%Dg^{-1}	%Dose	%Dg^{-1}	%Dose
BLOOD	18.5 ±0.4	47.9 ±2.3	20.0 ±0.0	55.6 ±0.7
KIDNEYS	5.7 ±0.8	2.5 ±0.3	5.8 ±0.1	2.6 ±0.0
LIVER	8.3 ±1.2	13.3 ±2.0	8.0 ±0.2	13.8 ±0.2
LUNGS	7.5 ±0.4	1.3 ±0.0	7.8 ±0.5	1.4 ±0.2
SPLEEN	5.8 ±0.1	0.4 ±0.0	5.0 ±0.4	0.4 ±0.0

Table 4.4 *Biodistribution data for pH 4 conventional labelling 21 hours; phenolic cyclam; no.of mice per dataset=2.*

The PD10 purified sample gave a biodistribution profile which was superior to that obtained using a PD10 purified pre-labelled ^{64}Cu-mac-ab conjugate (Table 4.2). This illustrates the success of the low pH strategy for reducing non-specific ^{64}Cu binding. The fact that the HPLC-purified material gave a marginally higher blood and lower liver activity may reflect the removal of aggregated protein from the PD10-purified material. The level of activity in the liver is slightly higher than expected even for the HPLC sample. It is conceivable that HPLC failed to separate the IgG and aggregate peaks cleanly - they elute in close proximity on a size-exclusion system. This illustrates the importance of using freshly "trauted" IgG and of capping excess thiols to prevent intermolecular cross-linking. It is possible that a low pH

régime damages the Mab in some way which is recognised by the liver, although this seems less likely if exposure to the pH 4 labelling buffer is limited to 30 minutes.

4.4 CONCLUSIONS

The conventional labelling of cyclam-antibody conjugates with ^{64}Cu at neutral pH produces an excessive amount of non-specifically bound radiolabel which dissociates *in vivo* and accumulates in the liver and kidneys.

Although pre-labelling eliminates the problem of non-specific binding, a better solution is to label conventionally at low pH where the binding of copper(II) to the protein backbone is minimised. This approach may be improved still further using a single, rapid chelate wash with excess free cyclam, EDTA or DTPA.

The biodistribution profile obtained for the ^{64}Cu-mac-ab conjugate, labelled at pH 4, is close to being acceptable for clinical use. The cardiovascular activity at 24 hours is close to the expected value, indicating that ^{64}Cu forms kinetically inert complexes with unsubstituted (at N) cyclam macrocycles which are stable *in vivo*. Hence the four carboxylic side-arms of Meares' Cu-binding cycle TETA[4] are at best superfluous and at worst potentially destabilising (section 1.5.5). This is substantiated by the work of Volkert *et al.*[5] who found that the ^{64}Cu complex of a di-N-alkylated cyclam, which also lacks carboxylic acid groups, is stable in serum (although no animal data has been reported).

The level of activity in the liver remains slightly elevated; probably due to the presence of damaged protein rather than to the

instability of the radiolabel. Further steps must be taken to minimise protein damage since HPLC will not be available in a hospital to remove aggregates.

The chemistry of ^{64}Cu is certainly more amenable to its successful attachment to Mab's than that of ^{99m}Tc. The results reported in this chapter are certainly very encouraging and will be pursued further in experiments with ^{67}Cu in Chapter 6. The prospects for the further development of ^{64}Cu radiopharmaceuticals for *in vivo* imaging depend more upon financial considerations than upon its chemistry and *in vivo* performance. ^{64}Cu is much more expensive to produce than either ^{99m}Tc or ^{111}In. Moreover PET cameras are currently up to 10 times more expensive than conventional Anger cameras. Recently however, a new and much cheaper type of positron camera has been developed at the Royal Marsden Hospital. If further cost-reductions are realised, the superior definition of PET could make ^{64}Cu an important radioisotope for radioimmunoimaging.

4.5 REFERENCES

1. L.D. Pettit and G. Formicka-Kozlowska, *Neuroscience Letts.*, 50, 53 (1984)
2. L.D. Pettit, I. Steel, G. Formicka-Kozlowska, T. Tatarowski and M. Bataille, *J.Chem.Soc.Dalton Trans.*, 535 (1985)
3. M. Kodama and E. Kimura, *J.Chem.Soc.Dalton Trans.*, 1473 (1977)
4. M.K. Moi, C.F. Meares, M.J. McCall, W.C. Cole and S.J. DeNardo, *Anal.Biochem.*, 148, 249 (1985)
5. J. Franz, G.M. Freeman, E.K. Barefield, W.A. Volkert, G.J. Ehrhardt and R.A. Holmes, *Nucl.Med.Biol.Int.J.Radiat.Appl.Instrum. Part B*, 14(5), 479 (1987)

CHAPTER FIVE

KINETIC STUDIES ON COPPER(II) COMPLEXES OF [13]- AND [14]-MEMBERED TETRAAMINE MACROCYCLES

5.1 INTRODUCTION

5.1.1 Why study Kinetics?

Copper-64 and copper-67 are potentially useful radioisotopes for positron imaging and radiotherapy respectively. Work by Pettit *et al.*[1] established that copper(II) ions do not bind to oligopeptides at a pH below 5 (see section 4.3.1). Moreover we have found that copper does not bind "non-specifically" to the protein backbone of derivatised antibodies at pH 4 (section 4.3.2). This is an important advance over the prior art since at lower pH, antibody-bound macrocycles may be labelled to produce a radiopharmaceutical which does not lose copper *in vivo*.

The proverbial "fly-in-the-ointment" concerns the extremely slow rate of incorporation of copper by antibody-bound tetraamine macrocycles at low pH. The poor kinetics can be explained in part by the very low concentration of "carrier-free" isotope which must be used in the labelling procedure, typically 10^{-15} mol dm^{-3}. More importantly, the protonated forms of the macrocycle, predominant at low pH, are much less reactive than the free ligand or indeed than their analogous open-chain equivalents.

It is of paramount importance to optimise the kinetics of complexation in view of the short half-life of these isotopes, especially ^{64}Cu (12.8 hours), and the need to avoid exposing potentially pH sensitive antibodies to excessively long periods of acidity.

5.1.2 Mechanistic Considerations Determining Rate

It has been known for some time that the protonated forms of tetraamine

macrocycles form metal complexes at a much slower rate than their open-chain equivalents[2]. In contrast, unprotonated forms of cyclic and acyclic ligands react at a similar rate. To understand these kinetic effects, it is necessary to distinguish between mono- and di-protonated forms of the macrocycle, which exhibit different reactivities and react *via* different mechanisms.

Both cyclam and $13N_4$ exist predominantly as the diprotonated form (LH_2^{2+}) at pH 4 (see Table 5.1 for pK_a values). Although the mono-protonated form (LH^+) is rare, it is still kinetically significant by virtue of its much higher reactivity.

	pK_1	pK_2	pK_3	pK_4
$13N_4$	11.1	10.1	~1.7	~1.0
CYCLAM	11.5	10.2	~1.7	~1.0

Table 5.1[3] *I=0.20 mol dm^{-3}; 25^{o}C*

In a study of a series of macrocycles, $12N_4$ - $16N_4$, Kaden *et al.*[4] found that the reactivity of LH_2^{2+} towards Cu^{2+} was dependent on the ring size of the macrocycle, there being a correlation between rate and pK_3. In fact pK_3 decreases with decreasing cavity size due to larger electrostatic repulsion of 3 protons in a smaller ring. Similarly electrostatic repulsion between LH_2^{2+} and Cu^{2+} in the "outer-sphere complex" was cited as an important factor in determining rate.

Generally the reactivity of LH^+ was found to be relatively independent of ring size implying that electrostatic repulsion alone could not be responsible. The lower reactivity of LH^+ relative to the unprotonated ligand and open chain systems was explained in terms of a rate-determining pre-equilibrium involving two conformations, only one of which is able to bind the metal.

As a general rule, Kaden found the rate of complexation of Cu^{2+} to

increase with increasing ring size. However the reactivities of the [13]- and [14]-membered systems were exceptional in that $13N_4$ was faster than cyclam. Moreover, there was a decrease in the reactivity of both LH^+ and LH_2^{2+} forms of cyclam relative to $13N_4$ and this decrease was of a similar magnitude for both forms (Table 5.2).

($l\ mol^{-1}s^{-1}$)	k_{LH_2}	$10^{-6}\ k_{LH}$
$13N_4$	1.9 ± 0.9	9.2 ± 0.9
CYCLAM	0.39 ± 0.03	1.8 ± 0.2

Table 5.2 *I=0.5 mol dm^{-3}; 25°C*

The explanation for such a trend reversal is not clear but suggests that the expected increase in the electrostatic repulsion between LH_2^{2+} and Cu^{2+} in the outer-sphere complex for $13N_4$ is offset by some other effect, perhaps a more favourable conformational pre-equilibrium similar to that proposed earlier for LH^+. Since the reactivity of LH^+ itself is equally dependent upon the change of ring size, the conformational pre-equilibrium for $13N_4$ must also be more favourable than for cyclam. It is noteworthy that the difference in the rate of complexation between $13N_4$ and cyclam is less pronounced for a monocationic copper species, $Cu(CH_3CO_2)^+$, than for Cu^{2+} implying that electrostatic effects are still important[3,5].

Although by no means the only factor explaining the slow rate of complexation at low pH, electrostatic repulsion is an important consideration and steps must be taken to minimise it. Kimura and Kodama[3,5,6] found that the incorporation of copper by a series of polyamine macrocycles at low pH was significantly faster in acetate buffer, by virtue of the reduced repulsion between monocationic $CuAc^+$

(Ac = CH_3COO^-) and LH_2^{2+} relative to Cu^{2+} and LH_2^{2+}. The LH^+ species is less reactive in acetate buffer. The rate constants for cyclam and $13N_4$ are given in Table 5.3.

(1 $mol^{-1}s^{-1}$)	$k_{LH^+}^{Cu^{2+}}$	$k_{LH_2^{2+}}^{Cu^{2+}}$	$k_{LH^+}^{CuAc^+}$	$k_{LH_2^{2+}}^{CuAc^+}$
CYCLAM	$1.7x10^7$	0.14	$5.6x10^6$	10.1
$13N_4$	$7.9x10^6$	$7.9x10^{-2}$	$5.0x10^6$	7.9

Table 5.3 *I=0.20 mol dm^{-3}; 25°C*

Later Kaden and Wu[7] studied the reactivity towards cyclam of a series of copper complexes incorporating anionic carboxylate donors and found that succinate produced the most significant rate-enhancing effect. In contrast to the acetate system, the reactivities of both ligand species, LH^+ and LH_2^{2+}, are greater towards CuSucc (Succ = $^-O_2CCH_2CH_2CO_2^-$) than Cu^{2+}, although the reduction in electrostatic repulsion has a more pronounced effect upon the rate constant for the diprotonated form ($k_{LH_2^{2+}}^{CuSucc}$, see Table 5.4†).

(1 $mol^{-1}s^{-1}$)	$k_{LH^+}^{Cu^{2+}}$	$k_{LH_2^{2+}}^{Cu^{2+}}$	$k_{LH^+}^{CuSucc}$	$k_{LH_2^{2+}}^{CuSucc}$
CYCLAM	$2.4x10^6$	0.39	$5.6x10^7$	48.0

Table 5.4 *I=0.50 mol dm^{-3}; 25°C*

5.1.3 Potential Rate-Enhancing Effects

Buffer

The reactivity of copper species towards LH_2^{2+} (cyclam) increases in the order: Cu^{2+}< $CuAc^+$< CuSucc. This suggested a direct correlation between

†The precise values for the rate constants involving CuSucc will later be shown to be incorrect (section 5.3) but the trends which they portray are nonetheless valid.

the number of carboxylate groups bound, which determines overall charge, and the reactivity of the species. On this basis, it was decided to study whether this trend would be continued when three carboxylate groups were available, by using a citrate buffer. In fact, it would be wise to study each of the combinations of ligands (cyclam, $13N_4$) and buffer (acetate, succinate, citrate) to establish which would give the most rapid overall incorporation.

Phenols

We have found that phenolic cyclam (2) incorporates technetium faster at pH 9 than cyclam itself (section 3.4.1). A similar effect for copper at pH 4 is unlikely on electrostatic grounds since the phenol in the copper complex of (2) is extensively protonated at this pH (*viz.* Kimura[8], pK_a 9.2). However the observed effect for technetium may not be purely electrostatic in nature but may involve a pre-orientation of technetium by the phenol for rapid uptake by the nitrogens of the ring. If true a catalytic effect by the phenols (56) and (2) may still be possible at low pH.

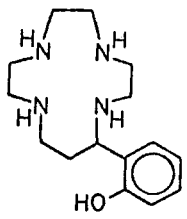

(56)

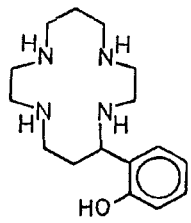

(2)

Temperature

A twofold rate increase for each 10^oC rise in temperature is commonly found for reactions which obey the Arrhenius law: $k_2 = A \exp(-E_a/RT)$. The antibody should withstand a temperature of 40^oC, perhaps 45^oC in some cases, so a useful rate enhancement over room temperature is possible.

Ionic Strength

According to Debye-Huckel Theory, the rate of reaction, (k) at a given ionic strength (I) is related to the rate at zero ionic strength (k_0) by the equation:

$$\log (k/k_0) = 1.018\ Z_A Z_B \sqrt{I} \quad (H_2O;\ 298\ K)$$

$$\text{where} \quad I = 1/2\ \Sigma_i c_i z_i^2$$

Rate increases with I for reactant ions of like charge and decreases for ions of opposite charge, since the surrounding ionic atmosphere (of equal but opposite charge) stabilises an encounter pair of like charges but destabilises one of opposite charges.

Evidence from the literature suggests that copper complexes of tetraamines are formed by reaction of positive ligand species with positive or neutral copper species, in which case a positive or zero ionic strength dependence should be observed. If the rate increases with increasing ionic strength, steps should be taken to raise the salt concentration in the radiolabelling buffer.

5.1.4 Measurement of Rate

The effect of each of the above factors, ring size, buffer, phenol-pendency, temperature and ionic strength, on rate was studied at first in a qualitative manner by varying one factor whilst keeping the others constant. However no attempt was made to control ionic strength for the different buffer systems, since the experiments were intended to investigate order-of-magnitude rate-enhancing effects rather than to measure precise values for rate constants. By comparing the rate of a given reaction for a series of different buffers of constant molarity, but varying ionic strength, we obtain information which is of direct relevance to the choice of radiolabelling buffer, for which ionic

strength is not really an important consideration. However the observed relative rates are not necessarily truly representative of the intrinsic relative rates which would have been obtained had the ionic strength been held constant.

In reality, the kinetics for the reaction of copper and ligand are second-order but the mathematical calculation of the rate constant can be simplified by using a ten-fold excess of one component. We can make the approximation that the concentration of this component at any time during the reaction does not differ significantly from its initial concentration. Since this concentration is constant, it can be incorporated into a new rate constant, k_{obs}, the pseudo-first order rate constant. In most experiments described here, the ligand will be used in excess, in which case the rate expression will simplify as follows:

$$\text{Rate} = k_2[Cu]_{tot}[L]_{tot} = k_{obs}[Cu]_{tot}$$

k_{obs} can be calculated directly from the increasing intensity of the "d-d" band (500-600 nm) as the copper-ligand complex is formed. The absorbance (A_t) increases exponentially with time and k_{obs} can be found from the slope of a plot of ln $\{(A_\infty - A_t)/(A_\infty - A_o)\}$ against time, according to the first-order integrated rate equation:

$$\ln\left(\frac{A_\infty - A_t}{A_\infty - A_o}\right) = -k_{obs}.t$$

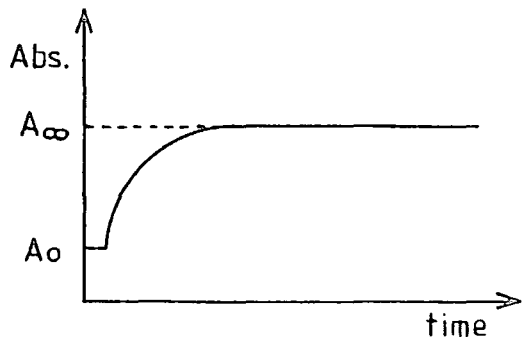

For relatively fast reactions such as these, the absorbance must be monitored using the "stopped-flow" method. The solutions of copper and ligand are injected by syringe into a mixing cell where they react. When the flow is stopped by a third syringe, the absorbance is monitored at a fixed observation point using a photomultiplying light guide. The pseudo-first order rate constants can be calculated routinely from the absorbance profile using a least-squares linear regression program (Hitech ADS-1 package).

5.2 RELATIVE RATE EXPERIMENTS

Experimental details are given in Section 5.4.

5.2.1 Kinetic Effect of Ring Size and Complexing Buffer Type

The effects of varying ring size (13 vs 14) and buffer type (acetate vs succinate vs citrate) were studied under the same experimental conditions (Experiment 1.1). Solutions of copper perchlorate (10^{-3} M) and of ligands, cyclam and $13N_4$ (10^{-2} M), were prepared in each of the carboxylate buffers (0.2M) at pH 4.0. The ligand was used in ten fold excess (pseudo-first order in copper) since copper ions were found to be insufficiently soluble in succinate buffer to provide a 10^{-2} M solution. The total concentrations of copper ions and ligand after mixing would therefore be 5×10^{-4} M and 5×10^{-3} M respectively. The pseudo-first order rate constants are given in Table 5.5. As expected the $13N_4$ cycle is faster than cyclam in every case - 7 times faster for acetate; 6 times for succinate and 2.7 times for citrate. For $13N_4$, succinate buffer provides the fastest incorporation, followed by citrate then

acetate. For cyclam, citrate buffer is slightly better than succinate and much better than acetate.

$k_{obs}(s^{-1})$	ACETATE	SUCCINATE	CITRATE
$13N_4$	0.530	2.550	1.670
CYCLAM	0.077	0.422	0.627

Table 5.5 *pH4; [buffer]=0.20M; [Cu]=5x10^{-4}M; [L]=5x10^{-3}M; 25^{o}C*

In a separate experiment (1.2), the effect of varying the buffer was investigated under 2 different pH régimes. The same concentrations of copper and ligand were used. Acetate (0.2M), succinate (0.05M) and citrate (0.1M) buffers were used at pH 4.50 and pH 5.40. The results are tabulated in Table 5.6.

For cyclam in acetate and succinate buffers, the rate shows the expected increase as the concentration of free copper decreases and the concentration of monoprotonated ligand increases. However in citrate buffer, the rate decreases with increasing pH for both cyclam and $13N_4$ ligands.

$k_{obs}(s^{-1})$	ACETATE		SUCCINATE		CITRATE	
	4.50	5.40	4.50	5.40	4.50	5.40
$13N_4$					2.83	1.94
CYCLAM	0.144	0.428	0.526	1.38	0.752	0.403

Table 5.6 *[Cu]=5x10^{-4}M; [L]=5x10^{-3}M; 25 ^{o}C*

It is interesting to note that the difference in rate between cyclam and $13N_4$ is at a minimum at low pH in citrate buffer (2.8 times at pH 4.0), then increases with increasing pH.

There seems to be uncertainty in the literature about the range of citrate complexes formed by copper(II). Warner and Weber[9] reported that 1:1 complexes were formed exclusively under their set of conditions (0.012M Cu^{2+}; 0.012M citrate) and that at pH 7, all four ionisable protons were displaced from the ligand (3 carboxylate and 1 alkoxide donors). At pH values below these, other 1:1 complexes were formed, in which fewer than 4 protons were displaced. The species distribution plot (Figure 5.1) suggests that the observed decrease in rate at higher pH may be due to conversion of more reactive protonated forms *e.g* $HCiCu^-$ to less reactive fully deprotonated forms *e.g* $CiCu^{2-}$. The neglect of the species H_2CiCu is a mistake.

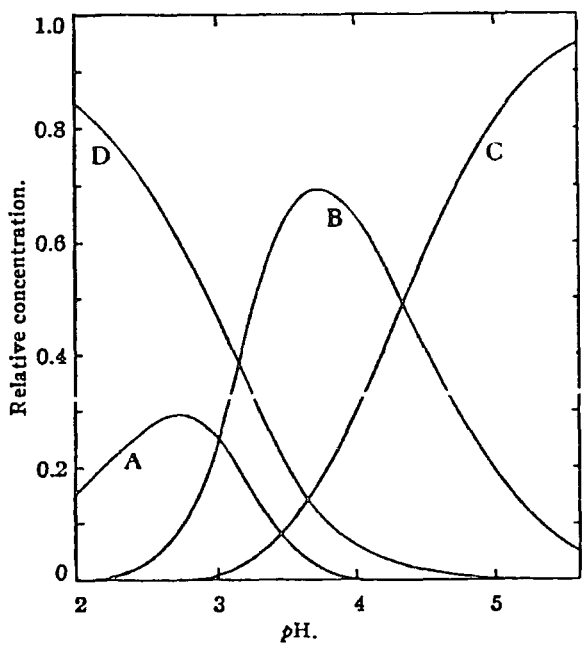

Figure 5.1 *Relative concentration of copper(II) citrate species as a function of pH. A=H_3CiCu^+; B=$HCiCu^-$; C=$CiCu^{2-}$; D=Cu^{2+}*

Campi *et al.*[10] insist that dinuclear species must be considered under the same set of conditions (pH range 3-8; equimolar amounts of Cu^{2+} and citrate), namely $HCiCu_2^+$ (log K = 13.2) and $CiCu_2$ (log K = -0.87). Rajan and Martell[11] also report the formation of dimeric species

of the type $(HCi)_2Cu_2^{2-}$ (log K = 13.2) and $Ci_2Cu_2^{4-}$ (log K = -8.03). However under our conditions of excess citrate, it is unlikely that species containing more than one copper need be invoked. Indeed it is more likely that copper will form complexes in which more than one citrate ligand is bound, as reported by Parry and Dubois[12].

It is interesting that the copper(II) complexes of di- and tricarboxylic acids are reported[10] to be unusually stable if an additional alcoholic donor group is available. This could explain the qualitative difference in trends observed here for the citrate and succinate systems.

In conclusion, it appears that the best kinetics for cyclam at pH 4.0 are observed in citrate buffer whereas at higher pH, succinate buffer is preferred. However the best overall rate of uptake was observed using the $13N_4$ ligand in succinate buffer.

5.2.2 Kinetic Effect of Phenol-Pendency

Solutions of copper perchlorate (10^{-3} M) and phenolic ligands (2) and (56) (10^{-2} M) were prepared in 0.2M succinate buffer, since this system provided the most favourable kinetics at pH 4.0 in experiments (1.1) and (1.2). The rate constants for these ligands, obtained in experiment (2.1), are given below:

LIGAND:	CYCLAM	(2)	$13N_4$	(56)
$k_{obs}(s^{-1})$	0.422	0.387	2.55	complex

The phenolic derivative of cyclam (2) incorporates copper marginally slower than cyclam itself. The [13]-membered phenol (56) appears to react by a more complex mechanism than the other ligands since no single

exponential curve could be resolved from the absorbance profile. Instead the profile was fitted to three separate exponentials, comprising a very fast reaction complete within 50 milliseconds (k_{obs}~110), a slower reaction (k_{obs}=0.5323) and a very slow reaction (k_{obs}=0.0472) (Figure 5.2).

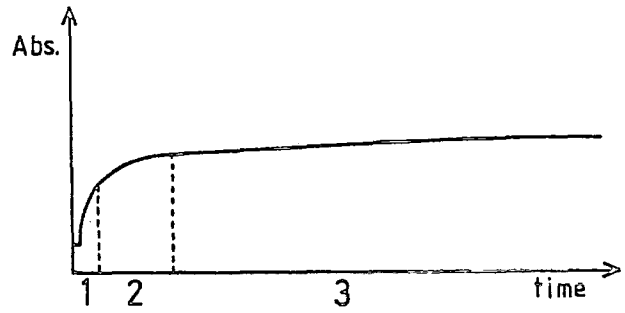

Figure 5.2 *Absorbance profile for the reaction between Cu(II) succinate and (56). Not drawn to scale. Reactions numbered: 1) k_{obs}~110; 2) k_{obs}=0.532; 3) k_{obs}=0.047*

Since this behaviour was not observed for the non-phenolic system, a stepwise mechanism is suggested, possibly involving participation by the phenol group. The initial very rapid step might involve dissociation of the succinate ligand to form a species with an N_3O donor set, followed by a slower step in which the fourth nitrogen is deprotonated to form an N_4O species. The final very slow step might be a rearrangement of the macrocycle from a folded conformation in the N_4O species to planar N_4 coordination.

Whilst the difference in rate between cyclam and (2) is not particularly significant at pH 4.0 in 0.2M succinate buffer, it is much more obvious in 0.1M citrate buffer at pH 4.25 (Experiment 2.2); cyclam reacts almost twice as rapidly (Table 5.7).

Interestingly in citrate buffer at higher pH (5.17), the "phenol" effect again becomes less apparent. It is improbable that the phenol will have any electrostatic effects in this pH range. However it is

conceivable that an intermediate copper species is formed involving the pendent phenol and one or more nitrogen donors.

$k_{obs}(s^{-1})$	CYCLAM	(2)
pH 4.25	0.4625	0.2437
pH 5.17	0.2001	0.1850

Table 5.7 *[citrate]=0.1M; [Cu]=5x10^{-3}M; [L]=5x10^{-4}M; 25^{o}C*

At low pH, the kinetic inertness of the diprotonated ligand might encourage reaction through this intermediate which is itself kinetically quite inert. At higher pH, the disappearance of the "phenol effect" might be attributed to the greater abundance of the monoprotonated form of the ligand providing an alternative pathway with a much lower kinetic barrier, not involving a stable intermediate. Therefore it seems possible that (2) is also reacting through a stepwise mechanism similar to that observed for (56), but the first two steps are too rapid to be observed separately in the absorbance profile.

In conclusion, the behaviour of phenol-pendent macrocycles is complex and does not seem to offer any obvious advantages over non-phenols in terms of the association kinetics at pH 4.0.

5.2.3 Kinetic Effect of Temperature

It seemed sensible to pursue the $13N_4$ ligand in succinate buffer in all further experiments since this system gave the best overall rate of incorporation of copper at pH 4. Solutions of copper (10^{-3}M) and $13N_4$ (10^{-2}M) were prepared in the usual manner in 0.2M succinate buffer at pH 4 (Experiment 3). The temperature was raised in 5^{o}C steps from 25^{o}C to 45^{o}C and the following rate constants were obtained:

^{o}C	25	30	35	40	45
$k_{obs}(s^{-1})$	2.30	3.21	5.32	8.31	12.55

The rate of uptake was found to increase quite sharply with temperature, by a factor of 2.3-2.4 times for each $10^{o}C$ rise. It is possible to obtain an indication of the activation energy (E_a) for the reaction using the Arrhenius equation:

$$k_2 = A \exp(-E_a/RT)$$

E_a may be determined from a plot of log k_{obs} (or k_2) against 1/T (Figure 5.3, see section 5.5.2). The plot gives a straight line indicating Arrhenius-type behaviour and gives a value of 63 (±5) kJ mol^{-1} for the activation energy. This value is only valid for these precise conditions and gives only a qualitative indication of the effect of temperature at different pH and for other concentrations of reactants, where the distribution of reactive species will differ. This study gives a rough guide to the effect of increasing temperature on the rate of uptake and suggests that as high a temperature as possible should be used within the constraints imposed by the presence of the antibody.

5.2.4 Kinetic Effect of Ionic Strength

Solutions were prepared containing 10^{-3} M copper perchlorate and 10^{-2} M $13N_4$ in 0.2M succinate buffer at pH 4. Sodium perchlorate was added to boost the ionic strength. The following rate constants were observed at 25 ^{o}C:

$[NaClO_4]$	0.0M	0.2M	1.0M
$k_{obs}(s^{-1})$	2.42	1.77	1.00

The observed trend, decreasing rate with increasing ionic strength, is the reverse of that expected for reaction between cationic copper and ligand species. If the reaction proceeded *via* cationic ligand and

neutral CuSucc, no ionic strength dependence would be expected. Since the ligand cannot be negatively charged, it would appear that anionic copper species must be involved. The formation of anionic copper-succinate species and their role in the reaction mechanism will be studied in section (5.3).

5.2.5 Conclusions

The preceding experiments demonstrate that the optimum association kinetics at pH 4.0 are observed for the non-phenolic $13N_4$ macrocycle in succinate buffer, with the temperature as high as possible and the ionic strength at a minimum. These suggestions were passed on to our collaborators at Harwell and pursued in radiochemical experiments using ^{64}Cu and ^{67}Cu, the results of which are given in section (4.3.2).

There are a number of interesting experiments which I would have performed had time permitted it and which may yet be pursued by other workers.

Although of no consequence to the choice of radiolabelling buffer, it would nonetheless be useful to measure the rates of incorporation of copper(II) by $13N_4$ and cyclam for the series of 3 buffers at constant ionic strength. For example it is conceivable that the observed differences in rate between citrate and succinate (Table 5.5) are related to the differences in ionic strength, being considerably greater for 0.2M citrate (~0.31) than for 0.2M succinate (~0.12). If anionic copper-citrate complexes are formed, as seems likely from the literature evidence, the same ionic strength dependence as for copper-succinate would be expected. The slow-down for the $13N_4$ system in citrate (k_{obs}= 1.67 s^{-1}), relative to succinate (k_{obs}= 2.55 s^{-1}), might then be explained partly or wholly in terms of the ionic strength difference.

Similarly, it is possible that some of the observed slowing effect in citrate buffer at higher pH (Table 5.6) is due to its increasing ionic strength.

Clearly an investigation of the mechanism by which tetraamines incorporate copper in citrate buffer is in order. By studying the ionic strength dependence, it would be possible to investigate a possible role for anionic copper-citrate species and gain an indication of their charge. It would also be interesting to study the variation of rate in citrate buffer over a wider pH range (pH< 4 and pH> 5.4) to ascertain whether the observed trends are continued.

The mechanism of reaction of the phenolic ligands (2) and, especially, (56), with copper-succinate seems to be complex and requires further investigation. The pH, succinate and ionic strength dependencies of the absorbance profiles and k_{obs} values should provide important information about the distribution of reactive species under different sets of conditions and their possible role in the reaction mechanism.

In the following section, the mechanism of the reaction between $13N_4$ and copper-succinate will be explored in detail.

5.3 KINETIC STUDIES ON COPPER(II) COMPLEXES OF 1,4,7,10-TETRAAZACYCLOTRIDECANE IN SUCCINATE BUFFER

5.3.1 Ionic Strength Dependence

The observed ionic strength dependence for the reaction between copper(II) succinate and $13N_4$, decreasing rate with increasing I (section 5.2.4), can only be explained in terms of a reaction between

oppositely-charged ions, essentially cationic ligand and anionic copper species. The $NaClO_4$ background cannot explain the observed trend since ClO_4^- ions do not coordinate to copper(II) in aqueous solution. Similarly the coordination of hydroxyl groups to copper(II) succinate to give anionic species is highly improbable at pH 4. The only plausible explanation requires the simultaneous coordination of more than one succinic acid molecule per copper ion.

5.3.2 Copper-Succinate Coordination Chemistry

The work of Wu and Kaden[7] on the kinetics of copper(II) succinate with cyclam made no mention of a possible role for anionic copper species. No ionic strength dependence was reported so it is difficult to judge whether their omission was an oversight or whether there was a valid reason for not including anionic species. Certainly their system would contain fewer copper(II) succinate species in which more than one ligand was bound. In our system, succinate was used as a buffer and was present in large (400 fold) excess. Kaden *et al.* used a borate buffer containing succinate in much smaller (<5 fold) excess. The question is whether anionic copper species are only formed in kinetically significant amounts at pH $\leq$4 when succinate is present in vast excess.

An extensive, but probably not exhaustive, search of the literature revealed only one reference to copper-disuccinate species. Garg *et al.*[12] reported formation constants (β values) for the neutral "CuSucc" species and the dianionic "$CuSucc_2^{2-}$" species of 4.00 and 6.570 respectively, determined polarographically. Other papers report a formation constant for a protonated form of CuSucc, $CuHSucc^+$, but contain no reference to copper-disuccinate species (Table 5.8). The reported values for the neutral complex CuSucc are reasonably consistent with the notable

exception of the value of Garg *et al.*, determined at I = 1.0, which is much larger (one would expect a lower value at higher ionic strength). This casts serious doubt on the validity of the β-value for $CuSucc_2^{2-}$ determined by the same workers.

I	log K_{CuL}	log K_{CuHL}	log K_{CuL_2}	Ref
1.0	4.000		2.570	13
0.2	2.26			14
0.1	2.6			15
0.1[a)]	2.93	1.70		16
0.1[b)]	2.58			17
0.1	2.85	1.87		18
0.1	2.608	1.86		19
0.1	2.5			19
0	3.33			20
0	3.22			14

Table 5.8 *25^oC except a) 20^oC; b) 30^oC; L= $Succ^{2-}$*

Given the absence of consistent β-values for copper-disuccinate species in the literature, it is not surprising that Wu and Kaden did not contemplate their involvement. However the failure to consider a possible role for the protonated complex, $CuHSucc^+$ is a curious oversight. It is therefore felt by the author that the quoted rate constants for the reactions between CuSucc and mono- and diprotonated forms of cyclam (5.6×10^7 and 48 respectively) are almost certainly too large. An additional inaccuracy concerns the use of a β-value for CuSucc, determined at I = 0.1, for analysing data acquired at I = 0.5.

In view of the conspicuous absence from the literature of trustworthy β-values for copper-disuccinate species, it was decided to determine our own values by pH potentiometry.

5.3.3 Equilibrium Studies on Copper(II) Complexes of Succinic Acid

A solution containing copper(II) perchlorate (2mM), succinic acid (4mM),

perchloric acid (2mM) and sodium perchlorate (0.1M) was titrated against standardised sodium hydroxide (Experiment 5). The pH potentiometric data was then analysed using the non-linear least squares programs, "SCOGS" and "SUPERQUAD"[21].

The β-values for CuSucc, $CuSuccH^+$, $CuSucc_2^{2-}$ and $CuSucc_2H^-$ were refined, holding constant the β-values for succinic acid. The pK_a values for succinic acid at I = 0.1 are known from the literature: pK_1 = 3.99; pK_2 = 5.20. The set of β-values which provided the best "fit" to the experimental data are given in Table 5.9.

	SCOGS	SUPERQUAD
$\log \beta_L$	5.20 *	5.20 *
$\log \beta_{HL}$	9.19 *	9.19 *
$\log \beta_{CuL}$	2.59	2.58
$\log \beta_{CuHL}$	7.03	7.03
$\log \beta_{CuL_2}$	4.30	4.35
$\log \beta_{CuHL_2}$	9.59	9.64

Table 5.9 *$[Cu]=2x10^{-3}M$; $[H_2Succ]=4x10^{-3}M$; $[HClO_4]=4x10^{-3}M$; $[NaClO_4]=0.1M$; 25^0C; L= $succ^{2-}$; * = held constant.*

The agreement between "SCOGS" and "SUPERQUAD" analyses was excellent, and the quality of the "fit" for "SUPERQUAD" was indicated by a low value for the chi-squared parameter (3.33). The formation constants for CuSucc and $CuHSucc^+$ were in good agreement with those reported in the literature (Table 5.8).

It has been demonstrated that the copper-disuccinate species, $CuSucc_2^{2-}$ and $CuHSucc_2^-$, are formed during the pH titration of solutions containing copper(II) ions and a 2 fold excess of succinic acid, albeit in very small quantities (Figure 5.4). Their concentration in a 0.2M succinate buffer (Experiment 4) would obviously be much greater. However we

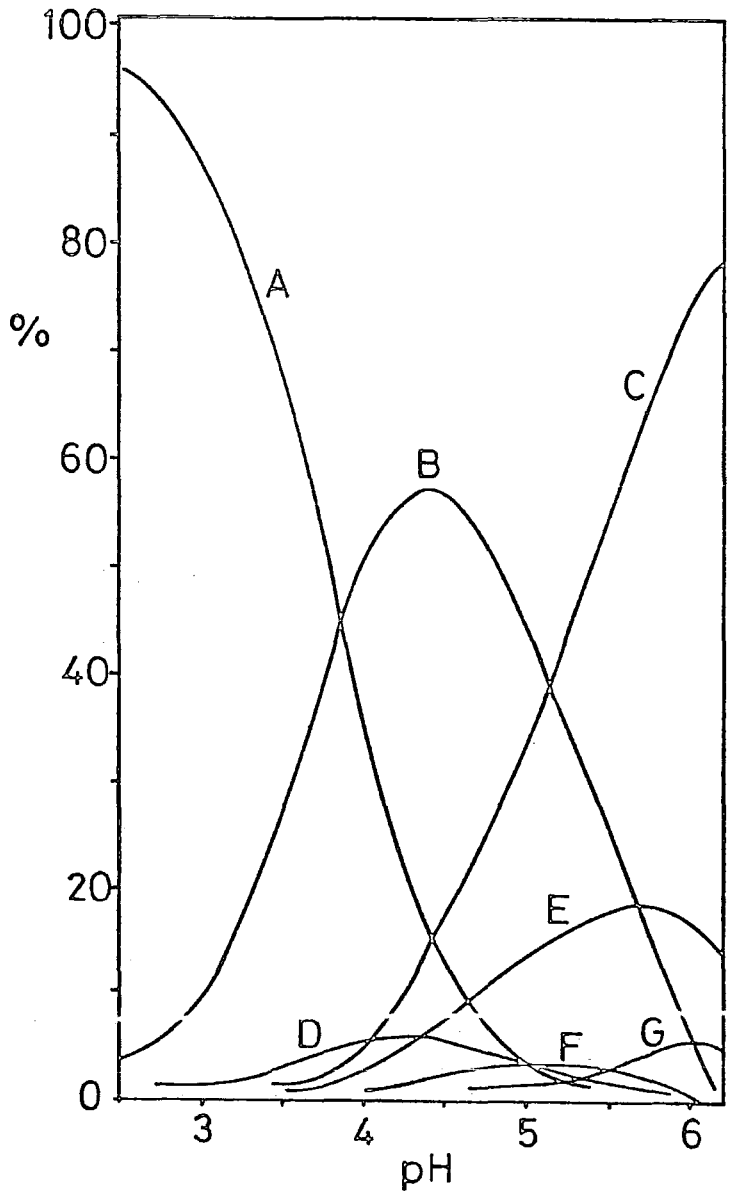

Figure 5.4 *Relative concentrations of copper(II) succinate species as a function of pH. A=H_2Succ; B=$HSucc$; C=$Succ^{2-}$; D=$CuHSucc^{+}$; E=$CuSucc$; F=$CuHSucc_2^{-}$; G=$CuSucc_2^{2-}$; [Cu]=2mM; [H_2Succ]=4mM; [$HClO_4$]=2mM; [$NaClO_4$]=0.1M.*

cannot say with absolute certainty that the presence of these species can explain the observed inverse dependence of rate upon ionic strength, unless we explore the exact nature of the reaction mechanism in more detail.

5.3.4 Kinetics of the Reaction of Copper(II) with $13N_4$ in Acetate Buffer[3]

As mentioned in section (5.1.2), Kimura and Kodama investigated the mechanism of the reaction of Cu(II) ions with $13N_4$ in acetate buffer at low pH and obtained the following rate expression:‡

$$\frac{d[Cu(13N_4)]}{dt} = k_{CuAc/H}[CuAc^+][13N_4H^+] + k_{CuAc/2H}[CuAc^+][13N_4H_2^{2+}]$$

The kinetically important species in the pH range 3.2 - 3.7 ([Ac]=0.05-0.15M) were therefore the (1:1) species, $CuAc^+$, and the mono-(LH^+) and diprotonated (LH_2^{2+}) forms of $13N_4$. The role of $CuAc^+$ was determined from the dependence of rate upon acetate concentration, the role of LH^+ and LH_2^{2+} from the dependence of rate upon pH.

The following equilibrium for copper(II) in acetate buffer was considered:

$$Cu^{2+} \underset{}{\overset{K_{CuAc}}{\rightleftharpoons}} CuAc^+ \overset{K_{CuAc_2}}{\rightleftharpoons} CuAc_2$$

At constant pH, the apparent rate constant (k_f) can be written:

---

‡Throughout this section, electrical charges will be omitted from the subscripts of rate and equilibrium constants for reasons of clarity

$$k_f = \frac{vel}{[Cu]_{tot}} = \frac{k_{Cu}[Cu^{2+}] + k_{CuAc}[CuAc^+] + k_{CuAc_2}[CuAc_2]}{[Cu]_{tot}}$$

thus:

$$k_f = (k_{Cu} + k_{CuAc}K_{CuAc}[Ac^-] + k_{CuAc_2}K_{CuAc}K_{CuAc_2}[Ac^-]^2/\ \beta$$

$$\text{where:}\quad \beta = 1 + K_{CuAc}[Ac^-] + K_{CuAc}K_{CuAc_2}[Ac^-]^2$$

Since a plot of k_f x β against $[Ac^-]$ gave a straight line with zero intercept, $CuAc^+$ was judged to be the only kinetically significant copper species under these conditions.

Kimura *et al.* also measured the variation of k_f with pH keeping constant the total ligand concentration and the concentration of Ac^-. Considering mono- and diprotonation of the ligand:

$$13N_4 \underset{}{\overset{K_{1H}}{\rightleftharpoons}} 13N_4H^+ \overset{K_{2H}}{\rightleftharpoons} 13N_4H_2^{2+}$$

$$k_f = \frac{vel}{[13N_4]_{tot}} = \frac{k_H[13N_4H^+] + k_{2H}[13N_4H_2^{2+}]}{[13N_4]_{tot}}$$

$$= k_HK_{1H}[H^+] + k_{2H}K_{1H}K_{2H}[H^+]^2\ /\ \alpha$$

$$\text{where } \alpha = 1 + K_{1H}[H^+] + K_{1H}K_{2H}[H^+]^2$$

Since all the reaction goes through a single Cu species, $CuAc^+$:

$$k_f = \frac{k_{Cu/H}K_{CuAc}K_{1H}[Ac^-][H^+]}{\alpha.\beta} + \frac{k_{Cu/2H}K_{CuAc}K_{1H}K_{2H}[Ac^-][H^+]^2}{\alpha.\beta}$$

A plot of $(k_f \text{ x } \alpha)/[H^+]$ against $[H^+]$ allows $k_{CuAc/H}$ and $k_{CuAc/2H}$ to be determined from the intercept and slope respectively.

5.3.5 The Mechanism of the Reaction between Copper(II) Succinate and $13N_4$

Mechanistically, the reaction between Cu(II) ions and $13N_4$ in succinate buffer is much more complex than in acetate. There are many more copper species of possible relevance since, unlike acetate ligands, coordinated succinate may be mono-protonated and still remain bound to the metal. Diprotonated ligand is not expected to remain bound to the metal and is not considered in the reaction mechanism. A reaction scheme involving 5 copper species and 2 ligand species was envisaged (Figure 5.5).

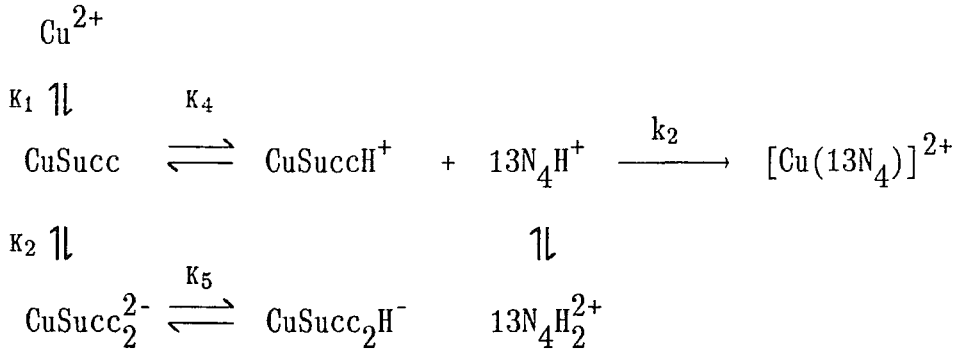

Figure 5.5 *Copper-succinate and ligand equilibria of possible kinetic significance at low pH.*

The role of the free ligand ($13N_4$), whose concentration is negligible in the pH range under study, and that of the copper species, CuH_2Succ_2, thermodynamically unstable with respect to CuSucc, are likely to be unimportant and may be neglected. All equilibria are sensitive to pH such that at higher pH, copper will be bound by an increasing number of less highly protonated succinate ligands. Since the direct dependence of rate on pH is a complex function of the redistribution of both copper and ligand species, we cannot separate the individual contributions of the 2 ligand species from a pH plot (*viz.* Kimura[3]). Thus we cannot determine exact values for the second order rate constants. However it

is possible, and indeed useful, to investigate the importance of different copper and ligand species at different pH and different buffer concentrations.

The slope of the *ionic strength* dependence of the rate at a particular pH will indicate the charge of the species involved in the rate-determining step. By varying the *succinate* buffer concentration at constant pH, we can also evaluate the relative contributions to the rate of free copper and its mono- and di-succinate complexes under a given pH régime.

5.3.6 Ionic Strength and Succinate Dependence - Experimental

The concentration of $[Cu(13N_4)]^{2+}$ required for rate measurements by stopped-flow spectrophotometry is ~2.5×10^{-4} M. Therefore solutions were prepared containing 5×10^{-4} M copper and 5×10^{-3} M $13N_4$, which on mixing would give this concentration of complex. A 10 fold excess of ligand was used to provide pseudo-first order conditions since copper(II) is too insoluble in succinate buffer to provide a 5×10^{-3} M solution.

The reactant solutions were prepared by diluting stock solutions of copper (5×10^{-3} M), ligand (5×10^{-2} M), succinic acid (0.5M), sodium hydroxide (1.0M) and sodium perchlorate (1.0M). Succinic acid is insufficiently soluble in water to provide a solution of greater concentration than 0.5M.

Both succinate and ionic strength dependencies were examined under different pH régimes: pH 5.7, 5.0, 4.0 and 3.6 for succinate; pH 5.6, 4.2 and 3.7 for ionic strength. In the succinate dependence experiments (6.1 - 6.4), the ionic strength was adjusted to a constant value of 0.3 using the appropriate amount of $NaClO_4$. In the ionic strength

experiments (7.1 - 7.3), the pH was adjusted to the given values using an appropriate amount of 1N NaOH or 1N $HClO_4$.

5.3.7 Ionic Strength Dependence Analysis

According to the "kinetic salt effect" and Debye-Hückel theory, the dependence of the rate constant upon ionic strength for non-ideal solutions, approximates to the relationship:

$$\log k = \log k_o + \frac{2A' Z_A Z_B \sqrt{I}}{1 + \sqrt{I}}$$

where k_o is the rate constant at zero ionic strength, Z_A and Z_B are the charges of the reactant species A and B and A' is a constant (0.509 $dm^{3/2}\ mol^{-1/2}$ in water; 298 K). By plotting log k against $\sqrt{I}/1+\sqrt{I}$, we can determine the product of the charges of the reactive species ($Z_A Z_B$) from the slope.

The ionic strength was calculated using:

$$I = 1/2\ \Sigma_i\ c_i z_i^2$$

taking account of the distribution of succinate between neutral, mono- and dianionic species.

Under all three pH régimes studied (5.6, 4.2 and 3.7), the rate of complexation was found to decrease with increasing ionic strength, in accord with the result of Experiment 4; the slope being steepest at pH 5.6. The calculated values for the abscissae and ordinates are given in Table 5.10 and the plots in Figure 5.6.

A slope of -2.2 for pH 5.6 can only be explained in terms of reaction of species whose mean charge-product ($Z_A Z_B$) is more negative than -2. There are many possible combinations of copper and ligand

species which collectively could explain this degree of slope; the most likely being: $Cu^{2-}/13N_4^{2+}$; $Cu^{-}/13N_4^{2+}$; $Cu^{2-}/13N_4^{+}$; $Cu^{-}/13N_4^{+}$.

The slopes for the pH 4.2 and 3.7 plots are very similar, both being considerably less steep than for 5.6. There is no need to invoke a contribution by $Cu^{2-}/13N_4^{2+}$, but whether this reaction is still important at lower pH cannot be ascertained from the ionic strength data alone. If the species pair, $Cu^{2-}/13N_4^{2+}$, is no longer relevant, a significant contribution from $Cu^{-}/13N_4^{2+}$ and/or $Cu^{2-}/13N_4^{+}$ must be considered.

5.3.8 Succinate Concentration Dependence Analysis

The rate of reaction accelerates with increasing succinate concentration under all four pH régimes studied (Table 5.11). By plotting log k_{obs} against log $[succ^{2-}]$, it is apparent that the dependence is noticeably steeper at higher pH (Figure 5.7). At high pH, the observed dependence may be due to conversion of less reactive copper-monosuccinate species to more reactive copper-disuccinate‡† species with increasing [succ]. At low pH, significant amounts of free copper will be present so the more gentle slope of the dependence may arise from the conversion of free copper to more reactive copper-succinate. At intermediate pH, the steepness of the slope is possibly determined by a combination of the effects of these two interconversions.

‡†Since electrostatic factors are important in determining the rate of incorporation (section 5.1.2), anionic copper-disuccinate species should be more reactive towards cationic ligand species.

5.3.9 The Role of Copper-Disuccinate Species

The kinetic significance of the 5 copper species envisaged in Figure 5.5 can be investigated more thoroughly by expressing the theoretical rate constant in terms of their formation and protonation constants and the protonation constants of succinic acid. For simplicity's sake, it is sensible to omit the role of different ligand species until a later stage of the analysis.

$$vel = k_2[Cu]_{tot}[13N_4]_{tot} = k_{obs}[Cu]_{tot}$$

$$k_{obs} = \frac{v}{[Cu]_{tot}} = \Big(k_{Cu}[Cu^{2+}] + k_{CuL}[CuL] + k_{CuHL}[CuHL] + k_{CuL_2}[CuL_2] + k_{CuHL_2}[CuHL_2] \Big) / [Cu]_{tot} \quad \ldots (I)$$

where $L = succ^{2-}$

We need to express the concentration of each Cu species in terms of known quantities, namely the equilibrium constants (K_1, K_2, K_4 and K_5) and the concentrations $[succ^{2-}]$ and $[H^+]$:

$$K_1 = \frac{[CuL]}{[Cu^{2+}][L]} \qquad K_2 = \frac{[CuL_2]}{[CuL][L]}$$

$$K_4 = \frac{[CuHL]}{[CuL][H^+]} \qquad K_5 = \frac{[CuHL_2]}{[CuL_2][H^+]}$$

$$[Cu]_{tot} = [Cu^{2+}] + [CuL] + [CuHL] + [CuL_2] + [CuHL_2]$$

Writing in terms of [CuSucc] gives:

$$[Cu]_{tot} = \frac{[CuL]}{K_1[L]} + [CuL] + K_4[CuL][H^+] + K_2[CuL][L] + K_2K_5[CuL][L][H^+]$$

$$[Cu]_{tot} = [CuL] \left(\frac{1}{K_1[L]} + 1 + K_4[H^+] + K_2[L] + K_2K_5[L][H^+] \right)$$

Writing [CuL] as a fraction of the total copper gives:

$$\frac{[CuL]}{[Cu]_{tot}} = \frac{K_1[L]}{\delta_1}$$

$$\text{where } \delta_1 = 1 + K_1[L] \left(1 + K_4[H^+] + K_2[L](1+K_5[H^+]) \right)$$

Since we know each concentration in terms of [CuL], we can write the other fractions:

$$\frac{[Cu^{2+}]}{[Cu]_{tot}} = \frac{1}{\delta_1} \qquad \frac{[CuHL]}{[Cu]_{tot}} = \frac{K_1K_4[L][[H^+]}{\delta_1}$$

$$\frac{[CuL_2]}{[Cu]_{tot}} = \frac{K_1K_2[L]^2}{\delta_1} \qquad \frac{[CuHL_2]}{[Cu]_{tot}} = \frac{K_1K_2K_5[L]^2[H^+]}{\delta_1}$$

Substituting for each fraction in equation (I) gives:

$$k_{obs} = \left(k_{Cu} + k_{CuL}K_1[L] + k_{CuHL}K_1K_4[L][H^+] + k_{CuL_2}K_1K_2[L]^2 + k_{CuHL_2}K_1K_2K_5[L]^2[H^+] \right) / \delta_1$$

$$\frac{k_{obs} \cdot \delta_1}{[L]} = \frac{k_{Cu}}{[L]} + k_{CuL}K_1 + k_{CuHL}K_1K_4[H^+] + \left(k_{CuL_2}K_1K_2 + k_{CuHL_2}K_1K_2K_5[H^+] \right)[L] \qquad \ldots \text{(II)}$$

According to equation (II), a plot of $k_{obs} \cdot \delta_1 / [L]$ against [L] will provide information about the role of copper-monosuccinate species from the intercept and copper di-succinate species from the slope.

For the pH 5.7 and pH 5.0 experiments, the concentration of $succ^{2-}$ (L) can be calculated directly from the amounts of NaOH and free ligand

added to the buffer solution. Since $[succ^{2-}]$ is so low at pH 4.0 and pH 3.6, it must be calculated from $[HSucc^-]$ using the following equation:

$$pH = pK_a + \log \frac{[succ^{2-}]}{[HSucc^-]} \qquad \ldots \text{(IIIa)}$$

The pK_a values of succinic acid at ionic strength 0.3 are approximately 4.0 and 5.2. Since the equilibrium constants K_1, K_2, K_4 and K_5 are known at I = 0.1 (Table 5.9), their values at I = 0.3 may be calculated using the Debye-Hückel equation:

$$\log K_I = \log K_o + \frac{2A.Z_A Z_B \sqrt{I}}{1 + \sqrt{I}} \qquad \ldots \text{(IIIb)}$$

e.g $\log K_1 = 2.58$ at I=0.1 ($Z_A Z_B = -4$)

From (IIIb):

$$\log K_{0.1} = \log K_o - 0.96$$
$$\log K_{0.3} = \log K_o - 1.42$$

$$\log K_1 = 2.58 - 0.46$$
$$\underline{K_1 \sim 150} \text{ (at I=0.3)}$$

The complete set of equilibrium constants is given in Table 5.12

	I=0.1	I=0.3
K_1	380	150
K_2	60	60
K_4	2.75×10^4	2.75×10^4
K_5	1.95×10^5	1.17×10^5

Table 5.12

K_2 and K_4 are essentially independent of ionic strength since the net charge is equal on both sides of the equilibrium. According to Debye-Hückel theory, neither products nor reactants will be stabilised more than the other by the presence of a more intense ionic atmosphere, of

equal but opposite charge, at I = 0.3.

The values of the cartesian coordinates, calculated using the equilibrium constants of Table 5.12, are given in Table 5.11 and are plotted in Figures 5.8 and 5.9.

The pH 3.6 and 4.0 data sets fit a reasonably straight line, with a positive slope and intercept, indicating that both copper mono- and disuccinate are kinetically significant species at this pH (Figure 5.8). At pH 5.7 and pH 5.0, there is also a positive slope suggesting that disuccinate species are again making an important contribution to the rate of reaction, but the lack of a positive intercept suggests that monosuccinate species are no longer of major importance. Moreover the intercept is negative, increasingly so with increasing pH, for a straight line drawn through these two sets of data points. This suggests that species with a greater than squared dependence upon the succinate concentration are contributing to the rate. The pH 5.7 data points in particular describe an upward curvature rather than the expected straight line if mono- and disuccinate species only were involved.

5.3.10 The Possible Role of Copper-Trisuccinate Species

The negative intercepts of Figure 5.9 signify terms with a cubed dependence upon the succinate concentration, suggesting that copper-trisuccinate species may be involved in the reaction mechanism at high pH. This introduces much greater complexity into our treatment of the data since there are several protonated forms to consider in addition to the tetra-anion form of copper-trisuccinate, $CuSucc_3^{4-}$ *e.g* $CuHSucc_3^{3-}$ *etc.* Ideally equation (II) should be amended to include all possible forms of copper-trisuccinate, but unfortunately this is not possible since we have no knowledge of the formation and protonation constants for such

species. It would be difficult, if not impossible, to determine their β-values using pH potentiometry since at low succinic acid concentrations, they are too rare to be detectable whereas at high concentrations, their endpoints would be swamped by the equivalence points of succinic acid itself. However a tentative value for the formation constant of $CuSucc_3^{4-}$ can be estimated, based on intuition and the known formation constants K_1 (150) and K_2 (60) - in the range 1 to 10 would seem appropriate. It would seem unwise to estimate more than a single equilibrium constant if the analysis is to be in any way meaningful. Thus we cannot realistically cover contributions from protonated forms of copper-trisuccinate. If, for simplicity's sake, we consider a model system in which contributions from non-protonated forms alone are important, Cu^{2+}, CuSucc, $CuSucc_2^{2-}$ and $CuSucc_3^{4-}$, we can envisage the reaction scheme given in Figure 5.10.

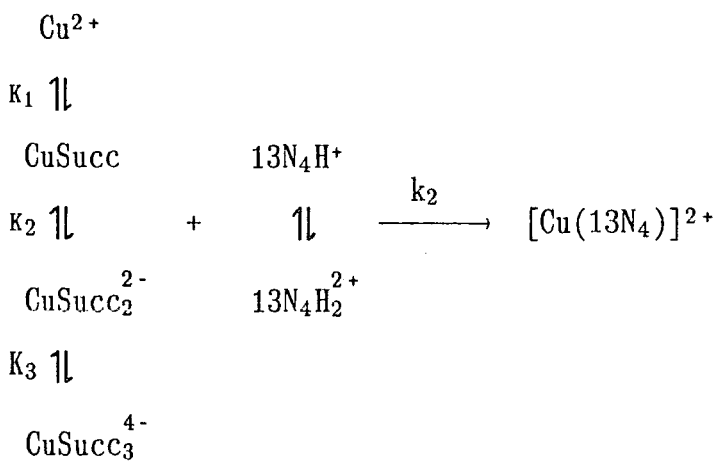

Figure 5.10 *A model reaction scheme involving copper-trisuccinate species*

The rate expression can then be written:

$$k_{obs} = k_{Cu}[Cu^{2+}] + k_{CuL}[CuL] + k_{CuL_2}[CuL_2] + k_{CuL_3}[CuL_3] \quad \ldots (IV)$$

$$K_1 = \frac{[CuL]}{[Cu^{2+}][L]} \qquad K_2 = \frac{[CuL_2]}{[CuL][L]} \qquad K_3 = \frac{[CuL_3]}{[CuL_2][L]}$$

$$[Cu]_{tot} = [Cu^{2+}] + [CuL] + [CuL_2] + [CuL_3]$$

As before, each concentration (as a fraction of the total copper) may be expressed in terms of the equilibrium constants (K_1-K_3). We can therefore substitute in equation (IV) to give:

$$k_{obs} = \frac{k_{Cu} + k_{CuL}K_1[L] + k_{CuL_2}K_1K_2[L]^2 + k_{CuL_3}K_1K_2K_3[L]^3}{\delta_2}$$

$$\text{where } \delta_2 = 1 + K_1[L]\left(1 + K_2[L](1 + K_3[L])\right)$$

Neglecting free Cu^{2+} which has no kinetic significance at any pH, we can write:

$$\frac{k_{obs}.\delta_2}{[L]^2} = \frac{k_{CuL}K_1}{[L]} + k_{CuL_2}K_1K_2 + k_{CuL_3}K_1K_2K_3[L] \qquad \ldots (V)$$

A plot of $k_{obs}.\delta_2 / [L]^2$ against [L] provides information about the role of $CuSucc_2^{2-}$ from the intercept and about $CuSucc_3^{4-}$ and CuSucc from the slope. Abscissae and ordinates, calculated using two estimated values of K_3 (1 and 10) are given in Table 5.13, and are plotted in Figures 5.11 and 5.12.

The data points for pH 5.7 and 5.0 describe straight lines with positive slopes and intercepts. Bearing in mind the oversimplified nature of this system, it would appear from the positive slopes of these plots that trisuccinate-copper species may be participating in the reaction mechanism at high pH. The steepness of the slope, reflecting the importance of the contribution of $CuSucc_3^{4-}$ to the rate, is obviously greater if its stability constant is estimated to be higher (10 versus 1). The positive intercepts confirm that copper-disuccinate species are also kinetically significant.

However at pH 4.0 the slope is slightly negative and at pH 3.6 it is much more steeply negative. In this simple system, the only species with an inverse dependence upon $[succ^{2-}]^2$ is the monosuccinate species, CuSucc. We can therefore conclude that at lower pH, the contribution from monosuccinate is more important than that from trisuccinate, particularly so at pH 3.6. For both pH régimes (4.0 and 3.6), a positive intercept indicates a contribution from copper-disuccinate species.

The involvement of trisuccinate species is not necessarily inconsistent with the ionic strength dependence data (section 5.3.7). The slope of the ionic strength plot at pH 5.6 (Figure 5.6) is -2.2. This could be explained in the model system by a dominant reaction in which $CuSucc_2^{2-}$ reacts with monoprotonated $13N_4$ (expected slope: -2), with a smaller contribution from $CuSucc_3^{4-}$ reacting with $13N_4H^+$ (-4). The reduced ionic strength slopes at pH 4.2 and 3.7 (-1.4 and -1.36) could then be explained in terms of a contribution of CuSucc (slope=0) and $CuSucc_2^{2-}$, reacting with either mono- or diprotonated macrocycle (slope: -2 or -4). Of course in the real system, protonated forms would be present, allowing a greater contribution to the rate from trisuccinate species without contradicting the ionic strength slope.

5.3.11 Conclusions

Unfortunately it has not proved possible to explore the mechanism of the reaction between copper(II) succinate and $13N_4$ at low pH in the detail we had hoped for or to determine a set of 2nd order rate constants. Other workers have reported rate constants for the reaction of CuSucc with mono- and diprotonated forms of the analogous [14]-membered cycle, cyclam, but we believe their neglect of disuccinate species and the protonated form of CuSucc invalidates their treatment. We have

established, by pH titration, that $CuSucc_2^{2-}$ and $CuHSucc_2^-$ are indeed formed, albeit in small amounts, in the presence of a 2 fold excess of succinate (Figure 5.4).

When protonated forms are taken into account, it is no longer possible to evaluate 2nd order rate constants for each individual species pair. The dependence of rate upon pH is a complex function of the degrees of protonation of both copper and ligand species. In our efforts to probe the reaction mechanism, we are therefore limited to exploring the ionic strength and succinate dependencies of the rate. The ionic strength dependence shows that anionic copper species play a dominant role in the reaction mechanism across the whole pH region studied (3.6-5.7). At high pH, both $CuSucc_2^{2-}$ and $CuHSucc_2^-$ would seem to be involved. From the succinate dependence plots (Figure 5.9) the absence of a positive intercept implies no significant role for monosuccinate species.

At lower pH, we conclude from the positive intercepts of the succinate dependence plots (Figure 5.8) that monosuccinate species are involved, but the ionic strength plot (Figure 5.6) indicates that anionic species, $CuSucc_2^{2-}$ or more likely $CuHSucc_2^-$, remain dominant.

The negative intercepts shown in Figure 5.9 cannot be explained by a rate expression involving mono- and disuccinate species alone. Retrospectively, it would have been useful to have obtained more than three data points for each pH régime, since it is often difficult to fit an accurate straight line to so few points. However the fact that both pH 5.7 and pH 5.0 data sets suggest negative intercepts lends credence to the view that this is a "real effect". If the effect is indeed more than an experimental artifact, we must invoke copper-trisuccinate species in the rate expression, in order to explain the greater than squared dependence of rate upon succinate concentration. Since we do

not know the β-values for such species, we have no option but to consider a simplified model system in which protonated species are neglected and the formation constant for $CuSucc_3^{4-}$ is estimated.

Using this simple system, we can obtain plots against $[succ^{2-}]$ which give positive intercepts (Figure 5.12). This implies that there are no further terms, with a higher dependence upon $[succ^{2-}]$, missing from the rate expression. Of course we cannot be sure that $CuSucc_3^{4-}$ is the only copper-trisuccinate species involved or indeed that it is involved at all. In fact $CuSucc_3^{4-}$ is likely to be a rare species even in the upper reaches of this pH range, by virtue of its high charge density and the characteristic reluctance of Cu(II) to bind fifth and sixth donors (except water itself) in aqueous solution (section 1.5.1). Indeed $CuSucc_3^{4-}$ cannot play a major role since the observed ionic strength slope (-2.2) is considerably less than would be expected from reaction of a tetra-anion with mono- (4-) or diprotonated (-8) forms of the ligand. Protonated forms of copper-trisuccinate are therefore more likely to explain the observed succinate dependence in this pH range.

In conclusion we have established that copper mono- and disuccinate species are rate determining in the pH range 3.6-4.2. At higher pH ($\geq$ 5), it seems necessary to consider both di- and trisuccinate species to explain the observed succinate dependence. It is not possible to distinguish between protonated and non-protonated forms from the succinate dependence plots. The ionic strength plots provide clues as to which species pairs are important at different pH. However the superimposed pH dependence of the copper and ligand equilibria prevents the quantification of these roles and the determination of rate constants, as was possible for the acetate system (*viz.* Kimura).

5.4 EXPERIMENTAL

5.4.1 Reagents

All purchased chemicals were used without further purification. Copper perchlorate, $Cu(ClO_4)_2.6H_2O$, was purchased from Aldrich for experiments (1) to (4), from Johnson-Matthey (99.9% purity) for experiments (5) and (6). Cyclam was obtained from Aldrich; $13N_4$, (2) and (56) were synthesised according to the methods outlined in section 7.3.5.

Acetate buffers were prepared from glacial acetic acid (Durham Chemicals) and anhydrous sodium acetate (BDH). Citrate buffers were prepared from citric acid monohydrate (Hopkin and Williams) and tri-sodium citrate dihydrate (Fluka). Succinate buffers were made using succinic acid (Fluka puriss p.a.) and analar sodium hydroxide (BDH). For experiments (5) and (6), sodium hydroxide was obtained as an analar volumetric 1.0M solution from BDH.

Perchloric acid was purchased as a 69-72% solution from Aldrich; sodium perchlorate monohydrate was obtained from Fluka (purum p.a.). Distilled water was used throughout.

5.4.2 Apparatus

Rates of reactions were measured using a Hitech SF-3L/30C stopped-flow spectrophotometer, on-line with an Apple IIe microcomputer with 80 column card. Hitech ADS-1 software (SF 051.0#05) was used to analyse the raw data and compute the pseudo-first order rate constant.

pH measurements were made using a Jenway 3020 pH meter in conjunction with a Russell microelectrode. Equilibrium constants were determined by pH potentiometry using a Mettler DL20 titrator and a

Mettler DG112 combination pH electrode in conjunction with a BBC microcomputer. The titration data was stored on a disc and transferred to the mainframe (NUMAC) using the program KERMIT. It was then analysed by the two non-linear least squares programs, SCOGS and SUPERQUAD.

5.4.3 Solution Preparation: Experiments (1) to (4)

In the following experiments, a minimum of 50 cm^3 of each of the copper and ligand solutions was found to be necessary. For experiments (1.1), (1.2), (2.1), (3) and (4), the concentrations of copper and ligand after mixing were 5 x 10^{-4} M and 5 x 10^{-3} M respectively (10 fold excess ligand). For experiment (2.2), the concentration of copper was 5 x 10^{-3} M and that of the ligand 5 x 10^{-4} M (10 fold excess copper).

Due to the hygroscopic nature of copper perchlorate, the percentage by mass of copper in our sample was found, by atomic absorption, to be lower than expected for the hexahydrate. The molar mass was therefore corrected for absorbed water and found to be 426.2 *i.e* $Cu(ClO_4)_2.9.09$ H_2O. Similarly the percentage sodium in our sample of sodium perchlorate was found to be consistent with the formula, $NaClO_4.1.88$ H_2O.

Experiments 1.1, 2.1, 3 and 4

Separate solutions of 10^{-3} M copper perchlorate and 10^{-2} M ligand were prepared in 0.2M buffer, calculated to provide a pH of 4.0. For the copper solutions, the buffer components were dissolved in water, 5 cm^3 of 10^{-2} M copper perchlorate stock solution (0.426g in 100 cm^3) was added and the volume was made up to 50 cm^3. For the ligand solutions, the buffer components and the ligand [0.5 mmol: 100mg cyclam; 93mg $13N_4$; 146mg (2); 139mg (56)] were dissolved in 50 cm^3 of water.

A solution of 0.2 M acetate buffer in water (50 cm^3) at pH 4.0 required 0.1477g sodium acetate and 0.4925g acetic acid. Similarly, succinate buffer required 1.1808g succinic acid and 0.160g sodium hydroxide, and citrate buffer required 1.2059g sodium citrate and 1.2398g citric acid.

In experiment 4, sufficient sodium perchlorate was added to provide 0.2 M (1.5636g) and 1.0 M (7.818g) solutions. If found to be necessary, the pH of each of the copper solutions was adjusted to pH 4.0 with 1.0 M NaOH and that of the ligand solutions with 1.0 M $HClO_4$.

Experiment 1.2

Solutions containing 10^{-3} M copper were prepared in acetate, succinate and citrate buffers, and solutions containing 10^{-2} M ligand were prepared in distilled water.

In addition to 10^{-2} M copper stock solution (5 cm^3 for acetate and succinate; 10 cm^3 for citrate), each copper solution required the following buffer components to provide the given molarities after mixing (total volume: 50 cm^3 for acetate and succinate; 100 cm^3 for citrate):

		ACID/g	SALT/g
0.20 M acetate	(pH 4.5)	0.7560	0.6071
0.20 M "	(pH 5.4)	0.1680	1.4110
0.05 M succinate	(pH 4.5)	0.5905	0.1336
0.05 M "	(pH 5.4)	0.5905	0.2736
0.10 M citrate	(pH 4.5)	2.0804	2.9706
0.10 M "	(pH 5.4)	1.0717	4.3824

For the 10^{-2} M ligand solutions, 400mg cyclam was dissolved in 200 cm^3 water and 93mg $13N_4$ in 50 cm^3 water.

Experiment 2.2

Solutions containing 10^{-2} M copper in 0.1M citrate buffer (pH 4.24 and

pH 5.17) and 10^{-3} M ligand in distilled water were prepared. The copper citrate solutions (100 cm^3) required at pH 4.25: 0.426g $Cu(ClO_4).9.09\ H_2O$, 2.9706g sodium citrate and 2.0804g citric acid; at pH 5.17: 0.426g $Cu(ClO_4).9.09\ H_2O$, 4.3824g sodium citrate and 1.0717g citric acid.

The solutions of cyclam and phenolic cyclam (2) in distilled water (100 cm^3) required 20mg and 29.2mg of ligand respectively.

5.4.4 Calculation of k_{obs} values: Experiments (1) to (4)

The formation of the complexes of cyclam, $13N_4$, (2) and (56) was followed at 516, 561, 506 and 557 nm respectively, corresponding to λ_{max} in each case. For each separate reaction, a minimum of 5 injections were made and k_{obs} was taken to be the average of these values. A typical data set is presented below:

$$[succ]_{tot} = 2 \times 10^{-1}\ M$$
$$[13N_4] = 5 \times 10^{-3}\ M$$
$$[Cu^{2+}] = 5 \times 10^{-4}\ M$$

1.	2.633
2.	2.571
3.	2.403
4.	2.569
5.	2.583
6.	2.542

Average k(obs) = 2.550
(Standard deviation = 0.071)

5.4.5 Solution Preparation and Titration - Experiment 5

A solution of approximate volume 490 cm^3 was prepared, containing 2mM $Cu(ClO_4)_2.6H_2O$ (0.3706g), 4mM succinic acid (0.2362g) and 0.1M $NaClO_4.H_2O$ (7.0230g). The pH was adjusted to ~2.5 with 2 cm^3 of 1.0M $HClO_4$ and the volume was made up to 500 cm^3 with distilled water. The titrant was a standardised 0.05M NaOH solution, obtained from BDH.

The combination pH electrode was standardised using 0.05M $KHPO_4$ (pH = 4.008 at 25°C) and 0.025M Na_2HPO_4 and 0.025M KH_2PO_4 (pH = 6.865 at 25°C). The temperature was maintained at 25°C throughout the titration. Sodium hydroxide was added, to a stirred solution of the above ingredients, until the pH reached 6, whereupon copper hydroxide precipitated.

5.4.6 Solution Preparation: Experiments (6) and (7)

Stock Solutions

Copper Stock: 200 cm^3 of 5mM solution (0.3706g $Cu(ClO_4)_2.6H_2O$).

Ligand Stock: 200 cm^3 of 50mM solution (1.863g $13N_4$).

Succinic Acid Stock: 1000 cm^3 of 0.5M solution (59.045g).

NaOH Stock: 1.0M solution purchased from BDH.

$NaClO_4$ Stock: 500 cm^3 of 1.0M solution (70.23g $NaClO_4.H_2O$).

Solutions were prepared by a 10 fold dilution of the copper and ligand stock solutions (5 cm^3) in the appropriate buffer (50 cm^3). The figures in parentheses indicate the volumes of stock solutions required in a total volume of 50 cm^3 to give the indicated pH and ionic strength. The remaining volume is made up of distilled water. All volumes were measured using "Grade A" volumetric pipettes.

Experiment 6.1

pH=5.7; I=0.3; [succ]= 1) 0.06M 2) 0.09M 3) 0.12M

1) 0.06M H_2Succ (6 cm^3); 0.10M NaOH (5 cm^3); 0.16M $NaClO_4$ (8 cm^3)

2) 0.09M H_2Succ (9 cm^3); 0.15M NaOH (7.5 cm^3); 0.09M $NaClO_4$ (4.5 cm^3)

3) 0.12M H_2Succ (12 cm^3); 0.20M NaOH (10 cm^3); 0.02M $NaClO_4$ (1 cm^3)

Experiment 6.2

pH=5.0; I=0.3; [succ]= 1) 0.07M 2) 0.14M 3) 0.21M

1) 0.07M H_2Succ (7 cm^3); 0.09M NaOH (4.5 cm^3); 0.19M $NaClO_4$ (8 cm^3)

2) 0.14M H_2Succ (14 cm^3); 0.18M NaOH (9 cm^3); 0.08M $NaClO_4$ (4.5 cm^3)

3) 0.21M H_2Succ (21 cm^3); 0.27M NaOH (13.5 cm^3); 0M $NaClO_4$ (0 cm^3)

Experiment 6.3

pH=4.0; I=0.3; [succ]= 1) 0.08M 2) 0.16M 3) 0.24M

1) 0.08M H_2Succ (8 cm^3); 0.04M NaOH (2 cm^3); 0.26M $NaClO_4$ (13 cm^3)

2) 0.16M H_2Succ (16 cm^3); 0.08M NaOH (4 cm^3); 0.22M $NaClO_4$ (11 cm^3)

3) 0.24M H_2Succ (24 cm^3); 0.12M NaOH (6 cm^3); 0.18M $NaClO_4$ (9 cm^3)

Experiment 6.4

pH=3.6; I=0.3; [succ]= 1) 0.12M 2) 0.18M 3) 0.24M

1) 0.12M H_2Succ (12 cm^3); 0.03M NaOH (1.5 cm^3); 0.27M $NaClO_4$ (13.5 cm^3)

2) 0.18M H_2Succ (18cm^3); 0.045M NaOH (2.25cm^3); 0.255M $NaClO_4$ (12.75cm^3)

3) 0.24M H_2Succ (24 cm^3); 0.06M NaOH (3 cm^3); 0.24M $NaClO_4$ (12 cm^3)

Experiment 7.1

pH=5.6; [succ]= 0.04M; I= 1) 0.08 2) 0.18 3) 0.28 4) 0.48

1) - 4) 0.04M H_2Succ (4 cm^3) + 0.06M NaOH (3 cm^3)

1) 0M $NaClO_4$; 2) 0.1M $NaClO_4$ (5 cm^3); 3) 0.2M $NaClO_4$ (10 cm^3); 4) 0.4M $NaClO_4$ (20 cm^3).

Experiment 7.2

pH=4.2; [succ]= 0.04M; I= 1) 0.02 2) 0.12 3) 0.22 4) 0.42

1) - 4) 0.04M H_2Succ (4 cm^3) + 0.02M NaOH (1 cm^3)

1) 0M $NaClO_4$; 2) 0.1M $NaClO_4$ (5 cm^3); 3) 0.2M $NaClO_4$ (10 cm^3); 4) 0.4M $NaClO_4$ (20 cm^3).

Experiment 7.3

pH=3.7; [succ]= 0.08M; I= 1) 0.02 2) 0.04 3) 0.08 4) 0.16

1) - 4) 0.08M H_2Succ (8 cm^3) + 0.02M NaOH (1 cm^3)

1) 0M $NaClO_4$; 2) 0.02M $NaClO_4$ (1 cm^3); 3) 0.06M $NaClO_4$ (3 cm^3); 4) 0.14M $NaClO_4$ (7 cm^3).

k_{obs} values were calculated in the same manner as for experiments (1) to (4) (section 5.4.4).

5.5 RESULTS TABLES AND PLOTS

5.5.1 Tables

pH	I	$\frac{\sqrt{I}}{1+\sqrt{I}}$	k_{obs}	log k_{obs}	SLOPE‡‡
	0.08	0.221	11.97	1.078	
5.6	0.18	0.298	8.22	0.915	-2.20
	0.28	0.346	6.27	0.797	
	0.48	0.409	4.65	0.667	
	0.02	0.124	1.32	0.121	
4.2	0.12	0.257	0.846	-0.073	-1.40
	0.22	0.319	0.700	-0.155	
	0.42	0.393	0.555	-0.256	
	0.02	0.124	0.464	-0.333	
3.7	0.04	0.167	0.407	-0.390	-1.36
	0.08	0.220	0.328	-0.484	
	0.16	0.286	0.283	-0.548	

Table 5.10 *Ionic strength dependence; 25°C; k_{obs} in s^{-1}*

‡‡ slope determined by linear regression

pH	$[succ]_{tot}$	$[succ^{2-}]$	k_{obs}	δ_1	$\frac{k_{obs}\cdot\delta_1}{[succ^{2-}]}$
	0.06	$4.5x10^{-2}$	9.40	32.28	6743
5.7	0.09	$6.5x10^{-2}$	11.46	60.62	10688
	0.12	$8.5x10^{-2}$	14.18	97.84	16322
	0.07	$2.5x10^{-2}$	3.93	23.58	3707
5.0	0.14	$4.5x10^{-2}$	5.77	59.22	7593
	0.21	$6.5x10^{-2}$	6.71	110.49	11406
	0.08	$2.8x10^{-3}$	0.468	21.90	3660
4.0	0.16	$5.4x10^{-3}$	0.664	42.91	5276
	0.24	$7.9x10^{-3}$	0.776	64.57	6343
	0.12	$1.2x10^{-3}$	0.240	44.27	8854
3.6	0.18	$1.8x10^{-3}$	0.286	66.20	10518
	0.24	$2.4x10^{-3}$	0.307	88.33	11299

Table 5.11 *Succinate dependence; 25°C; k(obs) in s^{-1}; I=0.3 mol dm^{-3}; [succ] in mol dm^{-3}.*

		K_3=1		K_3=10	
pH	$[succ^{2-}]$	δ_2	$\frac{k_{obs}\cdot\delta_2}{[succ^{2-}]^2}$	δ_2	$\frac{k_{obs}\cdot\delta_2}{[succ^{2-}]^2}$
	$4.5x10^{-2}$	26.80	124000	34.18	159000
5.7	$6.5x10^{-2}$	51.25	139000	73.49	199000
	$8.5x10^{-2}$	84.30	165000	134.05	263000
	$2.5x10^{-2}$	10.52	66000	11.78	74000
5.0	$4.5x10^{-2}$	26.80	76000	34.18	97000
	$6.5x10^{-2}$	51.25	81000	78.49	117000
	$2.8x10^{-3}$	1.49	89000	1.49	89000
4.0	$5.4x10^{-3}$	2.07	47000	2.09	48000
	$7.9x10^{-3}$	2.75	34000	2.79	35000
	$1.2x10^{-3}$	1.19	198000	1.19	198000
3.6	$1.8x10^{-3}$	1.30	115000	1.30	115000
	$2.4x10^{-3}$	1.41	75000	1.41	75000

Table 5.13 *Succinate dependence; 25°C; k(obs) in s^{-1}; I=0.3 mol dm^{-3}; [succ] in mol dm^{-3}.*

5.5.2 Plots

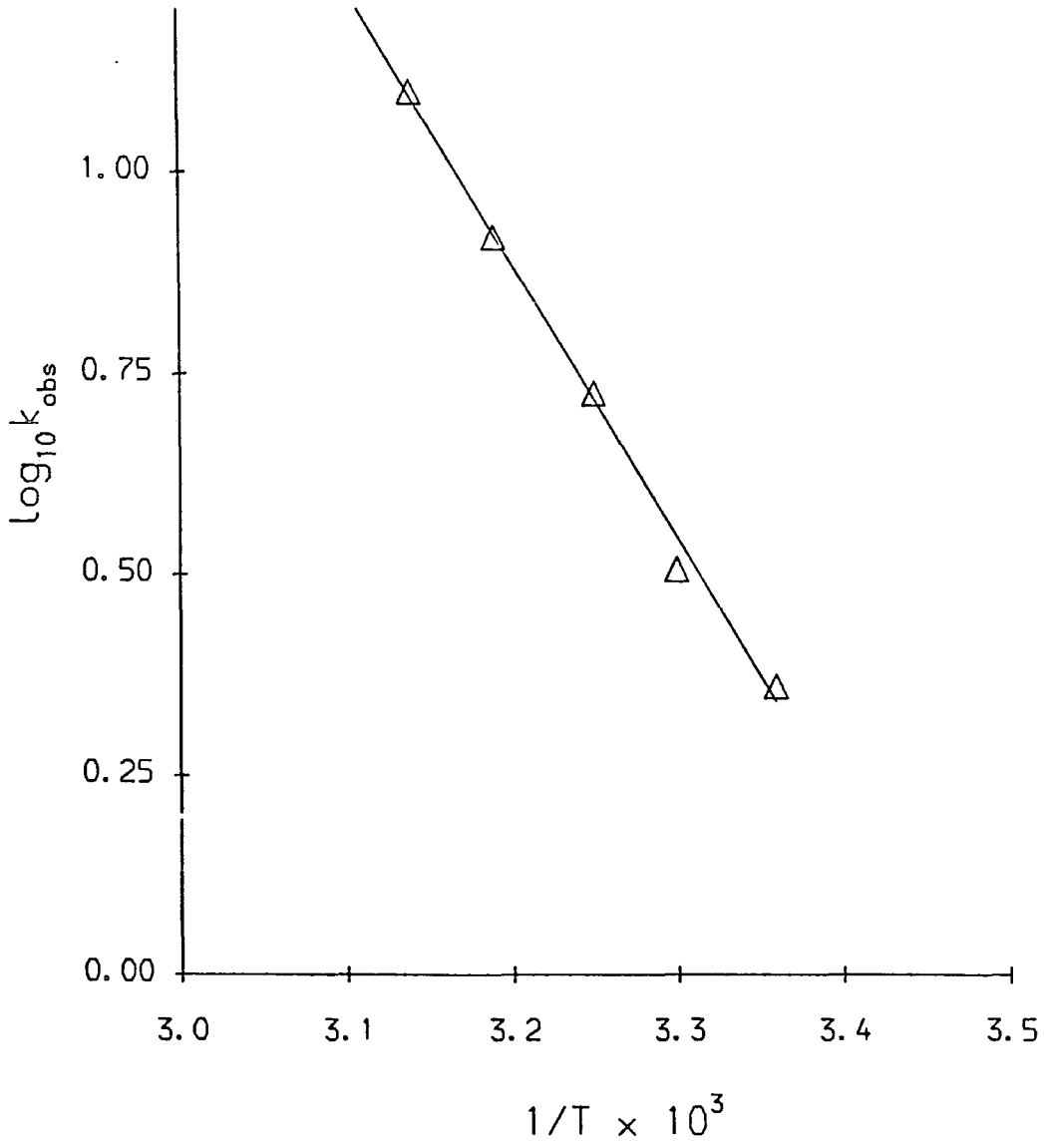

Figure 5.3 *Arrhenius plot for the reaction between Copper(II) Succinate and* $13N_4$

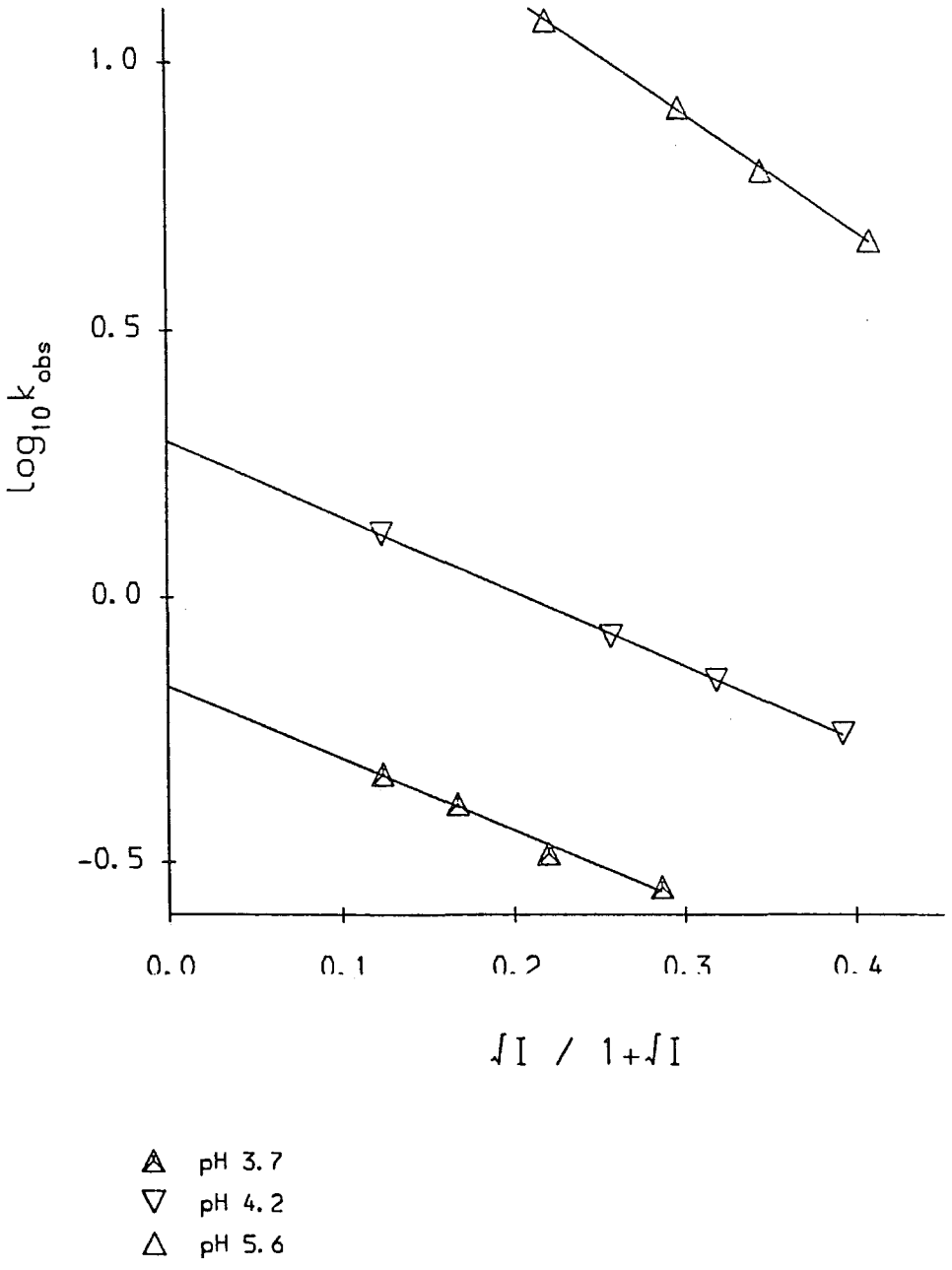

Figure 5.6 *Ionic Strength Dependence of the Rate of the Reaction between Copper(II) succinate and* $13N_4$

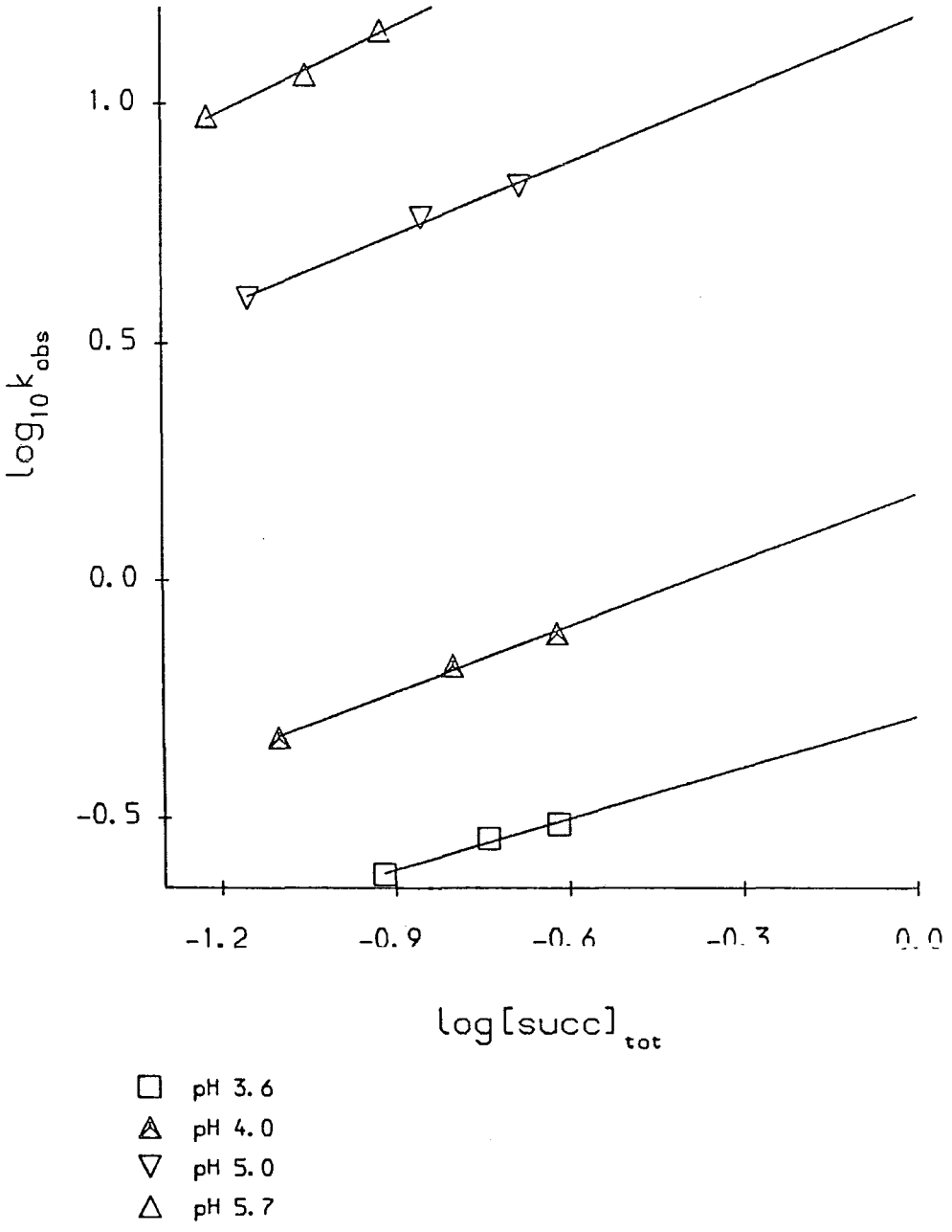

Figure 5.7 *Succinate Dependence of the Rate of the Reaction between Copper(II) Succinate and* $13N_4$

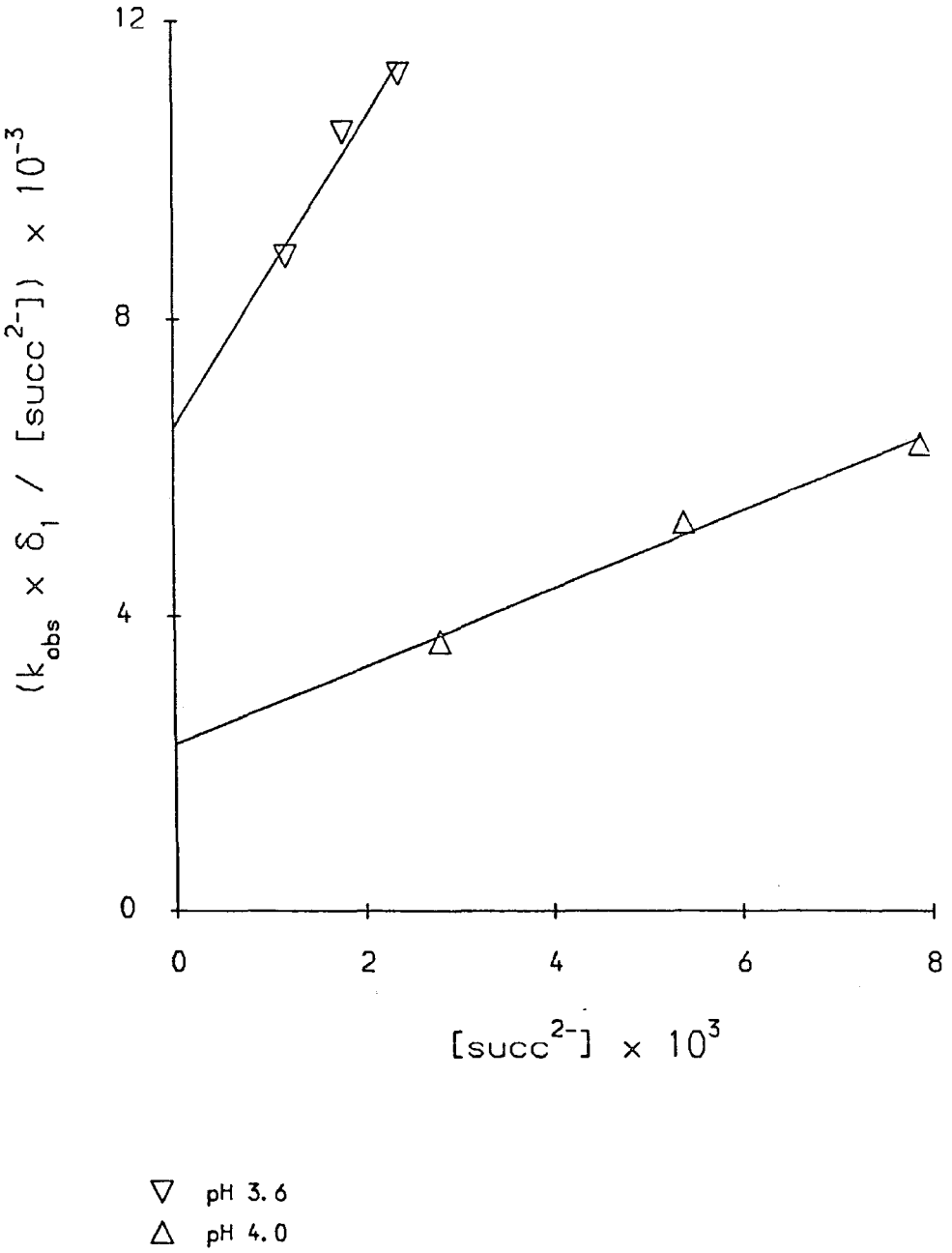

Figure 5.8 *Dependence of the Rate of complexation Upon the Concentration of* $Succ^{2-}$ *(Lower pH)*

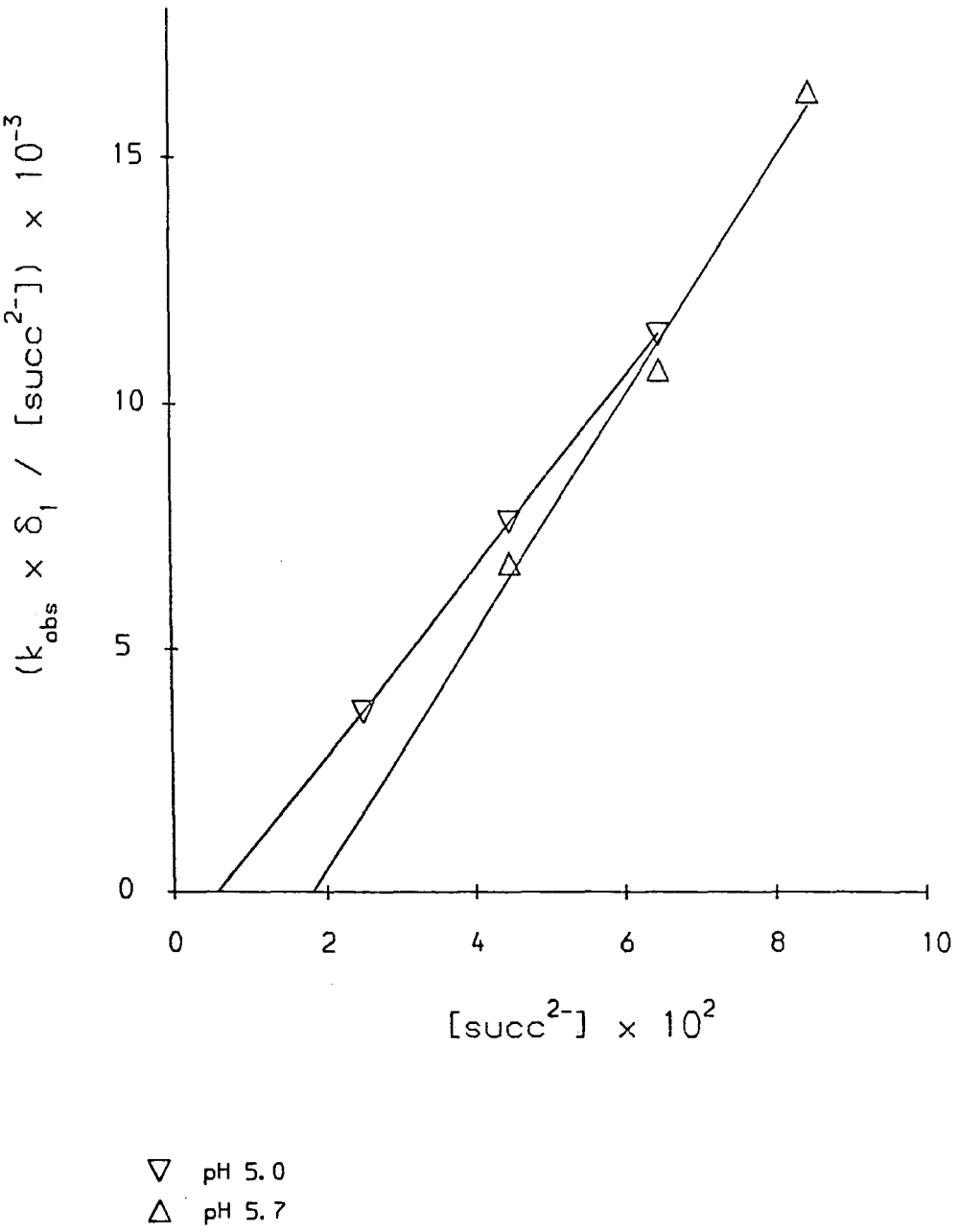

Figure 5.9 *Dependence of the Rate of Complexation Upon the Concentration of $Succ^{2-}$ (Higher pH)*

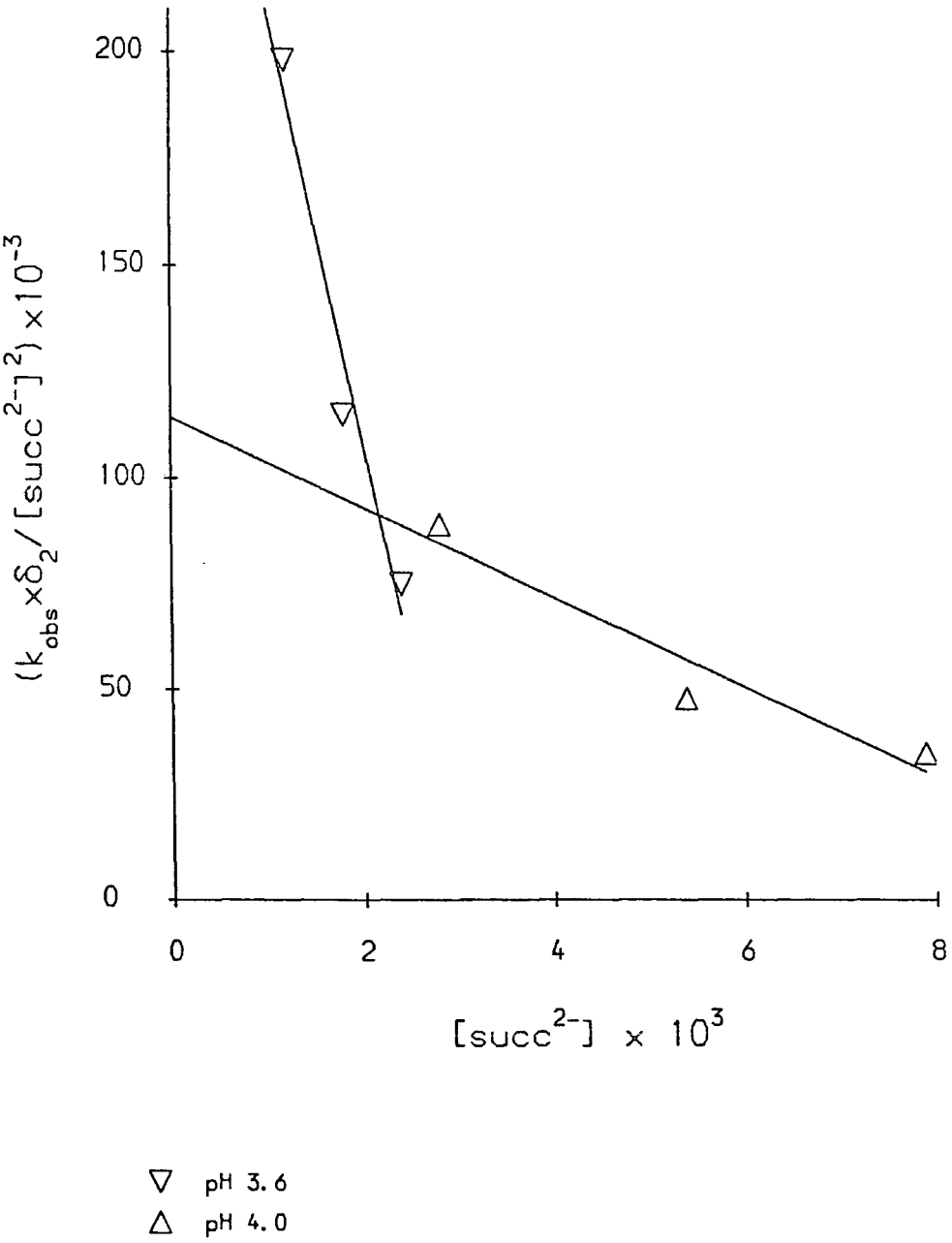

Figure 5.11 *Dependence of the Rate of Complexation Upon the Squared Concentration of $Succ^{2-}$ (Lower pH)*

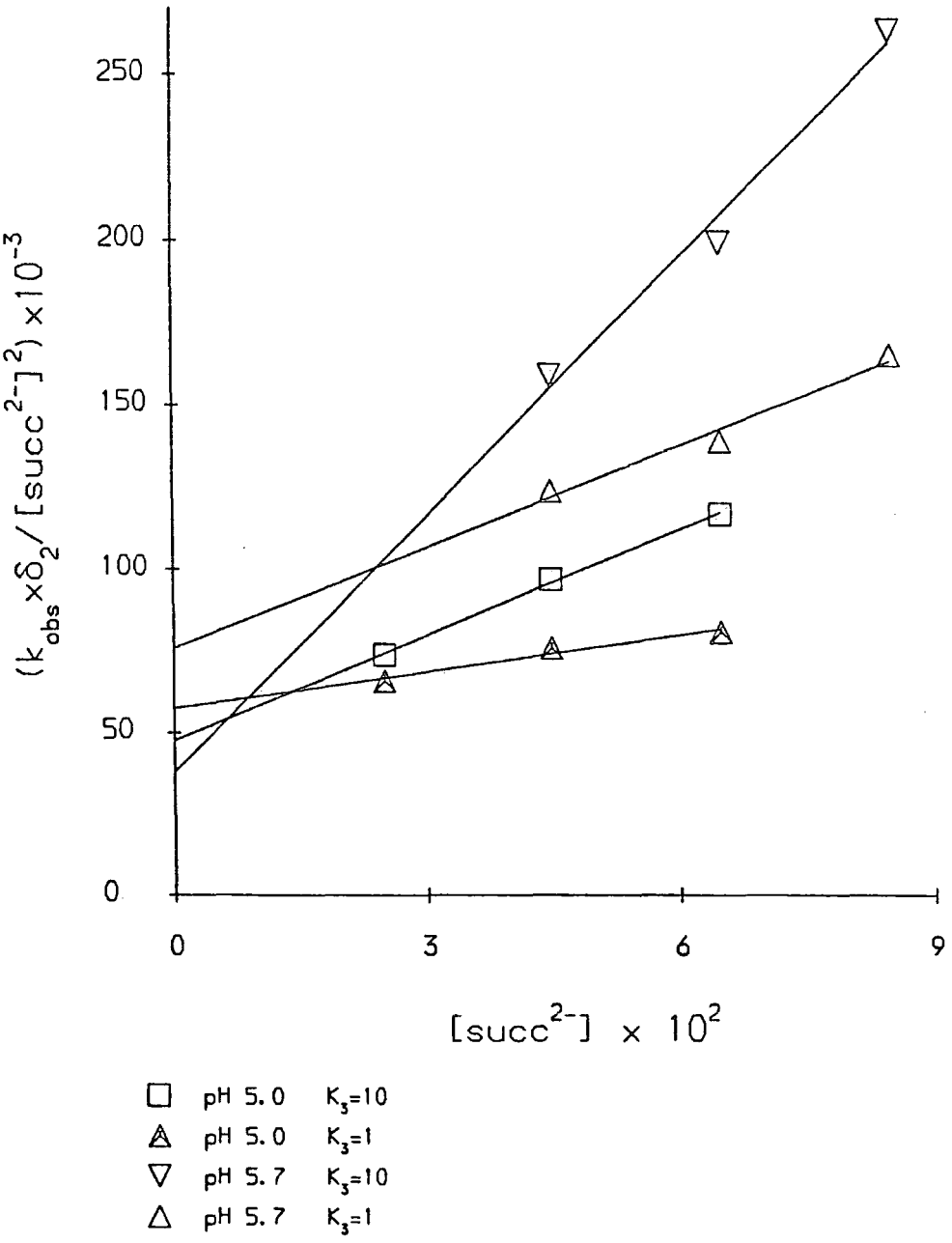

Figure 5.12 *Dependence of the Rate of Complexation Upon the Squared Concentration of* $Succ^{2-}$ *(Higher pH)*

5.6 REFERENCES

1. L.D. Pettit, I. Steel, G. Formicka-Kozloska, T. Tatarowski and M. Bataille, *J.Chem.Soc. Dalton Trans.*, 535 (1985)

2. T.A. Kaden, *Helv.Chim.Acta*, 53, 617 (1970)

3. M. Kodama and E. Kimura, *J.Chem.Soc. Dalton Trans.*, 1720 (1976)

4. A.P. Leugger, L. Hertli and T.A. Kaden, *Helv.Chim.Acta*, 61, 219 (1978)

5. M. Kodama and E. Kimura, *J.Chem.Soc. Dalton Trans.*, 1473 (1977)

6. M. Kodama and E. Kimura, *J.Chem.Soc. Dalton Trans.*, 116 (1976)

7. Y. Wu and T.A. Kaden, *Helv.Chim.Acta*, 68, 1611 (1985)

8. E. Kimura, M. Yameoka, M. Morioka and T. Koike, *Inorg.Chem.*, 25, 3883 (1986)

9. R.C. Warner and I. Weber, *J.Am.Chem.Soc.*, 75, 5086 (1953)

10. E. Campi, G. Ostacoli, M. Meirone and G. Sain, *J.Inorg.Nucl.Chem.*, 26, 553 (1964)

11. K.S. Rajan and A.E. Martell, *J.Inorg.Nucl.Chem.*, 29, 463 (1967)

12. R.W. Parry and F.W. DuBois, *J.Am.Chem.Soc.*, 74, 3749 (1952)

13. J.K. Garg, L.K. Agarwal, P.S. Verma and D.S. Jain, *J.Electrochem. Soc.India*, 31(4), 153 (1982)

14. A. McAuley, G.H. Nancollas and K. Torrance, *Inorg.Chem.*, 6, 136 (1967)

15. M Yas da, K. Yamasaki and K. Ohtaki, *Bull.Chem.Soc.Japan*, 33, 1067 (1960)

16. E. Campi, *Ann.Chim.Italy*, 53, 96 (1963)

17. E.G. Sase and D.V. Jahargirdar, *J.Inorg.Nucl.Chem.*, 37, 985 (1975)

18. P.G. Daniele, G. Ostacoli and A. Vanni, *Atti.Accad.Sci.Torino*, 109, 547 (1974-1975)

19. G. Arena, R. Cali, E. Rizzarelli and S. Sammartano, *Trans.Met. Chem.*, 3, 147 (1978)

20. J.M. Peacock and J.C. James, *J.Chem.Soc.*, 2233 (1951)

21. P. Gans, A. Sabatini and A.J. Vacca, *J.Chem.Soc.Dalton Trans.*, 1195 (1985)

CHAPTER SIX

RADIOIMMUNOTHERAPY

6.1 INTRODUCTION

6.1.1 The Potential For Antibody-Based Tumour Therapy[1]

Unlike normal cells, malignant cells will grow in any part of the body. Carried from primary tumours in the bloodstream they may set seed to form secondary deposits called *metastases*. Often relatively less hazardous forms of cancer *e.g* melanoma (skin cancer) become life-threatening when the malignancy spreads to critical organs of the body.

Surgical removal has proved to be the most effective way of treating easily accessible malignancies such as melanoma, and is likely to remain so. However, more deep-seated tumours, especially if close to vital organs, are generally more difficult to treat. Smaller growths, especially *micrometastases*, are difficult to detect let alone treat by conventional methods, yet all must be eliminated for the treatment to be effective.

There has been much interest in the potential of monoclonal antibodies which bind specifically to tumour associated antigens for the treatment of some of the more troublesome types of tumour *e.g* breast, lung, stomach and colorectal. Monoclonal antibodies alone are rarely cytotoxic unless they bind to and inactivate cell surface molecules which are necessary for survival or proliferation. In some cases however antibodies may elicit a response from the immune system through their effector functions (Fc region) which ultimately destroys the tumour cell. Indeed this is the mechanism by which malignant cells are normally destroyed by the body, thereby preventing the development of cancer. However many antibodies are incapable of promoting a satisfactory response from the immune system and must instead be tagged with an anti-cancer drug.

Most anti-cancer drugs presently in clinical use act by preventing the replication of DNA, thus inhibiting cell division and tumour growth. However the dose of drug which may be given is limited by its toxicity towards towards rapidly dividing normal tissues *e.g* bone marrow. The aim of antibody-based tumour therapy is to deliver a cytotoxic agent to the site of the tumour without exposing the rest of the body to toxic levels of the drug. Selective cytotoxic effects have been observed for a variety of monoclonal antibodies when coupled with biochemical toxins or radioactive isotopes.

6.1.2 Biochemical versus Radioactive Cytotoxicity

The coupling of chemotherapeutic drugs *e.g* methotrexate and of toxic proteins *e.g* ricin to Mab's has been much explored with the hope of combining the cytotoxic effect of the drug with the tumour specificity of the antibody. However this approach is often limited by the slow rate of internalisation of the toxin across the cell membrane. Since virtually all the cells of a tumour must be sterilised for long term remission, at least one cytotoxic agent must be incorporated per cell.

Within some tumours there are clusters of cells which lack the target antigen. These so-called "cold-regions" will escape the effects of the cytotoxin. Generally tumours which take the form of a loose association of cells (sarcomas) or which are well supplied with blood vessels will respond better to biochemical cytotoxins. Tumours consisting of a poorly vascularised solid mass of tightly-packed cells (carcinomas), providing only limited access for Mab's, will tend to respond relatively poorly.

Since radionuclides emit penetrating and ionising radiation throughout the localisation process, they are more indiscriminately

toxic than biochemical toxins. However it is precisely because their radiation may span more than one cell diameter, so-called "cross-fire", that certain types of radionuclides are more useful for the treatment of larger and more solid tumour masses. The emissions can kill cells which surround the targeted cell, allowing the destruction of neighbouring cells which lack the target antigen and of cells in poorly vascularised tumours which the antibody itself cannot reach.

6.2 RADIOIMMUNOTHERAPY

6.2.1 Choice of Emission[2-5]

Only particulate radiation interacts sufficiently strongly with bodily tissues, including cellular DNA, to cause large-scale sterilisation. Alpha particles are particularly effective cytotoxic agents since they dissipate a large amount of energy in a path length of only one or two cell diameters. Unfortunately most alpha-emitters are heavy elements (atomic number > 82) which decay to give hazardous daughter products. This is a major problem since the alpha recoil energy, typically several hundred keV, will rupture the radionuclide-antibody bond, leaving the daughter product to diffuse away from the tumour. ^{211}At and ^{212}Bi (^{212}Pb) are examples of α-emitting radionuclides which are suitable for therapeutic use. Another approach is to generate an alpha-emitter *in situ* by bombarding a stable isotope *e.g.* ^{10}B with low energy thermal neutrons. Unfortunately thermal neutrons penetrate tissues so poorly that this method has only limited application. Radionuclides which decay by neutron capture or internal conversion have been proposed for the treatment of very small tumours since they emit X-rays and Auger

electrons of very short range ($\leq 1\mu m$) which deliver a high radiation dose locally. Since sources of alpha particles and Auger electrons deliver their energy along a short path length they suffer from the same disadvantages as biochemical toxins. Thus they are of limited use for the treatment of larger and more poorly vascularised tumours which the antibody cannot penetrate effectively. In addition they rely upon almost every cell having a copy of the tumour-associated antigen (*i.e* no "cold" regions).

The true benefits of "cross-fire" can only be realised if longer-range particles are used, essentially β-rays. There is also a much wider choice of β-emitters which are potentially suitable for therapy, offering a range of particle energies and greater flexibility for the chemist who must attach them to the antibody. In fact the only radionuclides which satisfy all the general criteria outlined in section 1.3.1, as well as those specifically required for therapy, are β-emitters.

6.2.2 Criteria for choice of β-emitter

The following factors have been identified as being particularly important in the choice of a β-emitting radioisotope for therapy:

1) Physical half-life
2) Zero or low gamma emissions
3) β particle energy
4) Availability and cost
5) Stable daughter product
6) Appropriate chemistry for Mab attachment.

Physical half-life

The half-life must be sufficiently long to allow for the necessary tumour accumulation of the antibody, yet sufficiently short to ensure

that most of the possible "absorbed dose" is delivered before the antibody itself is completely catabolised and the radioisotope released. Wessels and Rogus[3] developed a series of models to predict the half-life of an isotope which would give a maximum target:non-target ratio. Simple models suggested that the half-life should be at least 1.5 - 3.0 times longer than the time necessary for satisfactory accumulation in the tumour and clearance from non-target areas. Since the time required for a maximum target:non-target biodistribution ratio is typically 2 days, the ideal half-life is of the order of 72 to 144 hours.

Gamma Emissions

In theory, pure β-emitters, of which there are relatively few suitable ones, are preferred for radioimmunotherapy since they deposit all their energy in a relatively short path-length (maximum target:non-target dose ratio). However it is often advantageous to have a small gamma component, of appropriate energy, for imaging the tumour whilst the patient is receiving radioimmunotherapy. Moreover the use of the same isotope at low dosage for pre-therapy imaging allows accurate dosimetric information for an individual tumour to be acquired, permitting the precise therapeutic dose required for its sterilisation to be calculated. If a radioisotope of a different element *e.g* ^{99m}Tc, ^{111}In is used for pre-therapy imaging one can never be sure that its target:non-target biodistribution will exactly match that of the therapeutic isotope[6].

Beta Energy[5]

A β-emitter may be selected on the basis of the energy of its β particle. This usually determines the size and morphology of tumour for which it is suitable. Generally the lower the β energy, the more

localised will be the energy deposition. This is especially important for smaller tumours which must be sterilised without β particles penetrating and damaging the surrounding normal tissue. However the relationship between particle energy and tumour size is complicated by the extent of the capillary vasculature and the density of the antibody expression, which may differ for different tumours. If the vasculature is inadequate or there are "cold regions" devoid of antigens, the need for "cross-fire" will be greater and a longer range β particle must be employed to sterilise less accessible cells.

Some radionuclides which appear eminently suitable for therapeutic applications on the basis of their decay characteristics must be discounted on other grounds *e.g* availability and cost, active daughters, inappropriate chemistry *etc.*

6.2.3 Radioisotopes of Potential Therapeutic Value

So far, only one radioisotope, ^{131}I, has been used for radioimmunotherapy in man[7]. However it is by no means ideal for this purpose because of its high yield of penetrating gamma radiation which can escape from most tumours and damage healthy tissues. Iodine isotopes also tend to deiodinate from Mab's *in vivo*. Metals are much better in this respect, being attached to antibodies using chelating agents (section 1.4). A number of β emitting radiometals which have been considered for radioimmunotherapy are given in Table 6.1 (^{131}I is also included for comparison). All of these radioisotopes produce abundant β emissions, which vary in range from 3.9 mm for ^{90}Y to 0.1 mm for ^{199}Au, and all decay to give stable daughter products. However some of these radiometals are more favoured than others mainly on the grounds of cost,

availability and/or difficulty of chemistry.

ISOTOPE	$t_{\frac{1}{2}}$(h)	β (max MeV %)[8]	Gamma (keV %)[8]	SOURCE
^{131}I	193	0.606 (90)	364 (79)	Reactor
^{90}Y	64	2.25 (100)	---	Generator
^{64}Cu	62	0.577 (20) 0.486 (35) 0.395 (45)	93 (17) 184 (47)	Accelerator
^{199}Au	75	0.250 (22) 0.296 (72)	158 (76)	Reactor
^{186}Re	90	0.933 (21) 1.071 (74)	137	Reactor
^{188}Re	17	1.96 (18) 2.12 (80)	155	Generator
^{111}Ag	179	1.04 (93)	342 (6)	
^{161}Tb	166	0.45 (26) 0.57 (64)	75 57 (21)	

Table 6.1 *Candidate Radioisotopes for Therapy*

For example, ^{161}Tb and ^{186}Re are potentially useful but are unusually difficult to obtain in a "carrier-free" form. Its low β energy makes ^{199}Au an attractive choice for treating small tumours, micrometastases, leukaemias *etc*. However the main drawback is the uncompromising nature of gold coordination chemistry, making its attachment to the antibody a major challenge. Similarly, the aqueous chelation chemistry of isotopes of rhenium and silver is little known; few potentially suitable chelates or macrocyclic complexes have been reported to date.

From this shortlist of radionuclide candidates, two are particularly promising - yttrium-90, by virtue of its cheapness, availability and high energy, long range β particle; and copper-67, by virtue of its ability to form "strong" complexes with macrocyclic ligands and its gamma ray, of suitable energy for imaging. These two isotopes are discussed further in sections 6.3 and 6.4 respectively.

6.3.1 The Nuclear Properties of ^{90}Y

^{90}Y is perhaps the most important radiometal which has been identified as a successor to ^{131}I. Since it is a pure β emitter, the majority of the absorbed dose will be to the tumour itself rather than to the surrounding tissues. The energy of the β particle is sufficiently high (max E: 2.25 MeV; range 3.9 mm) to allow successful treatment of larger tumours with extensive "cold regions". ^{90}Y has a physical half-life (64 hours) which achieves the right balance between the rate of antibody localisation and the rate of antibody catabolism. With regard to the more general selection criteria of section 1.3.1, ^{90}Y produces a stable daughter product (^{90}Zr) and is available cheaply and "carrier-free" from a ^{90}Sr generator.

One disadvantage of ^{90}Y arises from its lack of a suitable gamma ray. Being a pure β emitter, the tumour localisation of ^{90}Y-labelled antibodies cannot be visualised externally so the therapy dose distribution cannot easily be monitored. (The use of a gamma emitting isotope of yttrium *e.g* ^{86}Y, ^{87}Y may be necessary at the clinical trials stage to determine the precise dosimetry).

6.3.2 The Chemical Properties of ^{90}Y

Although yttrium belongs to group IIIa, its chemistry is often considered alongside that of the lanthanides[9]. The *lanthanide contraction*† is sufficiently large that the size of the Y^{3+} ion is

†The lanthanide contraction arises from the imperfect shielding of one 4f electron by another. Thus across the series, effective nuclear charge increases causing a reduction in the size of the 4f shell.

reached in the Ho^{3+}-Er^{3+} region. The heavier lanthanides (Gd-Lu) are often called "yttrium earths" since they share with yttrium many basic chemical properties which are determined by cation-charge/cation-size relationships *e.g* crystal structure, coordination number, stability of complex species. The relationship between effective ionic radius and coordination number is shown in Figure 6.1[10].

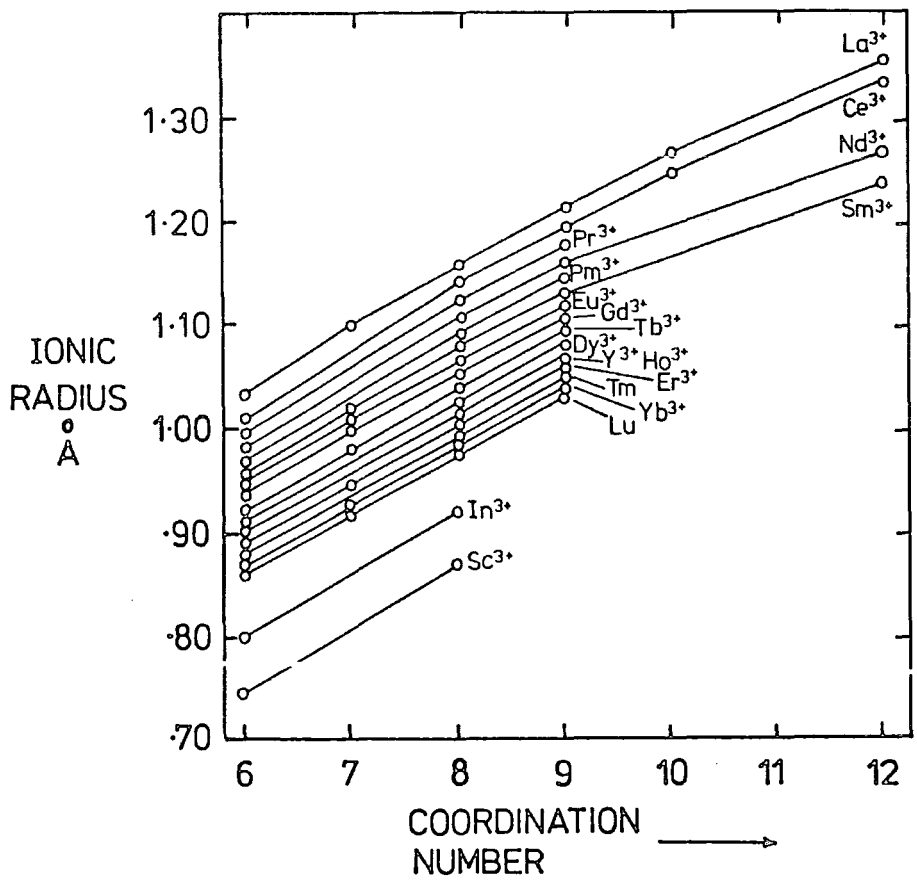

Figure 6.1 *The relationship between ionic radius and coordination number for yttrium and the lanthanides.*

In common with the heavier lanthanides, yttrium can form complexes with coordination numbers which vary between 6 and 9. However six-coordination is rare; 7, 8 or 9 being much more common *e.g* $Y(H_2O)_9^{3+}$ is

formed in aqueous solution.

In contrast to the "d" block metals which prefer "softer" donor atoms *e.g* N or S, lanthanides ("f" block) prefer "harder" oxygen donors; forming electrostatic non-directional bonds similar to those formed by the alkaline-earth or alkali metals.

6.3.3 The Selection of Suitable ^{90}Y Binders

Bifunctional derivatives of EDTA and DTPA have been employed for attaching ^{90}Y to antibodies[11,12]. The thermodynamic stability of these yttrium complexes is high (log K = 22.1 for DTPA; 18.1 for EDTA). However the stability constant is not the primary consideration for *in vivo* applications; kinetic inertness being much more important (section 1.4.3). Indeed, it is now known that ^{90}Y dissociates from EDTA and DTPA *in vivo* in much the same way as ^{67}Cu is lost (section 1.5.2). Once dissociated, ^{90}Y accumulates readily in bone whereupon it delivers a toxic dose of β radiation to the haematopoietic cells of the marrow. Hence there is an urgent need to replace ^{90}Y-DTPA with a more kinetically stable ^{90}Y-chelate which does not lose the radiolabel *in vivo*.

In 1976, Stetter and Frank[13] reported that the macrocycle, 1,4,7,10-tetraazacyclododecane-N,N^1,N^2,N^3-tetraacetic acid ("DOTA"), formed an extremely stable Ca^{2+} complex (log K = 17.2) (Figure 6.2). It was predicted that DOTA would also formed complexes with the lanthanides by virtue of the similarity in ionic radius between Ca^{2+} and Ln^{3+}. The following year, Desreux *et al.*[14] found that DOTA complexes of the heavier lanthanides were exceedingly stable over a wide pH range; ten orders of magnitude more stable than their EDTA complexes (Table 6.2).

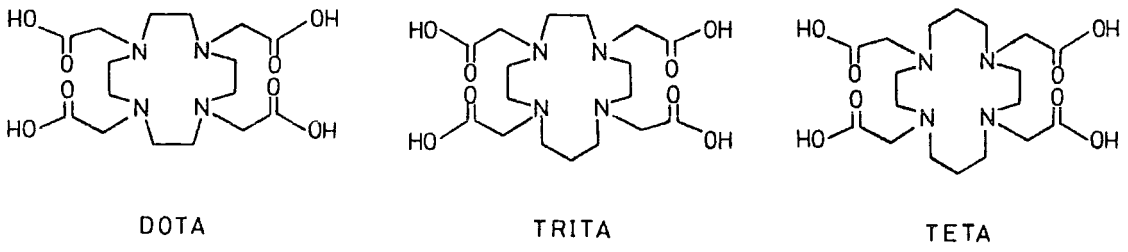

Figure 6.2 *Macrocyclic tetraamine tetracarboxylic acids for ^{90}Y binding.*

Ln^{3+}	DOTA	EDTA	DTPA
Eu^{3+}	28.2	17.3	22.4
Tb^{3+}	28.6	17.9	22.7
Lu^{3+}	29.2	19.8	22.4

Table 6.2 *Stability constants (log K) of Lanthanide-DOTA complexes[15]; 20 ^0C; I=1.0 mol dm^{-3}*

The stability of DOTA complexes increases with decreasing ionic radius of the metal ion. No stability constant for Y-DOTA has been reported but on the basis of its ionic radius, it might be expected to be similar to that of Tb-DOTA (28.6). DOTA behaves as a classical acyclic complexing agent; there being no metal ion diameter-cavity size correlation often associated with macrocyclic complexes. Indeed the metal does not reside within the macrocyclic cavity but sits above the N_4 plane, with carboxylic groups completing a nearly spherical "cage-like" structure[16]. The square antiprismatic structure of the Eu-DOTA complex, Na^+ $(EuDOTA.H_2O)^-.4H_2O$ is shown in Figure 6.3. The coordinated ligand is able to adopt the same stable, rigid conformation which is found in the free ligand. Moreover ^1H NMR studies have indicated that Ln-DOTA complexes adopt the same rigid, highly symmetrical structures in solution. This is highly unusual; lanthanides generally form highly

labile complexes in which Ln-oxygen bonds exchange very rapidly. Since the ligand undergoes little or no conformational change, the energy required for complexation is limited to that associated with desolvation of the metal ion. Overall the enthalpy term is very favourable, thereby contributing to the high thermodynamic stability of these complexes.

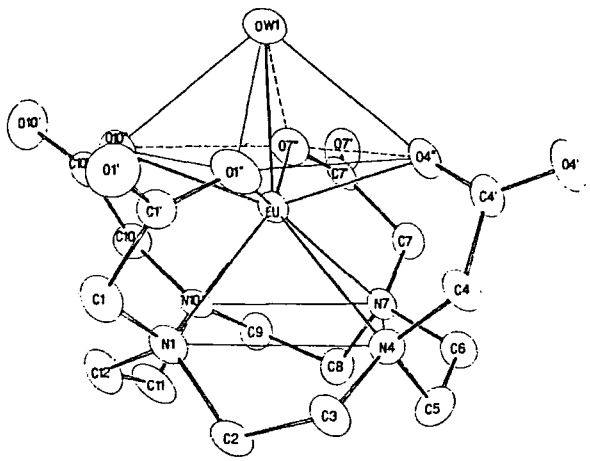

Figure 6.3 *The crystal structure of* $(EuDOTA.H_2O)^-$

It is reported[17] that the rate of complexation of heavy lanthanides by DOTA is very slow below pH 7. This was associated with the unusual conformational properties of the ligand. The rate-determining step may involve the rearrangement of an intermediate complex, in which the metal is not coordinated to all the carboxylic groups, to one in which the metal is completely encapsulated.

Lanthanide complexes of the [14]-membered system, TETA (Figure 6.2) have also been reported.[18] However these complexes are much less thermodynamically stable by virtue of the conformation of the coordinated ligand being more highly strained. The six-membered chelate rings of TETA complexes are more sterically crowded than the five-membered rings of DOTA complexes. The crystal structure of Tb^{III}-TETA

is shown in Figure 6.4. The ligand adopts a distorted dodecahedral structure which lacks the axial symmetry of DOTA complexes.

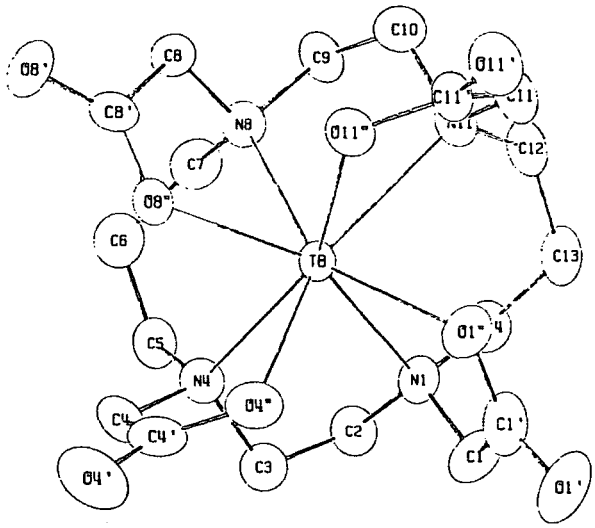

Figure 6.4 *The crystal structure of* $(TbTETA)^-$

The kinetics of association for Ln-TETA complexes are much more rapid than those of Ln-DOTA complexes presumably because the free ligand is less rigid and more easily distorts to accommodate the incoming metal ion.

In view of the similar nature of yttrium and the lanthanides, DOTA should be preferred to TETA for binding ^{90}Y *in vivo*. The rigid and symmetric structure of Y-DOTA is kinetically inert, resisting acid-induced decomplexation. However it was thought at the outset of this work, that its association kinetics at low pH (necessary to prevent non-specific ^{90}Y binding) might be too slow for its use to be practicable at the tracer level. Thus a [13]-membered analogue, TRITA (Figure 6.2) was contemplated, which it was hoped would combine the high kinetic stability of DOTA complexes with the more rapid association kinetics of TETA complexes. With this hope in mind, a functionalised derivative of TRITA was synthesised (section 6.3.4).

It has since transpired that Y-DOTA is formed more rapidly than had been expected on the basis of previous observations using lanthanides *e.g* terbium.[19] In preliminary radiolabelling experiments at Harwell, it would appear that the rate of formation of ^{90}Y-DOTA may actually be more rapid than that of ^{90}Y-TRITA or ^{90}Y-TETA; in which case its superior stability would make ^{90}Y-DOTA the preferred choice for *in vivo* yttrium binding.

6.3.4 The Functionalisation of TRITA

The selection of a side-chain functionality for TRITA is somewhat less critical than it was for unsubstituted tetraamine macrocycles (section 2.1.1) since the necessity for acylation of the exocyclic amine to be selective does not arise; the TRITA ring being peralkylated. However it seemed sensible to employ the same aminomethyl group as before to enable the use of a similar conjugation procedure.

The synthesis of the functionalised $13N_4$ cycle (28) has been described *vide ante* (section 2.3.4). Prior to alkylation of the 4 ring nitrogens, the exocyclic primary amine must be protected as an amide (59, Figure 6.5). Selective acylation was conducted under the same experimental conditions as the conjugation of (28) with the p-nitrophenyl ester of 2-vinylpyridine-methoxyacetic acid (section 2.6.4).

A 2.7 fold excess of p-nitrophenyl acetate in p-dioxane was stirred with (28) in "Pipes" buffer (pH 6.8) for 3 days at room temperature. A large excess of ester was required to drive the reaction to completion. The amide could then be recovered as a clear oil (pure by ^{1}H NMR) simply by extracting from aqueous base (KOH; pH 14) into chloroform. Attempts to peralkylate (59) directly using chloroacetic acid produced a crude mixture of partially alkylated products, from which the desired product

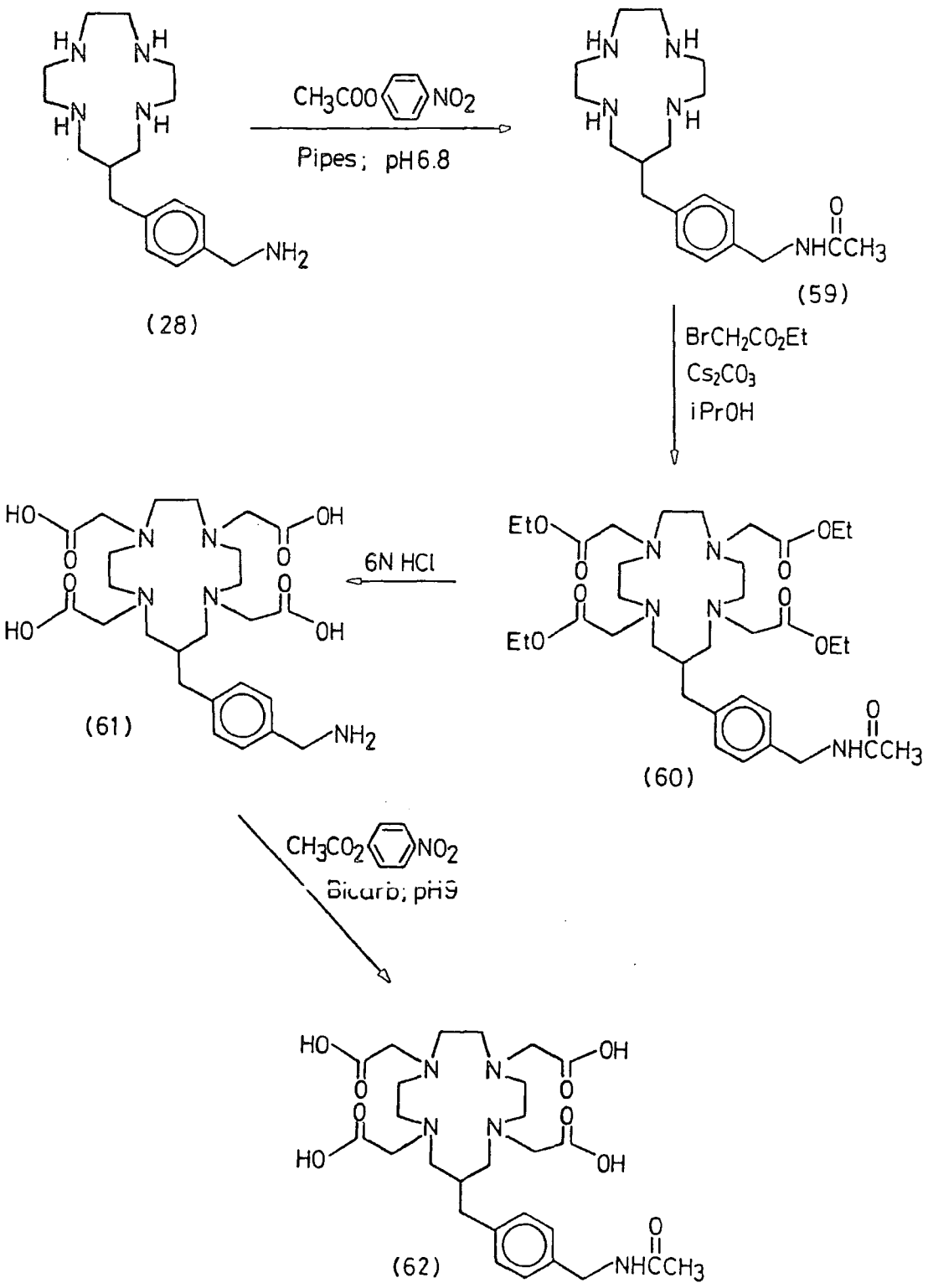

Figure 6.5 *A Synthetic Route to a Functionalised TRITA Derivative*

(61) could only be isolated by reverse phase HPLC. It was therefore more convenient to peralkylate (59) using ethyl bromoacetate, the product (60) being separable using conventional column chromatography (alumina), then hydrolyse the ester and amide groups simultaneously using 6N HCl.

The reaction with ethyl bromoacetate is cleaner, giving a higher yield of the peralkylated product (60), if caesium carbonate is used as a base (rather than sodium carbonate which is less basic) and anhydrous iso-propanol is used as the solvent (rather than acetonitrile which is normally used for such reactions). Although a small amount of trans-esterification (Et → iPr) occurred, this was not problematical since the ester is hydrolysed in the next step anyway (the use of anhydrous ethanol as a solvent would prevent this). Two successive alumina columns were necessary to isolate (60) as a pure "off-white" solid.

Deprotection proceeded smoothly in boiling 6N HCl to give the functionalised TRITA derivative (61) in a sufficiently pure form to be linked to a "trauted" Mab using the 2-vinylpyridine linker molecule whose synthesis is described in section 2.5.2.

A small amount of (61) was acetylated for future radiolabelling and biodistribution studies using ^{90}Y. On this occasion, selective acetylation was not necessary; pH 9 bicarbonate buffer being used instead of "Pipes". Following extraction of the excess ester and p-nitrophenol, the amide was purified from inorganic salts using a cation exchange resin (Dowex 50W H^+ form).

6.4 COPPER-67 FOR RADIOIMMUNOTHERAPY

6.4.1 The Nuclear Properties of ^{67}Cu

^{67}Cu is an attractive choice for radioimmunotherapy. In addition to abundant β particles (max E: 0.577, 0.486, 0.395 MeV), ^{67}Cu delivers moderately abundant gamma rays of an energy (91, 93, 184 keV) suitable for imaging. It has a half-life (62h), which is almost identical to that of ^{90}Y, and decays to give stable ^{67}Zn. In view of its much shorter β particle range (0.2 mm), ^{67}Cu should inflict less damage upon healthy tissue at the edge of the tumour than ^{90}Y. On the other hand, it is less suitable for the treatment of larger tumours especially those containing extensive "cold" regions.

The requirement to produce ^{67}Cu in a linear accelerator makes this isotope four times more expensive than ^{90}Y. It is produced from ^{68}Zn by a (p,2p) reaction:

$$^{68}Zn + p \longrightarrow {}^{67}Cu + 2p$$

$^{67}CuCl_2$ is available from the Los Alamos National Laboratory (New Mexico, USA) at a cost of ~ £40 per mCi.

6.4.2 The Chemical Properties of ^{67}Cu

Of course, the chemical properties of ^{67}Cu are identical to those already outlined in connection with the imaging isotope ^{64}Cu (section 1.5). It has already been established that antibody-bound cyclam and phenolic cyclam (2) form ^{64}Cu complexes which are stable *in vivo* (section 4.2.2). These ligands should be equally suitable for binding ^{67}Cu to Mab's.

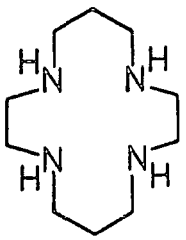

cyclam

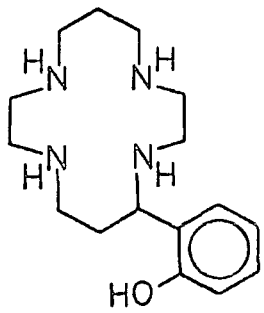

(2)

6.4.3 The Labelling and Biodistribution of ^{67}Cu-Macrocycle-Antibody Conjugates

A ^{67}Cu-mac-ab conjugate (mac=(2); ab=B72.3) was prepared from ^{67}Cu-succinate ($^{67}CuCl_2$ in succinate buffer) and the mac-ab according to the pH 4 labelling method which had worked so well for ^{64}Cu (section 4.3.4). After incubating for 30 minutes at 37^{o}C,‡ the labelled conjugate was washed with excess DTPA for 5 minutes to chelate the small amount of ^{67}Cu which may have bound non-specifically. The conjugate was purified using size-exclusion HPLC to remove aggregated protein (the sample of mac-ab conjugate was several months old and substantial cross-linking had occurred). The purified ^{67}Cu-mac-ab conjugate was then injected intravenously into "Thy 1.2" mice. The biodistribution profiles at 4, 24 and 72 hours are given in Table 6.3 (see section 3.1.3 for a review of the interpretation of animal data). ^{67}Cu biodistribution data for tumour-bearing mice obtained by Meares *et al.*[20] using the tetraamine-carboxylate macrocycle, TETA (section 1.5.2), conjugated to the Mab, "Lym-1" (anti-human B cell lymphoma), is given in Table 6.4 for

‡The higher temperature provides a kinetic enhancement over room temperature without damaging the antibody.

comparison.

TISSUE	4 hours %Dg^{-1}	4 hours %Dose	24 hours %Dg^{-1}	24 hours %Dose	72 hours %Dg^{-1}	72 hours %Dose
BLOOD	28.8±1.9	70.5±4.5	19.1±1.2	46.0±5.3	18.1±0.9	46.8±4.3
KIDNEYS	8.2±0.1	2.5±0.1	5.9±0.4	2.0±0.2	6.2±0.5	2.1±0.2
LIVER	9.3±0.4	13.8±0.1	6.5±0.6	8.6±1.6	5.1±0.3	8.7±1.3
LUNGS	10.1±0.1	1.9±0.1	7.7±0.8	1.2±0.4	8.6±0.3	1.7±0.1
SPLEEN	5.9±0.2	0.6±0.0	4.1±0.5	0.4±0.1	4.9±0.5	0.6±0.2
STOMACH	---	1.1±0.0	---	0.6±0.1	---	1.0±0.2
INTESTINES	---	5.1±0.7	---	4.6±0.4	---	4.6±0.0

Table 6.3 *Biodistribution data for ^{67}Cu-mac-ab; pH 4; conventional labelling; mac=(2); ab=B72.3; 2 mice for 4h and 72h time-points, 7 mice for 24h time-point.*

TISSUE	24 hours %Dg^{-1}	24 hours %Dose	72 hours %Dg^{-1}	72 hours %Dose	120 hours %Dg^{-1}	120 hours %Dose
BLOOD	13.8±2.5	28.0±5.0	8.7±1.2	17.8±2.4	5.8±1.2	11.8±2.4
TUMOUR	8.2±1.8	1.4±0.3	14.7±4.5	2.4±0.7	13.2±1.9	2.2±0.3
KIDNEYS	5.1±0.4	1.5±0.1	4.9±1.8	1.5±0.5	3.2±0.5	0.9±0.1
LIVER	10.9±0.6	10.9±0.6	9.4±2.3	9.4±2.3	4.8±2.3	4.7±2.3
LUNGS	5.4±0.5	0.8±0.1	4.8±1.6	0.7±0.2	2.9±0.7	0.4±0.1
SPLEEN	9.1±1.8	0.9±0.2	8.5±3.0	0.9±0.3	3.2±1.2	0.3±0.1
STOMACH	2.7±0.6	0.4±0.1	2.4±0.5	0.4±0.1	1.6±0.4	0.3±0.1
INTESTINES	4.7±0.5	4.9±0.5	3.8±1.0	4.0±1.1	1.7±0.5	1.8±0.5

Table 6.4 *Biodistribution data for Meares' ^{67}Cu-mac-ab in tumour-bearing mice; pH 8; conventional labelling (EDTA wash); mac=TETA; ab="Lym-1".*

TETA was conjugated to the "trauted" Mab *via* its α-bromoacetamide derivative (section 1.7.2). Since the conjugated macrocycle was labelled at pH 8 (citrate), extensive non-specific ^{67}Cu binding occurred. Apparently a single wash with EDTA (10 mM) successfully removed all non-specifically bound metal. The radiolabelled conjugate was purified using a gel centrifugation procedure (Sephadex G50) before being injected intravenously into tumour-bearing mice.

Comparison of the two sets of animal data must be done with a degree of caution. Not only was a different strain of mice used by

Meares *et al.*, but more importantly a xenograft was present; a tumour obviously alters the biodistribution of the radiolabel with respect to the other tissues. Therefore we cannot compare the tissue activities (g^{-1}) directly, since an implanted tumour removes from the blood activity bound by Mab's which recognise its associated antigens. However we can compare activity ratios: blood (g^{-1}):liver (g^{-1}). If there is no excess accumulation in the liver, such that its activity reflects only its blood content, the level of activity in the blood and liver will fall at essentially similar rates, as the radiolabelled Mab either accumulates in the tumour or is catabolised (*i.e* the blood:liver activity ratio will remain constant).

Between 24 and 72 hours, Meares reports a liver activity which falls much less rapidly than the blood level, such that the blood:liver ratio decreases from 1.27 to 0.93 (Table 6.4). This indicates retention of activity in the liver, over and above that expected from its blood content.

With reference to our own set of animal data, the blood:liver ratio remains essentially constant between 24 and 72 hours (2.94 → 2.92), indicating that the liver activity is falling at almost exactly the same rate as that of the blood. This suggests that the activity in the liver can be attributed almost entirely to its blood content (roughly 30% by weight). Since there is no xenograft, the decrease in cardiovascular activity is simply due to normal Mab catabolism in the liver and radiolabel excretion (see Figure 3.2) rather than to tumour localisation. The apparent increase in the cardiovascular % initial dose between 24 and 72 hours is an artifact arising from the use of differently-sized animals for different time-points.

The blood:organ ratios for the other tissues also do not change appreciably between 24 and 72 hours and are reasonably consistent with

their blood content (the apparent slight accumulation in the lungs and spleen at 72 hours may need further investigation). A further time-point at 120 hours or more is advisable, since therapeutic isotopes such as ^{67}Cu remain highly active for several days. The blood:kidney ratio cannot be interpreted simply upon the basis of its blood content since it is also the organ of excretion (several timepoints are required). However the fact that its activity appears to decrease at roughly the same rate as the blood (the blood:kidney ratios at 24 and 72 hours are broadly similar) suggests that there is no significant retention of the radiolabel in the kidneys.

6.4.4 Biodistribution Conclusions

On the basis of the evidence presented in section 6.4.3, it is readily apparent that our animal data is superior to that obtained by Meares *et al.* However this direct form of comparison is not entirely fair: our ^{67}Cu-mac-ab conjugate was purified by HPLC, which removes essentially all aggregated protein; Meares' conjugate was purified by gel chromatography (Sephadex G-50) which removes considerably less aggregated protein. Indeed Meares admits that the liver activity is too high and suggests that this may be due to cross-linked antibody molecules. Although 90% of the radiolabelled material had a molecular weight of ~150000 D (*i.e* IgG), 9% was labelled molecules of ~300000 D (*i.e* aggregates).

On the other hand, it is possible that the high liver levels recorded by Meares *et al.* are not entirely explained by the presence of aggregates and may be exacerbated by the dissociation of non-specifically bound copper (not removed by the EDTA wash) or by the loss of ^{67}Cu from TETA. (As an anionic complex, $[Cu\text{-}TETA]^{2-}$ should be less

kinetically inert *in vivo* than $[Cu\text{-}cyclam]^{2+}$, see section 1.5.5). However we must await the publication of further biodistribution results from Meares *et al.*, obtained using HPLC-purified conjugates, to establish which factors contribute to the high liver retention. In the meantime, it is hoped to determine the stability and localisation of our own conjugate in tumour-bearing animals.

6.5 REFERENCES

1. L.M. Franks and N. Teich (Editors), "*Introduction to the Cellular and Molecular Biology of Cancer*" (Oxford, 1986)
2. W. Wolf and J. Shari, *Nucl.Med.Biol.Int.J.Radiat.Appl.Instrum. Part B*, 13(4), 319 (1986)
3. B.W. Wessels and R.D. Rogus, *Med.Phys.*, 11(5), 638 (1984)
4. R.P. Spencer, "*Therapy in Nuclear Medicine*", 3 (1978)
5. J.L. Humm, *J.Nucl.Med.*, 27(9), 1490 (1986)
6. W.C. Enkelmann and C.H. Paik, *Nucl.Med.Biol.Int.J.Radiat.Appl. Instrum. Part B*, 13(4), 335 (1986)
7. S.E. Order, J.L. Klein, D. Ettinger *et al.*, *Cancer Res.*, 40, 3001 (1980)
8. R.C. Weast (Editor), "*CRC Handbook of Chemistry and Physics*", B255 (Table of Isotopes) (1982)
9. F.A. Cotton and G. Wilkinson, "*Advanced Inorganic Chemistry*", (4th Edition), 811 (1980)
10. R.D. Shannon, *Acta.Crystallogr.Sect.A: Cryst.Phys.,Diffr., Theor. Gen.Crystallogr.*, 751 (1976)
11. D.J. Hnatowich, F. Virzi and P.W. Doherty, *J.Nucl.Med.*, 26, 503 (1985)
12. L.C. Washburn, T.T. Hwa Sun, J.E. Crook, B.L. Byrd, J.E. Carlton, V.-W. Hung and Z.S. Steplewski, *Nucl.Med.Biol.Int.J.Radiat.Appl. Instrum. Part B*, 13(4), 453 (1986)
13. H. Stetter and W. Frank, *Angew.Chem.Int.Ed.Engl.*, 15, 686 (1976)
14. J.F. Desreux, A. Renard and G. Duyckaerts, *J.Inorg.Nucl.Chem.*, 39, 1587 (1977)

15. M.F. Loncin, J.F. Desreux and E. Merciny, *Inorg.Chem.*, 25, 2646 (1986)

16. M.-R. Spirlet, J. Rebizant, J.F. Desreux anf M.-F. Loncin, *Inorg. Chem.*, 23, 359 (1984)

17. J.F. Desreux, *Inorg.Chem.*, 19, 1319 (1980)

18. M.-R. Spirlet, J. Rebizant, M.-F. Loncin and J.F. Desreux, *Inorg. Chem.*, 23, 4278 (1984)

19. A. Harrison, J. Cox and K. Jankowski, unpublished observations (1988)

20. S.V. Deshpande, S.J. DeNardo, C.F. Meares, M.J. McCall, G.P. Adams, M.K. Moi and G. DeNardo, *J.Nucl.Med.*, 29, 217 (1988)

CHAPTER SEVEN

SYNTHETIC PROCEDURES

7.1 APPARATUS AND CHARACTERISATION

The chemical compounds reported in the procedural sections of this chapter have been characterised using a variety of analytical techniques in order of presentation: melting/boiling point, microanalysis, thin layer and high performance liquid chromatography, ultraviolet/visible spectroscopy, mass spectroscopy, infrared spectroscopy and proton and carbon-13 nmr spectroscopy.

Chromatography

Reported R_f values refer to silica gel TLC (Merck.Art.5735, Kieselgel 60 F_{254}), with the eluent system indicated. All HPLC analyses and purifications were performed using a Varian Vista 5500/Polychrom 9060 system fitted with a cation exchange column ("CM 300" Synchropak). The tetraamine macrocycles were retained on the column to a greater or lesser extent depending on the degree of charge, allowing for example dipositively charged species to be separated from tripositively charged species. For each 20 minute run, the flow rate was 1.4 cm^3 sec^{-1} and the composition of the eluent, unless indicated otherwise, was varied as follows:

A = H_2O; B = 1.0 M NH_4OAc; C = CH_3CN

TIME (mins)	%A	%B	%C
0	70	10	20
20	0	80	20

The retention time (R_t) of the macrocycle under these conditions is specified, together with the pH of the eluent used. All column chromatography employed "gravity" silica (Merck.Art.7734, Kieselgel 60, 0.063 - 0.200 mm) unless "flash" silica (Merck.Art.9385, Kieselgel 60,

0.040 - 0.063 mm) is specified. The "standard conditions" specified for the purification of macrocyclic amides and diamides were as follows:

A = aqueous NH_3 (0.890); B = CH_3OH; C = CH_2Cl_2

TIME (hours)	%A	%B	%C
0 - 1	1	12	87
1 - 3	2	23	75
3 - 6	4	36	60
6 +	6	44	50

Ultraviolet/Visible Spectroscopy

All spectra were recorded in water using a Perkin-Elmer Lambda 3 spectrometer. λ_{max} is given in nanometres (nm).

Mass Spectroscopy

All spectra were obtained using a VG 7070E spectrometer. Samples were analysed using CI/DCI techniques (iso-butane, ammonia) except where otherwise indicated. FAB spectra were recorded in the positive ion mode using a water/glycerol matrix unless indicated to the contrary.

Infrared Spectroscopy

Spectra were recorded using a Perkin-Elmer 577 spectrometer. Samples were prepared either as a potassium bromide disc, in solution in chloroform (0.1 mm KBr cell) or as a thin film on a NaCl plate. Frequencies are quoted in cm^{-1}.

NMR Spectroscopy

A Brüker AC 250 spectrometer was used with its spectral frequency set at 250.134 MHz for proton NMR and 62.896 MHz for carbon-13 nmr. The chemical shifts are indicated in parts per million, to higher frequency of TMS at δ = 0 ppm. For ^1H NMR, $CDCl_3$ samples are referenced to

internal TMS at δ = 0 ppm, CD_3OD samples to CD_2HOD at δ = 3.35 ppm and D_2O samples to HOD at δ = 4.80 ppm. For ^{13}C NMR, $CDCl_3$ and CD_3OD samples are referenced to solvent peaks at δ = 77.00 and δ = 49.00 ppm respectively, and D_2O samples are referenced externally to TMS at δ = 0 ppm. The following abbreviations are used: Ar = Aromatic; Py = Pyridine; Ak = Alkene. Proton coupling constants (J) and ^{13}C assignments are given for certain representative cycles.

7.2 REAGENTS

The following chemicals were purchased from the suppliers indicated and were used without further purification:

α-Bromo-p-tolunitrile (Aldrich); n-Butyllithium (Aldrich); Caesium carbonate (Aldrich); Copper(I) cyanide (Aldrich); Coumarin (Lancaster); Cyclam (Aldrich); Diborane-DMS (Aldrich); Diborane-THF (Aldrich); Dicyclohexylcarbodiimide (Aldrich); Diethyl malonate (BDH and Aldrich); Ethyl bromoacetate (Aldrich); Manganese dioxide (Fluka); Methyl bromo-acetate (Aldrich); 4-Nitrobenzyl bromide (Aldrich); 6-Nitrocoumarin (Lancaster); p-Nitrophenyl acetate (Aldrich); "Pipes" buffer (Aldrich); Pyridine dimethanol (Aldrich); 1,4,7,10-Tetraazadecane (Fluka); 1,4,8,11-Tetraazaundecane (Strem); Trimethylsilylmethylmagnesium chloride (Aldrich).

Solvents were dried using the following reagents: Methanol, Ethanol, Iso-propanol ($Mg(OR)_2$); Dichloromethane (CaH_2); Tetrahydrofuran (Na/benzophenone); Acetonitrile (CaH_2); Toluene (Na).

Water was pre-distilled, dimethylformamide (DMF) was of HPLC grade and all other solvents were of reagent grade.

7.3 EXPERIMENTAL

7.3.1 Functionalised Tetraamine Macrocycles

5-(2-Hydroxy-5-nitrophenyl)-1,4,8,11-tetraazacyclotetradecane-7-one (4)
Equimolar quantities of 1,4,8,11-tetraazaundecane (5g, 31.25 mmol) and 6-nitrocoumarin (6g, 31.41 mmol) were reacted in methanol (150 cm^3), under reflux for 5 days (argon atmosphere)[1]. On cooling, the solvent was removed under reduced pressure and the residue was chromatographed on silica (standard conditions) to give the desired product as an orange solid (2.3g, 21%). Mpt: 150-152 ^oC; Anal: Calcd for $C_{16}H_{25}N_5O_4.1.2\ H_2O$: C 51.51; H 7.40; N 18.78. Found: C 51.99; H 7.30; N 18.16; TLC: R_f 0.4 ($aq.NH_3/CH_3OH/CH_2Cl_2$ 6:44:50); UV(H_2O): 400 nm; m/e: 353$(M+2)^+$; 352 $(M+1)^+$; 227; 203; 192; 186; 185; 162; 161; IR(KBr): 3260(NH); 3050(CH); 2920(CH); 2840(CH); 1640(CO); 1590(Ar); 1550(NH); ^1H NMR(D_2O) δ 8.00(2H, mult,Ar); 6.50(1H,d,Ar); 4.29(1H,t,ArCHN); 3.56-2.48(14H,mult,CH_2N +CH_2CO); 1.84(2H,q,CH_2C); ^{13}C NMR (D_2O) δ 176.2; 174.4; 133.0;130.1; 126.8; 124.4; 119.8; 53.9; 49.3; 47.4; 42.3; 38.7; 25.2.

5-(2-Hydroxy-5-aminophenyl)-1,4,8,11-tetraazacyclotetradecane (8)
The trihydrochloride salt of (4) was dissolved in dry THF (20 cm^3) and refluxed with a 10 molar solution of diborane in methyl sulphide (4 cm^3, 40 mmol) for 9 days. The reaction mixture was cooled, quenched with methanol and the solvent removed under reduced pressure. The resulting aminoborane was hydrolysed with refluxing 6N hydrochloric acid (40 cm^3)

for 3 hours to give the hydrochloride salt as a dark-coloured solid. ^{13}C NMR (D_2O) δ 155.3; 126.9; 124.4; 122.2; 119.8; 118.0; 60.8; 54.6; 45.1; 43.2; 42.0; 41.6; 38.9; 28.2.

5-(2-Hydroxy-5-nitrophenyl)-1,4,8,11-tetraazacyclotetradecane (5)

The amide group of (4) (0.7g, 2 mmol) was selectively reduced using diborane-THF (15 cm^3, 15 mmol) at reflux for 24 hours under nitrogen. On cooling, the excess diborane was quenched with methanol and evaporated *in vacuo*. The residue was then hydrolysed with 6N HCl (30 cm^3) for 3 hours and evaporated to dryness. A solution of the crude hydrochloride salt (187 mg) in distilled water (2 cm^3) was basified with potassium hydroxide (1g) and extracted into chloroform (15 cm^3). A yellow gum (21.4 mg) was recovered on evaporation of the solvent which was found to be highly impure by ^1H NMR. Therefore a small amount (6 mg) of pure product was separated by cation exchange HPLC. HPLC: R_t 21 min (CM 300 "Synchropak"; $Et_3NH.HCO_3/H_2O$ 5→99/95→1); m/e (Neg.FAB): 336$(M-1)^-$; 257; 205; 183; 143; ^1H NMR (D_2O) δ 7.98(2H,mult,Ar); 6.49 (1H,d,Ar); 4.22(1H,dd,ArCHN); 3.19-2.60(14H,mult,CH_2N); 2.27-2.00 (4H,mult,CH_2C).

6-Aminocoumarin[2]

To a suspension of 6-nitrocoumarin (30g, 157 mmol) in 0.5N hydrochloric acid (700 cm^3) was added, in batches, iron powder (40g, 716 mmol) and stirred at 50-60 ^oC for 30 minutes. The reaction mixture was then refluxed for 5 hours to complete the reduction, then cooled and made alkaline with potassium bicarbonate. The solids were filtered off, dried *in vacuo*, then extracted repeatedly with hot chloroform. Having removed the chloroform under reduced pressure, the residue was dissolved in 0.2N HCl (500 cm^3) and washed with chloroform (2 x 250 cm^3) to remove

unreacted 6-nitrocoumarin. The dilute acid was then evaporated *in vacuo* to give the cream coloured hydrochloride salt of 6-aminocoumarin in 74% yield (22.8g). Mpt: 166-168 ^{o}C (Lit. 168 ^{o}C); Anal: Calcd for $C_9H_7NO_2$: C 67.08; H 4.38; N 8.69. Found: C 66.56; H 4.27; N 8.36; m/e: 163$(M+2)^+$; 162$(M+1)^+$; 161$(M)^+$; 133; ^{1}H NMR ($CDCl_3$) δ 7.58(1H,d,Ak); 7.15(1H,d,Ar); 6.88(1H,dd,Ar); 6.72(1H,d,Ar); 6.38(1H,d,Ak); 3.73(2H,br.s,NH).

6-Cyanocoumarin

The hydrochloride salt of 6-aminocoumarin (22.7g, 115 mmol) suspended in 3N HCl (103 cm^3) at 0 ^{o}C, was diazotised using a solution of sodium nitrite (8.36g, 121 mmol) in water (18 cm^3) added dropwise to avoid over-heating. The reaction mixture was neutralised with sodium carbonate, then added, in 5 cm^3 aliquots, to a cold (< 5 ^{o}C) aqueous solution (44 cm^3) of copper(I) cyanide (12.3g, 137 mmol) and potassium cyanide (16.9g, 260 mmol). Chloroform (400 cm^3) was added to prevent excessive foaming and the reaction mixture was allowed to warm to room temperature over a period of 3 hours. The diazotisation was completed by warming to 50 ^{o}C for 30 minutes. On cooling, a further 150 cm^3 of chloroform was added, the solids were filtered off and the organic layer was separated. The solvent was removed to yield 6-cyanocoumarin as an orange solid (15.9g, 81%). Mpt: 214-215 ^{o}C; Anal: Calcd for $C_{10}H_5NO_2$. 0.2 H_2O: C 68.72; H 3.09; N 8.02. Found: C 68.29; H 2.80; N 8.01; TLC R_f 0.10 (20% EtOAc/petrol); m/e: 171$(M)^+$; 143$(M\text{-}CO)^+$; IR(KBr): 2225(CN); 1730(CO) cm^{-1}; ^{1}H NMR ($CDCl_3$) δ 7.85(1H,d,Ar); 7.79(1H,dd,Ar); 7.73(1H, d,Ak); 7.43(1H,d,Ar); 6.55(1H,d,Ak); ^{13}C NMR ($CDCl_3$) δ 159.0; 156.4; 141.7; 134.7; 132.3; 118.8; 118.4; 117.5; 108.7.

11-(2-Hydroxy-5-cyanophenyl)-1,4,7,10-tetraazacyclotridecane-13-one (16)
A solution of 1,4,7,10-tetraazadecane (4.39g, 30.0 mmol) and 6-cyano-coumarin (5.12g, 29.9 mmol) in dry methanol (165 cm^3) was heated under reflux for 18 days. The methanol was evaporated and the crude residue was chromatographed on silica gel (standard conditions) to give the cyclic amide as an orange solid (1.57g, 17%). Mpt: 119-121 ^oC; TLC R_f 0.27 (aq $NH_3/CH_3OH/CH_2Cl_2$ 5:45:50); Acc. Mass (DCI): $C_{16}H_{23}N_5O_2$ requires $(M+1)^+$ 318.19298. Found: 318.23172; IR(KBr): 3250(NH); 3050(CH); 2930 (CH); 2840(CH); 1640(CO); 1600(Ar); 1470; 1430; ^1H NMR ($CDCl_3$) δ 7.69 (1H,br.s, NHCO); 7.37(1H,d,Ar,J=8.6 Hz); 7.35(1H,s,Ar); 6.76(1H,d,Ar, J=8.3 Hz); 4.18(1H,d,ArCHN,J=11.5 Hz); 3.73-2.44 (18H,mult,CH_2N+NH +CH_2CO); ^{13}C NMR (D_2O) δ 175.3(CO); 169.6; 133.9; 131.8; 130.5; 122.8; 120.2(Ar); 94.5(CN); 55.2(ArCHN); 47.7; 45.8; 45.1; 44.2; 43.0; 42.3; 39.3(CH_2N+CH_2CO).

11-(2-Hydroxy-5-aminomethylphenyl)-1,4,7,10-tetraazacyclotridecane (18)
The amide (16) (1.308g, 4.13 mmol) was reduced using molar diborane-THF (40 cm^3, 40 mmol). After 60 hours under reflux, the solution was cooled, quenched with methanol (10 cm^3) and evaporated to dryness. Following treatment with boiling 6N HCl (80 cm^3), the acid was removed *in vacuo* and the hydrochloride salt was re-dissolved in water (35 cm^3), washed with ether (100 cm^3), basified (15g KOH) and extracted into chloroform (2 x 250 cm^3) as the free amine (370 mg, 30%). HPLC: R_t 17.5 min (pH 6.5); UV(H_2O): 276 nm; m/e: 310$(M+2)^+$, 309$(M+1)^+$; 292; 204; 147; ^1H NMR ($CDCl_3$) δ 7.01(1H,dd,Ar,J=8.2 Hz); 6.87(1H,s,Ar); 6.71(1H,d,Ar, J=8.3 Hz); 3.81(1H,dd,ArCHN,J=10.8 Hz,J=2.4 Hz); 3.72(2H,s,ArCH_2N); 3.09-2.42(20H,mult,CH_2N+NH); 2.03-1.70(2H,mult,CH_2C); ^{13}C NMR ($CDCl_3$) δ 156.8; 133.4(Ar); 126.8; 116.5(Ar,CH); 66.5(ArCHN); 49.6; 48.5; 48.1; 47.5; 47.3; 46.7; 46.5; 46.0(CH_2N); 36.1(CH_2C).

5-(2-Hydroxy-5-cyanophenyl)-1,4,8,11-tetraazacyclotetradecane-7-one (17)

This was prepared from 1,4,8,11-tetraazaundecane (9.68g, 60.5 mmol) in a similar manner to (16). Yield: 4.0g (20%); Mpt: 136-138 ^{o}C; TLC R_f 0.32 (aq $NH_3/CH_3OH/CH_2Cl_2$ 5:45:50); UV(H_2O): 362 nm; Acc. Mass (DCI): $C_{17}H_{25}N_5O_2$ requires $(M+1)^+$ 332.20865. Found: 332.21757; IR(KBr): 3040 (CH); 2925(CH); 2830(CH); 2205(CN); 1635(CO); 1588; 1470; ^{1}H NMR (D_2O) δ 7.42(1H,s,Ar); 7.40(1H,dd,Ar); 6.63(1H,d,Ar); 4.28(1H,dd,ArCHN); 3.55-2.38(14H,mult,CH_2N+CH_2CO); 1.85(2H,q,CH_2C); ^{13}C NMR (D_2O) δ 174.9; 170.3; 133.5; 131.3; 130.8; 122.8; 120.2; 93.5; 53.5.

5-(2-Hydroxy-5-aminomethylphenyl)-1,4,8,11-tetraazacyclotetradecane (19)

The amide (17) (2.87g, 8.67 mmol) was treated with molar diborane-THF (90 cm^3, 90 mmol), under reflux for 48 hours, then quenched with methanol. The solvent was removed and the residue treated with boiling 6N HCl (180 cm^3) for 3 hours. The acid was evaporated *in vacuo* and the crude hydrochloride salt re-dissolved in distilled water (50 cm^3). After washing with diethyl ether (150 cm^3), the solution was basified (25g) and extracted into chloroform (2 x 400 cm^3). The solvent was removed to give the free amine as a clear oil (1.93g, 69%). HPLC: R_t 13.7 min (pH 7.4); UV(H_2O): 276 nm; Acc. Mass (DCI): $C_{17}H_{31}N_5O$ requires $(M+1)^+$ 322.26069. Found: 322.33893; IR($CHCl_3$): 3250(NH,OH); 2910(CH); 2830(CH); 1600(Ar); ^{1}H NMR ($CDCl_3$) δ 7.04(1H,dd,Ar); 6.91(1H,s,Ar); 6.73(1H,d,Ar); 3.81(1H,dd,ArCHN); 3.75(2H,s,$ArCH_2N$); 3.11-2.51(14H,mult,CH_2N+NH); 1.94-1.75(4H,mult,CH_2C+NH); ^{13}C NMR ($CDCl_3$) δ 156.6; 133.5; 126.8; 126.6; 116.4; 66.8; 51.2; 51.0; 50.1; 49.7; 49.4; 49.2; 47.4; 46.0; 36.4; 29.4.

N-(4-Nitrobenzyl)-1,4,8,11-tetraazacyclotetradecane (20)

A solution of 4-nitrobenzyl bromide (200 mg, 0.926 mmol) in chloroform

(10 cm^3) was added dropwise to a solution of cyclam (2g, 10 mmol) in chloroform (100 cm^3) in the presence of potassium carbonate (3g) at 0^oC. The reaction mixture was allowed to warm to room temperature and stirred for 18 hours. Having removed the chloroform under reduced pressure, the residue was extracted with diethyl ether (3 x 100 cm^3) and the excess cyclam was filtered off. This extraction procedure was then repeated to remove remaining traces of cyclam from the monoalkylated product (222 mg, 70%). Anal: Calcd for $C_{17}H_{29}N_5O_2$: C 60.87; H 8.71; N 20.88. Found: C 61.07; H 9.08; N 19.92; m/e: 345$(M+2)^+$; 344$(M+1)^+$; 343$(M)^+$; ^1H NMR ($CDCl_3$) δ 8.08(2H,d,Ar); 7.50(2H,d,Ar); 3.58(2H,s,CH_2Ar); 2.89-2.32(19H, mult,CH_2N+NH); 1.80(2H,q,CH_2C); 1.62(2H,q,CH_2C); ^{13}C NMR ($CDCl_3$) δ 147.1; 129.9; 129.5; 123.3; 57.6; 54.8; 53.5; 50.9; 49.3; 49.1; 48.6; 47.8; 47.1; 28.2; 26.0.

N-(4-Nitrobenzyl)-N^1,N^2,N^3-trimethyl-1,4,8,11-tetraazacyclotetradecane (21)

The monoalkylated cyclam, (20) (79.2 mg, 0.24 mmol) was trimethylated using a mixture of 37% aqueous formaldehyde solution (2 cm^3, 24.6 mmol) and formic acid (3.5 cm^3). After refluxing for 20 hours, molar hydrochloric acid (10 cm^3) was added and the solvent was removed *in vacuo*. The amine hydrochloride salt was then dissolved in water (12 cm^3) and a white insoluble material was filtered off. The filtrate was washed with dichloromethane (15 cm^3), basified with sodium hydroxide (2.5g) and extracted into dichloromethane (2 x 30 cm^3) to give the free amine. ^1H NMR ($CDCl_3$) δ 8.16(2H,d,Ar); 7.58(2H,d,Ar); 3.62(2H,s,ArCH_2N); 2.56-2.44(16H,mult,CH_2N); 2.25-2.21(9H,mult,CH_3N); 1.67(4H,mult,CH_2C).

N-(4-Cyanobenzyl)-1,4,8,11-tetraazacyclotetradecane (23)

This was synthesised in the same manner as (20) to yield a colourless

solid (0.257g, 82%). Mpt. 88-90 ^{o}C; Anal: Calcd for $C_{18}H_{29}N_5$: C 68.53; H 9.27; N 22.20. Found: C 68.52; H 9.59; N 22.04; m/e: 317$(M+2)^+$; 316 $(M+1)^+$; 199$(M-C_8H_6N)$; IR($CHCl_3$): 2920(CH); 2810(CH); 2235(CN); ^{1}H NMR ($CDCl_3$) δ 7.59(2H,d,Ar); 7.50(2H,d,Ar); 3.61(2H,s,$ArCH_2N$); 2.86-2.45 (19H,mult,CH_2N+NH); 1.86(2H,q,CH_2C); 1.71(2H,q,CH_2C); ^{13}C NMR ($CDCl_3$) δ 144.9; 131.8; 129.3; 119.0; 110.5; 57.7; 55.1; 53.4; 50.1; 49.2; 49.0; 48.6; 47.9; 47.1; 28.5; 26.1.

N-(4-Aminomethylbenzyl)-1,4,8,11-tetraazacyclotetradecane (24)

The nitrile group of (23) (200mg, 0.65 mmol) was reduced using diborane-THF solution (7 cm^3, 7 mmol), heated under reflux for 24 hours. After quenching with methanol, the solvent was removed and the residue treated with boiling 6N HCl (20 cm^3) for 3 hours. The hydrochloride salt was then dissolved in water (10 cm^3), basified (1g KOH) and extracted into dichloromethane (2 x 30 cm^3). The free amine was recovered as a clear oil (177mg, 85%); m/e: 321$(M+2)^+$; 320$(M+1)^+$; 220; ^{1}H NMR ($CDCl_3$) δ 7.22(2H,d,Ar); 7.16(2H,d,Ar); 3.76(2H,s,$ArCH_2N$); 3.49(2H,s,$ArCH_2N$); 2.70-2.30 (21H,mult,CH_2N+NH); 1.78(2H,q,CH_2C); 1.60(2H,q,CH_2C); ^{13}C NMR ($CDCl_3$) δ 141.9; 137.2; 129.4; 126.7; 57.4; 54.4; 53.3; 50.8; 49.4; 49.2; 48.9; 47.9; 47.3; 45.2; 28.5; 25.2.

Diethyl-4-cyanobenzylmalonate (25)

A solution of diethyl malonate (20g, 125 mmol) in dry ethanol (50 cm^3) was added dropwise under a nitrogen atmosphere to sodium ethoxide, prepared by dissolving sodium metal (1.5g, 65 mmol) in dry ethanol (125 cm^3). After stirring for 30 minutes at 20 ^{o}C, a solution of α-bromo-p-tolunitrile (12g, 61 mmol) in dry DMF (60 cm^3) was added dropwise. The reaction mixture was heated under reflux for 24 hours. On cooling to room temperature, the reaction was quenched with distilled water (150

cm^3). A white precipitate of dibenzylated malonate was filtered off and the filtrate was extracted with diethyl ether (440 cm^3). The ether was removed under reduced pressure and the desired product, a clear oil, was distilled from the residue at 150 ^oC (0.1 mm). Yield: 7.84g (47%); TLC: R_f 0.26 (20% EtOAc/petrol); m/e: 277$(M+2)^+$; 276$(M+1)^+$; 275$(M)^+$; 230(M+1 -EtOH)$^+$; 184(M+1-2EtOH); IR($CHCl_3$): 3010(CH); 2980(CH); 2235(CN); 1730 (CO); ^1H NMR ($CDCl_3$) δ 7.59(2H,d,Ar); 7.33(2H,d,Ar); 4.16(4H,mult,CH_2O); 3.36(1H,t,CH); 3.27(2H,d,CH_2); 1.22(6H,t,CH_3); ^{13}C NMR ($CDCl_3$) δ 167.3; 143.3; 132.1; 129.5; 116.5; 110.5; 61.6; 53.0; 34.4; 13.8.

12-(4-Cyanobenzyl)-1,4,7,10-tetraazacyclotridecane-11,13-dione (26)
The linear tetraamine, 1,4,7,10-tetraazadecane (4.18g, 28.6 mmol) was added to diethyl 4-cyanobenzyl malonate (7.84g, 28.5 mmol) in dry ethanol (58 cm^3) and heated for 10 days under reflux. A white precipitate of the required diamide was filtered off and recrystallised from hot ethanol (1.404g, 15%). Mpt: 244-247 ^oC (dec); Anal: Calcd for $C_{17}H_{23}N_5O_2.0.2\ H_2O$: C 61.31; H 7.08; N 21.03. Found: C 61.15; H 7.03; N 20.79; TLC: R_f 0.27 (aq $NH_3/CH_3OH/CH_2Cl_2$ 6:44:50); m/e: 331$(M+2)^+$; 330 $(M+1)^+$; 312; 286; IR(KBr): 3320(NH); 2930(CH); 2880(CH); 2810(CH); 2225(CN); 1665(NH); 1640(CO); 1550; 1525; ^1H NMR (CD_3OD) δ 7.63(2H,d,Ar, J=8.0 Hz); 7.41(2H,d,Ar,J=8.2 Hz); 3.64(2H,mult,CH_2N); 3.47(1H,t,CHCO); 3.26(2H,d,CH_2Ar); 3.02(2H,mult,CH_2N); 2.67(8H,mult,CH_2N).

12-(4-Aminomethylbenzyl)-1,4,7,10-tetraazacyclotridecane (28)
The macrocyclic diamide (26) (1.3g, 3.95 mmol) was reduced with molar diborane-THF (80 cm^3, 80 mmol) under reflux for 3 days. After treatment with boiling 6N HCl (100 cm^3) for 3 hours, the hydrochloride salt was dissolved in distilled water (50 cm^3), washed with ether (60 cm^3), basified (8g KOH) and extracted into chloroform (2 x 70 cm^3). A clear

oil was recovered upon removal of the solvent (1.19g, 99%). Anal: Calcd for $C_{17}H_{31}N_5.5HCl.4H_2O$: C 36.47; H 7.92; N 12.51. Found: C 36.71; H 7.82; N 12.11; m/e: 307$(M+2)^+$; 306$(M+1)^+$; 305$(M)^+$; 258; ^1H NMR ($CDCl_3$) δ 7.22(2H,d,Ar,J=8.0 Hz); 7.14(2H,d,Ar,J=8.0 Hz); 3.84(2H,s,$ArCH_2N$); 2.84-2.49(19H,mult,$CH+CH_2N+CH_2Ar$); 2.04(6H,br.s,NH); ^{13}C NMR ($CDCl_3$) δ 140.7 (Ar); 138.8(Ar); 128.9(Ar,CH); 126.8(Ar,CH); 54.6($ArCH_2N$); 48.8(CH_2N); 47.4(CH_2N); 47.2(CH_2N); 46.0(CH_2N); 40.2; 38.3($CH_2Ar+CHC$).

6-(4-Cyanobenzyl)-1,4,8,11-tetraazacyclotetradecane-5,7-dione (27)
A solution of 1,4,8,11-tetraazaundecane (2.768g, 17.3 mmol) and diethyl 4-cyanobenzyl malonate (4.75g, 17.3 mmol) in dry ethanol (35 cm^3) was heated under reflux for 5 days. The solvent was evaporated and the diamide was isolated from the residue through silica gel column chromatography (standard conditions) in 19% yield (1.1g). Mpt. 209-211^oC; Anal: Calcd for $C_{18}H_{25}N_5O_2.H_2O$: C 59.80; H 7.53; N 19.38. Found: C 60.06; H 7.17; N 18.68; TLC: R_f 0.25 (aq $NH_3/CH_3OH/CH_2Cl_2$ 6:44:50); m/e: 345$(M+2)^+$; 344$(M+1)^+$; 326; 309; 308; IR(KBr): 3290(NH); 2910(CH); 2805(CH); 2225(CN); 1638(CO); 1530; ^1H NMR ($CDCl_3$) δ 7.56(2H,d,Ar); 7.33 (2H,d,Ar); 6.65(2H,br.s,NH); 3.50(2H,mult,CH_2Ar); 3.25(5H,mult,CH_2NCO +CHCO); 2.82-2.57(8H,mult,CH_2N); 1.78(2H,br.s,NH); 1.65(2H,mult,CH_2C); ^{13}C NMR (CD_3OD) δ 171.2; 146.3; 133.3; 131.1; 119.7; 111.3; 56.5; 50.9; 39.4; 35.1; 28.3.

6-(4-Aminomethylbenzyl)-1,4,8,11-tetraazacyclotetradecane (29)
The diamide, (27) (0.969g, 2.82 mmol) was reduced by stirring with diborane-THF (47 cm^3, 47 mmol) for 24 hours under reflux. Once cool, the reaction was quenched with methanol and the solvent evaporated *in vacuo*. The residue was treated with boiling 6N HCl (60 cm^3) for 3 hours to convert the aminoborane to an amine hydrochloride salt. The acid was

removed under reduced pressure and the residue was re-dissolved in distilled water (45 cm^3). The aqueous solution was washed with diethyl ether (60 cm^3), basified with sodium hydroxide (2.5g) and extracted into chloroform (2 x 120 cm^3). The crude macrocycle was recrystallised from toluene in 83% yield (0.75g). Mpt. 149 ^oC; Anal: Calcd for $C_{18}H_{33}N_5.H_2O$: C 64.05; H 10.45; N 20.75. Found: C 64.61; H 10.16; N 20.10; m/e: 321 $(M+2)^+$; 320$(M+1)^+$; ^1H NMR ($CDCl_3$) δ 7.22(2H,d,Ar); 7.14(2H,d,Ar); 3.83 (2H,s,ArCH_2N); 2.40-2.85(19H,mult,CH_2N+CH_2Ar+CHCH_2Ar); 2.20(6H,br.s, NH); 1.71(2H,q,CH_2C); ^{13}C NMR ($CDCl_3$) δ 140.9; 139.0; 129.1; 127.0; 55.8; 50.7; 49.3; 46.2; 40.8; 38.6; 29.3.

7.3.2 Vinyl Pyridine Linker Molecule

2-Dimethoxytrityloxymethyl-6-hydroxymethyl-pyridine (32)

A solution of 2,6-bis(hydroxymethyl)-pyridine (16.1g, 116 mmol) in dry pyridine (200 cm^3) was added to a solution of dimethoxytrityl chloride (39.2g, 116 mmol) in pyridine (120 cm^3), dropwise over 4 hours. The reaction mixture was stirred for a further hour, then concentrated by evaporation *in vacuo*. The residual solution was then dissolved in dichloromethane (400 cm^3), washed with saturated sodium bicarbonate solution (400 cm^3), separated and dried. The solvent was removed under reduced pressure and the crude residue was purified by "flash" chromatography (diethyl ether/hexane 8:2) to give the mono-protected alcohol as a yellow glass in 61% yield (31.2g). Mpt. 38-40 ^oC; TLC: R_f 0.20 (diethyl ether/hexane 8:2).

2-Hydroxymethyl-6-methylmethoxyacetate pyridine (33)

The mono-protected alcohol (32) (30.96g, 70.2 mmol) was dissolved in dry THF (200 cm^3) and n-butyl lithium (48 cm^3, 1.6M solution in hexane, 77.2

mmol) was added by syringe at -78 °C under nitrogen. The brown suspension thus formed was added via a cannula to a solution of methyl bromoacetate (26.85g, 175mmol) in dry THF (50 cm^3) at -78 °C. The reaction mixture was allowed to warm to room temperature and stirred for 18 hours. The THF solution was poured into saturated sodium bicarbonate solution (250 cm^3) and extracted into dichloromethane (500 cm^3). The organic layer was separated, dried ($MgSO_4$) and evaporated to dryness *in vacuo*. The crude residue was re-dissolved in dry dichloromethane (300 cm^3) and zinc bromide (78.7g, 350 mmol) was added as a solid. After stirring for 15 minutes at room temperature, the reaction mixture was poured into saturated disodium EDTA solution (300 cm^3). The aqueous layer was separated, basified with sodium bicarbonate and extracted into chloroform (3 x 500 cm^3). The solvent was removed under reduced pressure to give the alcohol (3.0g) in 20% overall yield. TLC: R_f 0.46 (CH_3OH/CH_2Cl_2 1:9); Acc. Mass (DEI): $C_{10}H_{13}NO_4$ requires $(M)^+$ 211.08446. Found 211.08082; ^1H NMR ($CDCl_3$) δ 7.72(1H,t,Py); 7.41(1H,d,Py); 7.18(1H, d,Py); 4.76(4H,s,$PyCH_2O$); 4.22(2H,s,CH_2O); 3.75(3H,s,CH_3O); 3.07(1H, br.s,OH); ^{13}C NMR ($CDCl_3$) δ 158.3; 156.3; 137.5; 120.2; 119.4; 73.9; 67.9; 63.9; 51.9.

2-Formyl-6-methylmethoxyacetate pyridine (34)

The alcohol (33) (2.6g, 12.3 mmol) was dissolved in dry dichloromethane (50 cm^3) and oxidised with manganese dioxide (25g, 288 mmol). After stirring at room temperature for 15 hours, the excess oxidant was filtered off (using "Celite") and the filtrate evaporated *in vacuo*. The aldehyde was purified by silica gel "flash" chromatography, eluting with ether/hexane (8:2). Yield: 1.3g (51%); Anal: Calcd for $C_{10}H_{11}NO_4$: C 57.41; H 5.30; N 6.70. Found: C 56.59; H 5.00; N 6.39; TLC: R_f 0.45 (ether/hexane 4:1); Acc. Mass (DEI): $C_{10}H_{11}NO_4$ requires $(M+1)^+$

210.07663. Found 210.07255; ^{1}H NMR ($CDCl_3$) δ 10.05(1H,s,CHO); 7.90(2H, mult,Py); 7.78(1H,dd,Py); 4.86(2H,s,$PyCH_2O$); 4.29(2H,s,CH_2O); 3.80(3H, s,CH_3O); ^{13}C NMR ($CDCl_3$) δ 193.2; 158.4; 152.0; 137.7; 125.9; 120.6; 73.7; 68.0; 51.9.

2-Vinyl-6-methoxyacetic acid pyridine-methyl ester (35)

To a solution of the aldehyde (34) (1.3g, 6.22 mmol) in dry THF (20 cm^3) was added by syringe, a molar solution of trimethylsilylmethylmagnesium chloride in ether (6.84 cm^3, 6.84 mmol) at -78^{o} C under nitrogen. After stirring for 15 minutes at -78 ^{o}C, the reaction mixture was allowed to warm to 0 ^{o}C and thionyl chloride (0.81g, 6.81 mmol) was added dropwise. The solution was stirred at 0 ^{o}C for 20 minutes, then warmed to room temperature, cautiously basified with saturated sodium bicarbonate solution and extracted into dichloromethane. The solvent was dried ($MgSO_4$) and evaporated, and the residue "flash" chromatographed on silica (ether/hexane 1:1) to give the vinyl pyridine in 71% yield (0.91g). TLC: R_f 0.19 (Et_2O/hexane 1:1); m/e (DEI): 208$(M+1)^+$; 207$(M)^+$; 206$(M-1)^+$; ^{1}H NMR ($CDCl_3$) δ 7.68(1H,t,Py); 7.41(1H,d,Py); 7.29(1H,d,Py); 6.82(1H,dd,Ak); 6.19(1H,d,Ak); 5.49(1H,d,Ak); 4.76(2H,s,$PyCH_2O$); 4.25 (2H,s,CH_2O); 3.78(3H,s,CH_3O); ^{13}C NMR ($CDCl_3$) δ 170.6; 163.0; 156.4; 137.2; 136.6; 122.2; 120.3; 118.4; 73.9; 67.9; 51.8.

2-Vinyl-6-methoxyacetic acid pyridine-4-nitrophenyl ester (36)

The methyl ester (35) (0.80g, 3.87 mmol) was hydrolysed with lithium hydroxide (0.175g, 7.31 mmol) in a mixture of methanol (40 cm^3) and water (13 cm^3). After stirring for 15 minutes at room temperature, the reaction mixture was concentrated by evaporation *in vacuo* and passed down a pyridinium cation exchange column (20g Dowex 50W), eluting with pyridine. The UV active fractions were combined and the solvent removed

under reduced pressure. To a solution of the pyridinium salt in dry dichloromethane (50 cm^3) was added p-nitrophenol (840mg, 6 mmol) as a solid, and dicyclohexylcarbodiimide (DCC) (830mg, 4 mmol) as a solution in dry dichloromethane (25 cm^3). Having stirred the reaction mixture for 60 minutes at room temperature, the white precipitate of dicyclohexyl-urea was filtered off and the solvent evaporated under reduced pressure. The active ester was purified by silica gel "flash" chromatography, eluting with ether/dichloromethane (1:40). Yield: 0.81g (63%). TLC: R_f 0.32 (ether/CH_2Cl_2 1:40); Acc. Mass (DCI): $C_{16}H_{14}N_2O_5$ requires $(M+1)^+$ 315.09809. Found 315.09810; ^1H NMR ($CDCl_3$) δ 8.28(2H,d,Ar); 7.76(1H,t, Py); 7.41(2H,mult,Py); 7.32(2H,d,Ar); 6.84(1H,dd,Ak); 6.18(1H,dd,Ak); 5.53(1H,dd,Ak); 4.84(2H,s,$PyCH_2O$); 4.51(2H,s,CH_2O).

7.3.3 Macrocycle-Vinyl Pyridine Conjugation

2-Vinyl-6-methoxyacetic acid pyridine-12-(4-amidomethylbenzyl)-1,4,7,10-tetraazacyclotridecane (39)

The following procedure is generally applicable to the acylation of exocyclic primary amines using the active ester (36). The macrocycle (28) (10.5mg, 34.4 mmol) was dissolved in 0.5M "Pipes" buffer (1 cm^3) at pH 6.8 ("Pipes" = 1,4-piperazinebis(ethanesulphonic acid)). A solution containing a 2-fold excess of the active ester (36) (21mg, 69 μmol) in p-dioxane (1 cm^3) was added dropwise to the aqueous solution of the macrocycle and stirred at 40 ^oC for 4 hours. Exhaustive extraction of the reaction mixture with chloroform removed the unreacted p-nitrophenyl ester and the majority of the p-nitrophenol liberated in the acylation. Purification of the macrocycle-vinylpyridine conjugate was by cation exchange HPLC, the adduct eluting after 13 minutes (pH 6.5) in 55% yield (9mg); m/e(FAB): $482(M+1)^+$; $481(M)^+$; 243; UV(H_2O): 281 nm; ^1H NMR (D_2O)

δ 7.82(1H,t,Py,J=7.9 Hz); 7.54(1H,d,Py); 7.36(1H,d,Py); 7.22(4H,s,Ar); 6.79(1H,dd,Ak); 6.09(1H,d,Ak,J=17.7 Hz); 5.56(1H,d,Ak,J=11.0 Hz); 4.70(2H,s,$PyCH_2O$); 4.38(2H,s,CH_2O); 4.20(2H,s,$ArCH_2N$); 3.09-2.59(18H, mult,CH_2N+CH_2Ar); 2.21(1H,mult,$CHCH_2$); 1.89(6H,s,CH_3COO^-).

2-Vinyl-6-methoxyacetic acid pyridine-6-(4-amidomethylbenzyl)-1,4,8,11-tetraazacyclotetradecane (40)

Yield: 80%. HPLC: R_t 13 min (pH 6.5); m/e(FAB): 495$(M+1)^+$; 494$(M)^+$; 304; 185; 115; UV(H_2O): 280 nm; ^1H NMR (D_2O) δ 7.76(1H,t,Py); 7.48(1H,d,Py); 7.30(1H,d,Py); 7.17(4H,br.s,Ar); 6.74(1H,dd,Ak); 6.03(1H,d,Ak); 5.50(1H, d,Ak); 4.64(2H,s,$PyCH_2O$); 4.33(2H,s,CH_2O); 4.14(2H,s,$ArCH_2N$); 2.98-2.32 (19H,mult,CH_2N+CH_2Ar+$CHCH_2$); 1.84(2H,mult,CH_2C).

2-Vinyl-6-methoxyacetic acid pyridine-11-(2-hydroxy-5-amidomethyl-phenyl)-1,4,7,10-tetraazacyclotridecane (37)

Yield: 50%. HPLC: R_t 12.01 min (pH 6.5); m/e(FAB): 484$(M+1)^+$; 483$(M)^+$; 453; 378; 325; UV(H_2O): 280 nm; ^1H NMR (D_2O) δ 7.79(1H,t,Py); 7.52(1H, d,Py); 7.32(1H,d,Py); 7.07(2H,mult,Ar); 6.86(1H,d,Ar); 6.72(1H,dd,Ak); 6.05(1H,d,Ak); 5.53(1H,d,Ak); 4.67(2H,s,$PyCH_2O$); 4.31(2H,s,CH_2O); 4.18 (2H,s,$ArCH_2N$); 4.06(1H,dd,ArCHN); 3.32-2.54(14H,mult,CH_2N); 2.14-1.89 (8H,mult,CH_2C+CH_3COO^-).

2-Vinyl-6-methoxyacetic acid pyridine-5-(2-hydroxy-5-amidomethylphenyl)-1,4,8,11-tetraazacyclotetradecane (38)

Yield: 70%. HPLC: R_t 11.2 min (pH 6.5); UV(H_2O): 280 nm; ^1H NMR (D_2O) δ 7.78(1H,t,Py); 7.51(1H,d,Py); 7.30(1H,d,Py); 7.07(2H,mult,Ar); 6.85(1H, d,Ar); 6.71(1H,dd,Ak); 6.04(1H,d,Ak); 5.52(1H,d,Ak); 4.66(2H,s,$PyCH_2O$); 4.29(2H,s,CH_2O); 4.12(3H,mult,ArCHN); 3.31-2.60(14H,mult,CH_2N); 2.12-1.80(10H,mult,CH_2C+CH_3COO^-).

7.3.4 Selective Acetylation of Functionalised Macrocycles

12-(4-Acetamidomethylbenzyl)-1,4,7,10-tetraazacyclotridecane (59)

A solution of (28) (0.8g, 2.62 mmol) in 0.5M "Pipes" buffer (35 cm^3, pH 6.8) was added to a solution of p-nitrophenyl acetate (1.3g, 7.2 mmol) in p-dioxane (35 cm^3) and stirred for 3.5 days at room temperature. Having washed the reaction mixture with ether (2 x 150 cm^3), the aqueous layer was made basic with KOH (5g) and extracted into chloroform (2 x 200 cm^3), to give the free amine as a clear oil in 70% yield (0.636g). IR(film): 3260(NH); 3060(CH); 2915(CH); 2830(CH); 1650(CO); 1550; 1460; 1295; m/e: 350$(M+3)^+$; 349$(M+2)^+$; 348$(M+1)^+$; ^{1}H NMR ($CDCl_3$) δ 7.17(2H,d, Ar,J=8.1 Hz); 7.11(2H,d,Ar,J=8.1 Hz); 6.97(1H,br.s,NHCO); 4.35(2H,d, $ArCH_2N$,J=5.6 Hz); 2.80-2.41(23H,mult,CH_2N+$CHCH_2$+CH_2Ar+NH); 1.97(3H,s, CH_3); ^{13}C NMR ($CDCl_3$) δ 170.0; 139.5; 135.9; 129.1; 127.7; 54.8; 48.8; 47.4; 43.2; 40.3; 38.3; 23.0.

6-(4-Acetamidomethylbenzyl)-1,4,8,11-tetraazacyclotetradecane (52)

Synthesised using the same method as (59). Yield: 75%; ^{1}H NMR (AcO^- salt, D_2O) δ 7.26(4H,mult,Ar); 4.33(2H,s,$ArCH_2N$); 3.10-2.75(16H,mult, CH_2N); 2.63(2H,d,CH_2Ar); 2.23(1H,mult,$CHCH_2$); 2.02(3H,s,CH_3); 1.89(8H, mult,CH_2C+CH_3COO^-).

5-(2-Hydroxy-5-acetamidomethylphenyl)-1,4,8,11-tetraazacyclotetradecane (51)

Synthesised in a similar manner to (59) and (52). Yield: 51% (after recrystallisation from CH_3CN); Mpt. 151-153 ^oC; Anal: Calcd for $C_{19}H_{33}N_5O_2.1.3H_2O$: C 58.97; H 9.27; N 18.10. Found: C 59.02; H 9.04; N 17.87; UV(H_2O): 285 nm (phenol); 296 nm (phenolate); m/e: 365$(M+2)^+$; 364$(M+1)^+$; IR(KBr): 3240(NH); 3050(CH); 2925(CH); 2880(CH); 2820(CH);

1632(CO); 1545; 1500; 1460; 1270; ^{1}H NMR ($CDCl_3$) δ 7.00(1H,d,Ar); 6.87 (1H,s,Ar); 6.71(1H,d,Ar); 5.80(1H,br.s,NHCO); 4.29(2H,d,$ArCH_2N$); 3.79 (1H,dd,ArCHN); 3.05-2.49(18H,mult,CH_2N+NH); 2.00(3H,s,CH_3); 2.00-1.70 (4H,mult,CH_2C); ^{13}C NMR ($CDCl_3$) δ 157.5; 157.3; 128.2; 127.8; 127.7; 126.8; 116.5; 66.7; 51.2; 51.0; 50.1; 49.6; 49.3; 49.1; 47.4; 43.4; 36.3; 29.3; 23.3.

7.3.5 Parent Tetraamine Macrocycles

1,4,7,10-tetraazacyclotridecane-11,13-dione (63)

A solution of 1,4,7,10-tetraazadecane (20g, 0.137 mmol) and diethyl malonate (21.92g, 0.137 mmol) in dry ethanol (250 cm^3) was stirred under reflux for 2 weeks under nitrogen. On cooling a precipitate was deposited which was filtered off and found by TLC to be baseline material. The filtrate was evaporated to dryness and chromatographed on silica (standard conditions) to give the desired diamide as a white solid (5.57g, 19%). Mpt. 168-170^{o}C (dec); TLC: R_f 0.38 (aq NH_3/CH_3OH/ CH_2Cl_2 5:45:50); Acc.Mass (DCI): $C_9H_{18}N_4O_2$ requires $(M+1)^+$ 215.15080. Found 215.16653; IR(KBr): 3310(NH); 3040(CH); 2950(CH); 2930(CH); 2895(CH); 2830(CH); 1655(CO); 1532; 1440; ^{1}H NMR ($CDCl_3$) δ 7.64(2H, br.s,NHCO); 3.40(4H,q,CH_2NCO); 3.22(2H,s,CH_2CO); 2.74(4H,t,CH_2N); 2.70(4H,s,CH_2N); 1.73(2H,s,NH); ^{13}C NMR ($CDCl_3$) δ 168.2; 47.7; 46.7; 46.4; 39.4.

1,4,7,10-tetraazacyclotridecane ($13N_4$)

The cyclic diamide (63) (4.814g, 22.5 mmol) was dissolved in molar diborane-THF (180 cm^3, 180 mmol) and refluxed for 36 hours. After quenching the excess diborane with methanol, the solvent was removed and the residue treated with 6N HCl (230 cm^3) at 100 ^{o}C for 3 hours. The

crude hydrochloride salt was then re-dissolved in distilled water (75 cm^3), washed with ether (200 cm^3), basified (22g KOH) and extracted as the free amine into chloroform (2 x 300 cm^3) in 76% yield (3.2g). Mpt. 40-41.5 ^oC (Lit. 40-41 ^oC)[3]; Anal: Calcd for $C_9H_{22}N_4.0.6H_2O$: C 54.84; H 11.86; N 28.43. Found: C 55.01; H 12.39; N 28.10; m/e: 188$(M+2)^+$; 187 $(M+1)^+$; 99; ^1H NMR ($CDCl_3$) δ 2.76-2.66(16H,mult,CH_2N); 2.05(2H,br.s,NH); 1.67(2H,q,CH_2C); ^{13}C NMR ($CDCl_3$) δ 49.8; 48.7; 47.5; 47.2; 28.8.

11-(2-Hydroxyphenyl)-1,4,7,10-tetraazacyclotridecane-13-one (64)

A solution of 1,4,7,10-tetraazadecane (12.7g, 86.8 mmol) and coumarin (12.7g, 86.9 mmol) in dry methanol (420 cm^3) was boiled for 14 days. The solvent was removed and the desired amide was separated using the standard chromatographic conditions in 16% yield (3.989g). The trihydrochloride salt was recrystallised from ethanol/HCl. Mpt. 165-167^oC; Anal: Calcd for $C_{15}H_{24}N_4O_2.3HCl.2H_2O$: C 41.15; H 7.14; N 12.80. Found: C 40.90; H 7.07; N 12.29; TLC: R_f 0.54 (aq $NH_3/CH_3OH/CH_2Cl_2$ 10:40:50); m/e: 294$(M+2)^+$; 293$(M+1)^+$; 276$(M+1-NH_3)$; 275$(M-NH_3)$; 213; 171; IR(KBr): 3260(NH); 3050(CH); 2920(CH); 2840(CH); 1635(CO); 1450 (NH); ^1H NMR ($CDCl_3$) δ 7.42(1H,br.s,NHCO); 7.13(1H,t,Ar,J=8 Hz); 7.05 (1H,d,Ar,J=7.5 Hz); 6.78(2H,mult,Ar); 4.46(3H,br.s,NH); 4.21(1H,dd, ArCHN); 3.88-2.47(15H,mult,CH_2N+CH_2CO); ^{13}C NMR ($CDCl_3$) δ 172.0; 157.1; 128.4; 128.3; 125.4; 119.1; 116.5; 60.3; 47.9; 47.3; 46.3; 45.3; 44.7; 43.6; 39.1.

11-(2-Hydroxyphenyl)-1,4,7,10-tetraazacyclotridecane (56)

The cyclic amide (64) (3.95g, 13.5 mmol) was reduced using molar diborane-THF (130 cm^3, 130 mmol), under reflux for 36 hours. The residue, after quenching (CH_3OH) and removal of solvent, was hydrolysed with boiling 6N HCl (200 cm^3) for 3 hours. The hydrochloride salt was

dissolved in distilled water (50 cm^3), washed with ether (80 cm^3), basified (12g KOH) and the free amine extracted into chloroform (2 x 200 cm^3) in 49% yield (1.833g). Mpt. 69-71°C (Lit. 72-74 °C)[4]; Anal: Calcd for $C_{15}H_{26}N_4O.1.7H_2O$: C 58.29; H 9.59; N 18.13. Found: C 58.26; H 9.32; N 18.19; m/e: 281(M+2)$^+$; 280(M+1)$^+$; 147; 85; ^{1}H NMR ($CDCl_3$) δ 7.11 (1H,-t,Ar,J=7.9 Hz); 6.92(1H,d,Ar,J=7.3 Hz); 6.75(2H,mult,Ar); 3.83(1H, dd,-ArCHN); 3.11-2.60(19H,mult,CH_2N+NH); 2.02-1.71(2H,mult,CH_2C); ^{13}C NMR ($CDCl_3$) δ 158.7; 158.1; 128.1; 118.7; 116.7; 66.4; 49.6; 48.5; 48.1; 47.5; 46.7; 46.5; 36.1.

5-(2-Hydroxyphenyl)-1,4,8,11-tetraazacyclotetradecane-7-one (65)

Synthesised in a similar manner to (64). Yield: 1.68g (17%); TLC: R_f 0.35 (aq $NH_3/CH_3OH/CH_2Cl_2$ 5:45:50); m/e: 308(M+2)$^+$; 307(M+1)$^+$; 164; 147; ^{1}H NMR ($CDCl_3$) δ 7.78(1H,br.s,NHCO); 7.11(1H,t,Ar); 7.03(1H,d,Ar); 6.80-6.73(2H,mult,Ar); 4.20(1H,dd,ArCHN); 3.84-2.45(20H,mult,CH_2N+CH_2CO+NH); 1.73(2H,mult,CH_2C); ^{13}C NMR ($CDCl_3$) δ 171.6; 156.6; 128.2; 125.5; 119.0; 116.1; 59.0; 49.6; 48.9; 47.8; 45.3; 42.9; 38.2; 28.1.

5-(2-Hydroxyphenyl)-1,4,8,11-tetraazacyclotetradecane (2)

Synthesised in a similar manner to (56), then recrystallised from CH_3CN. Yield: 520mg (55%); Mpt. 141-143 °C (Lit. 142-143 °C)[4]; Anal: Calcd for $C_{16}H_{28}N_4O.H_2O$: C 61.90; H 9.74; N 18.05. Found: C 61.79; H 9.26; N 17.97; m/e: 294(M+2)$^+$; 293(M+1)$^+$; 161; 131; 130; ^{1}H NMR ($CDCl_3$) δ 7.10(1H,t,Ar); 6.93(1H,d,Ar); 6.74(2H,mult,Ar); 3.81(1H,dd,Ar); 3.09-2.45(18H,mult,CH_2N+NH); 1.93(2H,mult,CH_2C); 1.74(2H,mult,CH_2C); 0.75(1H, br.s,OH); ^{13}C NMR ($CDCl_3$) δ 157.7; 127.8; 126.5; 118.5; 116.2; 66.5; 51.1; 50.8; 49.9; 49.5; 49.2; 49.1; 47.2; 36.2; 29.2.

7.3.6 Modified Phenol-Pendent Macrocycles

5-(2-Hydroxy-3-sulphonic acid-5-aminomethylphenyl)-1,4,8,11-tetraaza-cyclotetradecane (55)

A solution of (19) (84mg) in 98% H_2SO_4 (1 cm^3) was heated to 100 ^oC for 1 hour. On cooling, the darkened solution was poured onto crushed ice (15g) and the pH was adjusted to 3-4 with sodium hydroxide. On addition of excess methanol, sodium sulphate was precipitated and was filtered off. Remaining sodium sulphate was removed by evaporating the solution to dryness, then extracting the macrocycle into methanol. The required monosulphonated product was separated from unreacted starting material using cation exchange HPLC: R_t 10.0 min (pH 7.4); m/e(FAB): 402$(M)^+$; 389; 346; ^1H NMR (AcO^- salt,D_2O) δ 7.66(1H,d,Ar,J=2.2 Hz); 7.31(1H,d,Ar, J=2.1 Hz); 4.19(1H,dd,ArCHN); 4.06(2H,s,$ArCH_2N$); 3.23-2.71(14H,mult, CH_2N); 2.40-1.87(4H,mult,CH_2C+CH_3COO^-).

5-(2-Hydroxy-3-nitro-5-aminomethylphenyl)-1,4,8,11-tetraazacyclotetra-decane (54) *and 5-(2-hydroxy-3,5-dinitrophenyl)-1,4,8,11-tetraazacyclo-tetradecane* (53)

A solution of (19) (180mg, 0.56 mmol) in trifluoroacetic anhydride (2 cm^3) was stirred at room temperature for 15 hours. The excess anhydride was then evaporated *in vacuo* and the residue dissolved in ethyl acetate/ chloroform/dichloromethane (2:1:1). After stirring for 2 hours in the presence of water (10 cm^3), the organic layer was washed with more water (2 x 6 cm^3) and the solvent removed under reduced pressure. Diethyl ether was added to precipitate a white solid (263mg) which was filtered off. The nitration of the protected pentaamine (263mg) was carried out with a mixture of concentrated nitric (0.9 cm^3, 75%) and sulphuric (0.55 cm^3, 98%) acids. After stirring for 4 hours at room temperature, the

reaction mixture was poured into distilled water (25 cm^3) and a yellow precipitate was filtered off. The solid (203mg) was treated with a mixture of molar sodium hydroxide in water (1.2 cm^3) and methanol (5 cm^3) for 20 hours at room temperature. After evaporating the solvent *in vacuo*, molar acetic acid (5 cm^3) was added to the residue producing a yellow precipitate of the acetate salt of (53) which was filtered off. Overall yield: 45mg (16%); Mpt. 215-217^oC; m/e(Neg.FAB): 382$(M)^-$; 381 $(M-1)^-$; 365; 249; UV(H_2O): 261 nm (pH 2,phenol); 372 nm (pH 10, phenolate); ^1H NMR (D_2O) δ 8.81(1H,d,Ar); 8.08(1H,d,Ar); 4.16(1H,dd, ArCHN); 3.32-2.61(14H,mult,CH_2N); 2.27-1.87(4H,mult,CH_2C).

The aqueous layer was evaporated to dryness and the residue was twice recrystallised from water to remove further dinitro-compound. Cation exchange HPLC was used to remove further impurities, including sodium acetate. The acetate salt of (54) was isolated as a yellow-orange solid. Overall yield: 7mg (2.3%); HPLC: R_t 15 min (pH 6.5); UV(H_2O): 236 nm (pH 4,phenol); 411 nm (pH 9.2,phenolate); ^1H NMR (AcO^- salt,D_2O) δ 8.10(1H,d,Ar,J=2.1 Hz); 7.50(1H,d,Ar,J=2.1 Hz); 4.23(1H,dd,ArCHN); 4.10 (2H,s,$ArCH_2N$); 3.30-2.67(14H,mult,CH_2N); 1.92(13H,mult,CH_2C+CH_3COO^-).

7.3.7 Functionalised Yttrium Binder

12-(4-Acetamidomethylbenzyl)-1,4,7,10-tetraazacyclotridecane-N,N^1,N^2,N^3-tetraacetic acid, ethyl ester (60)

The monoprotected amine (59) (300mg, 0.86 mmol) was dissolved in dry isopropanol (15 cm^3). Caesium carbonate (1.173g, 3.6 mmol) was added as a solid, ethyl bromoacetate (600mg, 3.6 mmol) as a solution in dry isopropanol (2 cm^3). After stirring for 18 hours at 55-60 ^oC, the solids were filtered off and the solvent evaporated. The residue was

re-dissolved in chloroform (50 cm^3), washed with water (20 cm^3) and dried over potassium carbonate. The chloroform was removed under reduced pressure to give a crude oil (476mg). The crude material was chromatographed on alumina, eluting with 2% methanol/dichloromethane, to give the pure tetracarboxylate ester in 35% yield (205mg). Two successive columns were necessary to remove all remaining traces of baseline material. TLC: R_f 0.45 (ethyl acetate); m/e(EI): 694$(M+2)^+$; 693$(M+1)^+$; 680; 679; 666; 665; IR(film): 3270(NH); 3050(CH); 2980(CH); 2930(CH); 2825(CH); 1735(CO); 1655(CO); 1542; 1450; 1375; 1200; ^{1}H NMR ($CDCl_3$) δ 7.22(2H,d,Ar); 7.15(2H,d,Ar); 5.21(1H,br.s,NHCO); 4.40(2H,d, $ArCH_2N$); 4.15(8H,mult,CH_2O); 3.39-2.30(27H,mult,CH_2N+$COCH_2N$+$CHCH_2$+ CH_2Ar); 2.05(3H,s,CH_3CO); 1.26(12H,t,CH_3C); ^{13}C NMR ($CDCl_3$) δ 171.8; 171.3; 140.7; 135.4; 129.5; 127.8; 60.1; 57.5; 55.2; 52.3; 51.5; 50.6; 43.5; 39.6; 37.8; 21.9; 14.3.

12-(4-Aminomethylbenzyl)-1,4,7,10-tetraazacyclotridecane-N,N^1,N^2,N^3-tetra-acetic acid (61)

Treatment of (60) (110mg, 0.16 mmol) with 6N HCl (10 cm^3) for 24 hours hydrolysed the amide and ester functionalities simultaneously. The acid was removed *in vacuo* to give the tetraacid as a glassy solid (110mg, 96%); m/e(FAB): 538$(M+1)^+$; 494$(M+1-CO_2)^+$; 480; 462; ^{1}H NMR (D_2O) δ 7.36(2H,d,Ar); 7.30(2H,d,Ar); 4.11(2H,s,$ArCH_2N$); 4.00-3.70(8H,mult, NCH_2CO_2H); 3.60-2.40(19H,mult,CH_2N+CH_2Ar+$CHCH_2$); ^{13}C NMR (D_2O) δ 173.6; 141.5; 133.8; 132.4; 131.8; 62.4; 56.3; 55.8; 53.7; 51.4; 45.3; 38.9; 34.7.

12-(4-Acetamidomethylbenzyl)-1,4,7,10-tetraazacyclotridecane-N,N^1,N^2,N^3-tetraacetic acid (62)

The exocyclic amino group of (61) (110mg, 0.153 mmol) in water (1 cm^3)

was acetylated using excess p-nitrophenylacetate (76mg, 0.42 mmol) in p-dioxane (4 cm^3). The reaction mixture was neutralised with sodium carbonate and stirred for 3 days at room temperature. The solution was then acidified (pH 4) with molar acetic acid and washed with ether (2 x 50 cm^3) to remove excess ester and p-nitrophenol. The solvent was then removed under reduced pressure. The amide was separated from inorganic salts by passing down a cation exchange column (Dowex 50W H^+ form), eluting with 0.5M ammonium hydroxide. The alkaline fractions were collected and combined, and the solvent removed to give a glassy solid (55mg, 62%); ^1H NMR (D_2O) δ 7.27(4H,mult,Ar); 4.35(2H,s,$ArCH_2N$); 3.70-2.20(27H,mult,CH_2N+CH_2CO+CH_2Ar+$CHCH_2$); 2.04(3H,s,CH_3).

7.4 REFERENCES

1. E. Kimura, T. Koike and M. Takahashi, *J.Chem.Soc. Chem.Commun.*, 385 (1985)
2. G.T. Morgan and F.M.G. Micklethwaite, *J.Chem.Soc.*, 85, 1230 (1904)
3. L.Y. Martin, L.J. DeHayes, L.J. Zompa and D.H. Busch, *J.Am.Chem*, 96(12), 4046 (1974)
4. E. Kimura, T. Koike, K. Uenishi, M. Hediger, M. Kuramoto, S. Joko, Y. Arai, M. Kodama and Y. Iitaka, *Inorg.Chem.*, 26, 2975 (1987)

APPENDICES

APPENDIX 1

RESEARCH COLLOQUIA, SEMINARS AND LECTURES

The following lectures were organised by the Department of Chemistry during the course of my three years of research (October 1985 - September 1988); "*" indicating the authors's attendance:

17.10.85		Dr. C.J. Ludman (Durham) "Some Thermochemical Aspects of Explosions"
24.10.85		Dr. J. Dewing (UMIST) "Zeolites - Small Holes, Big Opportunities"
30.10.85		Dr. S.N. Whittleton (Durham) "An Investigation of a Reaction Window"
31.10.85	*	Dr. P. Timms (Bristol) "Some Chemistry of Fireworks"
05.11.85	*	Prof. M.J. O'Donnell (Indiana-Purdue University, USA) "New Methodology for the Synthesis of Amino Acids"
07.11.85		Prof. G. Ertl (Munich, W. Germany) "Heterogeneous Catalysis"
14.11.85	*	Dr. S.G. Davies (Oxford) "Chirality Control and Molecular Recognition"
20.11.85		Dr. J.A.H. McBride (Sunderland Polytechnic) "A Heterocyclic Tour on a Distorted Tricycle - Biphenylene"
21.11.85		Prof. K.H. Jack (Newcastle) "Chemistry of Si-Al-O-N Engineering Ceramics"
28.11.85	*	Dr. B.A.J. Clark (Kodak Ltd.) "Chemistry & Principles of Colour Photography"
28.11.85		Prof. D.J. Waddington (York) "Resources for the Chemistry Teacher"
15.01.86		Prof. N. Shephard (East Anglia) "Vibrational and Spectroscopic Determinations of the Structures of Molecules Chemisorbed on Metal Surfaces"
23.01.86		Prof. Sir Jack Lewis (Cambridge) "Some more Recent Aspects in the Cluster Chemistry of Ruthenium and Osmium Carbonyls"
29.01.86		Dr. J.H. Clark (York) "Novel Fluoride Ion Reagents"

30.01.85 * Dr. N.J. Phillips (Loughborough)
"Laser Holography"

12.02.86 Dr. J. Yarwood (Durham)
"The Structure of Water in Liquid Crystals"

12.02.86 Prof. O.S. Tee (Concordia University, Montreal)
"Bromination of Phenols"

13.02.86 Prof. R. Grigg (Queen's, Belfast)
"Thermal Generation of 1,3-Dipoles"

19.02.86 * Prof. G. Proctor (Salford)
"Approaches to the Synthesis of some Natural Products"

20.02.86 * Dr. C.J.F. Barnard (Johnson Matthey Group)
"Platinum Anti-Cancer Drug Development"

26.02.86 Miss C. Till (Durham)
"ESCA and Optical Emission Studies of the Plasma Polymerisation of Perfluoroaromatics"

27.02.86 Prof. R.K. Harris (Durham)
"The Magic of Solid State NMR"

05.03.86 Dr. D. Hathway (Durham)
"Herbicide Selectivity"

05.03.86 * Dr. M. Schroder (Edinburgh)
"Studies on Macrocyclic Complexes"

06.03.86 * Dr. B. Iddon (Salford)
"The Magic of Chemistry"

12.03.86 Dr. J.M. Brown (Oxford)
"Chelate Control in Homogeneous Catalysis"

14.05.86 Dr.P.R.R. Langridge-Smith (Edinburgh)
"Naked Metal Clusters - Synthesis, Characterisation and Chemistry"

09.06.86 Prof. R. Schmutzler (Braunschweig, W. Germany)
"Mixed Valence Diphosphorus Compounds"

23.06.86 Prof. R.E. Wilde (Texas Technical University, USA)
"Molecular Dynamic Processes from Vibrational Bandshapes"

16.10.86 Prof. N.N. Greenwood (University of Leeds)
"Glorious Gaffes in Chemistry"

23.10.86 * Prof. H.W. Kroto (University of Sussex)
"Chemistry in Stars, between Stars and in the Laboratory"

29.10.86 * Prof.E.H. Wong (University of New Hampshire, USA)
"Coordination Chemistry of P-O-P Ligands"

05.11.86 Prof. D. Döpp (University of Duisburg)
"Cyclo-additions and Cyclo-reversions Involving Captodative Alkenes"

06.11.86 * Dr. R.M. Scrowston (University of Hull)
"From Myth and Magic to Modern Medicine"

13.11.86 * Prof. Sir G. Allen (Unilever Research)
"Biotechnology and the Future of the Chemical Industry"

20.11.86 * Dr. A. Milne and Mr. S.Christie (International Paints)
"Chemical Serendipity: A Real Life Case Study"

26.11.86 Dr. N.D.S. Canning (University of Durham)
"Surface Adsorption Studies of Relevance to Heterogeneous Ammonia Synthesis"

27.11.86 Prof. R.L. Williams (Metropolitan Police Forensic Science)
"Science and Crime"

03.12.86 Dr. J.J. Miller (Dupont Central Research, USA)
"Molecular Ferromagnets; Chemistry and Physical Properties"

08.12.86 Prof. T. Dorfmüller (University of Bielefeld)
"Rotational Dynamics in Liquids and Polymers"

22.01.87 Prof. R.H. Ottewill (University of Bristol)
"Colloid Science a Challenging Subject"

28.01.87 Dr. W. Clegg (University of Newcastle-upon-Tyne)
"Carboxylate Complexes of Zinc; Charting a Structural Jungle"

04.02.87 * Prof. A. Thomson (University of East Anglia)
"Metalloproteins and Magneto-optics"

05.02.87 Dr. P. Hubberstey (University of Nottingham)
"Demonstration Lecture on Various Aspects of Alkali Metal Chemistry"

11.02.87 Dr. T. Shepherd (University of Durham)
"Pteridine Natural Products; Synthesis and Use in Chemotherapy"

12.02.87 * Dr. P.J. Rodgers (I.C.I. Billingham)
"Industrial Polymers from Bacteria"

17.02.87 * Prof.E.H. Wong (University of New Hampshire, USA)
"Symmetrical Shapes from Molecules to Art and Nature"

19.02.87 * Dr. M. Jarman (Institute of Cancer Research)
"The Design of Anti Cancer Drugs"

04.03.87 Dr. R. Newman (University of Oxford)
"Change and Decay: A Carbon-13 CP/MAS NMR Study of humification and Coalification Processes"

05.03.87 * Prof. S.V. Ley (Imperial College)
"Fact and Fantasy in Organic Synthesis"

09.03.87 Prof. F.G. Bordwell (Northeastern University, USA)
"Carbon Anions, Radicals, Radical Anions and Radical Cations"

11.03.87 Dr. R.D. Cannon (University of East Anglia)
"Electron Transfer in Polynuclear Complexes"

12.03.87 Dr. E.M. Goodger (Cranfield Institute of Technology)
"Alternative Fuels for Transport"

17.03.87 Prof. R.F. Hudson (University of Kent)
"Aspects of Organophosphorus Chemistry"

18.03.87 Prof. R.F. Hudson (University of Kent)
"Homolytic Rearrangements of Free Radical Stability"

03.04.87 * Prof. G. Ferguson (University of Guelph, Canada)
"X-Ray Crystallography for the Organic Chemist"

06.05.87 Dr. B. Bartsch (University of Sussex)
"Low Co-ordinated Phosphorus Compounds"

07.05.87 Dr. M. Harmer (I.C.I. Chemicals & Polymer Group)
"The Role of Organometallics in Advanced Materials"

11.05.87 Prof. S. Pasynkiewicz (Technical University,Warsaw)
"Thermal Decomposition of Methyl Copper and its Reactions with Trialkylaluminium"

27.05.87 Dr. M. Blackburn (University of Sheffield)
"Phosphonates as Analogues of Biological Phosphate Esters"

24.06.87 * Prof. S.M. Roberts (University of Exeter)
"Synthesis of Novel Antiviral Agents"

26.06.87 Dr. C. Krespan (E.I. Dupont de Nemours)
"Nickel(0) and Iron(0) as Reagents in Organofluorine Chemistry"

15.10.87 Dr. M.J. Winter (University of Sheffield)
"Pyrotechnics" (Demonstration Lecture)

22.10.87 * Prof. G.W. Gray (University of Hull)
"Liquid Crystals and their Applications"

29.10.87 Mrs. S. van Rose (Geological Museum)
"Chemistry of Volcanoes"

04.11.87 Mrs. M. Mapletoft (Durham Chemistry Teachers' Centre)
"Salters' Chemistry"

05.11.87 Dr. A.R. Butler (University of St.Andrews)
"Chinese Alchemy"

12.11.87 * Prof. D. Seebach (E.T.H. Zurich)
"From Synthetic Methods to Mechanistic Insight"

26.11.87 * Dr. D.H. Williams (University of Cambridge)
"Molecular Recognition"

.11.87 Dr. J. Davidson (Herriot-Watt University)
"Metal Promoted Oligomerisation Reactions of Alkynes"

03.12.87 * Dr. J. Howard (I.C.I. Wilton)
"Chemistry of Non-Equilibrium Processes"

10.12.87 Dr. C.J. Ludman (Durham University)
"Explosives"

16.12.87 Mr. R.M. Swart (I.C.I.)
"The Interaction of Chemicals with Lipid Bilayers"

19.12.87 * Prof. P.G. Sammes (Smith, Kline and French)
"Chemical Aspects of Drug Development"

21.01.88 * Dr. F. Palmer (University of Nottingham)
"Luminescence" (Demonstration Lecture)

28.01.88 Dr. A. Cairns-Smith (Glasgow University)
"Clay Minerals and the Origin of Life"

09.02.88 Mr. Lacey (Durham Chemistry Teacher's Centre)
"Double Award Science"

11.02.88 Prof. J.J. Turner (University of Nottingham)
"Catching Organometallic Intermediates"

18.02.88 Dr. K. Borer (Univ.of Durham Industrial Research Labs.)
"The Brighton Bomb - A Forensic Science View)"

25.02.88 Prof. A. Underhill (University of Bangor)
"Molecular Electronics"

03.03.88 Prof. W.A.G. Graham (University of Alberta, Canada)
"Rhodium and Iridium Complexes in the Activation of Carbon-Hydrogen Bonds

07.03.88 Prof. H.F. Koch (Ithaca College, U.S.A.)
"Does the E2 Mechanism Occur in Solution"

16.03.88 L. Bossons (Durham Chemistry Teachers' Centre)
"GCSE Practical Assessment"

07.04.88 * Prof. M.P. Hartshorn (Univ.of Canterbury, New Zealand)
"Aspects of Ipso-Nitration"

13.04.88 Mrs. E. Roberts (SATRO Officer for Sunderland)
Talk - Durham Chemistry Teachers' Centre
"Links between Industry and Schools"

18.04.88 Prof. C.A. Nieto De Castro (University of Lisbon and Imperial College)
"Transport Properties of Non-Polar Fluids"

25.04.88 * Prof. D. Birchall (I.C.I. Advanced Materials)
"Environment Chemistry of Aluminium"

27.04.88 Dr. R. Richardson (University of Bristol)
"X-Ray Diffraction from Spread Monolayers"

27.04.88 * Dr. J.A. Robinson (University of Southampton)
"Aspects of Antibiotic Biosynthesis"

28.04.88 Prof. A. Pines (Univ. of California, Berkeley, USA)
"Some Magnetic Moments"

11.05.88 * Dr. W.A. McDonald (I.C.I. Wilton)
"Liquid Crystal Polymers"

11.05.88 Dr. J. Sodeau (University of East Anglia)
Durham Chemistry Teachers's Centre:
"Spray Cans, Smog and Society"

08.06.88 Prof. J.-P. Majoral (Université Paul Sabatier)
"Stabilisation by Complexation of Short-Lived Phosphorus Species"

29.06.88 Dr. M.E. Jones (Durham Chemistry Teachers' Centre)
"GCSE Chemistry Post-mortem"

29.06.88 Prof. G.A. Olah (University of Southern California)
"New Aspects of Hydrocarbon Chemistry"

06.07.88 Dr. M.E. Jones (Durham Chemistry Teachers' Centre)
"GCE Chemistry A-Level Post-mortem"

APPENDIX 2

RESEARCH CONFERENCES

1.	Practical High Resolution NMR Spectroscopy, University of Sheffield	23th - 27th March 1988
2.	Molecular Recognition, University of Sheffield	14th December 1987
3.	R.S.C. Graduate Symposium, North-East Polytechnics and Universities	19th April 1987

APPENDIX 3

PUBLICATIONS

1. J.R. Morphy, D. Parker, R. Alexander, A. Bains, A.F. Carne, M.A.W. Eaton, A. Harrison, A. Millican, A. Phipps, S.K. Rhind, R. Titmus and D. Weatherby, *J.Chem.Soc. Chem.Commun.*, 156 (1988)

2. D. Parker, J.R. Morphy, K. Jankowski and J. Cox, *Int.Union.Pure Appl.Chem.*, submitted for publication, (1988)

3. I.M. Helps, D. Parker, J.R. Morphy and J. Chapman, *Tetrahedron*, submitted for publication (1988)